UNIVERSIDAD DE CÓRDOBA

Departamento de Biología Celular, Fisiología e Inmunología

DOCTORAL THESIS

MICRORNAS AND GRK2 AS MODULATORS OF KISS1/GPR54 SYSTEM: PHYSIOPATHOLOGICAL ROLE IN PUBERTAL ALTERATIONS AND OBESITY INDUCED HYPOGONADISM

MICRORNAS Y GRK2 COMO ELEMENTOS MODULADORES DEL SISTEMA KISS1/GPR54: PAPEL FISIOPATOLÓGICO EN ALTERACIONES PUBERALES E HIPOGONADISMO CENTRAL INDUCIDO POR OBESIDAD

Cecilia Mª Perdices López
Programa de Doctorado en Biomedicina
Córdoba, mayo de 2023

Los Directores,

Dr. Manuel Tena-Sempere
Catedrático de Fisiología de la Universidad de Córdoba

Dra. María Soledad Avendaño
Investigadora Postdoctoral Miguel Servet de la Fundación para la Investigación Biomédica de Córdoba

TITULO: *MicroRNAs and GRK2 as modulators of Kiss1/GPR54 system: Physiopathological role in pubertal alterations and obesity induced hypogonadism*

AUTOR: *Cecilia María Perdices López*

Campus de Rabanales
Ctra. Nacional IV, Km. 396 A
14071 Córdoba

https://www.uco.es/ucopress/index.php/es/
ucopress@uco.es

TÍTULO DE LA TESIS: MicroRNAs y GRK2 como elementos moduladores del sistema Kiss1/GPR54: papel fisiopatológico en alteraciones puberales e hipogonadismo central inducido por obesidad/ MicroRNAs and GRK2 as modulators of Kiss1/GPR54 system: Physiopathological role in pubertal alterations and obesity induced hypogonadism.

DOCTORANDO/A: Cecilia Mª Perdices López

INFORME RAZONADO DEL/DE LOS DIRECTOR/ES DE LA TESIS

El trabajo de Tesis Doctoral titulado "*MicroRNAs and GRK2 as modulators of Kiss1/GPR54 system: Physiopathological role in pubertal alterations and obesity induced hypogonadism*" ha sido completado de forma muy satisfactoria por la doctoranda Cecilia Mª Perdices López en la Sección de Fisiología del Departamento de Biología Celular, Fisiología e Inmunología de la Universidad de Córdoba, entre los años 2018 y 2023, bajo nuestra dirección. El objetivo general de esta Tesis doctoral ha sido profundizar nuestro conocimiento en los mecanismos de control del sistema Kiss1/GPR54, como elementos clave en la regulación de la pubertad y el eje reproductor en la edad adulta. En concreto, los resultados de este trabajo han permitido identificar por vez primera el papel del tándem de miRNAs, miR-137-3p y miR-325-3p, en el control de la pubertad, a través de su acción represora sobre el sistema Kiss1, así como la posible implicación de este sistema en la generación de condiciones de hipogonadismo central asociado a obesidad, igualmente gracias a su capacidad de reprimir la expresión de *Kiss1*/kisspeptinas en situaciones de sobrepeso persistente. Además, este trabajo de Tesis ha definido el papel del factor, GRK2, en el control del receptor de kisspeptinas, GPR54, actuando al menos en parte en neuronas GnRH, con implicaciones relevantes en la regulación puberal y su modulación por señales nutricionales, así como en la generación de hipogonadismo asociado a obesidad.

Durante todo el período de formación predoctoral, la doctoranda no sólo ha cumplido de manera muy satisfactoria los objetivos propuestos para su trabajo científico, sino que también ha aprovechado esta etapa formativa para (i) reforzar sus conocimientos en el área de estudio; (ii) familiarizarse y adquirir una considerable destreza en el manejo de diferentes técnicas de biología molecular y celular, así como de neuroendocrinología experimental, (iii) estimular su pensamiento crítico y (iv) colaborar activamente en otras líneas de investigación estrechamente relacionadas con su línea de Tesis Doctoral, lo que ha contribuido igualmente a expandir de forma considerable su bagaje formativo y su producción científica.

La excelente labor investigadora de la doctoranda durante este periodo se ha traducido hasta la fecha en: (i) 1 artículo científico como primera autora publicado en la revista *Metabolism – Clinical and Experimental*, en primer decil del área de Endocrinología y Metabolismo, y otros dos que se anticipan que serán completados en breve (correspondientes a las partes 1 y 2 de esta Tesis Doctoral), a fin de proceder con su envío a evaluación, a revistas de primer decil, en el segundo semestre del año en curso; (ii) 8 artículos científicos adicionales como co-autora, en revistas de primer cuartil o primer decil (incluyendo papers en *Nature Communications, Human Reproduction, American Journal of Obstetrics and Gynecology, Frontiers in Neuroendocrinology* y *European Journal of Neuroendocrinology*, entre otras), y (iii) 14 comunicaciones a congresos nacionales e internacionales, incluyendo comunicaciones orales en los congresos "X Simposio anual CIBERobn, 2019", "eECE Congress, 2020", "Congreso SEEN, 2021" y el "Kisspeptin Congress, 2022". Cabe resaltar la obtención del premio a la mejor comunicación oral en el X Simposio anual CIBERobn así como el premio a mejor comunicación oral en la sesión "Nutrición y enfermedades endocrinas y metabólicas",

enmarcada dentro las XII Jornadas de Jóvenes Investigadores del Instituto Maimónides de Investigación Biomédica de Córdoba (IMIBIC). Adicionalmente, la doctoranda ha completado una estancia de tres meses de duración en el grupo de la Dra. Nelly Pitteloud, del Centro Hospitalario Universitario de Vaudois, Lausana (Suiza), gracias a la obtención de fondos competitivos de la Universidad de Córdoba de ayuda a estancias predoctorales en el extranjero, así como gracias a la Ayuda a la Movilidad del Plan Propio del IMIBIC.

Todo ello, unido a las excelentes aptitudes y capacidades de la doctoranda para la investigación y el trabajo de laboratorio, nos hacen calificar su formación predoctoral como excelente.

Por todo lo anteriormente expuesto, se autoriza la presentación de esta Tesis Doctoral

Córdoba, 26 de mayo de 2023

Firma del/de los director/es

TENA SEMPERE MANUEL JOSE - 30534904N
Firmado digitalmente por TENA SEMPERE MANUEL JOSE - 30534904N
Fecha: 2023.05.26 07:20:12 +02'00'

AVENDAÑO HERRADOR MARIA SOLEDAD - 30986570G
Firmado digitalmente por AVENDAÑO HERRADOR MARIA SOLEDAD - 30986570G
Fecha: 2023.05.26 12:20:32 +02'00'

Fdo.: MANUEL TENA-SEMPERE

Fdo.: MARIA SOLEDAD AVENDAÑO

Index

INDEX

Summary

Resumen

Abbreviations

Introduction 1

1. Reproduction and the hypothalamic-pituitary-gonadal axis **2**
1.1. Hypothalamus 2
1.1.1. Hypothalamic nuclei 3
1.1.2. Gonadotropin-releasing hormone 4
1.2. Pituitary 5
1.2.1. Gonadotropins: LH and FSH 6
1.3. Gonads 7
1.3.1. Ovary and the ovarian cycle 7
1.3.2. Testis and spermatogenesis 9
1.3.2.1. Steroidogenesis 10
1.3.2.2. Androgen metabolism 11

2. The Kiss1/GPR54 system: Roles in puberty and maintenance of reproductive function **11**
2.1. *Kiss1* gene and kisspeptins 12
2.2. The kisspeptin receptor: GPR54 13
2.3. The Kiss1/GPR54 system along the lifespan 14
2.3.1. Sites and mechanisms of action 14
2.3.2. Roles in sex differentiation 15
2.3.3. Roles in puberty 17
2.3.4. Adult period: GnRH pulse generator 18

3. Main neuroendocrine regulators of the Kiss1/GPR54 system and the HPG axis **19**
3.1. Central regulators of the HPG axis 20
3.3.1. Neurokinin B and tachykinins 20
3.3.2. Glutamate and ϒ-aminobutyric acid 20
3.3.3. Other neuropeptides 20
3.2. Peripheral regulators of the HPG axis 22
3.2.1 Gonadal steroids 22
3.2.2. Peripheral metabolic mediators 22

4. Molecular mechanisms for the regulation of the Kiss1/Gpr54 system **23**
4.1. *Kiss1* regulation 23
4.1.1. Transcriptional regulation 23
4.1.2. Epigenetic regulation 24
4.2. GRK2 regulation of GPR54 signaling 25

5. MicroRNAs: Pleiotropic epigenetic regulators **28**
5.1. General features of miRNAs 28
5.2. Synthesis and mechanism of action 29
5.3. Potential roles of miRNAs in reproduction 31
5.4. MiRNAs as regulators od kisspeptin 33
5.5. MiRNA data bases for *in silico* studies 33

6. Interplay between metabolism and reproduction - **35**
6.1. Central signals for the metabolic control of reproduction 36
6.2. Peripheral hormones in the metabolic control of reproduction 37

6.3. Central cell energy sensors and the metabolic control of reproduction 40
6.4. The Kiss1/GPR54 system and the metabolic control of reproduction 40
6.4.1. The Kiss1/GPR54 system and the metabolic control of puberty 40
6.4.2. The Kiss1/GPR54 and obesity-induced central hypogonadism 41

Objectives 47

Materials and Methods 51
1. Ethic statement 51
2. Animals 51
2.1. Rat models 51
2.2. Mouse models 51
2.2.1. *Kiss1*$^{Cre:GFP}$ mouse model 51
2.2.2. *Kiss*$^{Cre\_EYFP}$ mouse model 51
2.2.3. G-GRKO mouse model 51
3. Drugs 52
4. General experimental procedures 52
4.1. Sample collection 52
4.1.1. Hypothalamus, preoptic area and mediobasal hypothalamus 52
4.1.2. Blood collection 53
4.1.3. Heart and tibia 53
4.1.4. Prostate hyperplasia determination 53
4.1.5. Ovary and testis isolation 53
4.2. Phenotypic evaluation of pubertal maturation 53
4.3. Mouse habituation for tail-tip blood collection and LH pulsatility test 54
4.4. Systolic blood pressure ..... -54
4.5. Vascular components determination 54
4.6. Body composition 56
5. General surgical procedures 57
5.1. Cannulation and ICV 57
5.2. Stereotaxic injections 57
6. General analytical procedures 57
6.1. Genotyping 57
6.2. RNA extraction, retrotranscription and quantitative PCR from tissues 58
6.3. RT reactions and qPCR from cells 59
6.4. Radioimmunoassay 60
6.5. ELISA assays 61
6.5.1 LH ELISA assay 61
6.5.2. Insulin and leptin serum levels 61
6.6. Western Blot 62
6.7. Determination of plasma cytokines 62
6.8. Immunohistochemistry 63
6.9. RNAscope 64
6.10.Fluorescence-activated cell sorting 65
6.11. *In vitro* validation of miRNA repression 65
6.12. *In vitro* calcium mobilization assay 66
7. Bioinformatic analysis 67
8. Statistical analysis 68
8.1. General analysis 68
8.2. Area under the curve 68

9. Experimental designs 68
Part 1. MicroRNAs and the physiological control of puberty 69
Part 2. Pathophysiological role of miR-137-3p and miR-325-3p in male OIH 73
Part 3. GRK2 regulation of Kiss1/GPR54 signaling during nutritional deprivation 77
Part 4. Analysis of roles of GRK2 in male OIH 82

Results 87
Part 1. MiRNAs in the physiological control of puberty 87
1.1. *In silico* prediction of putative miRNA regulators of *KISS1/Kiss1* 87
1.2. Hypothalamic expression of miR-137/miR-325 in postnatal maturation and delayed puberty 88
1.3. *In vitro* validation of miR-137-3p and miR-325-3p repression over *Kiss1* 90
1.4. Assessment of miR-137-3p and miR-325-3p repression of *Kiss1 in vivo* 91
1.5. Blockade of miR-137-3p/miR-325-3p repression of *Kiss1 in vivo advances puberty onset* *94*
1.6. MIR137HG copy number variants in human precocious puberty 95
Part 2. Pathophysiological role of miR-137-3p and miR-325-3p in male OIH 96
2.1. Hypothalamic expression analysis of kisspeptin, miR-137-3p and miR-325-3p in OIH model 96
2.2. *In vivo* validation of miR-137-3p repressive actions on *Kiss1* in adult male rats 98
2.3. Virogenetic over-expression of miR-137 in the ARC in $Kiss1^{Cre:GFP}$ and $Kiss^{Cre:EYFP}$ mice 98
2.4. Hormonal and phenotypic characterization of the male rat OIH model 100
2.5. Central blockade of miR-137-3p/325-3p repression of *Kiss1 in vivo* in the OIH model 101
2.6. Effects of central Kp-10 or testosterone treatment on the OIH model 104
Part 3. GRK2 as a novel regulator of GPR54: Roles in puberty and nutritional deprivation 108
3.1. Evaluation of GRK2-mediated modulation of responses to Kp-10 *in vitro* and *in vivo* 108
3.2. Hypothalamic GRK2 expression through postnatal maturation and in delayed puberty 109
3.3. Blockade of GRK2 and pubertal development: Pharmacological and genomic approaches 111
3.3.1. Central pharmacological inhibition of GRK2 and puberty onset 112
3.3.2. Conditional ablation of *Grk2* in GnRH neurons and puberty onset 112
3.4. Blockade of GRK2 and pubertal development: Studies in models of delayed puberty 115
3.4.1. Central pharmacological inhibition of GRK2 in conditions of nutritional deprivation 116
3.4.2. Conditional ablation of *Grk2* in GnRH neurons in conditions of delayed puberty 117
Part 4. Roles of central GRK2 in obesity-induced hypogonadism of the male 119
4.1. Inhibition of GRK2 enhances gonadotropin responses to repeated kisspeptin stimuli 119
4.2. Hypothalamic expression of GRK2 in the rat model of OIH 120
4.3. Effects of central pharmacological blockade of GRK2 in the rat model of OIH 120
4.4. Effects of conditional ablation of *Grk2* in GnRH neurons in the mouse mode of OIH 122
Discussion 127
Conclusions 143
Bibliography 145

Summary

1. Introduction

The reproductive function is governed by the so-called hypothalamic-pituitary-gonadal (HPG) axis, where an intricated network of central, peripheral and external factors determine hormonal balance and proper functioning of the reproductive system and the gonadal function, guaranteeing the perpetuation of the species [1–3]. In recent years, it has been documented that a plethora of central (glutamate, GABA, NKB, NPY) [4–7], peripheral (insulin, leptin, ghrelin) [8,9] and external (nutritional availability, endocrine disruptors, circadian rhythms) [10–13] cues converge (either acting directly or indirectly) onto Kiss1 neurons in the hypothalamus, as major signaling hub of the HPG axis [14], whose products, kisspeptins, act on the GnRH neurons, via its canonical receptor, GPR54[15], activating puberty onset and reproductive function. In addition, it is well recognized that reproductive function is altered under conditions of metabolic distress, ranging from subnutrition to obesity, type 2 diabetes and metabolic syndrome, which are bound to numerous perturbations, including disordered puberty, central hypogonadism (mainly in males) and cardiometabolic impairment[16,17].

MicroRNAs have been recently pointed out as essential players in the control of normal pubertal development[18–21], although no study has addressed the specific regulation of *Kiss1*, at central levels, exerted by miRNAs [21,22]. Further, the effects of miRNAs in the pathogenesis of central hypogonadism are completely unexplored. In parallel, the Kiss1/GPR54 system is a key element for the integration of the energetic status and reproductive capacity [23], where GPR54 inactivating mutations were described decades ago as underlying origin of hypogonadotropic hypogonadism [24,25]. The G-protein coupled receptor kinase 2 (GRK2) [26], which is largely recognized as pleiotropic regulator of cellular signaling [27–29], has been suggested *in vitro* as a modulator of GPR54[26]. Nevertheless, no studies had addressed to date its potential roles in proper pubertal development and maintenance of reproductive capacity.

In the above context, this Doctoral Thesis has addressed, as main aims, **(i)** the putative role of specific miRNAs in the physiological control of puberty via regulation of the Kiss1 system; **(ii)** the pathophysiological role of miRNAs in obesity-induced hypogonadism (OIH), their interplay with *Kiss1* and their potential therapeutic implications; **(iii)** the role of GRK2 in the control of puberty and the HPG axis through regulation of GPR54 in normal conditions and under nutritional stress; and **(iv)** the implication of GRK2 in OIH through GPR54 regulation.

2. Research contents

This Thesis has been divided into four main parts, subdivided into several experimental sets.

Part 1 and 2 of this Thesis assessed the putative role of miRNAs in the regulation of *Kiss1* expression during puberty and in conditions of obesity-induced hypogonadism in adult males, respectively. Both parts departed from one common *in silico* study, that set up the subsequent experiments, and were supported by confirmatory functional *in vitro* assays, which documented that miR-325-3p and miR-137-3p are indeed specific regulators of Kiss1 system, as demonstrated also by a combination of studies *in vivo*. Importantly, both miRNAs were predicted to share the same seed binding region to the 3'UTR of *Kiss1*, they were found to be highly conserved in evolution and were sensitive to nutritional distress cues.

In **Part 1** of this Thesis, we performed initial hypothalamic expression analysis in preclinical models (female Wistar rats): during normal postnatal maturation and in conditions of perturbed puberty due to neonatal undernutrition (20 pups per mother), peripubertal subnutrition (30% subnutrition regarding controls, from PND 23) or modification of the sex steroid milieu, from birth. During normal development, we observed a gradual increase in the levels of miR-137-3p and miR-325-3p, especially from infantile stage to pubertal stage, that were paralleled by the increase observed in kisspeptin levels. Complementarily, our results showed that models of perturbed puberty -linked to delay of pubertal maturation- were linked to a prominent increase in the levels of both miRNAs. The role of these miRNAs was studied further via two complementary means: via mimicking their action, using miRNA mimics, and via target-specific blockade of miRNA repressive action *in vivo*, from post-weaning to puberty onset. In these studies, we observed that mimicking of both miRNAs induced a delay in the age of pubertal maturation, while blockade of miR-137-3p and miR-325-3p caused an advancement of the awakening of the hypothalamic-pituitary-gonadal axis at puberty.

In **Part 2** of this Thesis, we interrogated the potential functional role of miR-137-3p and miR-325-3p in OIH, using a suitable preclinical model. First, we found that the hypothalamic levels of miR-137-3p and miR-325-3p were highly elevated in the arcuate nucleus, and showed an opposite pattern to that observed for kisspeptin levels, under OIH. As a proof of concept, mimicking of miR-137-3p in control young male rats induced a decrease in the content of hypothalamic kisspeptin. Next we observed, in our model of OIH, cardiometabolic and reproductive improvement after central blockade of miRNA 137-3p/325-3p specific action on *Kiss1.* In contrast, comparative analysis of the effects of central treatment of Kp-10 or testosterone replacement did not show relevant cardiometabolic improvements despite (supra-physiologically) increased levels of LH or testosterone, respectively. Finally, overexpression of

miR-137-3p in the arcuate neurons of young male mice prompted increased body weight and decreased LH levels, linked to a drop of kisspeptin levels in isolated kisspeptin neurons.

In **Part 3** of this Thesis, evaluation of modulatory function of GRK2 in the regulation of GPR54, by *in vitro* approaches, showed a repressive role of GRK2 in acute responses to kisspeptin. Evidence for such a role were obtained also *in vivo*, using female rats pre-treated intracerebroventricularly with the inhibitor of GRK2 (β-ARK-1-I) or mice lacking GRK2 in the GnRH neuron, which displayed exaggerated responses to kisspeptin. Additionally, hypothalamic expression of GRK2 during normal development showed progressive increment until puberty in female Wistar rats, while models of perturbed puberty were linked to augmented content of GRK2 at hypothalamic level. Our studies evidenced also advanced puberty in female rats pre-treated with β-ARK-1-I and in our congenital mice model of *Grk2* ablation in GnRH neurons, which exhibited changes in the pattern of LH release and ovarian maturation. Notably, the negative impact of conditions of undernutrition in terms of pubertal maturation was partially prevented by central pharmacological inhibition of GRK2 or its genetic suppression in GnRH neurons.

Finally, in **Part 4** of this Thesis, we explored the role of GRK2 in OIH in males. First, we tested in adult male rats the central response to repeated injections of kisspeptin after GRK2 inhibition with β-ARK-1-I. This approach revealed augmented responses to kisspeptin, supporting a role of GRK2 in modulating kisspeptin/GPR54 signaling also in adulthood. Next, expression and functional analyses of GRK2 were conducted in our model of OIH. As most striking finding, when OIH animals were treated with β-ARK-1-I or after congenital ablation of *Grk2* in GnRH neurons, we observed significant improvement in the reproductive profiles, which were negatively affected by obesity, together with detectable amelioration of different metabolic parameters, although a greater cardiovascular improvement was found with the pharmacological blockade of GRK2 than in our conditional model of GnRH-specific GRK2 KO.

3. Conclusions

Based on the above results, the main conclusions of this Doctoral Thesis are the following:

1. The microRNAs, miR-137-3p and miR-325-3p, which are evolutionary conserved and share their seed region, operate as putative regulator of puberty, acting via repression of *Kiss1*, as documented by expression and functional studies in female rats. This mechanism may contribute to pubertal regulation in conditions of early nutritional stress and, based on initial findings in clinical databases, might operate also in humans.

2. The microRNAs, miR-137-3p and miR-325-3p, are also involved in the pathogenesis of obesity-induced hypogonadism in the male, as major driving force for suppression of hypothalamic *Kiss1* in conditions of obesity. Prevention of the repressive action of miR-137/ 325 on *Kiss1* not only ameliorates reproductive indices, but also improves metabolic, cardiovascular and inflammatory markers, outperforming the effects of pharmacological treatments with either Kp-10 or testosterone in a rat model of rat obesity.

3. GRK2, acting in GnRH neurons, exerts a repressive effect on kisspeptin signaling, likely via modulation of GPR54; this phenomenon plays a relevant role in the control of pubertal maturation in rats, and contributes to inhibition of puberty onset in conditions of early undernutrition.

4. GRK2 signaling, acting at least in part in GnRH neurons, contributes to central suppression of the gonadotropic axis in conditions of obesity, with a discernible role of central GRK2 in the manifestation of the cardiometabolic alterations linked to this condition.

As a sum, the results of this Doctoral Thesis allow us to set as global conclusion that:

5. Novel repressive regulatory mechanisms, involving both the direct interplay between miR-137-3p/miR-325-3p and *Kiss1*, and the inhibitory actions of GRK2 on GPR54 in GnRH neurons, play a major role in the regulation of pubertal timing and its modulation by metabolic cues, particularly in situations of undernutrition, and likely contribute to the reproductive and metabolic manifestations of OIH. These pathways pose clear physiological interest and may pave the way for the definition of novel targets for the personalized management of prevalent reproductive and metabolic disorders, ranging from pubertal alterations to adult obesity and infertility.

Bibliography

1. Avendaño, M. S., Vazquez, M. J. & Tena-Sempere, M. Disentangling puberty: novel neuroendocrine pathways and mechanisms for the control of mammalian puberty. *Hum Reprod Update* **23**, 737–763 (2017).

2. Sobrino, V., Avendaño, M. S., Perdices-López, C., Jimenez-Puyer, M. & Tena-Sempere, M. Kisspeptins and the neuroendocrine control of reproduction: Recent progress and new frontiers in kisspeptin research. *Front Neuroendocrinol* **65**, 100977 (2022).

3. Plant, T. M. & Zeleznik, A. J. *Physiology of Reproduction*. Elsevier (2015).

4. Navarro, V. M. *et al.* The integrated hypothalamic tachykinin-kisspeptin system as a central coordinator for reproduction. *Endocrinology* **156**, 627–637 (2015).

5. De Croft, S., Boehm, U. & Herbison, A. E. Neurokinin B activates arcuate kisspeptin neurons through multiple tachykinin receptors in the male mouse. *Endocrinology* **154**, 2750–2760 (2013).

6. Manfredi-Lozano, M., Roa, J. & Tena-Sempere, M. Connecting metabolism and gonadal function: Novel central neuropeptide pathways involved in the metabolic control of puberty and fertility. *Front Neuroendocrinol* **48**, 37–49 (2018).

7. Vazquez, M. J. *et al.* SIRT1 mediates obesity and nutrient-dependent perturbation of pubertal timing by epigenetically controlling Kiss1 expression. *Nat Commun* **9**, 1–15 (2018).

8. Talbi, R. & Navarro, V. M. Novel insights into the metabolic action of Kiss1 neurons. *Endocr Connect* **9**, R124–R133 (2020).

9. Vazquez, M. J., Velasco, I. & Tena-Sempere, M. Novel mechanisms for the metabolic control of puberty: implications for pubertal alterations in early-onset obesity and malnutrition. *J Endocrinol* **242**, R51–R65 (2019).

10. Castellano, J. M. *et al.* Early Metabolic Programming of Puberty Onset: Impact of Changes in Postnatal Feeding and Rearing Conditions on the Timing of Puberty and Development of the Hypothalamic Kisspeptin System. *Endocrinology* **152**, 3396–3408 (2011).

11. Ruiz-Pino, F. *et al.* Environmentally Relevant Perinatal Exposures to Bisphenol A Disrupt Postnatal Kiss1/NKB Neuronal Maturation and Puberty Onset in Female Mice. *Environ Health Perspect* **127** (10), 107011 (2019).

12. Castellano, J. M. *et al.* Changes in Hypothalamic KiSS-1 System and Restoration of Pubertal Activation of the Reproductive Axis by Kisspeptin in Undernutrition. *Endocrinology* **146**, 3917–3925 (2005).

13. Boden, M. J. & Kennaway, D. J. Circadian rhythms and reproduction. *Reproduction* **132**, 379–392 (2006).

14. Herbison, A. E. The Gonadotropin-Releasing Hormone Pulse Generator. *Endocrinology* **159**, 3723–3736 (2018).

15. Smith, J. T., Clifton, D. K. & Steiner, R. A. Regulation of the neuroendocrine reproductive axis by kisspeptin-GPR54 signaling. *Reproduction* **131**, 623–630 (2006).

16. Sánchez-Garrido, M. A. *et al.* Obesity-induced hypogonadism in the male: Premature reproductive neuroendocrine senescence and contribution of Kiss1-mediated mechanisms. *Endocrinology* **155**, 1067–1079 (2014).

17. George, J. T., Veldhuis, J. D., Tena-Sempere, M., Millar, R. P. & Anderson, R. A. Exploring the pathophysiology of hypogonadism in men with type 2 diabetes: kisspeptin-10 stimulates serum testosterone and LH secretion in men with type 2 diabetes and mild biochemical hypogonadism. *Clin Endocrinol* **79**, 100–104 (2013).

18. Messina, A. *et al.* A microRNA switch regulates the rise in hypothalamic GnRH production before puberty. *Nat Neurosci* **19**, 835–844 (2016).

19. Sangiao-Alvarellos, S. *et al.* Testicular expression of the Lin28/let-7 system: Hormonal regulation and changes during postnatal maturation and after manipulations of puberty. *Sci Rep 2015* ***5***, 15683 (2015).

20. Sangiao-Alvarellos, S. *et al.* Changes in hypothalamic expression of the Lin28/let-7 system and related microRNAs during postnatal maturation and after experimental manipulations of puberty. *Endocrinology* **154**, 942–955 (2013).

21. Roa, J. *et al.* Dicer ablation in Kiss1 neurons impairs puberty and fertility preferentially in female mice. *Nat Commun* **13**, 4663 (2022).

22. Romero-Ruiz, A. *et al.* Deregulation of miR-324/KISS1/kisspeptin in early ectopic pregnancy: mechanistic findings with clinical and diagnostic implications. *Am J Obstet Gynecol* **220** (5), 480.e1–480.e17 (2019).

23. Harter, C. J. L., Kavanagh, G. S. & Smith, J. T. The role of kisspeptin neurons in reproduction and metabolism. *J Endocrinol* **238**, R173–R183 (2018).

24. Roux, N. De *et al.* Hypogonadotropic hypogonadism due to loss of function of the KiSS1-derived peptide receptor GPR54. *Proc Natl Acad Sci U S A* **100**, 10972 -10976 (2003).

25. Seminara, S. B. *et al.* The GPR54 gene as a regulator of puberty. *N Engl J Med* **349**, 1614–1627 (2003).

26. Pampillo, M. *et al.* Regulation of GPR54 signaling by GRK2 and β-arrestin. *Mol Endocrinol* **23**, 2060–2074 (2009).

27. Evron, T., Daigle, T. L. & Caron, M. G. GRK2: multiple roles beyond G protein-coupled receptor desensitization. *Trends Pharmacol Sci* **33**, 154–164 (2012).

28. Ciccarelli, M., Cipolletta, E. & Iaccarino, G. GRK2 at the Control Shaft of Cellular Metabolism. *Curr Pharm Des* **18**, 121–127 (2012).

29. Cipolletta, E. *et al.* Antidiabetic and Cardioprotective Effects of Pharmacological Inhibition of GRK2 in db/db Mice. *Int J Mol Sci* **20** (6), 1492 (2019).

Resumen

1. Introducción

La función reproductora está determinada por el correcto funcionamiento del eje hipotálamo-hipofiso-gonadal (HHG), donde una compleja red de factores centrales, periféricos y externos determinan el balance hormonal necesario para la adquisición de la capacidad reproductora y, en consecuencia, para el mantenimiento de las especies [1–3]. De este modo, se ha documentado que una multitud de factores centrales (GABA, glutamato, NKB, NPY) [4–7], periféricos (leptina, insulina o ghrelina) [8,9] y externos (disruptores endocrinos, aporte energético, ritmos circadianos) [10–13] convergen (actuando directa o indirectamente) en las neuronas Kiss1 hipotalámicas como principal núcleo del eje HHG [14] y cuyo producto, las kisspeptinas, transmitirán información a la neurona GnRH, por medio de su receptor canónico, GPR54[15] , activando la pubertad y la función reproductora. Al mismo tiempo, existen evidencias sobre la afectación de la función reproductora como consecuencia del desequilibrio homeostático presente en situaciones como la subnutrición o la obesidad, diabetes mellitus tipo 2 o síndrome metabólico, que se encuentran vinculadas a numerosos desórdenes, incluyendo alteraciones de la edad de pubertad, el hipogonadismo central (principalmente masculino) y la enfermedad cardiovascular [16,17].

Datos recientes señalan que los microRNAs (miRNAs) son elementos implicados en la correcta transición puberal [18–21], aunque existen pocos estudios dirigidos a evaluar al papel de los miRNAs en la regulación específica de la expresión de *Kiss1,* a nivel central[19,22]. Además, la desregulación de determinados miRNAs en condiciones de hipogonadismo central, su impacto sobre el sistema Kiss1 y su implicación fisiopatológica en esta condición, permanecen inexplorados. En paralelo, el sistema Kiss1/GPR54 es un elemento clave en la integración del estado energético y la capacidad reproductora[23], estando descrito que mutaciones inactivantes en *GPR54* son una causa subyacente en determinados casos de hipogonadismo hipogonadotropo [24,25]. La quinasa de receptor acoplado a proteína G (GRK2) [26] está reconocida como un regulador pleiotrópico de la señalización celular [27–29] y ha sido demostrada su capacidad para regular GPR54, *in vitro* [26]. En cualquier caso, no existen estudios relacionados con su potencial implicación en la correcta maduración puberal y en el mantenimiento de la capacidad reproductora *in vivo*.

En base a lo anterior, esta Tesis Doctoral ha abordado, como objetivos principales, (i) el estudio del papel específico de microRNAs en la regulación puberal a través de la regulación del sistema Kiss1; (ii) el papel fisiopatológico de los microRNAs en el hipogonadismo central inducido por obesidad (HIO) y sus potenciales implicaciones terapéuticas; (iii) el papel de GRK2 en el control

de la puberal y el eje HHG mediante la regulación de GPR54 en condiciones control y de estrés nutricional; y (iv) la implicación de GRK2 en HIO a través de la regulación de GPR54.

2. Contenido de la investigación

Esta Tesis Doctoral se ha dividido en cuatro grandes partes. Entre ellas, la parte 1 y 2 están enfocadas al estudio del papel ejercido por microRNAs específicos en la regulación epigenética de *Kiss1* durante la entrada en pubertad, así como en condiciones de hipogonadismo masculino central inducido por obesidad. Ambas partes partieron de un análisis *in silico* común, que estableció el inicio de los subsiguientes estudios experimentales, y fueron amparadas por ensayos *in vitro* confirmatorios, que documentaron que miR-137-3p y miR-325-3p son reguladores específicos del sistema Kiss1, así como por una amplia base de estudios *in vivo* en diversos modelos. De manera relevante, ambos miRNAs presentan la misma región semilla de unión a la región 3'UTR de *Kiss1*, están altamente conservados en la evolución y son sensibles a estrés nutricional.

La **parte 1** de la Tesis se inició con análisis de expresión de tejido hipotalámico en modelos animales (ratas Wistar hembra), a lo largo del desarrollo ontogénico normal y en condiciones de pubertad alterada debido a subnutrición neonatal (camadas de 20 crías por madre), subnutrición peripuberal (reducción de un 30% del aporte energético respecto a los controles) o modificación del ambiente esteroideo. Con relación al desarrollo ontogénico postnatal, observamos un aumento paulatino en los niveles de miR-137-3p y miR-325-3p, particularmente desde el estadío infantil al puberal, que incrementaron de forma paralela al aumento en los niveles hipotalámicos de kisspeptina. De manera complementaria, también observamos un acusado incremento en los niveles de miR-137-3p/miR-325-3p en nuestros modelos de pubertad alterada, los cuales están asociados al retraso en la maduración puberal. Ante estos resultados, la evaluación de ambos miRNAs en el desarrollo puberal se abordó mediante dos estrategias complementarias: el empleo de miméticos de los miRNAs y el empleo de bloqueadores específicos, que evitan la represión ejercida por miR-137-3p y miR-325-3p endógenos, sobre *Kiss1*. De este modo, los miméticos de los miRNAs indujeron retraso puberal, mientras que el bloqueo selectivo de la actividad represora de estos miRNAs sobre Kiss1 provocó un adelanto de la maduración puberal.

En la **parte 2** de esta Tesis, abordamos el papel funcional de miR-137-3p y miR-325-3p en condiciones de HIO utilizando un modelo animal adecuado. En primer lugar, nuestro modelo preclínico de hipogonadismo central mostró niveles hipotalámicos de miR-137-3p y miR-325-3p significativamente aumentados en el núcleo arcuato hipotalámico respecto al grupo control. A su vez, mostraron un patrón de expresión opuesto al observado en los niveles de kisspeptina.

Como prueba de concepto, empleamos miméticos del miR-137-3p en ratas macho jóvenes adultas, donde observamos la reducción significativa de los niveles de kisspeptina hipotalámica inducida por el mimético. A continuación, el tratamiento de un modelo preclínico de HIO con el bloqueante o represor de la interacción represiva entre miR-137-3p/miR-325-3p y *Kiss1* indujo mejoras cardio-metabólicas y reproductivas vinculadas a la inhibición de la actividad endógena de ambos miRNAs. Comparativamente, los tratamientos realizados en paralelo con kisspeptina o testosterona no fueron capaces de normalizar dichos parámetros. Adicionalmente, la sobreexpresión específica de miR-137-3p en neuronas Kiss1 hipotalámicas de ratón indujo un incremento del peso corporal, disminución de los niveles de LH, así como caída de los niveles de kisspeptina en neuronas Kiss1 aisladas.

En la **parte 3** de esta Tesis, evaluamos la capacidad reguladora de GRK2 sobre GPR54, mediante ensayos *in vitro* e *in vivo*. La aproximación *in vitro* reveló el papel represor de GRK2 ante la respuesta a la estimulación aguda de kisspeptina en presencia del inhibidor de GRK2, β-ARK-1-I. La respuesta a kisspeptina se vio igualmente incrementada *in vivo* en ratas hembra previamente tratadas con β-ARK-1-I, así como en ratones cuyas neuronas GnRH presentaban una ablación específica de GRK2. El análisis de expresión hipotalámica durante el desarrollo ontogénico normal mostró un aumento progresivo en los niveles de GRK2 desde el nacimiento hasta la pubertad, que se vio incrementado aún más en modelos de pubertad alterada debido subnutrición postnatal o restricción calórica. Más allá de todo ello, nuestro estudio ha evidenciado el adelanto puberal sufrido tras el bloqueo farmacológico de GRK2, en línea con el adelanto puberal observado en el modelo de ablación congénita de GRK2 en neuronas GnRH de ratón, el cual mostró un patrón de secreción de LH y maduración ovárica alterados, así como, la normalización de la entrada en pubertad ante condiciones de estrés nutricional.

Finalmente, en la **parte 4** de esta Tesis, exploramos el papel de GRK2 en el HIO. En primer lugar, analizamos el aumento de la respuesta central frente a la administración repetida de kisspeptina en ratas macho adultas pre-tratadas con β-ARK-1-I, donde observamos el papel relevante de GRK2 en la modulación de la respuesta a kisspeptina. A continuación, evaluamos la expresión de los niveles de GRK2 en nuestro modelo de HIO, donde sorprendentemente hallamos una significativa caída en sus niveles a nivel hipotalámico. A pesar de ello, tanto el bloqueo farmacológico como la ablación congénita de GRK2 (en este último caso, selectivamente en neuronas GnRH) indujeron una mejora del perfil reproductivo en los modelos de HIO. Por su parte, el bloqueo farmacológico de GRK2 fue capaz al mismo tiempo de provocar una mejora cardio-metabólica en el grupo hipogonadal, mucho más marcada que la causada por la ablación selectiva de GRK2 en neuronas GnRH.

3. Conclusiones

Las principales conclusiones de esta Tesis Doctoral son las siguientes:

1. Los microRNAs, miR-137-3p y miR-325-3p, los cuales se encuentran conservados evolutivamente y comparten la misma región semilla, se postulan como potenciales reguladores de la pubertad, vía represión de Kiss1, como se demuestra mediante los análisis de expresión y funcionales en ratas hembra. Este mecanismo podría contribuir a la regulación puberal en condiciones de estrés nutricional y, en base a la exploración preliminar de bases de datos clínicas, podría igualmente operar en humanos.
2. Los microRNAs, miR-137-3p y miR-325-3p, están involucrados en la patogénesis del HIO, como potente señal represora de la expresión hipotalámica de *Kiss1* en condiciones de obesidad. La prevención de la acción represora de miR-137-3p/miR-325-3p sobre Kiss1 mejora, además de los parámetros reproductivos, los marcadores metabólicos, cardiovasculares e inflamatorios, sobrepasando los efectos del tratamiento farmacológico con Kp-10 o testosterona en el modelo de obesidad en rata.
3. GRK2, actuando a través de la neurona GnRH, ejerce su acción represora en la señalización kisspeptidérgica mediante modulación de GPR54; este fenómeno jugaría un papel relevante en el control de la pubertad en ratas, contribuyendo a la inhibición de la pubertad en condiciones de subnutrición temprana.
4. La señalización vía GRK2, mediada al menos parcialmente a través de la neurona GnRH, contribuye a la supresión central del eje hipotálamo-hipofiso-gonadal en condiciones de obesidad, contribuyendo a la manifestación de las alteraciones cardio-metabólicas ligadas a esta patología.

En conjunto, los resultados de esta Tesis Doctoral nos permiten establecer la siguiente conclusión global.

5. La nueva interacción reguladora, establecida entre miR-137-3p/miR-325-3p y *Kiss1*, y la acción inhibitoria de GRK2 sobre GPR54 en la neurona GnRH, juegan un papel primordial en la regulación de la temporalización puberal y en su modulación por señales metabólicas, especialmente en condiciones de déficit energético, contribuyendo igualmente a las manifestaciones reproductivas y metabólicas del HIO. Estas vías poseen un claro interés fisiológico y sientan las bases para el establecimiento de nuevas dianas en el manejo personalizado de desórdenes reproductivos y metabólicos prevalentes, desde las alteraciones puberales a la infertilidad y obesidad en la edad adulta.

Bibliografía

1. Avendaño, M. S., Vazquez, M. J. & Tena-Sempere, M. Disentangling puberty: novel neuroendocrine pathways and mechanisms for the control of mammalian puberty. *Hum Reprod Update* **23**, 737–763 (2017).

2. Sobrino, V., Avendaño, M. S., Perdices-López, C., Jimenez-Puyer, M. & Tena-Sempere, M. Kisspeptins and the neuroendocrine control of reproduction: Recent progress and new frontiers in kisspeptin research. *Front Neuroendocrinol* **65**, 100977 (2022).

3. Plant, T. M. & Zeleznik, A. J. *Physiology of Reproduction*. Elsevier (2015).

4. Navarro, V. M. *et al.* The integrated hypothalamic tachykinin-kisspeptin system as a central coordinator for reproduction. *Endocrinology* **156**, 627–637 (2015).

5. De Croft, S., Boehm, U. & Herbison, A. E. Neurokinin B activates arcuate kisspeptin neurons through multiple tachykinin receptors in the male mouse. *Endocrinology* **154**, 2750–2760 (2013).

6. Manfredi-Lozano, M., Roa, J. & Tena-Sempere, M. Connecting metabolism and gonadal function: Novel central neuropeptide pathways involved in the metabolic control of puberty and fertility. *Front Neuroendocrinol* **48**, 37–49 (2018).

7. Vazquez, M. J. *et al.* SIRT1 mediates obesity and nutrient-dependent perturbation of pubertal timing by epigenetically controlling Kiss1 expression. *Nat Commun* **9**, 1–15 (2018).

8. Talbi, R. & Navarro, V. M. Novel insights into the metabolic action of Kiss1 neurons. *Endocr Connect* **9**, R124–R133 (2020).

9. Vazquez, M. J., Velasco, I. & Tena-Sempere, M. Novel mechanisms for the metabolic control of puberty: implications for pubertal alterations in early-onset obesity and malnutrition. *J Endocrinol* **242**, R51–R65 (2019).

10. Castellano, J. M. *et al.* Early Metabolic Programming of Puberty Onset: Impact of Changes in Postnatal Feeding and Rearing Conditions on the Timing of Puberty and Development of the Hypothalamic Kisspeptin System. *Endocrinology* **152**, 3396–3408 (2011).

11. Ruiz-Pino, F. *et al.* Environmentally Relevant Perinatal Exposures to Bisphenol A Disrupt Postnatal Kiss1/NKB Neuronal Maturation and Puberty Onset in Female Mice. *Environ Health Perspect* **127** (10), 107011 (2019).

12. Castellano, J. M. *et al.* Changes in Hypothalamic KiSS-1 System and Restoration of Pubertal Activation of the Reproductive Axis by Kisspeptin in Undernutrition. *Endocrinology* **146**, 3917–3925 (2005).

13. Boden, M. J. & Kennaway, D. J. Circadian rhythms and reproduction. *Reproduction* **132**, 379–392 (2006).

14. Herbison, A. E. The Gonadotropin-Releasing Hormone Pulse Generator. *Endocrinology* **159**, 3723–3736 (2018).

15. Smith, J. T., Clifton, D. K. & Steiner, R. A. Regulation of the neuroendocrine reproductive axis by kisspeptin-GPR54 signaling. *Reproduction* **131**, 623–630 (2006).

16. Sánchez-Garrido, M. A. *et al.* Obesity-induced hypogonadism in the male: Premature reproductive neuroendocrine senescence and contribution of Kiss1-mediated mechanisms. *Endocrinology* **155**, 1067–1079 (2014).

17. George, J. T., Veldhuis, J. D., Tena-Sempere, M., Millar, R. P. & Anderson, R. A. Exploring the pathophysiology of hypogonadism in men with type 2 diabetes: kisspeptin-10 stimulates serum testosterone and LH secretion in men with type 2 diabetes and mild biochemical hypogonadism. *Clin Endocrinol* **79**, 100–104 (2013).

18. Messina, A. *et al.* A microRNA switch regulates the rise in hypothalamic GnRH production before puberty. *Nat Neurosci* **19**, 835–844 (2016).

19. Sangiao-Alvarellos, S. *et al.* Testicular expression of the Lin28/let-7 system: Hormonal regulation and changes during postnatal maturation and after manipulations of puberty. *Sci Rep 2015* ***5***, 15683 (2015).

20. Sangiao-Alvarellos, S. *et al.* Changes in hypothalamic expression of the Lin28/let-7 system and related microRNAs during postnatal maturation and after experimental manipulations of puberty. *Endocrinology* **154**, 942–955 (2013).

21. Roa, J. *et al.* Dicer ablation in Kiss1 neurons impairs puberty and fertility preferentially in female mice. *Nat Commun* **13**, 4663 (2022).

22. Romero-Ruiz, A. *et al.* Deregulation of miR-324/KISS1/kisspeptin in early ectopic pregnancy: mechanistic findings with clinical and diagnostic implications. *Am J Obstet Gynecol* **220** (5), 480.e1–480.e17 (2019).

23. Harter, C. J. L., Kavanagh, G. S. & Smith, J. T. The role of kisspeptin neurons in reproduction and metabolism. *J Endocrinol* **238**, R173–R183 (2018).

24. Roux, N. De *et al.* Hypogonadotropic hypogonadism due to loss of function of the KiSS1-derived peptide receptor GPR54. *Proc Natl Acad Sci U S A* **100**, 10972 -10976 (2003).

25. Seminara, S. B. *et al.* The GPR54 gene as a regulator of puberty. *N Engl J Med* **349**, 1614–1627 (2003).

26. Pampillo, M. *et al.* Regulation of GPR54 signaling by GRK2 and β-arrestin. *Mol Endocrinol* **23**, 2060–2074 (2009).

27. Evron, T., Daigle, T. L. & Caron, M. G. GRK2: multiple roles beyond G protein-coupled receptor desensitization. *Trends Pharmacol Sci* **33**, 154–164 (2012).

28. Ciccarelli, M., Cipolletta, E. & Iaccarino, G. GRK2 at the Control Shaft of Cellular Metabolism. *Curr Pharm Des* **18**, 121–127 (2012).

29. Cipolletta, E. *et al.* Antidiabetic and Cardioprotective Effects of Pharmacological Inhibition of GRK2 in db/db Mice. *Int J Mol Sci* **20** (6), 1492 (2019).

Abbreviations

ABP: Androgen binding protein
ADH: Antidiuretic hormone
AGO: Argonaute
AgRP: Agouti-related protein
AH: Anterior hypothalamic nucleus
AK: Adenylate kinase
AKT: Protein kinase B
AMPK: AMP-activated protein kinase
ANS: Autonomous nervous system
AP-2α: Activator protein-2alpha
AR: Androgen receptors
ARC: Arcuate nucleus
AUC: Area under the curve
AVP: Arginine vasopressin
AVPV: Anteroventral periventricular area
BPS: Balano-preputial separation
CART: Cocaine and amphetamine regulated transcript
CD: Control diet
CNS: Central nervous system
CNV: Copy number variant
CPP: Central precocious puberty
CUX1-p200: CCAAT displacement protein 1 -p200
DAG: Diacylglycerol
DHEA: Dehydroepiandrosterone
DHEAS: DHEA sulfate
DHT: Dihydrotestosterone
DMEM: Dulbecco's modified Eagle's medium
DMH: Dorsomedial nucleus
DNMT: DNA methylase
Dyn: Dynorphin
E2: Estradiol
EB: β- estradiol 3-benzoate
ELISA: Enzyme-Linked Immunosorbent Sandwich
ER: Estrogen receptor
f: Fornix
FACS: Fluorescence Activated Cell Sorting
FI: Food intake
FSH: Follicle-stimulating hormone
FSHR: Follicle stimulating hormone receptor
Fw: Forward
GABA: g-aminobutyric acid
gc: Genome copies
gDNA: Genomic DNA
GH: Growth hormone
GHSR: Ghrelin receptor
Gluc: Gaussia luciferase
GnIH: Avian gonadotropin inhibitory hormone
GnRH: Gonadotropin-releasing hormone
GnRHR: Gonadotropin releasing hormone receptor
GPCR: G protein-coupled receptor
GRK: G protein-coupled receptor kinases
GTT: Glucose tolerance test
GWAS: Genome-wide association
hCG: Chorionic gonadotropin hormone
HFD: High fat diet
HPG: Hypothalamic-Pituitary-Gonadal
i.p.: Intraperitoneal
icv: Intracerebroventricular
IGF-1: Insulin growing factor 1
IHC: Immunohistochemistry
iHH: Idiopathic hypogonadotropic hypogonadism
INF: Infantile
IP3: 1,4,5-triphospahte
IRS: Insulin receptor substrate
ITT: Insulin tolerance test
IU: International units
JUV: Juvenil
KHS: Krebs-Henseleit solution
KOR: K-receptor
Kp: Kisspeptin
LEPR: Leptin receptor
LH: Luteinizing hormone
LHA: Lateral hypothalamic area
LHR: Luteinizing hormone receptor
LHRH: Luteinizing hormone-releasing hormone
LL: Large litter
LM: Lateral mammillary nucleus
LNA: Locked nucleic acid
lncRNAs: Long noncoding RNAs
LRR: Leucine-rich repeat
MBH: Mediobasal hypothalamus
MC3R: Melanocortin receptor 3
MC4R: Melanocortin receptor 4
miRNAs: MicroRNAs
MKRN3: Makorin RING-fingerprotein-3
MPO: Medial preoptic area

MRA: Mesenteric resistance artery
MS: Median eminence
mTOR: Mammalian target of rapamycin
ncRNA: Non-coding RNA
NEO: Neonatal
NKA: Neurokinin A
NKB: Neurokinin B
NL: Normal litter
NN: Normonutrition
NO: Nitric oxide
NPY: Neuropeptide Y
OC: Optic chiasm
OIH: Obesity-induced hypogonadism
OPD: O-phenylenediamine
PACAP: Pituitary adenylate cyclase-activating polypeptide
PBS: Phosphate buffer saline
PcG: Polycomb group
PCR: Polymerase chain reaction
PeF: Perifornical nucleus
PeP: Posterior periventricular
PePO: Preoptic periventricular
PFA: Paraformaldehyde
PFA: Perifornical area
PGCs: Primordial germ cells
PH: Pleckstrin homology
PHA: Posterior hypothalamic area
Phe: Phenylephrine
PIP2: Phosphatidyl inositol diphosphate
piRNAs: PIWI-interacting RNAs
PIWI: P-element induced wimpy testis
PK: Protein kinase
PK: Protein kinase
PKC: Protein kinase C
PLC: Phospholipase C
PMD: Dorsal premammillary nucleus
PMV: Ventral premammillary nucleus
PND: Postnatal day
POA: Preoptic area
Pol II: RNA-polymerase II
POMC: Pro-opiomelanocortin
PR-A: Progesterone A
PR-B: Progesterone B
PUB: Peripubertal
PVDF: Polyvylidene difluoride
PVN: Paraventricular nucleus
QMR: Quantitative magnetic resonance
qPCR: Quantitative PCR
Rev: Reverse
RFI: Relative fluorescence units
RFRP-3: RFamide-related peptide-3
RGS: Regulator of G protein signaling
RH: N-terminal RGS homology
RISC: RNA induced silencing complex
ROI: Region of interest
RP3V: Rostral periventricular area of the third ventricle
RT: Retrotranscription
RT: Room temperature
s.c.: Subcutaneously
SBP: Systolic blood pressure
SCN: Suprachiasmatic nucleus
SE: Synchronization episodes
shRNAs: Short-hairpin RNAs
siRNAs: Small interferent RNAs
SIRT1: Sirtuin 1
SL: Small litter
SNP: Single nucleotide polymorphism
SO: Supraoptic nucleus
SOR: Shortest overlapping region
Sp1: Specificity protein 1
SST: Somatostatin
StAR: Steroidogenic acute regulatory
stRNAs: Small temporal RNA
SuM: Supra-mammillary nucleus
T: Testosterone
TF: Transcription factor
TP: Testosterone propionate
Trx: Trithorax group
TSB: Target site blockers
TSH: Thyroid-stimulating hormone
TTF1: Thyroid Transcription Factor 1
UN: Undernutrition post-weaning
VEH: Vehicle
VMH: Ventromedial nucleus
VO: Vaginal opening
WB: Western blot
YY1: Ying-Yang
ZFN: Zinc finger domains

Introduction

Introduction

Reproduction is a vital function for the perpetuation and evolution of species, which is acquired at puberty. Therefore, pubertal maturation and timing are exquisitely controlled and pubertal alterations can result in perturbations in reproductive capacity. Puberty is defined as the period in which sexual and somatic maturation is completed, leading to the acquisition of full reproductive function. In this context, recent evidence has documented alterations in pubertal timing, especially in girls, which are seemingly associated with increased risk of: 1) behavioral disorders, 2) development of certain types of cancer, and 3) occurrence of metabolic syndrome, characterized among other features by cardiovascular diseases, the latter being the main causes of death and morbidity in developed countries [1,2]. Among the factors involved in the generation of these pubertal perturbations, metabolic alterations, such as childhood obesity/overweight and anorexia, are thought to play a prominent role [3,4]. This tight connection with the metabolic status is based on the fact that reproduction is a costly process in terms of energy consumption, which requires adequate body energy stores to proceed. Notably, both the increase or deficiency of these energy reserves in early stages of life translates into an advance or delay in the age of puberty [5,6]. Moreover, the persistence of states of energy deficiency or excess in the adult stage can perturb reproductive health, if this metabolic stress is prolonged over time. In particular, persistence of a state of protracted overweight or obesity can lead to central suppression of the hypothalamic-pituitary-gonadal axis, establishing the condition of obesity-induced hypogonadotropic hypogonadism [5,7]. While this metabolic condition can primarily impact on reproductive health, it is also a risk factor that may contribute to the poor prognosis and even mortality of highly prevalent pathologies, such as cardiometabolic diseases, some types of cancer, and recently, COVID-19 [8–10].

1. REPRODUCTION AND THE HYPOTHALAMIC-PITUITARY-GONADAL AXIS

It is well known that the hormonal control of reproduction is directed by the integrated action of signals from the so-called Hypothalamic-Pituitary-Gonadal (HPG) axis, or gonadotropic axis. The understanding of the functional organization of this axis is crucial for the correct interpretation of pubertal and reproductive disorders. Functioning of the HPG axis depends on the pulsatile secretion of gonadotropin-releasing hormone (GnRH), produced by a population of neurons in the hypothalamus, into the portal circulation to stimulate the biosynthesis and release of gonadotropins, luteinizing hormone (LH) and follicle-stimulating hormone (FSH), by the pituitary gland. These gonadotropins induce gonadal maturation, promoting both gametogenesis and gonadal hormone production. In turn, gonadal hormones, of steroidal and protein nature, regulate, via positive and negative feedback mechanisms, their upstream regulators (GnRH, FSH and LH) mentioned above (**Figure 1**).

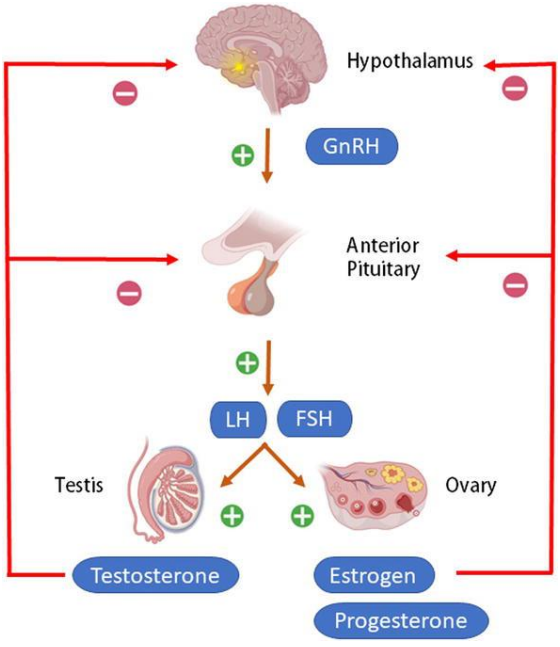

Figure 1. Hypothalamic-pituitary-gonadal axis. *Central and peripheral factors are integrated at the hypothalamic level to promote the secretion of GnRH, which stimulate the synthesis and secretion of gonadotropins (LH and FSH) by the pituitary. Both hormones bind to their receptors in the gonads, inducing the secretion of sex hormones, which regulate this pathway through negative/positive feedback mechanisms on the hypothalamus, modulating the homeostasis of LH and FSH levels. Taken from Gupta et al., 2019.*

1.1. Hypothalamus

The hypothalamus is located inside the brainstem, as part of one of the most developed regions of the central nervous system (CNS), the ventral section of the diencephalon. It integrates the functions of the autonomous nervous system (ANS) and regulates the release of endocrine hormones from the pituitary gland, controlling almost every single bodily function, including

maintenance of body temperature, regulation of food intake and thirst, control of sleep and circadian rhythms, and regulation of reproduction and other multiple endocrine vital functions (e.g., growth and metabolism) [11,12]. It is characterized by a heterogeneous structure, divided into four rostrocaudal regions, with the following coordinates in rodents (**Figure 2**): preoptic (approximately 0.00 to -1.20 mm from the bregma), supraoptic (approximately -1.20 to -2.00 mm from the bregma), tuberal (approximately -2.00 to -3.20 mm from the bregma) and mammillary (approximately -3.20 to -4.50 mm from the bregma) [12]. There are three distinct longitudinal zones in the medial lateral plane (periventricular, medial and lateral), analyzed in the next section.

1.1.1. Hypothalamic nuclei

The hypothalamic nuclei are organized into three medio-lateral areas (**Figure 2**) [13,14]:

- **Periventricular area** is formed by thin nuclei surrounding the third ventricle. They regulate synthesis of endocrine hormones in the anterior pituitary. In this region, the preoptic area (POA) is found. In rodents, inside the POA, there exist relevant nuclei for reproduction, which include the anteroventral periventricular area (AVPV) and surrounding zones, altogether referred as rostral periventricular area of the third ventricle (RP3V) [15]. Also in the periventricular area, the suprachiasmatic nucleus (SCN) regulates mainly circadian rhythms, while the ventromedial nucleus (VMH) and the dorsomedial nucleus (DMH) are involved in food intake and energy balance. Finally, the arcuate nucleus (ARC) is also located in this area and is known to exert control over hormonal secretion from anterior pituitary, influencing also feeding and reproduction.

- **Medial area** is an essential region in the regulation of the autonomous nervous system and other critical bodily functions via the paraventricular nucleus (PVN), which produces oxytocin, and through the supraoptic nucleus (SO), that produces antidiuretic hormone (ADH) or arginine vasopressin (AVP). They are released from neuronal axons into the capillaries of the posterior pituitary and act as hormones and neurotransmitters.

- **Lateral area** is formed by neuronal populations that integrate signaling from the limbic system towards the hypothalamus and mesencephalon and constitute a common pathway for the control of emotion and behavior. The medial area is separated from the lateral area by the fornix, a tract connecting structures from the limbic system. The lateral hypothalamic area (LHA) is also related with feeding behavior and the lateral mammillary bodies are linked to emotion and memory.

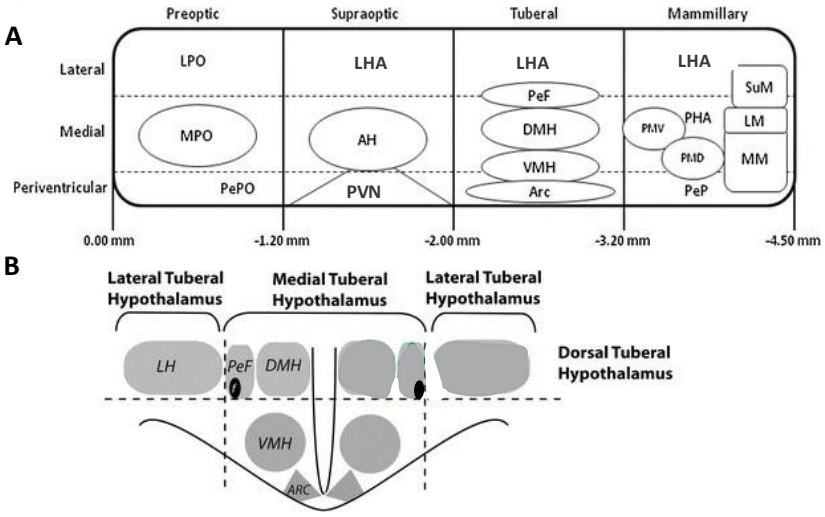

Figure 2. Structure of the hypothalamus. A) *Hypothalamic nuclei organization in four rostrocaudal regions and three mediolateral areas of the hypothalamus. Numbers represent mm from the bregma.* ***B)*** *Simplified scheme of a coronal section of the tuberal region. ARC arcuate nucleus, AH anterior hypothalamic nucleus, DMH dorsomedial nucleus, f fornix, LHA lateral hypothalamus, LM, lateral mammillary nucleus, LPO lateral preoptic area, MM medial mammillary nucleus, MPO medial preoptic nucleus, PVN, paraventricular nucleus, PeF perifornical nucleus, PeP, posterior periventricular, PePO preoptic periventricular nucleus, PHA posterior hypothalamic area, PMD dorsal premammillary nucleus, PMV ventral premammillary nucleus, SuM, supra-mammillary nucleus, VMH ventromedial nucleus. Taken from Marchant et al., 2012.*

1.1.2. Gonadotropin-releasing hormone

GnRH neurons are key in the control of reproduction. In rodents, ruminants and pigs, cell bodies of GnRH neurons are mainly located in the rostral hypothalamic regions, such as the POA and septum [16–19], while in primates, including humans, a considerable number of GnRH neuron cell bodies are located in the mediobasal hypothalamus (MBH). From there, GnRH neurons project their axons to the median eminence (MS) to release GnRH, in the form of highly synchronized pulses, into the pituitary portal circulation to control gonadotropin release [20,21].

GnRH was originally called luteinizing hormone-releasing hormone (LHRH) because it induced greater increases in LH than FSH secretion from the pituitary [22]; actually, the existence of a hypothalamic releasing factor specific for FSH was also postulated, although conclusive evidence for such a factor has not been provided. In fact, it is now recognized that GnRH stimulates the release of both gonadotropins in numerous mammalian species [23]. GnRH was sequenced and characterized in the early 70s by the pioneering work of the groups of Andrew Schally and Roger Guillemin, who described the GnRH decapeptide (pGlu-His-Trp-Ser-Tyr-Gly-Leu-Arg-Pro-Gly·NH2) containing a cyclized proline at the N-terminal and a glycine-amide residue at C-terminal that make it partially resistant to terminal peptidases [24]. There are more than twenty different forms of GnRH across the species, meaning that GnRH functionalization occurred early in evolution. The mammalian functional form is GnRH-I (from here onwards, GnRH), while GnRH-

II (pGlu-His-Trp-Ser-His-Gly-Trp-Tyr-Pro-Gly-NH2) and GnRH-III were first identified in chicken brain and fish, respectively [23].

The biological actions of GnRH are carried out after binding to the GnRH receptor (GnRHR), a surface G protein-coupled receptor (GPCR), whose Gα-subunit is of the q type, activating phospholipase C on its signaling cascade, thereby resulting in a intracellular increase in the levels of Ca^{2+}. *Gnrhr* expression in the pituitary is regulated by GnRH itself and by gonadal steroids, which increase before the preovulatory gonadotropin surge [18].

Appropriate, patterned secretion of GnRH is essential for adequate stimulation of gonadotropin release and therefore for proper gonadal function. This pulsatile pattern of release is the result of the interaction between the intrinsic oscillatory nature of the GnRH neurons and, more importantly, the interplay of a wide range of excitatory and inhibitory afferents that are integrated into the so-called GnRH pulse generator [25]. For further details, see Section 2.3.4.

1.2. Pituitary

The pituitary or hypophyseal gland is a neuroendocrine organ connected to the hypothalamus by the infundibulum or pituitary stalk. It is regulated by releasing factors from the hypothalamus through the portal-hypophyseal circulation. This organ contains two main regions: adenohypophysis and neurohypophysis.

The **neurohypophysis** contains the axons of neurons whose cell bodies reside inside the hypothalamus. Those axons cross the pituitary stalk and release granules containing oxytocin and vasopressin, that operate as neurohormones. Those neurohormones are beyond the study of this thesis.

The **adenohypophysis** is divided into three regions: anterior pituitary gland (*pars distalis*), the *pars tuberalis* and the *pars intermedia*. The anterior pituitary gland constitutes the biggest portion (up to 70%); the *pars tuberalis* is formed by groups of cells surrounding the pituitary stalk; and the *pars intermedia* is a small region of cells between the *pars distalis* and the neurohypophysis that exist in different species but is sparse or absent in the adult human [14]. The adenohypophysis contains several types of endocrine cells controlled by hypothalamic hormones. These include gonadotroph cells, which synthesize and release LH and FSH (gonadotropins); lactotroph cells, which secrete prolactin; somatotroph cells, which produce growth hormone (GH); thyrotroph cells, which synthesize thyroid-stimulating hormone (TSH); and corticotroph cells, which synthesize a precursor protein called pro-opiomelanocortin (POMC) to give rise, by proteolytic cleavage, to various biologically active peptides, including prominently at the level of the pituitary, the adrenocorticotropic hormone (ACTH) [26,27].

1.2.1. Gonadotropins: LH and FSH

LH and FSH belong to the family of glycoprotein hormones, and they are synthesized as heterodimers, composed of two different (α and β) subunits. The α-subunit, which is common for LH, FSH and human chorionic gonadotropin hormone (hCG), as well as TSH, is a 92-amino acid (aa) protein, containing two N-linked glycosylation sites (N52 and N78). Receptor binding specificity is conferred by the β-subunit (LH: 121 aa; hCG: 145 aa; FSH: 111 aa) [28], which contains one (β-LH) or two (β-FSH) glycosylation sites and where a cysteine loop between aa 93 and 100 of the β-subunit participates in the specific interaction with the receptor [29]. While intra-subunit tertiary structure is due to cysteine disulfide bonds, α and β covalent interaction conforms the heterodimer that is also necessary for binding to the receptor. Additionally, glycosylation sites have been reported to affect clearance of the hormones and bioactivity. Differentially glycosylated isoforms have relevance in puberty and the ovarian cycle by influencing downstream signaling after binding to their receptors [28].

Gonadotropins operate via specific surface receptors, the gonadotropin receptors, which are seven transmembrane (7TM) glycoprotein-hormone receptors, with complete ligand specificity for either LH or FSH. They are GPCRs, expressed mainly on the surface of gonadal cells: the LH receptor (LHR) and the FSH receptor (FSHR). In both receptors, the activation of the $G\alpha_s$-subunit activates the classical intracellular signaling, where the adenylyl cyclase enzyme is activated to produce cAMP. In addition, as example of "biased agonism", activation of inositol phosphate/ Ca^{2+}, MAPK, and phosphatidylinositol 3-kinasa/AKT signaling has also been documented upon LHR and FSHR activation. Gonadotropin receptors are characterized, among another GPCRs, by having a long extracellular N-terminal domain (ECD; >320 aa) containing a cysteine-rich domain and several leucine-rich repetitions (LRRs). LRR curve solenoid conformation allows the hormone to be coupled into its inner surface. Those conformations, together with the ECL/7TM domains or "hinge region" are fundamental for the activation of the receptor after hormone binding [28].

In the ovary, the LHR is expressed in theca cells, luteal cells, and interstitial cells, regulating actions such as steroid hormone synthesis, ovulation and *corpus luteum* formation. In the testis, the LHR is expressed in Leydig cells where its activation stimulates testosterone (T) synthesis [30]. On the other hand, the FSHR is expressed in the ovary, exclusively in granulosa cells. Its activation stimulates the synthesis of ovarian peptide hormones, as inhibins, and contributes to follicular development. In addition, FSH induces aromatase expression and thus modulates ovarian estrogen synthesis. In the testis, the FSHR is expressed in Sertoli cells, it being essential

for proper proliferation of this cell population during critical developmental windows and stimulation of the synthesis of protein hormones, such as the androgen-binding protein (ABP)[30].

1.3. Gonads

The reproductive functions of the gonads can be divided into: 1) the production of mature gametes or gametogenesis, and 2) the synthesis and release of hormones of protein or steroid nature (hormonogenesis). Gonadal hormones, in turn, regulate the production of gametes, the growth of the internal and external genital, and the expression of secondary sexual characteristics [26].

1.3.1. Ovary and the ovarian cycle

Ovarian follicles inside the stroma of the ovaries are responsible of female hormonal secretion and mandatory for proper development of the female gamete, the ovum. During human embryonic development, in the 7th week of gestation, primordial germ cells (PGCs) migrate from the yolk sac endoderm to the gonadal crest and synchronize their entry into mitotic divisions. Mitotically active PGCs (oogonia) continue mitotic proliferation until the 5th month of gestation, when the oogonia enter meiosis and become primary oocytes. The primary oocytes constitute primordial follicles as they become individually enclosed by pre-granulosa cells, separated from adjacent stroma by the basal lamina. Then, oocytes begin meiosis and remain arrested in the diplotene stage of prophase I until puberty onset [31,32]. These primordial follicles are the origin of the ovarian reserve (**Figure 3**). After birth, primordial follicles become primary follicles, which exhibit the cuboidal granulose cells responsible of the constitution of the pellucid membrane between them and the oocyte. Ultimately, oocyte-containing follicles arrested in prophase I of meiosis undergo one of three options: 1) they experience atresia, 2) they lie dormant, or 3) they are recruited for growth. From puberty onwards, numerous primary follicles are recruited to enter the growth phase and to conclude the first meiotic division, when they become secondary oocytes [33]. At this stage, when the external layer encircling the granulosa cells is formed (internal thecal layer), and granulose cells proliferate and initiate the production of estrogens, secondary follicles are constituted. Only some of them develop enough monthly to become tertiary or Graaf follicles, where aqueous material, from granulosa cells, conforms the antral cavity and where a theca external layer is formed surrounding the follicle. Here, the oocyte conforms the cumulus oophorus, with the oocyte surrounded by a layer of granulose cells (*corona radiata*) that occupies an eccentric position. This Graaf follicle will break to liberate the oocyte and the *corona radiata* in the process called ovulation **(Figure 3)**. Follicular residues in the ovary will

transform into *corpus luteum*, responsible of hormonal secretion during the luteal phase, mainly progesterone and estradiol. Each menstrual cycle, the non-dominant antral follicles become atretic and break down to nourish the dominant follicle, which will ovulate [33,34].

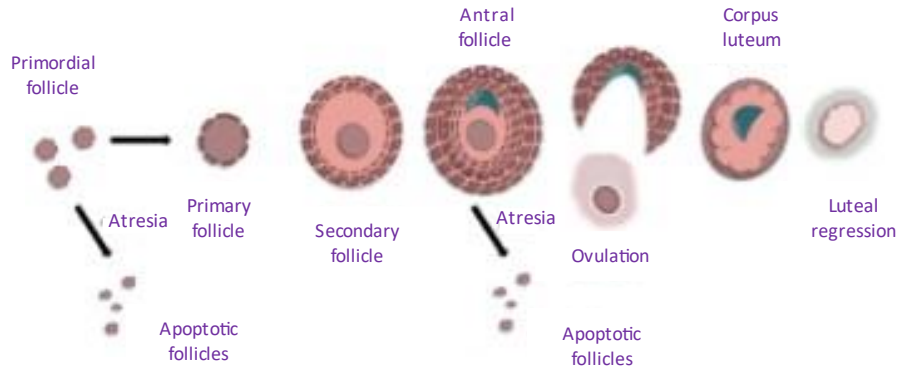

***Figure 3. Stages of follicle development**. After ovulation, the corpus luteum produces progesterone and some estradiol, and will degenerate into corpus albicans, if no fertilization occurs, ultimately leading to degradation. Taken from Park et al., 2021.*

Estradiol (E2) and progesterone, steroid hormones derived from cholesterol, are involved in the regulation of folliculogenesis and ovulation in the ovary. Gonadal steroid production is mainly confined to granulosa cells, theca cells and corpus luteum. The most important and potent estrogen secreted by the ovary is 17β-estradiol (commonly known as estradiol), although small amounts of estrone are also secreted. Although estrone does not play a relevant role during the ovarian cycle, it becomes the dominant estrogen after the menopause, since the levels of estradiol and progesterone become undetectable when their synthesis ceases with the establishment of menopause [26,34].

In primates including humans, ovarian and menstrual cycle are intimately linked. In these species, menstrual cycle last for 28 days and has three phases: proliferative, secretory or luteal, and menstrual phase. Ovulation occurs before the luteal phase. Hormonal levels, ovarian and menstrual cycle are depicted in **Figure 4**. In the case of non-primate mammals, including rodents studied in this thesis, the estrous cycle is analogous to the menstrual cycle. The main difference with the menstrual cycle is that the endometrium of non-primate mammals is reabsorbed and reorganized during the cycle, and hence there are no menses [35]. In **Figure 4**, human menstrual cycle and rodent estrous cycle are compared.

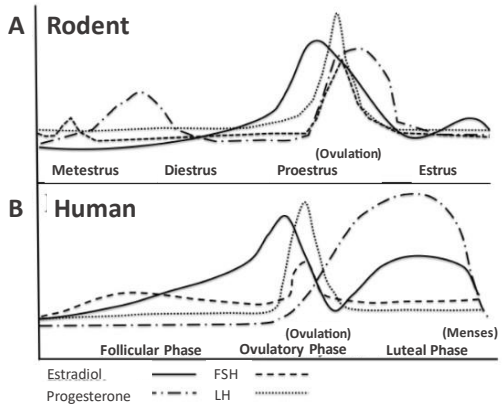

Figure 4. *Estrous and menstrual cycle comparison between rodent and humans.* ***A)*** *The rodent estrous cycle is organized into four phases, that last for 4 days in rat and for 4-5 days in mice. Proestrus is the shortest when critical levels of 17b-estradiol trigger LH surge and induce ovulation. In estrus, LH, FSH and progesterone decline to basal levels. An increase in the concentration of progesterone and some estradiol secretion from the corpus luteum occur after ovulation, between metestrus and diestrus. B) Human menstrual cycle. Taken from Koebele & Bimonte-Nelson, 2016.*

1.3.2. Testis and spermatogenesis

The capacity to produce functional gametes in the male is a dynamic process in which spermatogonia become mature spermatozoa. This process occurs inside the testis, continuously during reproductive lifetime of the male individual [36].

The mammalian testis has two basic compartments. The interstitial (aka, intertubular) compartment is highly vascularized and contains the Leydig cells around the vessels. Leydig cells are sensible to LH and are responsible for testosterone production. Testosterone accumulates in the second compartment, the seminiferous tubules, which contains Sertoli cells and developing germ cells that will undergo spermatogenesis, stimulated by T [36]. Sertoli cells provide cellular support to germ cells and are stimulated by FSH, promoting their proliferation and inducing the synthesis of numerous proteins (such as ABP, activins and inhibins) that participate in the regulation of spermatogenesis and the synthesis of FSH itself [37].

Spermatogenesis has common features in multiple species and can be divided in three phases. The initial phase or spermatocytogenesis is the proliferative stage, where stem spermatogonia divide through mitosis into new stem cells or differentiating spermatogonia. The latter undergo successive divisions, begin meiosis and become preleptotene spermatocytes. The attainment of first meiosis leads to the primary spermatocyte (2n), that is divided into two secondary spermatocytes (1n) to complete the second meiotic division. Then, secondary spermatocytes produce two immature haploid (1n) gametes, the spermatids. Last, the spermiogenic phase involves morphological and functional changes of the spermatids, which will become mature spermatozoa [36].

1.3.2.1. Steroidogenesis

The synthesis of all steroid hormones starts from cholesterol reservoirs in intracellular lipid droplets. In Leydig cells, it is synthesized *de novo* from acetyl-CoA, or taken from circulation by receptor-mediated endocytosis. Cholesterol is transferred to the inner membrane of the mitochondria, where the steroidogenic acute regulatory (StAR) protein is the limiting factor [36]. Main steps of steroid synthesis are depicted in **Figure 5**. The human testis synthesizes 6-7 mg of testosterone daily, as well as other steroid hormones, which act as weaker androgens or are metabolized in peripheral organs. In circulation, only about 2% of testosterone travels free. Mainly, it is bound to the SHBG in humans (44%), albumin and other proteins [36]

In the early 40's, Talbot described the increase of adrenal androgens in the peri-pubertal period or adrenarche; the contribution of such phenomenon to gonadarche or pubertal growth spurt remained unclear [38]. The adrenal gland produces a wide range of steroids, including dehydroepiandrosterone (DHEA), DHEA sulfate (DHEAS), androstenedione (A4), androstenediol or 11b-hydroxyandrostene-dione (11OHA), all of them mainly produced in this organ and named adrenal androgens. Although they have reduced androgenic activity, they are able to be transformed into testosterone or estradiol in peripheral tissues. In this sense, the adrenal gland contributes around 1% to the total testosterone concentration in males. Those adrenal androgens are employed to determine adrenal contribution to androgen excess diseases [39]

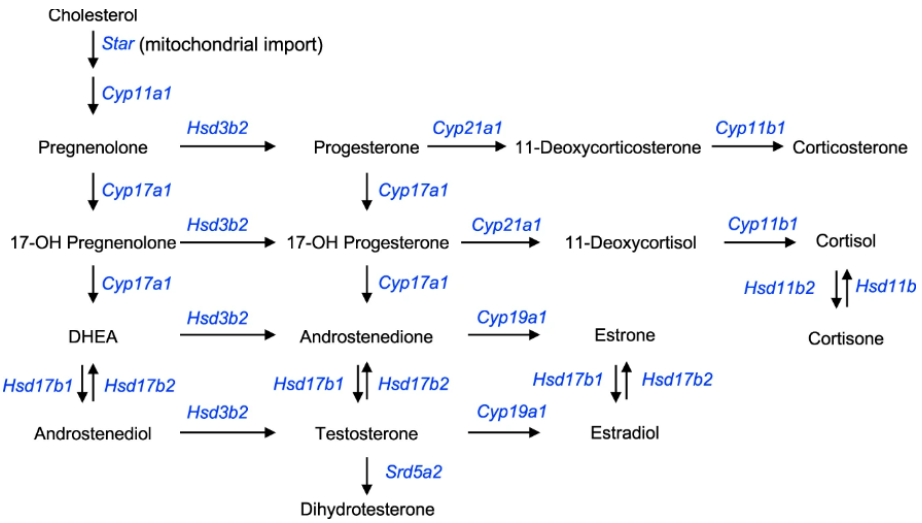

Figure 5. Steroidogenesis. *Inside the mitochondria, cholesterol is converted to pregnenolone by the CYP11A1. CYP17A1 enzyme catalyzes the hydroxylation of progesterone to generate 17α-hydroxyprogesterone, followed by the cleavage of the C17-C20 bond to form androstenedione. The enzyme, HSD17B3, catalyzes the conversion of androstenedione into testosterone using NADPH as a cofactor. Cyp19a1 or aromatase can convert testosterone into estradiol. Taken from Martin & Touaibia, 2020.*

1.3.2.2. Androgen metabolism

More than 95% of circulating T proceeds from the testis after puberty, while the remaining percentage comes from extragonadal conversion of precursors with minimal androgenic potency, that mainly originate in the adrenal cortex.

Testosterone can be directed into one of four major pathways and only a small portion of T becomes active, through conversion into two bioactive metabolites: estradiol and dihydro-testosterone (DHT) (**Figure 6**). Around 5-10% of circulating T is disposed in the amplification pathway, where it is converted into DHT by the 5α-reductase enzyme, that is expressed in tissues as the liver, kidney, skin, brain or prostate. Therefore, the androgenic effect of T in target peripheral tissues requires its metabolization to DHT. However, the actions of T at the level of the CNS are carried out mainly after aromatization to estradiol once T is disposed into the diversification pathway, which is mainly governed by the enzyme aromatase (CYP19). The remainder T suffers inactivation by hepatic metabolism to inactive oxidized and conjugated metabolites, for urinary and biliary excretion [40].

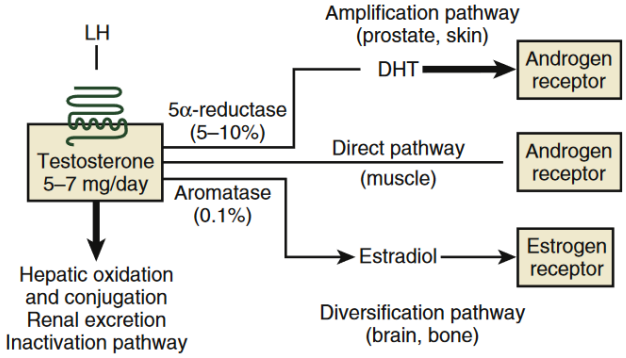

***Figure 6**. Pathways of testosterone action. The main four pathways are presented. The direct pathways is dominant in the skeletal muscle, where T bind to the androgen receptors (AR); amplification pathway occurs in prostate and skin tissues after the conversion of T into DHT in the liver; the diversification pathway is characteristic of brain and bones, where T is converted into estradiol to exert its actions through estrogen receptor (ER); finally, the inactivation pathway takes place mainly in the liver. Taken from Handelsman, 2015.*

2. THE Kiss1/GPR54 SYSTEM: ROLES IN PUBERTY AND MAINTENANCE OF REPRODUCTIVE FUNCTION

Kisspeptin (Kp) was firstly identified in 1996 as a metastasis suppressor, encoded by the gene *KISS1* [41]. It was proposed to induce inhibition of melanoma in human cell cultures and was also designated as metastin. The *KISS1* gene product was later discovered to be able of cleavage into different biologically active peptides: Kp-54, Kp-14, Kp-13 and Kp-10 [42], that were called kisspeptins.

On the other hand, in 1999 the orphan receptor GPR54 was discovered in rat brain tissue [43]. Proof of kisspeptins as natural ligands of GPR4 was obtained in 2001, when it was demonstrated that all kisspeptins efficiently activate this receptor, and that the Kp-10 fragment was sufficient to achieve the maximal activation of GPR54 [44]. There-after, 2003 was the year that brought into light the relevant role of *KISS1* and *GPR54* in the control of reproductive function. Patients with idiopathic hypogonadotropic hypogonadism (iHH) carrying inactivating *GPR54* mutations were identified independently by the groups of De Roux and Seminara [45,46]. This was the first evidence connecting the Kiss1/GPR54 system with reproduction. This finding was reinforced by the observation that mouse models of genetic inactivation of *Gpr54* and *Kiss1* were a complete phenocopy of affected humans [47]. Thus, mice with loss-of -function mutations in *Gpr54* or *Kiss1* were found to display absence of puberty and infertility, while "activating" *GPR54* mutations in humans were associated to precocious puberty [48].

2.1. *Kiss1* gene and kisspeptins

In mammals, kisspeptins are encoded by the *Kiss1* gene. They belong to the RF-amide family of peptides and contain the Arg-Phe-NH_2 C-terminus that confers them strong specificity to bind their receptor. In humans, the *KISS1* gene is in chromosome 1 (1q32) and contains 4 exons. The gene encodes a 145aa precursor with a PEST (proline, glutamic acid, serine, threonine, and aspartic) acid residue-rich sequence, susceptible to ubiquitination that confers Kp a short half-life. As mentioned above, Kp precursor can be cleaved into peptides with different aa size: Kp-54, Kp-14, Kp-13 and Kp-10 (**Figure 7**), all containing the common C-terminal RF-amide motif for high affinity binding to their receptor. While the larger fragments are more variable between species, Kp-10 is well conserved, differing only in one aa between human, rat and mouse species[48].

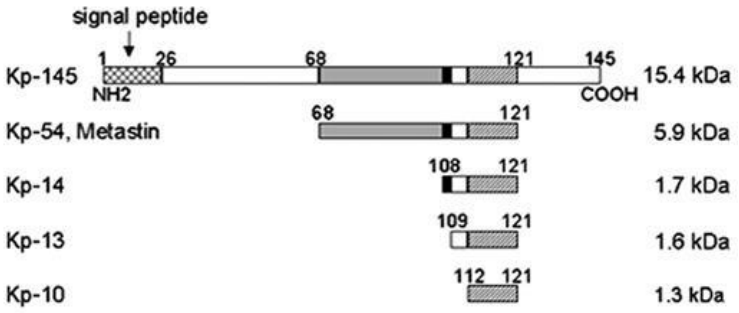

Figure 7. Structure and sequence of kisspeptins*. Human kisspeptin proteolytic cleavage showing kisspeptins and common C-terminal region. Taken from Bilban et al., 2014.*

2.2. The kisspeptin receptor: GPR54

G-protein-coupled receptor, GPR54, is a Gαq/11 coupled 7 transmembrane receptor (7TMR), encoded in humans by a gene in chromosome 19 (p13.3). Structural characterization showed homology (>40%) with the transmembrane regions of galanin receptor [47]. It contains 5 exons and 4 introns, and it is translated into a 398 aa protein and shows a homology close to 80% and 85% with the rat and mouse translated sequence, respectively, that achieves a 100% homology in the transmembrane regions [49].

Upon activation by kisspeptin, GPR54 signaling cascade leads to increasing Ca^{2+} levels inside the GnRH cells [47]. Activation of the receptor induces the dissociation of the Gαq subunit, promoting the activation of phospholipase C (PLC) and leading to phosphatidyl inositol diphosphate (PIP_2) hydrolysis into 1,4,5- triphosphate (IP_3) and diacylglycerol (DAG). DAG activates the PKC pathway, which induces phosphorylation of MAP kinases, such as ERK1/2 and p38. IP_3 mediates mobilization of Ca^{2+} from intracellular stores, resulting in changes in the ion channel permeability and promoting depolarization responses (**Figure 8**) [47,50].

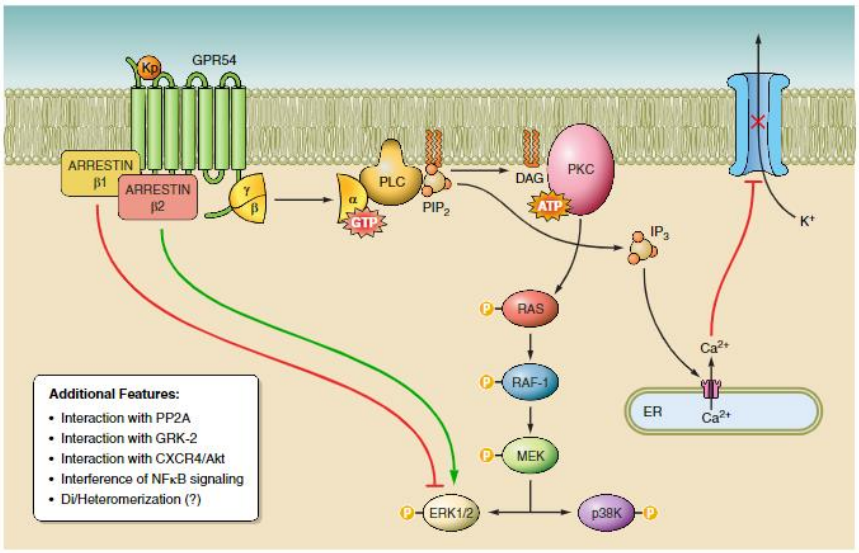

***Figure 8. GPR54 cellular signaling pathways**. Schematic presentation of the major signaling pathways recruited upon GPR54 activation by kisspeptins, including the Gαq/11-dependent pathway leading to calcium release, activation of protein kinase C (PKC) and the phosphorylation of different MAP kinases as ERK1/; and the Gαq/11-independent pathway signaling through β-arrestin-1 and -2 to stimulate the phosphorylation of ERK1/2. Taken from Pinilla et al., 2012.*

The Kiss1/GPR54 signaling function is dependent on cellular context. As indicated above, activation of GPR54 leads to activation of MAPKs, which is linked also to the antimetastatic role of kisspeptins. In the context of this thesis, kisspeptin signaling through GPR54 in the GnRH neuron is intimately related to the signaling cascade driving to the production and release of GnRH.

2.3. The Kiss1/GPR54 system along the lifespan

The Kiss1 system is functional from early life. *Gpr54* is expressed in the MBH of mice from the 13.5 day of embryonic life onwards, as it is the case also for *Kiss1.* Importantly, this period grossly coincides with GnRH neuronal arriving to the MBH. Moreover, kisspeptin increases GnRH neurite growth [51]. Yet, GnRH neuronal migration occurs in the absence of functional kisspeptin signaling. More importantly, the Kiss1 system has been shown to have a paramount influence on multiple aspects of reproductive function, from placentation and gonadal/brain differentiation to reproductive success and even reproductive senescence.

2.3.1. Sites and mechanisms of action

Kiss1/Kisspeptins are expressed in different tissues. Among them, expression in placenta has been claimed to have a role in implantation and trophoblast invasion [52]. Kisspeptins are also expressed in tissues such as pancreas, liver, testis, ovary and small intestine, and can be detectable in plasma. Nevertheless, there is no doubt that the main site of expression and action of *Kiss1*/Kisspeptins is the brain. Kiss1 neurons in the hypothalamus where first identified in the infundibular/ARC nucleus [53], where they are consistently detected across species. Evidence of a second population of hypothalamic Kiss1 neurons is species-specific, it being well defined in rodents [54] while it remains less well-defined in humans [55]. More specifically, this second population resides inside the RP3V region in rodents, and in the analogous POA in other mammals. The primary site of actions of kisspeptins for the control of reproduction takes place at the hypothalamic level, where they are known to control GnRH secretion, as reflected also by the fact that more than 75% of GnRH neurons co-express *Gpr54* [53,56]. In the following paragraphs, we will summarize the implications of the POA/ RP3V and ARC Kiss1 neuronal populations of the hypothalamus in the control of GnRH secretion (**Figure 9**).

POA/R3PV population. Kiss1 population in the RP3V area is especially relevant in female rodents, it being responsible of the control of the pre-ovulatory surge of GnRH, which is governed by the positive feedback exerted by estrogens during the pre-ovulatory phase. The analogous zone in other mammals including ruminants, primates, pigs and musk shrews corresponds to the POA [57]. For the sake of simplicity, rodents R3PV area will be designated as POA along this Thesis.

ARC population (KNDy neurons). Kiss1 neurons in this area highly co-express neurokinin-B (NKB) and dynorphin (Dyn) neuropeptides and were designated as KNDy (Kisspeptin/NKB/ Dynorphin) neurons. This concept was based on the initial findings on the co-expression of NKB and Dyn in the sheep and rat brain [58,59]. Further work demonstrated that majority of Kiss1 cells in the sheep

co-expressed those neuropeptides [60]. While the actual co-expression levels in rodents is not perfectly defined, in humans up to 75% of Kiss1 neuronal cell bodies showed co-expression of NKB, although this percentage may change depending on sex and age [61–64]. KNDy neurons are governed by estrogen levels, which mainly suppress *Kiss1* and *Tac2*, mediating by this way the negative feedback of estrogens over GnRH secretion in mammals [57]. Additionally, calcium events in KNDy neurons are known to be synchronized with pulsatile LH secretion in mice, as a proof of their function as the GnRH pulse generator [25], which will be covered in section 2.3.4.

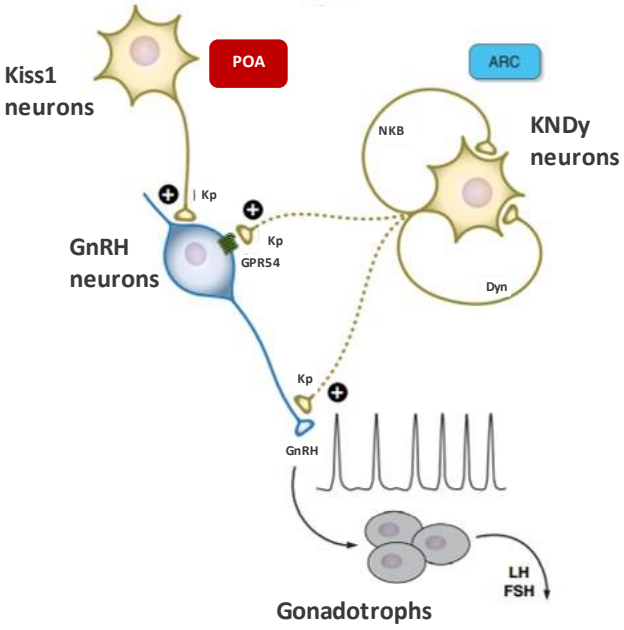

Figure 9. Central control of the HPG axis by the Kiss1 system. *Current scenario of Kiss1 neural networks governing GnRH secretion and thus reproductive function in rodents, where Kiss1 neurons activate pulsatile GnRH secretion by GnRH neurons. Kp, kisspeptins; NKB, Neurokinin B; Dyn, dynorphin; KNDy, Kiss1/NKB/Dyn neuron; ARC, arcuate nucleus; POA, preoptic area. Taken from Pinilla et al., 2012.*

Regarding *Gpr54* expression, it is also detectable in different tissues across the body, such as pancreas, placenta, pituitary, limbic system and especially at the hypothalamus [48,65].

2.3.2. Roles in sex differentiation

Sex differentiation of the brain starts in the utero, when gonadal formation begins, with durable influence later in life. Firstly, chromosomic sex endowment of the embryo determines the differentiation of the bipotential gonad. Then, gonadal secretion occurring between the 2nd and 7th month of embryo development will affect the maturation of internal and external genitalia and, importantly, the male or female CNS development and phenotype [66]. In more detail, according to the aromatization hypothesis, masculinization of the rodent brain is attributed to androgens produced in the developing testis, after central aromatization to estrogens [67]. Additionally, there is evidence that androgen and estrogen secretion during this critical period

influences brain sex differentiation via changes in epigenetic patterns, which for instance seem to contribute to the maintenance of the brain sex differences over time [68].

In this context, the hypothalamus constitutes one recognized region to be rich in estrogen receptors (ER), and thereby subjected to the steroid influence since early stages of development. It has been found that POA in the neonatal male rats expresses lower levels of ERα than females; a difference that persists during adulthood [53]. Importantly, there is also remarkable evidence of the influence of the gonadal hormone milieu during early development of the Kiss1 neuronal populations, especially in the POA region. For example, estrogens promote the development of a population of Kiss1 neurons in the POA that is larger in females rats than in males, while modification of the sex steroid milieu during the neonatal period severely impact the normal development of this population (**Figure 10**) [47].

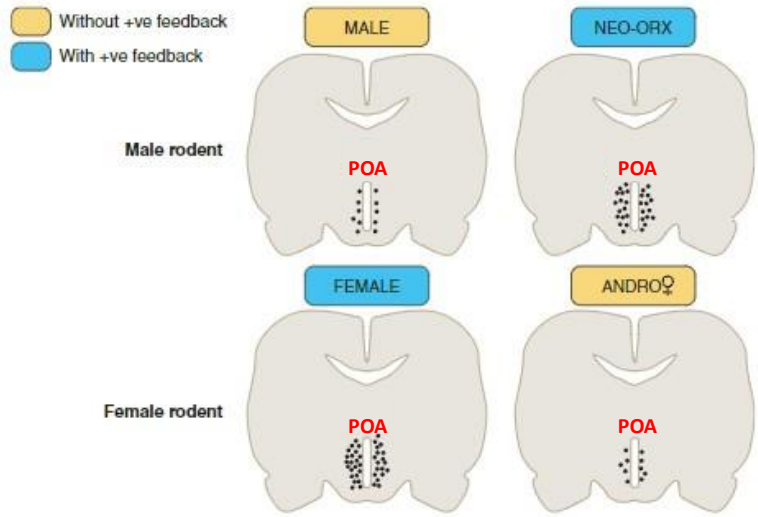

Figure 10. Sexual differentiation of the Kiss1 system in rodents. *Male neonatal orchidectomy enhances Kiss1 expression in the POA, while female neonatal androgenization decreases Kiss1 mRNA levels in the AVPV. Neonatal orchidectomy in males (NEO-ORX); neonatal androgenization in females (ANDRO♀). Blue boxes: presence of positive feedback; yellow boxes: absence of positive feedback. Modified from Pinilla et al., 2012.*

Additionally, "mini-puberty", which is defined by a transient increase of gonadotropin secretion -after birth and before puberty onset-, is present in rodents, monkeys and humans, during comparable windows of postnatal maturation. In humans, LH and FSH secretion increases 1 or 2 weeks after birth, lasting until 6-9 months of age in boys. In girls, LH secretion decreases the same age than in boys, but FSH secretion can be elevated until the 3-4 years of life [69,70], although hormonal patterns appear more complex and variable than in males [71]. Regarding rodents, LH levels peak around PND14 in female mice, [72] while in males, FSH and LH levels peak around PND23 and PND30, respectively. The involvement of the Kiss1 pathway in this phenomenon is yet to be defined [73]. Interestingly, in males, the occurrence of a testosterone surge within hours from birth is shared by several species, ensuring external genitalia masculinization and

suppression of the LH surge mechanism observed in females after puberty onset. Compelling evidence suggests the involvement of a Kiss1-GnRH signaling mechanism as driver of this testosterone surge [74]. After the above-mentioned events, the "juvenile hiatus" begins, it being dependent on gonadal and non-gonadal factors, with difference in magnitude and duration depending on the species.

2.3.3. Roles in puberty

It is well known that pubertal activation requires a progressive increase in GnRH levels secretion from the prepubertal period to puberty onset. The mechanisms controlling this change are likely multiple and seemingly include an increase in kisspeptin release and in the number and signaling efficiency of GPR54 in GnRH neurons [75]. During the prepubertal period, kisspeptin synthesis and release is suppressed in a variable degree between species. In rodent and sheep females, this inhibitory action over *Kiss1* expression appears to be exerted by ovarian estrogens, acting via ERα, with inhibitory effects that decrease across pubertal transition in accordance with the "gonadostat hypothesis"[57,76]. In primates, where the juvenile hiatus in terms of gonadotropin secretion is more pronounced, kisspeptin synthesis and release from KNDy neurons are thought to be suppressed through ϒ-aminobutyric acid (GABA) or via neuropeptide Y (NPY) neurons, as the estrogen-dependent suppression of gonadotropin secretion is manifested just shortly before puberty onset in monkeys [57].

In females, the first ovulation is a landmark of puberty onset. It depends on the first GnRH surge, which has been demonstrated to be gonadal dependent in rodents and primates. Firstly, activation of GnRH pulse generator (reviewed in section 2.3.4) in a gradual manner is necessary for increasing the levels of circulating estradiol that will induce positive feedback in the POA in the form of afternoon mini surges, short before puberty onset (**Figure 11**). In this way, estradiol constitutes one of the core elements of the GnRH surge, while the neuronal trigger is species-specific. The action of estradiol is exerted on the POA Kiss1 neuronal population in rodents and over Kiss1 neurons in the MBH in sheep and primates [77]. Additionally, it has been found that VMH nitric oxide (NO) neurons and rostral Kiss1 neurons also participate in the GnRH surge in sheep [77]. In rodents, NO activity has been shown to be regulated by estrogens in rats [78,79]. Also, recent studies in mice have shown that this regulation is exerted by the interplay between NO containing neurons, which express *Gpr54* in the preoptic region, and Kiss1 neurons. In this sense, it has been demonstrated that NO is needed for kisspeptin dependent preovulatory activation of the GnRH neurons [80]. In any case, full development of the positive feedback in spontaneous ovulatory species allows the whole LH surge linked to ovulation and puberty onset.

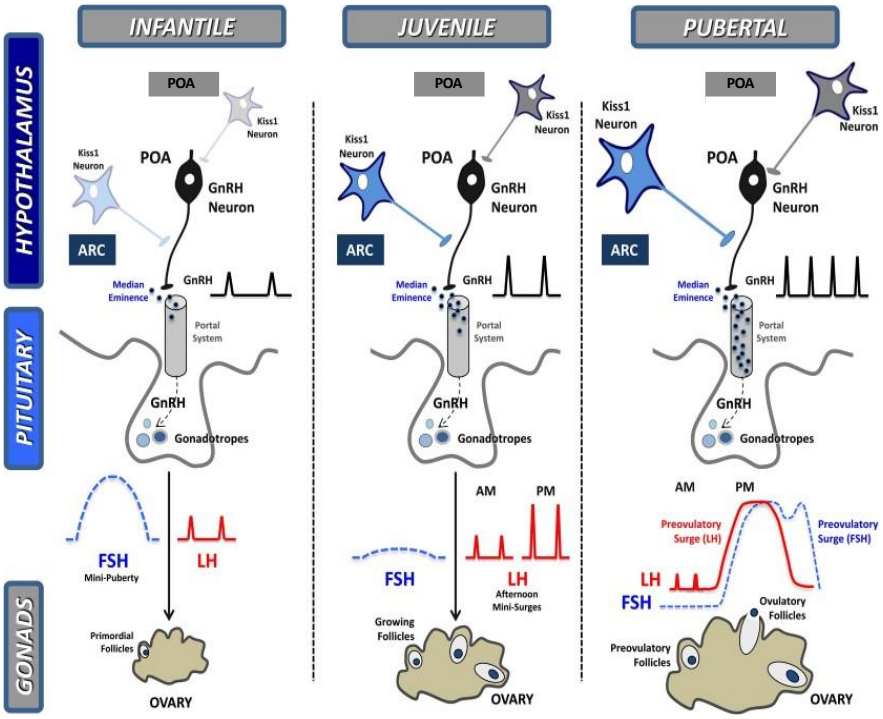

Figure 11. Elements of the HPG axis through the infantile to the pubertal stage. *Changes in GnRH pulsatile secretion, LH and FSH secretory profiles; and maturation of the ovary are depicted. In addition, changes in the Kiss1 neuronal populations are depicted showing the increase expression of Kiss1 and increased number of projections to GnRH neurons, by magnification of the neurons in the scheme. Taken from Avendaño et al., 2017.*

2.3.4. Adult period: GnRH pulse generator

Pulsatile LH release depends on pulsatile GnRH secretion from at least a subpopulation of GnRH neurons that are under the control of a pulse generator, which was initially postulated to be intrinsic and/or extrinsic [81]. Research studies in humans, monkeys, sheep, rats and mice have defined the pattern of LH secretion as a pulse occurring every 45-60 minutes in the diestrus phase in female rodents. This frequency decreases during the luteal/estrous phase. In contrast, pulses in males occurs once every 3 hours approximately [77].

Recent data have proven that the extrinsic "GnRH pulse generator" is mainly composed by the ARC population of KNDy neurons, as documented in mice [25]. This neuronal population has been also postulated to be the GnRH pulse generator in other mammalian species, where KNDy neurons communicate with GnRH neurons mainly at the distal axon close to the median eminence [77]. In this regard, KNDy neurons display an interconnected network capable of synchronization episodes (SEs) preceding an individual pulsatile event. Imaging single-cell resolution in freely behaving mice have provided evidence that the order in which cells depolarizes during these SEs is temporally organized. The experimental recorded data showed that a subpopulation of cells – named "leader" cells- reached the peak amplitude or peaked earlier than the rest, while the mid-time or end-time peaking neurons -named "follower" cells-

did it at this time point in repeated SEs. This information has provided the foundation for considering that the GnRH pulse generation is dictated by the coordinated activation of KNDy neurons in a patterned manner, which seems to be driven by the sequential activation of "leader" and "follower" cells within the KNDy network [27].

Importantly, KNDy neuron function is governed by additional signaling factors, besides NKB and Dyn, which contribute to synchronize GnRH release, while the terminal axon of GnRH neurons in the median eminence also receives further information [77]. A summary of these main regulators of KNDy and Kiss1 POA neurons is presented in the next sections.

3. MAIN NEUROENDOCRINE REGULATORS OF THE Kiss1/GPR54 SYSTEM AND THE HPG AXIS

Given the paramount importance of kisspeptins in the control of puberty and reproductive function, as summarized in the previous chapter, it makes biological sense that multiple signals and mechanisms regulating the HPG axis impinge on the Kiss1 system to convey their modulatory actions. This section focuses on the main central activators and inhibitors, as well as peripheral regulators of the Kiss1 system, as main driver of GnRH expression and release.

3.1. Central regulators of the HPG axis

The reproductive axis is finely modulated by a number of transmitters, of neuronal but also of glial origin, that can regulate directly or indirectly, Kiss1-GnRH neuronal circuits. The most prominent examples of central regulators of the HPG axis are summarized below.

3.1.2. Neurokinin B and tachykinins

The tachykinin family of neuropeptides is composed by substance P (SP), neurokinin A (NKA), and NKB, which bind preferentially to the receptors, NK1R, NK2R, and NK3R, respectively [82].

Regarding NKB, it is encoded by the *TAC3* gene in humans and by *Tac2* in rodents. NKB activates the NK3R in the membrane of the KNDy neurons, which depolarize and increase their action potentials, subsequently leading to kisspeptin release. In rodents, full NKB action needs the activation of the three tachykinin receptors, while in the sheep, NK3R alone seems to be sufficient for complete NKB effects, suggesting that NKB signaling partially varies between species [83]. This notion is supported by the fact that mutations in the gene encoding NK3R in humans result in hypogonadotropic hypogonadism, whereas rodents with pharmacologically or genetically impaired NK3R signaling show only moderate pubertal and reproductive

phenotypes[84]. SP and NKA are both encoded by the tachykinin gene, *Tac1*. SP-expressing neurons are placed mainly in the VMH in rodents and exert stimulatory effect over KNDy neurons, at least in females. Additionally, half of the KNDy neurons express the NK1R [83], that is also found in POA GnRH neurons [85–87]. This evidence points to a role for SP in the central regulation of HPG axis, probably through kisspeptin-dependent mechanisms [87–89]. Regarding NKA, its participation in pubertal timing is exerted through mechanisms independent of NKB, but dependent on sex steroids and kisspeptins [87–91].

3.1.2. Glutamate and γ-aminobutyric acid

The amino acid glutamate, the main excitatory neurotransmitter of the CNS, is released by neurons and glial cells. Glutamatergic pathways are involved in neuronal plasticity, memory and learning, as well as other complex functions. In the reproductive context, glutamate has been considered a key neurotransmitter in the generation of GnRH pulses [92]. Nevertheless, GnRH neurons receive limited glutamate input themselves, while glutamatergic signaling to kisspeptin neurons occurs in an estradiol regulated manner. Thus, estradiol increases glutamatergic transmission to POA Kiss1 neurons in mice, while decreases glutamatergic transmission in KNDy neurons at proestrus, i.e., during estradiol positive feedback. At diestrus, during the estradiol negative feedback, glutamatergic signaling is decreased in the POA Kiss1 neurons and increased in KNDy neurons [93].

On the opposite, γ-aminobutyric acid (GABA) is an amino acid found in high concentrations in the mammalian CNS, which mainly acts as an inhibitory neurotransmitter. During the peripubertal period, GABA exerts its inhibitory role over *Kiss1* expression through $GABA_B$ receptors, as demonstrated in monkeys. Nevertheless, GABA seems to play a conspicuous role as its effects (stimulatory vs. inhibitory) depends on the specific neuronal population and stage of development [94].

3.1.3. Other neuropeptides

Dynorphin (Dyn). Dyn belongs to the family of endogenous opioid neuropeptides and it is expressed in the KNDy neuron population [75]. There, Dyn exerts an inhibitory role over kisspeptin release and likely contributes to the negative feedback effect of progesterone over LH secretion [83]. Dyn acts through the κ-opioid receptor (KOR) [95] that has been detected in KNDy and GnRH neurons. This suggests that the inhibitory effect of Dyn on GnRH secretion can occur directly or indirectly through the inhibition of KNDy neurons [96].

Pituitary adenylate cyclase-activating polypeptide (PACAP). PACAP is a neuropeptide expressed in the hypothalamus, mainly in the ventral premammillary nucleus (PMV) and VMH. In rodents, PACAP increases LH levels in male rats and augments mating frequency in female mice. Further, PACAP neurons from the PVN establish direct contacts with KNDy and POA Kiss1 neurons, which express its receptors [83]. In this sense, elimination of PACAP expression negatively impacts both the number of cycles and their duration in female mice. In addition, the lack of PACAP induces a considerable reduction in the population of KNDy neurons, with an opposite impact on the POA. These effects suggest a fertility-facilitating role for PACAP mediated by Kiss1 neurons [97].

RFRP-3. The RFamide-related peptide-3 (RFRP-3) is the mammalian analog of the avian, gonadotropin inhibitory hormone (GnIH). It suppresses GnRH secretion, although there exists controversy about the nature and magnitude of its inhibitory effects in rodents [83]. In this context, studies in rodents have demonstrated co-expression of RFRP-3 and kisspeptin in the DMH in female rats [98], while adult mice deficient for the RFRP-3 canonical receptor, NPFF1R, showed increased ARC Kiss1 expression [99]. Those data point to an inhibitory function of RFRP-3 over kisspeptin expression.

Somatostatin. Somatostatin (SST) is a neuropeptide that acts as a growth hormone (GH) inhibitory substance. Regarding reproduction, it is a potent inhibitor of GnRH when infused icv in animal models. Indeed, SST neurons are found to be juxtaposed with KNDy neurons on male and female rats, where one third of Kiss1 neurons express the SST receptor, SSRT1 [100]. On the other hand, SST exerts its inhibitory effects during lactation periods in rats via SSTR2, directly through KNDy neurons expressing this receptor subtype or through glutamatergic intermediate neurons [101].

Additional central regulators of the HPG axis include POMC-derived melanocortins, cocaine and amphetamine regulated transcript (CART), NPY or agouti-related protein (AgRP). In the context of this Thesis, these have been reviewed in Section 6, as they hold a prominent role in the metabolic control of reproduction; a topic that will be covered there.

3.2. Peripheral regulators of the HPG axis

The reproductive axis is also precisely regulated by the action of various peripheral signals that interplay, in a coordinated manner, with factors of central origin to modulate the reproductive function.

3.2.1. Gonadal steroids

Sex steroids (androgens, estrogens, and progesterone) are mainly produced in the gonads and participate in the regulation of multiple circuits [102,103]. Most of their actions are mediated through their binding with intranuclear receptors, such as androgen receptor (AR), progesterone A and B receptors (PR-A and PR-B), and ERα and ERβ; yet, a fraction of sex steroid actions are carried out by their interplay with ion channels and surface receptors coupled to G proteins[102,104]. The ERs are widely distributed in the CNS and the pituitary gland, and prominently present in the ARC, where they are involved in the control of reproductive function and energy homeostasis [102,104,105].

Androgens and estrogens mediate the negative feedback effect on LH and FSH secretion through their interaction with AR and ERs in the ARC. In addition, specifically in females, estrogens participate also in positive feedback loops, involved in the generation of the LH preovulatory surge, through their interaction with ERs in the POA [106,107]. The positive and negative feedback effects of estrogen on LH release are primarily mediated by ERα [107,108]. Intriguingly, the only ER subtype expressed in the GnRH neurons seems to be ERβ, but most of the effects of estrogens on GnRH release are carried out by interneurons that express ERα and ERβ [105,107]. Among these, Kiss1 neurons stand out for a prominent role, as they express ERα. In fact, numerous reports have documented that *Kiss1* expression is modulated by estradiol signaling, with a bipartite mode of action: (i) it is stimulated at the POA, to impinge on the generation of the LH surge, through the positive estrogenic feedback; and (ii) it contributes to the maintenance of the pulsatile LH secretion, through the negative estrogenic feedback operating in the ARC [109–112]. In addition, classical studies in mice, where the juvenile hiatus is gonadal dependent, have demonstrated a differential influence of E2[113] -presumably on *Kiss1* expression- depending on the stage of development [110].

3.2.2. Peripheral metabolic mediators

As mentioned earlier, the reproductive axis is highly sensitive to the metabolic and energetic state of the organism. The different peripheral metabolic factors that will interact with the HPG axis, modulating reproductive capacity, will be described in detail in section 6.2.

4. MOLECULAR MECHANISMS FOR THE REGULATION OF THE Kiss1/GPR54 SYSTEM

4.1. *Kiss1* regulation

As indicated in previous sections, there are plenty of signals impinging on the regulation of *Kiss1* to precisely modulate the reproductive capacity. Further from the hormonal and neuropeptide influences described above, in the next section, we will focus on the transcriptional and epigenetic regulation of *Kiss1.*

4.1.1 Transcriptional regulation

While our knowledge on the transcriptional regulation of *Kiss1* is still uncomplete, substantial progresses in the last two decades has surfaced relevant information regarding the molecular control of *Kiss1* gene expression. In this sense, studies have shown how the 3' downstream region of *Kiss1* constitutes the specific enhancer region of the POA population of Kiss1 neurons, whilst the 5' upstream region has a more prominent role as enhancer region in the ARC Kiss1 neurons. Here, binding of the ERα to the 5' enhancer, that promotes the conformation of a loop between this zone and the promoter of *Kiss1*, exhibits a putative role in the specific regulation of *Kiss1* expression [114].

Additionally, several transcription factor (TF) binding sites have been identified by *in silico* studies [114]. Among them, only the Creb1 coactivator, Crtc1, has been experimentally validated[115]. Additional TFs have been shown to regulate *Kiss1* expression until now. For instance, activator protein-2alpha (AP-2α) and specificity protein 1 (Sp1), have been identified in *in vitro* studies, performed in breast cancer cell lines, as activators of the *Kiss1* promoter. These studies showed that AP2α and Sp-1 interact to form complexes which bind to two Sp1 binding sites of the *Kiss1* promoter [116]. Also, studies on the human *KISS1* gene have demonstrated that Thyroid Transcription Factor 1 (TTF1) and CCAAT displacement protein 1-p200 (CUX1-p200) are activators of the *Kiss1* promoter, that on the contrary, is repressed by the Enhanced at puberty 1 (EAP1), Ying-Yang (YY1), and CUX1-p110 TFs [117]. As mentioned, Crtc1 TF has been demonstrated to regulate the promoter activity of *Kiss1*, together with Tbx3 in mice[118]. Finally, one recent study performed in mice demonstrated the sex-specific, transcriptional regulatory role of the member of the helix-loop-helix (bHLH) TF, Nhlh2, over *Kiss1* expression. This study showed that Nhlh2 regulates *Kiss1* and *Tac2* expression, with a discernible role in the metabolic control of reproduction and puberty onset, specifically in male mice [119]. Finally, RNAseq transcriptomic analysis of Kiss1 cells from female mice have identified up to ten E2-

dependent TFs in the POA, which are not predicted to interact with the ERα; and seventy E2-dependent in the ARC nucleus, of which eight of them are predicted to bind to the ERα [111]

4.1.2. Epigenetic regulation

Epigenetics address the study of modifications in DNA that lead to changes in gene expression without alteration of the underlying DNA sequence [120]. This regulation can be conducted via histone modification (the most prominent being acetylation/deacetylation and methylation), DNA methylation and via non-coding RNA (ncRNA) regulation. Epigenetics spans from fertilization, fetal development and imprinting of the parental genomes necessary for the normal embryonic development, to the time of puberty onset and beyond [84]. In this section, we will briefly recapitulate the major mechanisms of histone modification and DNA methylation as major contributors in epigenetic regulatory mechanisms. Note that, due to its particular importance for this Thesis, ncRNAs regulation, focused on microRNAs (miRNAs), will be described independently in a later section (see Section 5).

Polycomb group and related factors. The polycomb group (PcG), as repressors, and the Trithorax group (Trx), as activators, are linked to the epigenetic regulation of multiple genes, including *Kiss1* expression [121]. In addition, DNA methylation is bound to gene repression, it being mediated by DNA methyl-transferase 1 (DNMT1), DNMT3 and DNMT3b. In Kiss1 neurons, methylation in the promoter of *Eed* and *Cbx7* genes, both members of the PcG, occurs during the pubertal transition [122]. As consequence, EED and CBX7 levels decrease and are thus displaced from the regulated genes, inducing an open conformational state in chromatin by reducing levels of H3K9me and H3K27me, which dominate in silenced genes [121,122]. At the same time, transcription activators signaling also occurs through the trimethylation of H3 at lysine 4 (H3k4me3), a mark of active transcription which is mediated by the Trx group [122].

SIRT1. In addition, sirtuin 1 (SIRT1) deacetylase suppresses *Kiss1* expression through interaction with the PcG, inducing a switch in local chromatin conformation from a permissive to a repressive state, e.g., in conditions of energy deprivation linked to pubertal delay [123]. This switch is promoted by deacetylation of markers of gene activation (H3K16 and H3K9ac) and promotion of methylation of H3K9me3, a modification related with gene silencing [122].More detailed information about SIRT1 influence on reproduction and energetic sensing will be provided in Section 6.3.

Mkrn3/Imprinting. As a conspicuous example of epigenetic regulation, the maternally imprinted *MKRN3/Mkrn3* gene plays a prominent role in pubertal control. Genetic imprinting modulates gene expression through epigenetic modifications of chromatin structure, depending

on methylation of the genes. The protein, makorin RING-fingerprotein-3 (MKRN3), is similar to IRF2BPL, another protein with a RING finger domain implicated in the onset of puberty [124]. In humans, primates and experimental animals, MKRN3 has been suggested to repress *Kiss1* and *Tac2* promoter activity in KNDy neurons. Thus, the drop of Mkrn3 levels observed preceding puberty has been suggested to contribute to inducing puberty onset [125,126]. Indeed, mutations in the gene encoding *MKR3* are the main genetic cause of central precocious puberty (CPP) in humans [127] and it has been reported that *Mkrn3* acts as a repressor of puberty onset in mice, under the co-regulation of microRNA, miR-30 [128]. While the repressive effect of MKRN3 over *Kiss1* expression has been suggested to play a role in pubertal control [129], regulation over GnRH pulsatile release seems to be mediated, at least partially, through the E3 ubiquitin ligase activity of Mkrn3 [127].

GATAD1. *GataD1* and *Znf573*, two genes with Zinc finger domains (ZFN), display decreased expression in the hypothalamus of peripubertal female monkeys; a phenomenon that is associated with an increase in *Kiss1* levels. Conversely, its overexpression in the rat hypothalamus delays puberty onset as consequence of repression over *Kiss1*. These data strongly suggest that the regulatory protein, GATAD1, directly represses *Kiss1* promoter through recruitment of histone demethylase, KDM1A, which induces demethylation of the activating mark, H3K4me2. Eviction of the GATAD1/KDM1A complex from the *Kiss1* promoter during pubertal transition allows activation of *Kiss1* transcription and puberty onset [122,130]. The translational relevance of this mechanism in humans is supported by the findings of genome-wide association studies (GWAS) showing that single nucleotide polymorphisms (SNPs) located near some ZNF genes are linked to an earlier age of menarche [131,132].

4.2. GRK2 regulation of GPR54 signaling

Because of the relevance for this Thesis, attention will be paid to the regulation of GPR54, the canonical receptor for kisspeptins in GnRH neurons, mainly through the action of GRK2, which was historically designed as β-ARK-1 [133] and is encoded by the *Adrbk1* gene.

GRKs, arrestins and regulation of GPCRs. In mammals, G protein-coupled receptor kinases (GRKs) are a group of 7 serin/threonine protein kinases (PK). They belong to the family of AGC kinases (as PKA, PKB and PKC), which present a catalytic domain characterized by a bilobular fold of the protein [134]. By recognition and phosphorylation of GPCRs, GRKs in one side and β-arrestins in another are central players in the switching off of GPCRS, by homologous desensitization and internalization of the agonist-occupied receptor. This mechanism has been widely recognized in the regulation of adrenergic receptors [135,136]. Specifically, agonist activation

of the GPCRs induces a conformational change in the receptor which allows binding of GRKs. GRKs phosphorylate residues in the intracellular loop and C-terminal regions provoking high-affinity binding of the cytosolic proteins β-arrestins to GPCRs. In this way, further interaction between GPCRs and G-proteins is prevented, leading to desensitization of the receptor[133]. Arrestins participate in clathrin-mediated endocytosis of GPCRs, which decrease in number in the cell membrane to be recycled and re-sensitized. Additionally, β-arrestins act as scaffolds able to recruit signaling intermediates to the receptor complex, such as c-Src, JnK-3, Raf/MEK/ERK signaling components, PDE4 phosphodiesterase or ubiquitin ligase, Mdm2 [137]. Therefore, participation of GRKs is essential to modulate important intracellular signaling of GPCRs (**Figure 12**).

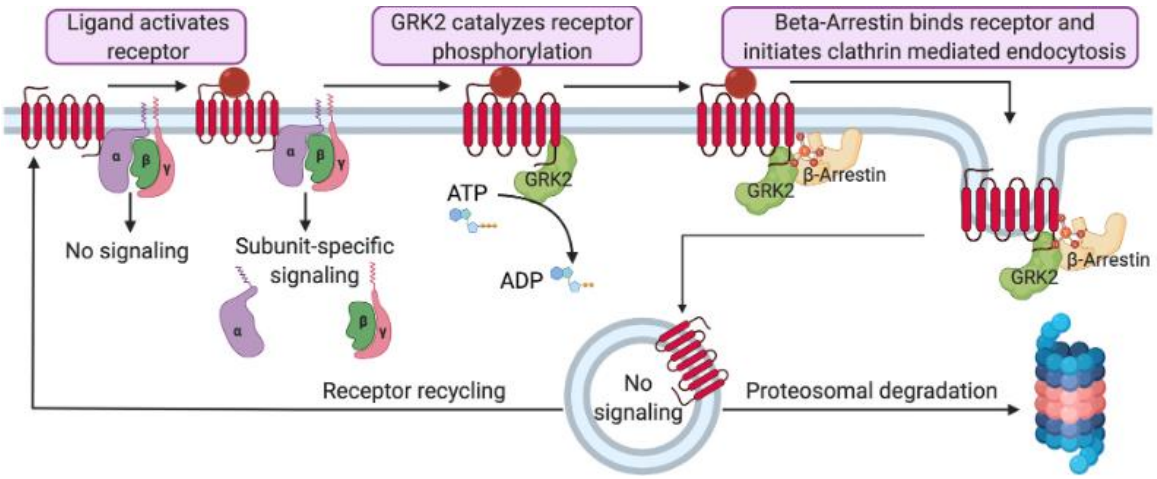

Figure 12. GRK2 regulation of GPCRs. *After activation of the GPCR by their ligand, GRK2-mediated desensitization and trafficking of GPCRs by phosphorylation of the receptor mediated by GRKs. Additionally, GRK phosphorylation promotes β-arrestin binding, which causes G-protein uncoupling. Taken from Zhai et al., 2022.*

GRK members are divided in three main groups:

- Rhodopsin-kinase or visual GRKs family (GRK1 and GRK7), mainly located in the retina.
- Kinase β-adrenergic family (GRK2 and GRK3), ubiquitously expressed in mammalian tissues.
- GRK4 family (GRK4, GRK5 and GRK6).

All of them contain the same functional domains. These include a N-terminal region, necessary for receptor recognition, next to the N-terminal RGS (regulator of G protein signaling) homology (RH) domain, that associates with the G_α protein subunit; a central and conserved catalytic domain; and the C-terminal region that confers them ability to bind to the plasma membrane[138].

In the context of this doctoral thesis, due to its pleiotropic nature and the documented regulation of GPR54 by GRK2, we will focus on the description of the features of this kinase.

GRK2 structure. The GRK2 RH domain interacts with the $G_{\alpha q/11}$ subunit, thus blocking its interaction with their effectors (see **figure 8** for further details) [134]. Anchorage to membrane phospholipids and to $G_{\beta\gamma}$ subunits is mediated by the C-terminal pleckstrin homology (PH) domain, common to GRK2 and GRK3 [134]. Binding of the PH to the $G_{\beta\gamma}$ mediates translocation of the cytosolic GRK2 to the membrane and eases regulation of active GPCR [133]. This property of the PH domain has been exploited by using the C-terminal peptide (β-ARKct) to interfere with GRK2 mediated desensitization [133]. Additionally, GRK2 contains several residues subjected to phosphorylation by different kinases (PKA, PKC ERK, s-SCr, RKTs), which impacts the kinase catalytic activity of GRK2, substrate selection, as well as docking of GRK2 to specific subcellular localizations (Penela et al., 2019). In contrast to AGC kinases, which become active by phosphorylation in regulatory hydrophobic motifs placed at the kinase domain, GRK2 transition from inactive to active conformation requires conformational induced arrangement (**Figure 13**). Those conformational changes are based on interactions between the N-helix, the RH and the PH domains, the agonist-occupied GPCR, the $G_{\beta\gamma}$ subunits, and PIP2 [134].

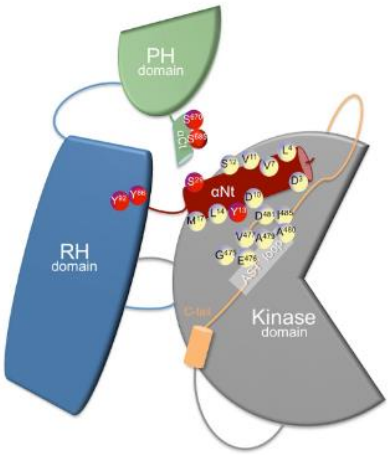

Figure 13. Domains of GRK2. *The N-terminal RGS (regulator of G protein signaling) homology (RH) domain (in blue), the bilobular central kinase domain (gray), and the C-terminal pleckstrin homology (PH) domain (green). The RH domain contacts the kinase and PH domains. The RH domain–PH domain interface allows a possible route for allosteric communication. Binding of diverse molecules (proteins, phospholipids) to PH and RH or posttranslational modifications (phosphorylation sites denoted in red) may affect the interface between RH and kinase lobes, and thus GRK2 catalytic activity. Taken from Penela et al., 2019.*

GRK2 and cell metabolism. Because of its predominant expression in heart tissue, most studies have been performed mainly in the cardiovascular system. Nevertheless, GRK2 expression and regulation have been studied also in other tissues [139]. Besides adrenergic receptor desensitization and phosphorylation of GPCRs, GRKs are able to inactivate non-GPCR receptors and to interact with different cytosolic intermediates of cell homeostasis. In particular, GRK2 navigates between the cellular compartments, being capable of regulating ATP production inside the mitochondria and mitochondrial biogenesis depending on the metabolic state of the

cell [140]. Additionally, obesity and type 2 diabetes lead to overexpression of GRK2 in tissues, such as liver or adipose tissue [134,139], especially in males [141], and insulin itself up-regulates GRK2 and promotes its association with the insulin adaptor protein 1 (IRS1), which becomes phosphorylated and consequently degraded, leading to impairment of the insulin signaling pathway [140]. In addition to regulate insulin signaling, it has been suggested that estrogens modulate Grk2 mRNA expression and protein stability, acting likely via ERα or ERβ. Reciprocally, GRK2 might influence estrogen action in specific cell types by modulating ERα or ERβ [141,142]. GRK2 has also been described to interact with β-tubulin in brain tissue, or with HDAC6 in fibroblasts and epithelial cells, showing its role in the modulation of cytoskeletal function [143,144]. Otherwise, GRK2 binds to the heat shock protein 90, which promotes its translocation to the mitochondria and alters oxidative stress and metabolism in cardiac myocytes under stress conditions [145]. Finally, S-nytrosylation of GRK2 has also been described in cardiac tissue, as an additional modulatory mechanism of the GRK2 activity [146].

GRK2 and GPR54. As previously stated, GRK2 is known to regulate the activity of different GPCR and non-GPCR intermediates in various tissues. Among them, *in vitro* evidence suggests GRK2 mediated regulation of GPR54 in HEK293 cells, where it has been demonstrated that association of GPR54 with GRK2 and β-arrestins occurs through sequences in the cytoplasmic tail of the receptor and through the second intracellular loop, the later known to mediate GPR54 binding to $G_{\alpha q}$. GRK2 exerts desensitization of the active GPR54 receptor via a phosphorylation-independent mechanism, acting via sequestration of activated $G_{\alpha q/11}$, which switches off the GPR54 activated receptor [136]. Despite this fragmentary knowledge, *in vivo* demonstration of GRK2 relevance for GPR54 signaling is missing and has been undertaken as one of the objectives of this Thesis.

5. MICRORNAS: PLEIOTROPIC EPIGENETIC REGULATORS

5.1. General features of miRNAs

MicroRNAs (MiRNAs) are small, endogenous, single-stranded, non-coding oligonucleotides (~ 22 nucleotides in length) that mainly act as gene repressors by inhibiting translation or by inducing mRNA degradation. They are one out of the three kinds of small RNAs described until date: microRNAs, small interferent RNAs (siRNAs) and the P-element induced wimpy testis (PIWI)-interacting RNAs (piRNAs) [147]. MiRNAs were discovered during the early 90's in the *C. elegans* nematode, where lin-4 became the first identified miRNA after demonstration of its regulatory

role over *lin-14* gene expression [148]. Later, a second regulatory miRNA, namely, let-7, was discovered also in *C. elegans*. Both, lin-4 and let-7 showed imperfect complementarity to conserved regions in the 3'UTRs of different mRNA, leading to the model in which they exert translational repression through antisense interactions [149]. Lin-4 and let-7 were identified to control developmental transitions and were initially named small temporal RNAs (stRNAs). Although it was first believed that miRNAs did not exist beyond nematodes, homologs of let-7 were identified in flies and let-7 itself was detected in humans, *Drosophila* and other bilateral animals [148]. Since then, hundreds (if not thousands) of miRNAs have been discovered across species. Interestingly, miRNA sequence conservation has been documented through evolution. Nevertheless, unlike lin-4 and let-7, most miRNAs appeared to be more related with cell type origin than with temporal expression and thus "miRNA" denomination was preferred and has become consensus nowadays [148].

5.2. Synthesis and mechanism of action

MiRNAs can be intragenic, being submerged in intronic sequences of other host genes, or can be intergenic, occupying their own genes and, in some cases, with particular regulation by their own promoters [150,151]. In this context, canonical miRNAs are transcribed by RNA-polymerase II (Pol II) [148], mainly as intronic clusters inside protein-coding pre-mRNAs. They appear as independent gene units, or can be encoded inside long non-coding RNAs (lncRNAs) [152]. Nevertheless, there also exist non-canonical miRNA genes which bypass some of the catalytic steps of the canonical miRNAs. Among them, we find "mirtrons", which are introns and miRNAs at the same time; the endogenous short-hairpin RNAs (shRNAs), which can be Pol II or Pol III products; and miRNA products of chimeric hairpins, which are transcribed in tandem with or as part of another type of small-RNA (Bartel, 2018). In this Thesis, we will focus on canonical miRNAs, as the most representative and relevant class of small non-coding RNAs.

For those canonical miRNAs, after Pol II transcription, the first step of the synthesis is the conformation of hairpin primary transcripts (pri-miRNA). Specific structural and sequence features recognized by the microprocessor complex in the nucleus are needed. This micro-processor transforms the pri-miRNAs into pre-miRNAs, which are exported to the cytoplasm, to undergo further processing and maturation [153]. Pri-miRNAs features include a stem length of around 33-39 nucleotides and apical loop sizes of 3-23 nucleotides. At the same time, bulges or sequence mismatches are also important for pri-miRNAs identification and processing, as pri-miRNAs are bulge enriched at 5-9 nucleotides from the stem base. The presence of specific motifs, such as the CNNC or the UG motif, is also enriched [153]

Microprocessor is a hetero-trimeric complex conformed by Drosha endonuclease and two DCGR8 molecules. The two RNase III domains of Drosha cut each strand of the pri-miRNA hairpin with an offset of 2bp. Then, the 60 nt stem-loop or pre-miRNA produced is transported to the cytoplasm through the action of exportin-5 and RAN-GTP. At the cytoplasm, it is processed by the endonuclease, Dicer, which does not need protein partners in mammals. The two RNase III domains of Dicer cut both strands close to the loop of the pre-miRNA and allow miRNA duplex generation. MiRNA duplex contains the miRNA or guide strand paired to the passenger strand, the latter being also named "miRNA*" or "miRNA star". The miRNA duplex is loaded into Argonaute (AGO) protein, conforming the pre-RNA induced silencing complex (pre-RISC). Subsequently, the mature RISC complex is formed after extrusion of the miRNA star strand. The mature RISC is able to target mRNAs and exerts it posttranscriptional repression after binding of target miRNAs complementary to their guide (**Figure 14**) [147].

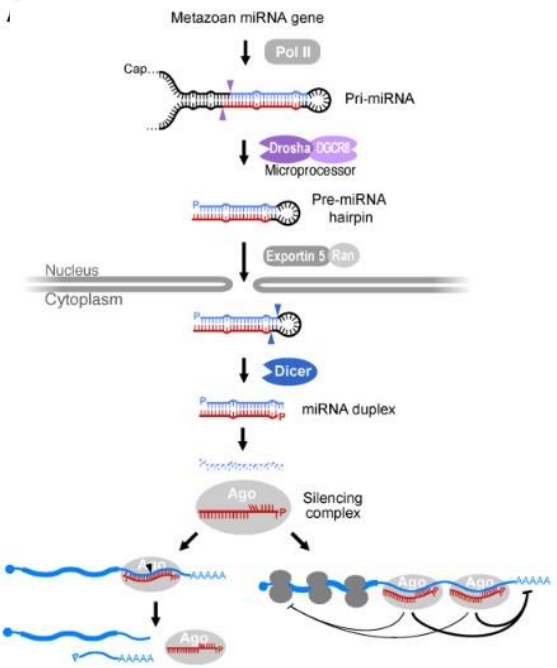

***Figure 14. MicroRNA synthesis and posttranscriptional repression**. Binding of the silencing complex to the target occurs through the interaction with miRNA nucleotides 2-5. MiRNA can induce target cleavage when the pairing extends beyond nucleotide 7-8 (left black arrow), while if it is not, repression of translation occurs. Taken from Bartel et al. 2018.*

Regarding regulation of miRNA expression, Pol II transcribed miRNA are under Pol II transcriptional control, regardless of whether they are processed from introns under regulation of host genes or not. Once transcribed, they are subjected to different regulatory factors. One of the best known is the mechanism by which the protein produced by the targeted mRNA induces oligo(U)-tailing at the 3' end of the pre-miRNAs. This way, oligo(U) blocks Dicer processing and induces pre-miRNA decay through 3'-5' exonucleases. The best-known example is the let-7 decay induced by LIN28. In any case, addition of a single nucleotide can instead enhance miRNA processing in other contexts [149]. Additionally, when miRNAs are part of the silencing complex, their half-live last for days, showing high stability in most cases. However, neuronal miRNAs exhibit some variability in this regard, with some being constitutively unstable, and more susceptible to transcriptional changes (Bartel, 2018).

The mechanisms of action of miRNA may be two-fold, depending on the length of pair-binding with their targets. Binding pair occurs mainly at 3'UTR site of mRNAs, although 5'UTR binding

can also occur. If base-pairing includes the seed region and it extends to the central region, target RNA cleavage is produced [147]. The main mode of action of miRNAs in mammals is, nevertheless, translational repression and mRNA decay. The later involves de-adenylation, decapping and exonucleotic degradation of the target mRNA (**Figure 15**) [147]

Most miRNAs are not uniquely complementary to a single mRNA and, therefore, can simultaneously regulate more than one gene. In addition, different miRNAs can bind to the same target RNA, finely regulating gene expression [154]. This multiplicity of miRNAs and their targets allows the generation of sophisticated regulatory networks that can affect complex biological processes in an integral manner.

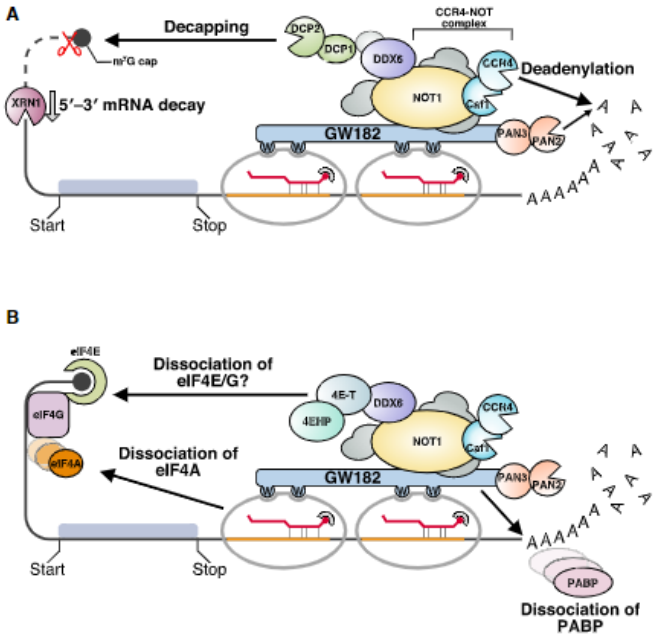

Figure 15. MicroRNA mechanism of action. *In detail, GW182 protein promotes dissociation of the poly(A) binding protein (PABP) from the poly(A) tail in the mRNA.* ***A)*** *Then, two de-adenilatyon complexes are recruited: CCR4-NOT and PAN2-PAN3. CCR4-NOT also induces the recruitment of decapping factors and activators. Taking together, all these actions allow XRN1 5′ to 3′ exoribonuclease to degrade the deadenylated and decapped target mRNA.* ***B)*** *In the other hand, translational repression starts by recruiting translational inhibitors as DDX6, 4E-T or 4HP. Additionally, PABP translational enhancer is dissociated, as well as other factors, e.g., eIF4a. Taken from Iwakawa & Tomari, 2022.*

5.3. Potential roles of miRNAs in reproduction

MiRNAs are implied in the regulation of a wide range of cellular processes, from differentiation to apoptosis, metabolism or reproduction [155]. Their contribution at central level to modulation of normal pubertal development have been suggested in the recent past years. Thus, the let-7 family of miRNAs, the first ones identified in humans, have been shown to participate in the regulation of several endocrine systems, which include the HPG axis. Let-7 family is under the regulation of LIN28, who acts as a post-transcriptional regulator by repressing let-7. At the same time, let-7 itself repress LIN28 expression in a double inhibitory loop. Experiments where LIN28 was overexpressed in mouse models showed delayed puberty, besides increased weight gain[156]. In addition, there is a link between changes in LIN28 expression in the hypothalamus and the pubertal transition. Additional miRNAs, as miR-132 and miR-145, which are detected in the hypothalamus, affect LIN28 expression [155]. At the same time, let-7, miR-132 and miR-145

expression are altered by caloric restriction [157]. On the other hand, miR-200 and miR-9 are involved in differentiation of olfactory progenitor cells, which influence GnRH neuronal migration after regulation of fork head transcription factor (Foxg1). Here, Dlx5 homeobox regulates miR-200 and miR-9 expression and consequently olfactory receptor neuron (ORN) differentiation and normal GnRH neuron development [155].

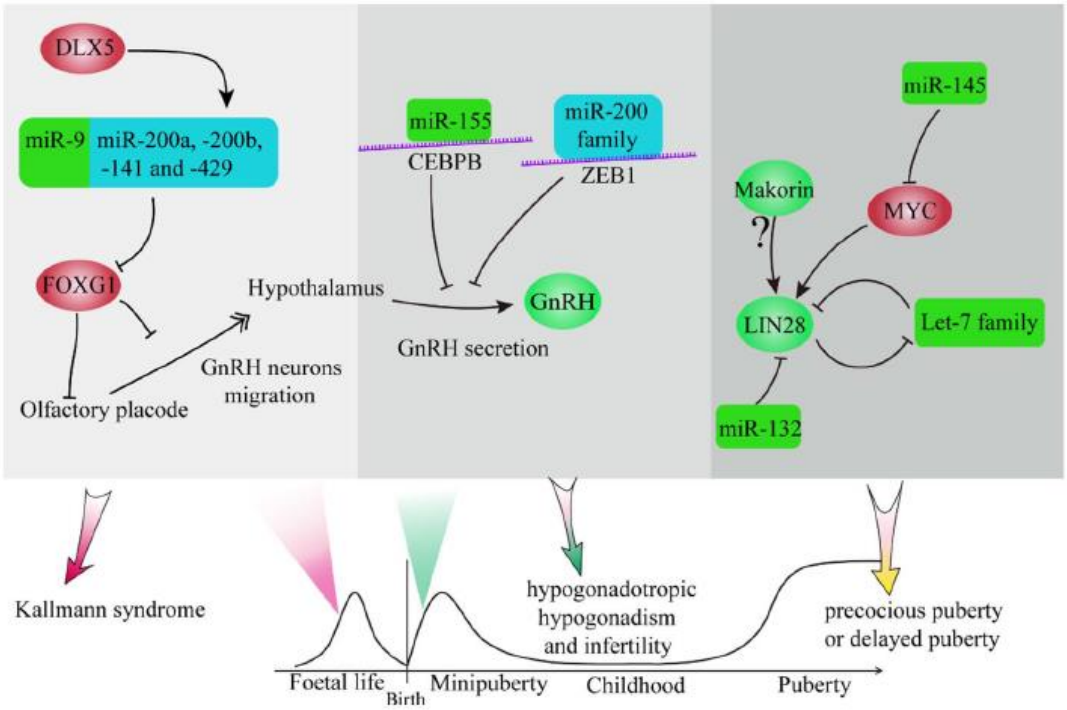

Figure 16. Regulation of key reproductive events by microRNAs. *Main documented miRNAs in the control of reproductive function in different stages of development. Taken from Cao et al., 2018.*

Additionally, highly relevant information has been obtained from conditional Dicer KO mice models. Thus, mice with gonadotroph-specific deletion of Dicer designed to suppress miRNA expression in gonadotroph cells, displayed reduced expression of gonadotropin β-subunit proteins and severely reduced fertility [158]. Subsequently, it was demonstrated that Dicer ablation in GnRH neurons causes hypogonadotropic hypogonadism and infertility, due mainly to hypothalamic GnRH deficiency. Specifically, miR-200 and miR-155 were shown to be implied in the switch governing GnRH transcriptional repression to GnRH transcriptional activation during the course of pubertal maturation **(Figure 16)** [159]. In 2019, Iivonen et al. suggested that mutations in the sequences of some miRNAs, such as miR-200a, were associated with congenital hypogonadism in humans [160]. More recently, miR-7 [161] was shown to have a critical role for maintaining HPG function, since mice constitutively lacking miR-7a in the pituitary exhibited hypogonadotropic hypogonadism and infertility linked to hypopituitarism and decreased levels of gonadotropins, LH and FSH. MiR-7 actions on gonadotrophs cells are exerted via BMP4 and prostaglandin signaling in the pituitary [162]

5.4. MiRNAs as regulators of kisspeptins

Regarding kisspeptin expression, to date only one publication has documented a repressive functional interaction *in vitro* between the 3'UTR region of human *KISS1* mRNA and miR-324-3p[163]. This repressive interaction is evidenced in altered states, such as ectopic pregnancy, and it is correlated with low levels of kisspeptins, as a consequence of the repression induced by miR-324-3p in placental tissue [163]. Other repressive interactions between kisspeptins and other miRNAs have been suggested, through negative correlations in cellular systems, specifically in the context of cancer. This is the case of miR-345 and let-7i [164,165]. On the other hand, it has also been suggested that kisspeptin signaling might be influenced in part by RNA-binding proteins, involved in control of miRNA synthesis, especially the Lin28/Lin28B family, and its target miRNA family, let-7, since mice deficient in *Gpr54* showed altered patterns of expression of these factors. In addition, it was observed that treatment with hCG produced a rescue of these altered expression patterns [166]. Nevertheless, evidence regarding kisspeptin regulation by miRNAs remains scarce and fragmentary, thus making necessary more studies in this area. In this sense, a recent study from our group has shown that specific deletion of Dicer in Kiss1 neurons, as a means to block canonical miRNA biosynthesis, has an impact on pubertal progression, with more dramatic effects in females, and causes profound central hypogonadism in both sexes in adulthood [167]. In this context, identification of miRNAs specifically involved in the control of kisspeptin expression in hypothalamic Kiss1 neuronal population appears mandatory, as a means to enlarge our knowledge on the molecular mechanisms for the control of puberty and fertility.

5.5. MiRNA databases for *in silico* studies

MiRNAs can bind multiple targets and 3'UTRs also contain binding sites for multiple miRNAs. Difficulties in predicting miRNA targets reside in the nature of miRNAs, as the miRNA:mRNA pair contains several mismatches, gaps, and G:U base pairs in many positions [168]. In any case, the functional roles of miRNAs reside in the transcripts they target and in the effect caused after binding. Numerous databases have been developed with the aim to assist in prediction of miRNA::mRNA interactions and for the registry of miRNA information. The main ones employed in this work are listed below:

MiRBase. This database constitutes the primary public repository and online resource for microRNA sequences and annotation. It was established in 2002 and provides miRNA nomenclature for new discovered miRNAs since then. Last version, v22, contains 48860 mature microRNAs from 271 organisms (Kozomara et al., 2019).

TargetScan. This was the first database employing an algorithm related to the concept of seed matches [168]. This algorithm scans ortho-logous 3'UTR sequences and conserved miRNAs across a group of organisms. The seed region is the sequence that confers specificity and function to miRNAs, located at nucleotides 2 to 7 of their 5' end[170]. This must necessarily be complementary to the mRNA of its target, it being defined by the presence of 8mer (exact match to positions 2-8 of the mature miRNA, followed by an "A"), 7 mer-m8 (match to positions 2-8), 7mer-A1 (match in position 2-7 followed by an "A") or 6mer (match to positions 2-7 of the mature miRNA) sites that match the seed region of each miRNA **(Figure 17)** [171].These matches are extended, allowing G:U pairs. Second structure of the heteroduplex is predicted for each putative target to provide folding energy value, as well as a Z-score based on the number of matches and free energies. Putative regulatory miRNAs are ranked by score; predictions with only poorly conserved sites and non-conserved miRNAs are also provided [168].

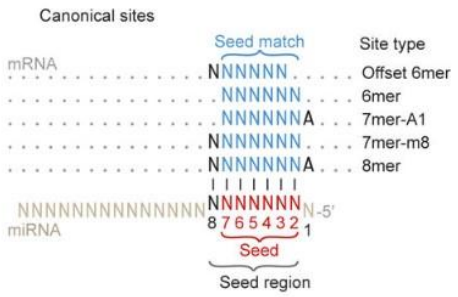

Figure 17. *Different kinds of matching between the seed region of miRNAs and their targets. Taken from Bartel, 2018.*

MiRDB. MiRNA-target prediction is based on the MiRTarbase algorithm, which employs a machine learning method developed by learning thousands of miRNA-target interactions found in high-throughput sequence experiments [172].

MiRMap. This is a bioinformatics algorithm for the prediction of miRNA target repression strength. It combines several existing approaches (thermodynamic, evolutionary, probabilistic and sequence based) to precisely predict miRNA targets [173].

MiRWalk. MiRWalk is supported by the machine learning algorithm TarPmiR, which employs miRNA-mRNA experimental data to predict miRNA target sites [174].

miRanda. miRanda is an algorithm for the detection of potential microRNA target sites in genomic sequences. Target sites are predicted using a two-step strategy. First, the query miRNA sequence and the reference sequence are aligned, producing scores based on sequence complementarity (A:U and G:C; G:U wobble is also permitted). The second phase of the algorithm estimates the thermodynamic stability of RNA duplexes based on the high-scoring alignments from the previous alignment process after using folding routines from the ViennaRNA package [175].

DIANA-tools. This database provides the user with a range of algorithms, databases of validated miRNA targets as well as software for pathway predictions. A summary is provided in **Table 1** below.

Tool	Prediction
microT-CDS	Target prediction
TarBase 7.0	Experimentally supported miRNA targets
miRPath	Enriched pathways
DIANA-miRExtra	Effect to the expression level of target

Table 1. *Bioinformatics tools from DIANA-tools related to the information provided by each of them.*

RNA-hybrid. This tool is designed to find the minimum free energy for hybridization between a long RNA and a short RNA, in this case between a mRNA and a miRNA [176].

miTALOS. Given a list of miRNAs, miTALOs employs TargetScan, MiRanda/mirSVR or StarBase 2 to localize targets in given pathways. It also allows running a search filtered by gene expression obtained from cell lines and tissue datasets [177]

TissueAtlas. This database contains information about miRNA tissue expression in 61 tissues from 2 individuals [178].

miRNASNP v3. This is a database for predicting the effects of miRNA SNPs, including effects of pri-miRNA SNPs and their impact on miRNA as well as target gain or loss of function [179].

6. INTERPLAY BETWEEN METABOLISM AND REPRODUCTION

Besides the genetic and epigenetic factors outlined in previous sections, the nutritional state can profoundly influence the HPG axis. Evidence for the influence of metabolic status on reproduction is provided by the well-known need of minimum threshold of energy reserves to achieve sexual maturation and reproductive success [87]. In this sense, puberty onset appears to be more closely related with body weight than to chronologic age [180]. Situations of energy deficit, such as anorexia nervosa, induce amenorrhea, while metabolic conditions, such as obesity or diabetes, are linked to miscarriage, anovulation or infertility in women [181] and to hypogonadotropic hypogonadism in men [182]. Indeed, states of metabolic unbalance, ranging from nutritional deprivation to excessive energy stores, operating via different energetic sensors and transmitters, are known to modulate (either in a repressive or stimulatory manner) multiple intermediate signals controlling GnRH neurons. In this context, Kiss1 neurons appear as major check-point for the metabolic control of GnRH neuronal regulation. For instance, in different

mammalian models, fasting has been shown to reduce *Kiss1* expression at hypothalamus; a response that is reversed by food intake [183]. In parallel, mounting evidence also suggests a regulatory role of kisspeptin over metabolic status. Thus, the presence of GPR54 in different tissues, as pancreas or liver, is well documented [184,185]. The presence of GPR54 has been suggested also in neuronal populations of paramount importance in the control of energy balance, as POMC or AgRP/NPY [186,187]. In this section, we will summarize the main aspects of the metabolic modulation of the reproductive system, with a particular focus on the regulation of the Kiss1 system, and its potential role in the metabolic control of puberty and gonadal function (including also central hypogonadism linked to obesity).

6.1. Central signals for the metabolic control of reproduction

While numerous central transmitters seem to be involved in this phenomenon, we will summarize below the main central mediators for the metabolic control of reproduction.

Proopiomelanocortin. The POMC precursor protein produces different active peptides: α-melanocyte-stimulating hormone (α-MSH), corticotropin (ACTH), and β-endorphin. In the CNS, α-MSH binds mainly to the G-protein coupled melanocortin receptors 3 and 4 (MC3R and MC4R)[188]. Regarding metabolic regulation of POMC, POMC neurons express the gene *Lepr*, encoding leptin receptor (see Section 6.2.). Additionally, mouse knockout models for *Pomc*, *Mc4r* and *Mc3r* show obese phenotypes, as humans displaying mutations of *POMC* and *MC4R* do [188]. Interestingly, some of these mouse lines also exhibit subfertility in adulthood [189]. Importantly, there is documented evidence of stimulatory actions of α-MSH on Kiss1 neurons, that consequently affect GnRH output to regulate puberty onset [189].

CART. Cocaine and amphetamine regulated transcript is the third most abundant transcript in the hypothalamus. In addition to the ARC, it is also expressed in the PVN, DMH, LHA, and perifornical area (PFA) [190]. Different studies in animal models have shown that the expression of *Cart* decreases in the ARC in fasting situations [190,191], while central administration of this peptide causes a reduction in food intake [192]. Regarding regulation of Kiss1 neurons, there is experimental evidence in mice that fibers from Cart-expressing neurons contact with Kiss1 cells in the ARC and POA, whose activation can induce post-synaptic depolarization of ARC Kiss1 neurons. This points out to a role of CART for direct and indirect -via Kiss1 neurons- stimulation of GnRH neurons [193].

AgRP and NPY. Agouti-related peptide (AgRP) and neuropeptide Y (NPY) are expressed in ARC neurons [194] where they act to increase food intake and decrease energy expenditure [181]. A rise in NPY and AgRP levels is observed in the obese leptin deficient (*ob/ob*) mouse, pointing out to

inhibitory actions of leptin over this neuronal population. AgRP/NPY neurons have been implicated also in the control of reproduction, as documented by their inhibitory role over GnRH and Kiss1 neurons, and the reported restoration of fertility in leptin-deficient *ob/ob* mice after ablation of AgRP neurons [195]. On the other hand, energy deficit leads to activation of AgRP neurons in mice, which secrete AgRP and GABA on ARC KNDy neurons and on POA Kiss1 neurons, thereby contributing to suppress fertility in conditions of negative energy balance (**Figure 18**)[196].

6.2. Peripheral hormones in the metabolic control of reproduction

Leptin. Leptin is an anorexigenic hormone synthesized in adipocytes and secreted proportionally to the amount of body fat storages. Although leptin deficiency can lead to delayed puberty, hypogonadotropic hypogonadism or infertility [87], energy excess conditions are linked to leptin resistance, and an excess of leptin can also favor infertility in both sexes [197]. Additionally, leptin appears to have a role in early reproductive programming, as there exists an increase in its levels during the gestational third trimester or neonatal period untied to fat mass increase or appetite regulation [197], with reproductive consequences later in life [198]. However, GnRH neurons do not express leptin receptor and Kiss1 neurons, while sensitive to changes in leptin concentrations, seem to express *Lepr* at low levels, suggesting that leptin could act indirectly on Kiss1 neurons to control the reproductive axis. In any event, KNDy neurons receive contacts from important cell populations known to mediate hunger and satiety and to be sensitive to leptin actions, such as POMC and NPY neurons [199,200]. Also, GABAergic neurons are a putatively relevant intermediate link between leptin and reproductive neurons, as mice engineered to lack *Lepr* in GABAergic neurons resemble the reproductive phenotype of leptin deficient female mice, and display reduced expression of *Kiss1* in POA and the ARC [87]. There exists sexual dimorphism regarding the effects of leptin in the control of reproduction, as *Lepr* deficiency appear to be less detrimental for adult reproductive function in male than in female mice [87].

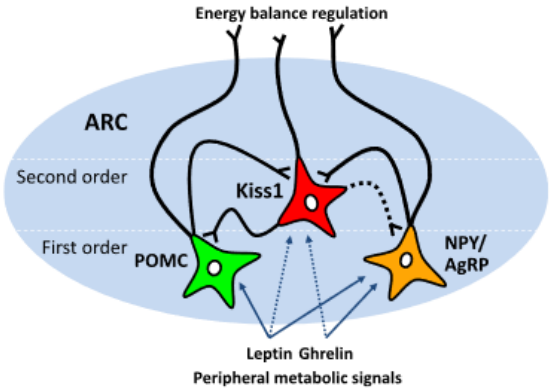

Figure 18. *Integration of peripheral and central cues for the metabolic control of Kiss1 neurons. Taken from Patel et al., 2021.*

Insulin. Insulin is a peptide secreted by pancreatic β cells, which signals into different ARC populations. Thus, insulin has been shown to excite POMC neurons, while it inhibits AgRP/NPY neurons [201]. Via this inhibitory signaling to AgRP/NPY neurons [202], central administration of insulin, in monkeys and rodents, reduces food intake and body weight [203], while the administration of insulin at the central level increases the expression of Pomc mRNA in the ARC[202]. Yet, insulin actions on the central pathways governing reproduction may be conducted not only indirectly (via primary actions in POMC and/or AgRP/NPY neurons), but to some extent also directly, since the insulin receptor seems to be present also in Kiss1 neurons [204,205] , where insulin may participate in the correct maturation of the reproductive system, although it is not apparently required for maintaining reproductive function in adulthood. Any case, insulin signaling in the brain is required for correct GnRH secretion and states of insulin resistance are frequently linked to central hypogonadism [87].

Ghrelin. Ghrelin is an orexigenic hormone produced in the gut that has been demonstrated to influence *Kiss1* and *Gnrh* expression at central level [83,87,206]. Two forms of ghrelin exist in circulation, acyl-ghrelin and unacyl-ghrelin, both affecting LH secretion *in vivo* [206]. In fasting situations, there is a rise in the circulating levels of ghrelin, which decrease after ingestion [207]. Its central and peripheral administration induces, in rodents, an increase in food intake and hypothalamic Npy mRNA expression. This increase in food intake is suppressed by the administration of NPY and AgRP antagonists in rats and knockout mice, demonstrating the role of these neuropeptides in mediating the effects of ghrelin on energy homeostasis [208,209]. Ghrelin gene also produces another peptide, named obestatin, with demonstrated effect over gonadotropin secretion, as documented in sheep [210]. Of note, although KNDy neurons appear to express ghrelin receptors (*Gshr*) in direct proportion to estradiol levels, global deletion of ghrelin does not impair fertility in mice [87].

Estrogens and testosterone. Both steroidogenic factors have been mentioned in previous sections, but a brief description of their roles in terms of metabolic control is worth also here. Regarding estrogens, compelling evidence has shown that estradiol, acting via ERα, has a specific action in the hypothalamus to modulate energy homeostasis, particularly within the ARC and VMH [211]. The functional relevance of such actions is supported by the fact that central administration of estradiol induces a potent anorexigenic effect [212]. In addition, estrogen acting at the VMH can induce thermogenesis, as key component for its role in energy homeostasis [213]. Interestingly, ablation of KNDy neurons in the ARC prevents the expected ovariectomy (OVX)-induced gain in body weight [214]. Similarly, elimination of KNDy neurons mitigated the body weight loss response induced by estradiol administration [214]. In general, these findings suggest

that KNDy neurons are essential to carry out the actions of estradiol on energy homeostasis. In the case of androgens, and specifically testosterone, they also play important roles in regulating energy homeostasis, with a predominant orexigenic effect [215]. Nevertheless, the underlying mechanisms for this action remain largely unknown.

6.3. Central cell energy sensors and the metabolic control of reproduction

Cells are able to sense the environment to adapt their energetic expenditure to the nutrient availability. This premise is also true for the neuronal populations controlling reproduction. To date, key cell energy/metabolic sensors, such as the mammalian target of rapamycin (mTOR), AMP-activated protein kinase (AMPK) and SIRT1, have been pointed out as putative components of the neuroendocrine pathways linking the state of energy resources and reproductive capacity, at least in part by modulating the activity of Kiss1 and GnRH neurons.

AMPK. AMPK is the main AMP/ATP ratio sensor in eukaryotic cells. It is well known that almost every function inside the cells consumes ATP, which is catabolized to ADP and phosphate (P). To maintain the ATP-ADP equilibrium needed for cell homeostasis, ADP is converted to ATP via ATP synthase or via adenylate kinase (AK), being the latter highly abundant at the cellular level. AK reaction converts 2 ADP into ATP and AMP; this is the reason why the AMP/ATP ratio is, together with ADP/ATP ratio, a reflection of cell energy status [216]. The link between AMPK signaling and reproduction has been demonstrated in animal models. Thus, conditions of undernutrition are associated to an increase in hypothalamic phosphor-AMPK levels and a delay of puberty onset in rodents; a delay that is largely prevented by the conditional ablation of the catalytic subunit of AMPK in Kiss1 neurons [217]. In the same vein, ablation of AMPK specifically in GnRH neurons induces early puberty in females and partially prevents the deleterious effects exerted by undernutrition/fasting on the gonadotropic axis [218]. Altogether, this evidence suggests that AMPK signaling in Kiss1 and GnRH neurons participates in the metabolic gating of puberty and reproduction, in conditions of nutritional deprivation.

mTOR. mTOR is a highly conserved serine/threonine kinase with two complexes, mTORC1 and mTORC2. mTOR signaling pathway is coupled to insulin/insulin-like-growth factor 1 (IGF-1) pathways, which activates mTOR via protein kinase B (PKB/AKT). In turn, mTOR inhibits IRS and consequently the insulin/IGF-1 pathway. Thereby, states of energetic excess activate mTOR, promoting cell growth, protein and lipid synthesis, glucose metabolism, mitochondrial function and active transcription. In contrast, energy deprivation switches off mTOR to promote catabolic processes for the survival of the cells [219]. At the hypothalamus, mTOR has been involved in sensing nutrient availability and hormonal milieu (e.g., insulin, leptin and ghrelin) to couple

energetic status and reproductive function. In this context, experimental data have shown that mTOR modulate *Kiss1* expression in the ARC and preserved brain mTOR signaling is required for the permissive effects of leptin on puberty onset in female rats, therefore suggesting the existence of a leptin-mTOR-Kiss1 pathway [220].

SIRT1. SIRT1, a key epigenetic regulator mentioned at section 4, is under the influence of the NAD^+/NADH ratio, it being activated by an increase in this ratio, as signal of energy deprivation. As NAD^+-dependent class III deacetylase, NAD^+ links this sirtuin to active states under nutrient restriction, with the consequent inhibitory effect over *Kiss1* transcription [220]. Thereby, SIRT1 plays a major role connecting metabolic state with reproductive function, and particularly puberty onset, through the epigenetic control of *Kiss1* expression. For further details, see Section 4.

6.4. The Kiss1/GPR54 system and the metabolic control of reproduction

Solid evidence, gathered in recent years, points out that the Kiss1/GPR54 system is a major component for the connection between the energy/metabolic state of the organism and the function of the reproductive axis at different stages during the lifespan of the individual. This is epitomized by the roles of the Kiss1/GPR54 system in the control of puberty, but also in conditions such as hypogonadal states bound to metabolic alterations in the adults. Given the objectives of this Thesis, these aspects are briefly summarized in the following sections.

6.4.1. The Kiss1/GPR54 system and the metabolic control of puberty

In humans, childhood obesity influences hormonal production and pubertal development and, at the same time, is bound to metabolic and cardiovascular diseases during adulthood, among other pathologies [149]. Controversial information exists regarding the impact of obesity on kisspeptin levels in prepubertal girls and boys, as some studies have pointed out changes in circulating levels of kisspeptin in obese children, while others failed to detect such changes[221,222]. In any event, the putative impact of such potential alterations in kisspeptin levels in plasma remains dubious, as the main role of kisspeptins in the control of puberty is conducted at central levels. In this context, and given the rise in alterations related to age of pubertal onset in girls and boys, numerous studies in animal models have aimed to explore changes at central levels affecting the Kiss1/GPR54 system in conditions of metabolic stress, as a means to assess its putative role as effector of the effects of metabolic cues onto the reproductive system. Indeed, as mentioned in previous sections, the Kiss1/GPR54 system has been shown to connect reproductive function and energetic status of the organism. Thus, alterations in the energy

balance, due to excess or energy deficiency, have been reported to alter hypothalamic expression of *Kiss1*.

In detail, conditions of negative energy balance have been shown to suppress the hypothalamic Kiss1 system, by decreasing Kiss1 mRNA expression and kisspeptin content in the hypothalamus, thereby causing a drop in circulating LH levels [75]. This state can be reversed with the administration of leptin in several species *in vivo* [54,223–225]. Similarly, in calorie-restricted female rats, central administration of Kp-10 was able to increase GnRH and gonadotropin secretion, rescuing the delay in puberty onset linked to energy deficit [226]. In the same vein, studies in adult male mice, employing short fasting periods, showed a reduction in *Kiss1* and *Gpr54* expression when compared with control fed mice [227].

In addition, conditions of persistent energy excess, such as obesity, have been shown to have a significant impact on the Kiss1 system. In one hand, postnatal overfeeding in female rats advanced puberty onset, together with an increase in circulating levels of leptin and hypothalamic Kiss1 mRNA during the pubertal period [7]. As previously mentioned, Kiss1 neurons have been pointed out as mediators of leptin signaling to the GnRH neurons. Strikingly, persistently elevated leptin levels, as a consequence of excess of adipose reserves, impact the Kiss1 system in different manner depending on the developmental period. While overfeeding during peripubertal period increases *Kiss1* expression with the associated pubertal advancement, obesity in adulthood is linked to reduced *Kiss1* expression and hypogonadism in rodents [5,220], as will be highlighted in the next section.

6.4.2. The Kiss1/GRP54 system and obesity-induced central hypogonadism

As mentioned earlier, adult obesity induces central hypogonadism, especially in men and male animal models [228,229]. Prevalence of obesity in humans has likely contributed to rise the prevalence of hypogonadism, which seems to affect between 2.1% and 12.8% of adult men in the general population, with an estimated prevalence that will reach 6.5 million affected men by 2025 [230]. Diabetes, coupled or not with obesity, is also linked to development of male hypogonadism as 35-57 % of patients with diabetes are affected by this condition [231]. Besides impairment of fertility, hypogonadism leads to sexual dysfunction, decreased muscle mass, alterations in bone mineralization and lipid metabolism disorders [230].

By definition, hypogonadism is a condition of altered gonadal function and androgen deficiency as compared to what is expected for age. Different forms of hypogonadism range from primary or testicular hypogonadism (due to primary alteration of testicular function) to central or hypogonadotropic hypogonadism, which refers to a condition of testicular failure due to

impaired GnRH pulse generator and/or impaired pituitary gonadotropin production [232]. While the causes of central hypogonadism are diverse and include those congenital forms, due to specific genetic defects, other acquired conditions, including inflammatory diseases, medication, stress, and, importantly, obesity, can contribute also to the development of central hypogonadism [233]. Here, we will focus on adult-onset male hypogonadism developed as a consequence of obesity, referred hereafter as obesity induced hypogonadism (OIH). In this sense, OIH is a form of central hypogonadism, in which alteration of metabolic cues impact on the HPG axis promoting reduction of gonadotropins, leading to gonadal insufficiency. As mentioned above, a primary mechanism for such drop of gonadotropic drive in obesity is linked to altered Kiss1/GPR54 signaling.

Indeed, obesity has been shown to suppress *Kiss1* expression in the hypothalamus of rats and mice, which leads to the development of hypogonadotropic hypogonadism [7,229]. Different mechanisms seem to be involved in such effect, as summarized below:

- Hyperestrogenism. As obesity cause adiposity expansion, the increase in estrogen levels in the adipose tissue correlates with overexpression of aromatase, which transform testosterone into estradiol. Hyperestrogenism in turn decreases LH secretion, through the negative feedback mechanism exerted on LH secretion [234]. As mentioned earlier in this Thesis, since GnRH neurons lack ERα, Kiss1 neurons, which express the receptor, are postulated to be the mediators of the impact of excess of estrogen on the reproductive axis, observed in morbidly obese men [235].
- Inflammatory state. Increased fat mass is associated with adipocyte dysfunction, linked to decrease adiponectin and increase pro-inflammatory adipokines, as leptin, IL-1, IL-6 and TNF-α, from adipocytes and macrophages. Those adipokines induce inflammation and systemic insulin resistance. At least partially, adipokines may promote hypogonadism by impairing kisspeptin signaling after interfering with GPR54, leading to reduced GnRH secretion [236,237], although the underlying mechanisms remain unfolded.
- Leptin resistance. Expansion of adipocytes causes hyperleptinemia and leptin resistance at central level, putatively decreasing central activation of *Kiss1* gene expression. Additionally, high leptin levels inhibit testosterone production directly on Leydig cells [230].
- Insulin resistance. Excess of fatty acids from visceral fat promotes higher production of glucose in the liver and decreased insulin uptake. This leads to hyperinsulinemia and insulin resistance coupled to additional release of insulin by pancreatic cells. It has been documented that persistent hyperinsulinemia decreases kisspeptin signaling and, thereby, GnRH and LH release[237]. In addition, hyperinsulinemia negatively affects liver function, as major determinant in humans [238].

Despite the above evidence, the ultimate mechanisms whereby OIH is established and progresses remain largely unknown, and further research efforts are needed to expose the molecular pathways whereby obesity affects the Kiss1/GPR54 system in adulthood.

As final note, the classic pharmacological treatment used to address hypogonadism in men to date has been testosterone replacement therapy. Despite the fact that this therapeutic option has been documented to generate multiple beneficial effects at the metabolic level in patients[239], its pharmacological dosage may not be exempt from adverse effects and it has numerous contraindications, such as prostate hypertrophy, prostate cancer risk, lower sperm count, swelling, heart failure, gynecomastia, sleep apnea or blood hyper-coagulability [233]. These alterations could be a consequence, in part, of the high levels of testosterone in the blood following this treatment, as the concentrations reached are well above the physiological levels of testosterone in a healthy adult [230,240]. For this reason, despite the fact that there are encouraging studies on testosterone treatment [241], it is necessary to better understand the mechanisms involved in OIH, which may help to develop new therapies that regulate better testosterone levels and their mediators in a physiological range.

Objectives

Objectives

Reproductive capacity is indispensable for the maintenance of the species. Proper functioning of the reproductive axis is determined by the precise regulation of the hypothalamic-pituitary-gonadal axis. Adequate integration of genetic, epigenetic, metabolic, hormonal, and environmental factors is essential for the acquisition and maintenance of reproductive function. The mechanisms involved in the decline or impairment of reproductive capacity are not fully understood yet. In any event, there are growing concerns, both in the scientific community and general population, about the detrimental effects of current lifestyle factors and harmful environment over the correct timing of puberty and the maintenance of reproductive capacity. At the same time, functioning of reproductive system is closely linked to adequate metabolic status and body energy reserves, while preserved gonadal function seemingly contribute to the maintenance of metabolic homeostasis and the prevention of metabolic complications, such as obesity, cardiovascular diseases or type 2 diabetes, whose escalating prevalence represents a major societal and economic burden in Europe and worldwide.

In the above context, the **GLOBAL AIM** of this doctoral thesis is to deepen our understanding of the mechanisms of reproductive control and its modulation by metabolic signals, by characterizing the roles of microRNAs and GRK2 in the regulation of the reproductive system and evaluating their eventual pathophysiological contribution to pubertal alterations and central hypogonadism linked to obesity.

This global aim is divided into four **SPECIFIC OBJECTIVES**:

1. To characterize the putative role of specific **microRNAs in the physiological control of puberty** via regulation of the Kiss1 system.

2. To define the pathophysiological role of **microRNAs in obesity-induced hypogonadism (OIH)**, including their interplay with Kiss1 and potential therapeutic implications in this condition.

3. To determine the role of **GRK2 in the control of puberty and the gonadotropic axis** via regulation of the kisspeptin receptor, GPR54, in normal conditions and under nutritional stress.

4. To evaluate the implication of **GRK2 in the development of OIH** through the regulation of GPR54.

Materials & Methods

Materials and methods

1. Ethic statement

The experimental procedures were approved by the Córdoba University Ethical Committee for Animal Experimentation and were conducted in accordance with the European Union normative for care and use of experimental animals.

2. Animals

Wistar rats and mice employed in this Thesis were bred in the vivarium of the University of Córdoba. The day the animals were born was considered day 1 of age. The animals were kept under constant conditions of light (12h of light, from 7:00 am) and temperature (22°C). They were weaned on postnatal day (PND) 21 and were provided with free access to tap water and pelleted food (A04, Panlab; 2.90 Kcal/g), unless otherwise stated.

2.1. Rat models

Female and male Wistar rats, employed in this Thesis, were bred in normal litters (NL; 12 pups per litter) unless otherwise stated. Additionally, models of delayed puberty and adult obesity-induced hypogonadism (OIH) were generated, as described in the corresponding experimental protocols section.

2.2. Mouse models

2.2.1. *Kiss1*$^{Cre:GFP}$ mouse model

The mouse line, *Kiss1*$^{Cre:GFP}$ (v2) (RRID:IMSR_JAX:033169) was obtained from Dr Richard Palmiter (University of Washington, Seattle, WA) [242]. *Kiss*$^{Cre:GFP}$ model express Cre recombinase, fused to GPF reporter in neurons expressing the *Kiss1* gene.

2.2.2. *Kiss1*$^{Cre:EYFP}$ mouse model

The mouse line *Kiss1*$^{Cre:EYFP}$ was generated in our laboratory by our colleague, Dr Juan Roa Rivas, by crossing the *Kiss1*$^{Cre:GFP}$ (v2) mouse (see 2.2.1.) with the *R26R-EYFP* mouse *(B6.129X1-Gt(ROSA)26Sortm1(EYFP)Cos/J; RRID:IMSR_JAX:006148)* [243]. In the *Kiss1*$^{Cre:EYFP}$ model, Cre recombinase activity driven by the Kiss1 promoter, deletes the stop sequence coupled to EYFP locus and allows expression of EYFP in Kiss1 cells of the double mutant mice.

2.2.3. G-GRKO mouse model

Mice lacking functional GRK2 specifically in GnRH-expressing cells were generated by crossing the *GnRH*$^{Cre+/-}$ mouse line *(Tg(Gnrh1-cre)1Dlc/J; RRID:IMSR_JAX:021207)* [244] with mice harboring LoxP sites flanking exons 3 to 6 of the *Adrbk-1* gene, encoding GRK2 *(Grk2tm1Gwd/J;*

RRID:IMSR_JAX:012458) [245]. The *GnRH*$^{Cre+/-}$ mouse line carries Cre recombinase expression under the control of GnRH promoter. The resulting genotypes, *GnRH*$^{Cre+/-}$*:Grk2*$^{loxP/-,}$ were self-crossed to generate all possible genotypic combinations. For experiments, only mice with genotypes *GnRH*$^{Cre+/-}$*:Grk2*$^{loxP/loxP}$ (named G-GRKO) and *GnRH-*$^{Cre-/-}$*:Grk2*$^{loxP/loxP}$ (control group) were used.

3. Drugs

The GRK2-inhibitor, methyl[(5-nitro-2-furyl)vinyl]-2-furoate (β-ARK1-I; Calbiochem, La Jolla, CA, USA) was dissolved in DMSO and administered intracerebroventricularly (icv), in a final volume of 5 µL per rat, at a dose of 6.53 nmol, as employed in previous studies [246,247]. β-estradiol 3-benzoate (EB, Ref: E8515S; Sigma Chemical Co., USA) and testosterone propionate (TP, Ref: 86541; Sigma Chemical Co., USA) were dissolved in olive oil and administered subcutaneously at a dose of 100 µg/mL. Rat/mouse kisspeptin-10 (Kp-10; KISS-1 (110–119)-NH_2), analogue of the human C-terminal KISS-1 decapeptide KISS-1 (112–121)-NH_2, was obtained from Phoenix Pharmaceuticals. Depending on the experiments, doses of 10 pmol, 50 pmol, 1nmol of Kp-10, as capable to either sub-maximally or maximally elicit LH and FSH secretion [248] were used. The NK3R agonist, Senktide, (Sigma Chemical Co.) was administered at a dose of 600 pmol in rats, as previously reported [249]. Kp-10 and Senktide were dissolved in physiological saline (0.9% sodium chloride) and administered icv in a final volume of 5 µL. Glucose (GL01271000, Scharlab, Spain) and insulin (mouse: ref. 2643, rat: ref. 109081; Sigma Chemical Co., USA) were administered intra-peritoneally (i.p.). For glucose tolerance tests (GTT), a bolus of 2 g/kg of body weight (BW) per mouse or 1 g/kg of BW per rat was employed. For insulin tolerance tests (ITT) 0.75 international units (IU) bolus was i.p. administered in rat and mice.

4. General experimental procedures

4.1. Sample collection

4.1.1. Hypothalamus, preoptic area and mediobasal hypothalamus

After decapitation of the animals, brains were placed on foil paper over dry ice, with the hypothalamus upwards until they got frozen, and were stored at -80°C for protein, RNA and RNAScope analytical protocols. For mRNA, miRNA and western blot (WB) procedures, the hypothalami were placed on ice, mild-thaw and dissected from the brain following the lateral delimitation of the circle of Willis, the rostral boundaries of the optic chiasm (OC) and the caudal limits of the rostral part of the mammillary bodies. To analyze independently POA and MBH, POA was dissected from MBH by a coronal cut posterior to the optic chiasm.

For immunohistochemistry analyses, mice were intraperitoneally anesthetized with ketamine/ xylazine in a 2:1 proportion. Next, mice were perfused with 0.9 % saline followed by 4 % of paraformaldehyde (PFA). Whole brains were collected, postfixed in PFA during 24 hours at 4°C, washed in phosphate buffer saline (PBS) for 24 additional hours and dehydrated in sucrose at 30% in PBS 0.1 M for 48 hours.

4.1.2. Blood collection

Blood, for hormonal and cytokine measurement, was obtained by jugular venipuncture or trunk collection after decapitation of the animals. Serum was stored at -20°C after centrifugation of the samples at 3000 g for 20 min. For LH pulsatile profile hormonal assays, blood was obtained by tail-tip nick and blood serial collection as described in Section 4.3.

4.1.3. Heart and tibia. For cardiac hypertrophy determination, hearts were removed and the length of the tibia was annotated. The ratio between dry weight of heart and the length of the tibia was calculated.

4.1.4. Prostate hyperplasia determination. For prostate hyperplasia determination, prostate was removed from each animal. The ratio between the prostate dry weight and the length of the tibia was calculated.

4.1.4. Ovary and testis isolation. For relative ovary and testis weights, left ovary and left testis were removed and weighted. Weight was normalized to the body weight of the animals.

4.2. Phenotypic evaluation of pubertal maturation

External indicators of pubertal development were assessed in mice and rats from PND24, in parallel with the recording of somatic development parameters, as body weight and food intake. Validated pubertal markers for female and male rodents included age of vaginal opening (VO) in females, and age of balano-preputial separation (BPS) in males. Additionally, in females, vaginal smears were taken and visualized since the day of VO to determine the age of first estrus (FE) (defined by the first appearance of cornified epithelial cells on vagina), as indicative of first ovulation. At the end of the experiments, uterus and left ovary weights were registered, while right ovary was reserved for histological analysis, to apply a method employed to precisely determine age of first ovulation. Those ovaries were collected and maintained >24h on Bouin medium to fix them. Ovaries were serially sectioned (10 µm), stained with hematoxylin- eosin and viewed with Elipse 400 microscope to analyze follicular development and *corpus luteum* progression by the validated methodology, Pub-score [250].

4.3. Mouse habituation for tail-tip blood collection and LH pulsatility test

Previous to blood collection by tail-tip nick for LH pulsatility test, mice were handled 5 min per mouse daily during three weeks. Habituation of the mice to human contact -smell and pressure exerted on their tails during performance of the test-, was done in parallel by the two investigators required for the sample collection: the mouse handler and the sample collector. When performing test on female mice, pulsatility test was done in the morning of diestrus [251]. LH pulsatility test consisted in blood collection from the tail-tip of the mouse, placed on a paper role, every 5 minutes for a period of 3 hours. By this mean, 4 µL of blood were 1:12.5 (normal conditions) or 1:7.14 diluted (undernutrition conditions) in 0.1 M PBS 0.05% Tween-20 and immediately frozen on dry ice. Blood samples were stored at -80°C until performance of the high-sensitivity LH ELISA assay, described in section 6.5.

4.4. Systolic blood pressure

Systolic blood pressure (SBP) measurements were performed in conscious rats by tail-cuff plethysmography (CIBERTEC Nerem 2000, Non-Invasive Blood Pressure System) before and after treatments. Rats were kept under warm conditions to better detect the pulse of the animals, with an overhead heating lamp. Prior to register SBP data (Niprem 1.5 software), animals were habituated to the experimental protocol. For each animal, several blood pressure readings were obtained and averaged, being expressed as mmHg. A systolic blood pressure ≤125 mmHg was considered normotensive.

4.5. Vascular components determination

Studies of vascular structure and function were made on the same day on fresh tissue; these studies were performed in collaboration with the team of Prof. Mercedes Salaices and Ana María Briones group (Universidad Autónoma de Madrid). Protocols were as follows:

Vascular tissue preparation: Third order branches of the mesenteric resistance artery (MRA) were removed and placed in cold (4°C) Krebs-Henseleit solution (KHS) (115 mM NaCl, 25 mM $NaHCO_3$, 4.7 mM KCl, 1.2 mM $MgSO_4.7H_2O$, 2.5 mM $CaCl_2$, 1.2 mM KH_2PO_4, 11.1 mM glucose, and 0.01 mM Na_2 EDTA) bubbled with a 95% O_2-5% CO_2 mixture (pH = 7.4).

Vascular function: Reactivity of rat mesenteric artery was studied in a wire myograph (**Figure 19**), as reported [252]. After a 30 min equilibration period in oxygenated KHS, arterial segments were stretched to their optimal lumen diameter for active tension development. Contractility of segments was then tested by an initial exposure to a high-K^+ solution (K^+-KHS, 120 mM). The presence of endothelium was determined by the ability of 10 µM acetylcholine (ACh) to relax

arteries precontracted with phenylephrine (Phe) at approximately 50% of K^+-KHS contraction. Afterwards, a single concentration-response curve to ACh (1 nM-100 µM), Phe (1 nM-300 µM) and the NO donor, DEA-NO (1 nM-100 µM), was performed. All drugs were dissolved in distilled water; further dilutions were made in distilled water. l-Phe hydrochloride, ACh chloride and DEA-NO were purchased from Sigma-Aldrich (St Louis, MO, USA).

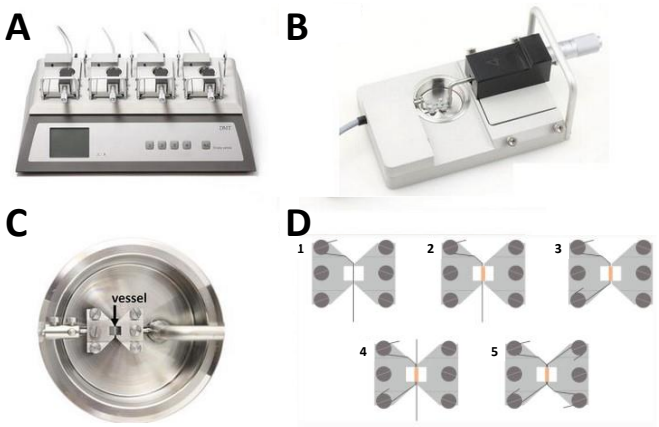

Figure 19*. Example of a wire myograph.* ***A)*** *Multichambered myograph.* ***B)*** *Single wire myograph unit with the force transducer on the left and the right, both connected to the jaws to support the vessel inside the chamber.* ***C)*** *Chamber, jaws and a mounted vessel segment.* ***D)*** *Scheme of the procedure to mount the wires and vessel step by step from 1 to 5. Adapted from www.dmt.dk and* Griffiths & Madhani, 2022.

Pressure myography: The structural and mechanical properties of MRA were studied with a pressure myograph (Danish Myo Tech, Model P100, J.P. Trading I/S, Aarhus, Denmark) (**Figure 20**), according described protocols [254]. Vessels were placed on two glass micro-cannulae and secured with surgical nylon suture. After all small branches were tied off, vessel length was adjusted so that the vessel walls were parallel without stretch. Intraluminal pressure was then raised to 140 mmHg and the artery was unbuckled by adjusting the cannulae. The segment was then set to a pressure of 90 mmHg and allowed to equilibrate for 60 min at 37°C in calcium-free KHS ($0Ca^{2+}$; omitting calcium and adding 1 mM EGTA), intravascular and extravascular perfused, gassed with a mixture of 95% O_2 and 5% CO_2. Intraluminal pressure was reduced to 3 mmHg. A pressure-diameter curve was obtained by increasing intraluminal pressure in 20 mmHg steps from 3 to 140 mmHg. Internal and external diameters were continuously measured under passive conditions (Di0Ca, De0Ca) for 3 min at each intraluminal pressure. The final value used was the mean of the measurements taken during the last 30 s when the measurements reached a steady state. Finally, the artery was set to 90 mmHg in $0Ca^{2}$+-KHS and then pressure-fixed with 4% PFA in 0.2 M phosphate buffer, pH 7.2-7.4 at 37°C for 60 min and kept in 4% PFA at 4°C.

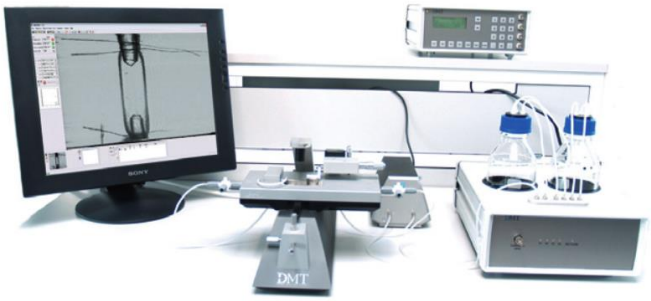

***Figure 20**. Pressure myograph is composed by a perfusion chamber, where the vessels are placed and mounted onto two glass cannulas; an inverted microscope stage; an interface unit with integrated buffer reservoir, heat control, force and pressure calibration procedure; and a diameter tracking software. Taken from http://www.bandetek.com.*

Calculation of passive structural and mechanical parameters: From internal and external diameter measurements in passive conditions, the following structural and mechanical parameters were calculated: Wall thickness (WT) = $(De_{0Ca} - Di_{0Ca})/2$

Wall:lumen = $(De_{0Ca} - Di_{0Ca})/2Di_{0Ca}$

Incremental distensibility represents the percentage of change in the arterial internal diameter for each mmHg change in intraluminal pressure and was calculated according to the formula:

$$\text{Incremental distensibility} = \Delta Di_{0Ca}/(Di_{0Ca} \times \Delta P) \times 100$$

Circumferential wall strain (ε) = (Di0Ca - D00Ca)/D00Ca, where D00Ca is the internal diameter at 3 mmHg and Di_{0Ca} is the observed internal diameter for a given intravascular pressure, both measured in $0Ca^{2+}$ medium.

Circumferential wall stress (σ) = (P × Di0Ca)/(2WT), where P is the intraluminal pressure (1 mmHg = 1.334 × 103 dynes·cm-2) and WT is wall thickness at each intraluminal pressure in $0Ca^{2+}$-KHS.

Arterial stiffness independent of geometry is determined by the Young's elastic modulus (E =stress/strain). In this case, its calculation has not been performed, as a result of no significant differences in stiffness between the different experimental groups.

4.6. Body composition

Percentage of lean and fat mass (body composition) in animals under study was analyzed by quantitative magnetic resonance (QMR) using the EchoMRI™ 700 analyzer (Houston, TX, software v.2.0). Adiposity index was calculated as follows: [fat mass (%) / fat + lean mass (%)]x100.

5. General surgical procedures

5.1. Cannulation and ICV

Icv cannulation was employed in experiments for central administration of drugs (through the lateral ventricle). Cannulas (BD INTRADEMIC™ polyethylene Tubing, Becton Dickinson, Sparks, MD, USA) 3 cm/4 cm long (neonatal rat and mouse/adult rat) were cut in bevel in one of the extremes. Adhesive tape was placed 2 mm/3mm (neonatal rat and mouse/adult rat) from the bevel to restrict to this length the insertion of the cannula inside the brain. After identification of bregma, perforation of the skull was done with a drill 1 mm posterior to bregma and 1.2 mm lateral to the midline. Cannulation was done at least 24 hours before first drug administration. Animals were placed individually to avoid falling of the cannula.

5.2. Stereotaxic injections

Stereotaxy was employed in experiments performed in mice requiring injection of an infective virus specifically in the ARC within the hypothalamus. Mice were anesthetized and placed in the stereotaxic device. According to the mouse brain atlas, targeting of the ARC was performed bilaterally after perforation of the skull at 2.1 mm posterior to bregma and ± 0.25 mm lateral to the midline. Administration of the viral particles was done with a 10 µL Nanofil™ syringe and needle NF33BL-2 (World precision instruments, LLC, USA) in the next coordinates: -2.1 mm from bregma, ± 0.25 lateral to the midline and -5.9 mm depth. Compounds were administered at a rate of 40 nL/min during 5 minutes. After infusion, the needle was left there for 5 minutes. Next, the needle was elevated 0.1 mm, position that was maintained during 5 additional minutes.

6. General analytical procedures

6.1. Genotyping

Mouse-ear tissue was collected to isolate genomic DNA. The tissue was digested 2 hours at 56°C in lysis buffer (1 M Tris pH 8.5; 0.5 M EDTA pH 8; NaCl 1M and SDS 10%) with 1:200 dilution of proteinase K (20 mg/ml Tris-ClH 0.01 M Promega). The lysate was centrifuged 5 min at 13,000 rpm. For DNA precipitation, the supernatant was mixed in 1:1 proportion with 2-propanol (EMSURE® ACS, ISO, Reag. Ph Eur). A second centrifugation step was performed followed by the decantation of the supernatant and washing with 70% ethanol. DNA was diluted in 50 µl of nuclease free water and stored at -20°C until genotyping. G-GRKO mice were genotyped using the combination of primers (10 µM) listed in **Table 1**. Polymerase chain reaction (PCR) was performed in a T100™ thermal cycler (Bio-Rad, Hercules, CA, USA), as it is indicated in the table below. PCR products were visualized by agarose gel electrophoresis (2% agarose in TBE 1X).

Primer	Sequence5' -3'	Amplicon size	Thermal cycler conditions
Cre forward (fw)	*5' CTG GTG TAG CTG ATG ATC CG 3'*	*400 bp*	5º- 5min 95º- 30seg 55º- 45seg 72º- 45seg 72º 5min 12º- ∞ x35
Cre reverse (rev)	*5' ATG GCT AAT CGC CAT CTT CC 3'*		
GRK2 GT2	*5' -TGA GGC TCA GGG ATA CCT GTC AT -3'*	*GT2-GT5:* *WT: 340 bp* *LoxP/LoxP: 400 bp* *GT4-GT5:* *Control: 1916 bp* *G-GRKO: 350 bp*	5º- 5min 95º- 30seg 60º- 45seg 72º- 45seg 72º 5min 12º- ∞ x40
GRK2-GT5	*5 ´-CAG GCA TTC CTG CTG GAC TAG -3'*		
GRK2- GT4	*5'- GTT AGC TCA GGC CAA CAA GCC -3'*		

***Table 1**: Primers used in PCR for the determination of G-GRKO vs WT animals.*

6.2. RNA extraction, retrotranscription and quantitative PCR from tissues

Total RNA extraction: Total RNA was isolated from hypothalamic samples with different reactive dependent on the experiment: 1) TRIsure isolation reagent (Bioline Reagents Ltd., UK) or 2) RNA extraction kit (Favorgen Tissue Total RNA Extraction Mini Kit, FATRK001). Manufacturer's instructions were followed in both cases. Nanodrop -10000 v.3.5.2 spectrophotometer (Nanodrop Technology®, Cambridge, UK) was used to determine RNA concentration and ratios 260/280 and 260/230.

Retrotranscription (RT) reaction for mRNA: cDNA synthesis, free of genomic DNA (gDNA) contamination from intron-less target genes, was performed with the iScript™ gDNA Clear cDNA Synthesis Kit (BioRad Laboratories Inc., USA). When target designed primers for quantitative-PCR (qPCR) span over an intronic region (intro-containing targets), RT reaction was performed with iScript™ cDNA Synthesis kit (Bio-Rad Laboratories Inc., USA).

In both cases, 0.5 µg of RNA were used as initial RNA amount. Manufacturer's instructions were followed to prepare the reactions and two negative controls were used: RNA free sample mix for detection of genomic DNA (gDNA) contamination, and RT mix free sample for detection of external contamination. A T100™ thermal cycler (Bio-Rad, Hercules, CA, USA) was used for RT incubation. cDNA samples were 1:4 diluted and stored at -20°C.

Retrotranscription reaction for miRNA: cDNA synthesis for miRNA quantification started from 5 ng/µL of RNA material and was performed with the miRCURY LNA RT Kit (Qiagen), following manufacturer's instructions. A T100™ thermal cycler (Bio-Rad, Hercules, CA, USA) was used for RT incubation; the cDNA obtained was stored at -20°C.

Quantitative-PCR for mRNA: Real-time qPCR reactions were performed in duplicate using: 5 µl of diluted cDNA from previous RT, 0.5 µl of specific forward (fw) and reverse (rv) primers (10 µM), 6.25 µl of GoTaq ® qPCR master mix (Promega) and 2.75 µl of nuclease free water. A reference gene, *Rps11,* was measured together with the target gene for standardization of the

RNA levels. Primer pairs employed are listed in **Table 2**. In addition to RT negative controls, a blank control was added to the plate. Standard curve, generated from serial dilutions of a cDNA reference pool, was also included to correct the obtained Ct values and to estimate the efficiency of the primers, that was evaluated with the qPCR efficiency calculator online tool (Thermo-Fisher). qPCR reactions were performed following GoTaq® manufacturer instructions in a CFX96™ Real-Time PCR thermocycler (Bio-Rad, Hercules, CA, USA).

Target		*Sequence 5'-3'*	*Annealing temperature (°C)*	*Amplicon size*
Kiss1	Fw	GCTGCTGCTTCTCCTCTGTG	61°	138 pb
(NM_181692.1)	Rev	GCATACCGCGGGCCCTTTT		
Grk2	Fw	TTCGGTGAGGTCTATGGG	53°	142 pb
(NM_012776.2)	Rev	CAGTGCTGACGAGGGAAA'		
Rps11	Fw.	CATTCAGACGGAGCGTGCTTAC	58°	240 pb
(NM_031110.1)	Rev	TGCATCTTCATCTTCGTCAC		

***Table 2**: Primers used in qPCR for the determination of Kiss1 and Grk2.*

Quantitative-PCR for miRNA: Immediately before reaction, cDNA samples were 1:60 diluted, and 3 µL were employed as cDNA starting material, as recommended by manufacturer. LNA™ primers rno-miR-137-3p, rno-miR-325 (Qiagen) and GoTaq ® qPCR master mix (Promega) were used, following manufacturer instructions, to perform the reaction in a CFX96™ Real-Time PCR thermocycler (Bio-Rad, Hercules, CA, USA). A reference gene, U6 snRNA, was measured in parallel, to perform relative expression normalization of our target miRNAs, by following the ΔCt method with a reference gene [255].

6.3. RT reactions and qPCR from cells

Previously to RT and qPCR reactions, RNA material obtained from lysates of cells isolated with FACS (Fluorescence Activated Cell Sorting) methodology (described in section 6.10), was inter-sample equalized considering as reference the lowest number of cells obtained per sample, in order to homogenize the starting amount of RNA material between different samples.

Retrotranscription reaction for mRNA and miRNAs from cells: 10 µL/3 µL (for mRNA/miRNA, respectively) of the inter-sample equalized cell lysate, were used as RNA starting material. Manufacturer's instructions were followed for mRNA RT reactions with the High-Capacity cDNA Reverse Transcription Kit (#4368814, Applied biosystem™, USA), where 10x random primers were included in the kit. For higher sensibility, miRNA RT reaction was performed following the TaqMan microRNA Assay (#4366596, Applied biosystem™, USA) instructions. For miRNA assay, TaqMan assay 5x specific primers are needed to perform target specific stem-loop RT and were independently purchased. Mmu-miR-137-3p (TaqMan™ MicroRNA Assay, #4427975, ID:

001129; Applied biosystem™, USA) and SNU6 RNA (TaqMan™ MicroRNA Assay, # 4427975- ID: 001973; Applied biosystem™, USA) primers were pooled in TE 1X buffer, as described by the manufacturer's instructions, prior to the performance of the RT in a T100™ thermal cycler (Bio-Rad, Hercules, CA, USA). The cDNA obtained was stored at -20°C.

qPCR for miRNA and mRNA from cells: Quantitative PCRs were performed with 2 µL of the previously synthesized cDNA material, using the TaqMan Universal Maser mix II (Thermo Fisher, Scientific Waltham, MA). Following the manufacturer instructions, amplification was carried out in CFX96™ Real-Time PCR thermocycler (Bio-Rad, Hercules, CA, USA). TaqMan® Gene Expression Assay primers (Applied biosystem™, USA) employed for mRNA quantification were: Kiss1 (#4331182, ID: Mm03058560_m1) and GAPDH (#4331182 ID: Mm99999915_g1). For miRNA analysis, TaqMan® MicroRNA Assays 20x primers (Applied biosystem™, USA) were employed: Mmu-miR-137-3p (TaqMan™ MicroRNA Assay, #4427975, ID: 001129; Applied biosystem™, USA) and SNU6 RNA (TaqMan™ MicroRNA Assay, # 4427975- ID: 001973; Applied biosystem™, USA). Calculation of expression levels of each target was conducted with the ΔCt method with a reference gene [255]. GAPDH and U6 snRNA served as the internal reference for mRNA or miRNA analyses, respectively.

6.4. Radioimmunoassay

Serum LH and FSH levels were measured using RIA kits supplied by the National Institutes of Health (Dr. A. F. Parlow, National Hormone and Peptide Program, Torrance, CA, USA). Hormonal determinations were performed in duplicates. Rat LH-I-10 and FSH-I-9 were labelled with ^{125}I by the chloramine-T method, and hormone concentrations were expressed using reference preparations LHRP-3 and FSH-RP-2 as standards. Intra- and inter-assay coefficients of variation were less than 8% and 10% for LH and 6% and 9% for FSH, respectively. The sensitivity of the assay was 5 pg/tube for LH and 20 pg/tube for FSH. Accuracy of hormone determinations was confirmed by assessment of rat serum samples of known concentrations (used as external controls).

Testosterone levels from serum samples were determined using the ImmuoChem™ Testosterone Double Antibody RIA Kit (MP07189102, MP Biomedical™, USA). Intra and inter assay coefficients of variation were 10% and 11%, respectively. The sensitivity of the assay was 0.1 ng/mL.

6.5. ELISA assays

6.5.1. LH ELISA assay

LH levels from samples obtained through tail-tip collection were assessed by employing a super-sensitive LH Enzyme -Linked Immunosorbent Sandwich (ELISA) assay [256]. First, coating was performed in 96-well plates (Costar Assay Plate, 96 well, Corning) that were covered with 50 µL of capture antibody (monoclonal antibody 518B7, bovine LHβ, from Lillian E Sibley, UC Davis) diluted 1:1000 in PBS 0.1M. Plates were incubated overnight at 4°C in a humidity chamber. The following day, blocking step for 2 hours was done at room temperature (*RT*) by adding 200 µL of blocking buffer (5% skim milk powder in PBS-T (0.1M PBS and 0.05% Tween-20, pH 7.4)). Standard curves were prepared by performing 1:2 serial dilutions of LH reference, rLH-RP3 (AFP5306A; from Dr. A.F. Parlow, National Hormone and Pituitary program, CA, USA) in PBS-T. After washing steps, 50 µL of standards and samples were loaded into the plate and were incubated 2 hours at *RT* with constant shaking. 50 µL of polyclonal antibody AFP240580Rb (from Dr. A F Parlow, National Hormone and Pituitary Program, CA, USA) diluted 1:10000 in blocking buffer was added. After 1.5 hours and washing steps, secondary antibody (P-0048 Dako Cytomation polyclonal goat anti-rabbit IgG/HRP; 1:1000 diluted in 50% PBS 1X and 50% blocking buffer) was incubated during 1.5 hours at *RT* and agitation. 100 µL of OPD (o-phenylenediamine, Sigma-Aldrich Corp., St. Louis, MO) diluted in citrate buffer with 0,1% of H_2O_2, were added to the plate after washing steps and was incubated during 30 minutes at room temperature. Reaction was stopped by adding 50 µL of HCl 3M. Absorbance was read at 490 nm and at 665 nm (for subtraction of the background) in a Bio-Rad iMARK™ microplate reader. Sensitivity of the assay was 0.002 ng/mL. Concentrations were obtained by interpolation using a sigmoidal dose-response curve. Pulse peak was determined as a LH rise 125% over the basal ones (determined as the mean of the 5 lowest LH levels), in keeping with previous references [251].

6.5.2. Insulin and leptin serum levels

Insulin levels in serum from rats were measured with the Rat ELISA kit (80-INSRT-E01; American Laboratory Products Company, ALPCO, USA). Sensitivity of the kit was 0.124 ng/mL and, coefficient of intra-assay and inter-assay variation were 5.05% and 7.9, respectively.

Leptin levels in serum from rats were measured with the Rat Leptin ELISA kit (90040, Crystal Chem Inc., Elk Grove Village, Illinois, USA). Sensitivity of the kit was 0.2 ng/mL and coefficient of intra-assay and inter-assay variation were <10%.

Insulin and leptin levels in serum from mice were measured with the MILLIPLEX MAP Mouse Adipokine Magnetic Bead Panel - Endocrine Multiplex Assay (Millipore, Merck KGaA, Darmstadt,

Germany). Sensitivity of the assay was 13 pg/mL for insulin and 4.2 pg/mL for leptin. Intra and inter-assay variation were <10% and <20%, respectively.

6.6. Western Blot

Protein samples were obtained: 1) by processing of hypothalamic samples with RIPA buffer (Canvax Biotech, S.L, Cordoba, Spain); or 2) by precipitation with acetate of the flow through obtained with mRNA Purification kit (Favorgen). Protein concentration was determined using RC DC™ Protein Assay (Bio-Rad), to equalize concentration levels between samples. Before performance of western blot, absorbance of the assay was quantified by spectrophotometry (Beckman DU530). Twenty µg of protein per sample were submitted to SDS-PAGE on 7% polyacrylamide gels, electro-transferred on polyvinylidene difluoride (PVDF) membranes (Millipore) and probed overnight at 4°C. Primary antibodies employed for the immunodetection of kisspeptins, NKB and GRK2 were as follows: anti-kisspeptin, diluted 1:200 (ab226786, Abcam); anti-NKB diluted 1:500 (ab123388, Abcam) and anti-GRK2 diluted 1:500 (sc-562, Santa Cruz Biotechnology Inc.). Protein levels were normalized to β-actin, with anti- β-actin primary antibody diluted 1:5000 (A5060, Sigma Aldrich); or to GAPDH, with anti-GAPDH diluted 1:500000 (ab181602, Abcam). Anti-rabbit horseradish peroxidase-conjugated secondary antibody (ab6721, Abcam) was incubated for 90-min and WBs were developed with chemiluminescence ECL Western Blotting Substrate (Thermo Scientific). Densitometric analysis of protein bands were conducted using the open-source image processing software, ImageJ (https:// imagej.net/Image; Image Processing and Analysis in Java, National Institutes of Health).

6.7. Determination of plasma cytokines

Changes in serum relative levels of cytokines were determined using Proteome Profiler Arrays (Proteome Profiler™ #ARY030 R&D Systems, Minneapolis, MN, USA). Serum samples were pooled (130 µL) and loaded in the array membranes to detect differentially expressed cytokine levels, following the manufacturer's instructions. The average signal of the pair of duplicate spots, representing each detectable protein, was calculated after subtraction of background values (pixel density) from negative control spots and was normalized to average values from positive control spots by using HLImage++ software (Version 22.0.0a; R&D Systems, Minneapolis, MN, USA).

6.8. Immunohistochemistry (IHC)

Brains were cut (30 µm) and divided in four sets of coronal sections in a freezing microtome (Leica CM1850 UV). One set was employed for identification of correctly infected mice, by performing single immunofluorescence against mCherry; another set was used for double GFP-mCherry immunofluorescence; and a third set was employed for double detection of mCherry and kisspeptin/NiDAB (rabbit anti Kp nº 566; gift from A. Caraty, Physiologie de la Reproduction et des Comportements-Institut National de la Recherche Agronomique, Nouzilly, France). The antibodies used were from Abcam, Jackson Immuno Research, Thermo Fischer and PhD. Caraty, as listed in **Table 3** and **Table 4**.

Name	*Reference*	*Host specie*	*Dilution*
Anti-mCherry	Ab205402	Chicken	1:2000
Anti-mCherry	Ab183628	Rabbit	1:2000
Anti-GFP	Ab13970	Chicken	1:2000
Anti-Kp	Caraty, nº566	Rabbit	1:10000

Table 3: *Primary antibodies used for IHC.*

Name	*Reference*	*Host specie*	*Dilution*
Biotin-SP conjugated anti-chicken	Jackson, 703066155	Goat	1:200
Biotin-SP conjugated anti-rabbit	Jackson, 711066152	Goat	1:500
Alexa Fluor 555 anti-chicken	Thermo Fisher, 1917941	Goat	1:1000
Alexa Fluor 594 anti-rabbit	Thermo Fisher A21207	Goat	1:1000

Table 4: *Secondary antibodies used for IHC.*

First, antigen retrieval was done in 10mM sodium citrate buffer, pH 6, for 10 min at 90°C. Containers were cooled down under cold running tap water. Sections were blocked for 1 hour in 0.1 M glycine and 4% donkey serum diluted in TBS 1X/0.3 % Triton/0.25 % BSA. Sections were incubated with the primary antibody diluted in incubation buffer (TBS 1X/0.3 % Triton/0.25 % BSA/Sodium Azide 0,01% and 2% donkey serum). Primary antibody incubation lasted 90 minutes at *RT* for single detection or 72 hours at 4°C for double antibody detection. After three TBS 1X washes, the sections were incubated with the secondary antibodies (sequentially if double-labelled) diluted in incubation buffer without azide, during 90 minutes at *RT*. For single immunofluorescence of mCherry, samples were incubated for 3 h with Alexa Fluor 555, then washed and mounted with Fluoroshield (Sigma; F6057) mounting medium. For double labelling of GPF and mCherry, GFP secondary antibody was first incubated (Biotin-SP conjugated anti-chicken), three washes were performed, and sections were incubated with Vector Elite ABC peroxidase kit (Vector Laboratories) for 90 minutes. Then, tree washes were done and sections

were incubated 10 minutes with Alexa Fluor 488 Tyramide Superboost (Fisher, B40932). Next, samples were incubated for 3 hours with Alexa Fluor 594 anti-rabbit, washed and mounted with Fluoroshield. For double labelling of mCherry and Kp/NIDAB, Biotin-SP conjugated anti-rabbit was employed as secondary antibody anti-Kp. After ABC peroxidase step, samples were incubated with glucose oxidase and NiDAB for 20 minutes, washed, and incubated with Alexa Fluor 555 anti-chicken, as previously described. Finally, samples were washed, and dehydrated before mounting them with Eukitt mounting medium (ITW Reagents, 253681).

Images were taken with Leica DM2500 microscope. Kisspeptin was quantified using ImageJ. Representative sections of the arcuate nucleus were selected for every animal, including controls. For kisspeptin, images were binarized by applying the same threshold to everyone. After delimitation of the area of interest, percentage of kisspeptin signal was registered for every side of the brain section, as well as the number of mCherry expressing cells, which were visually estimated.

6.9. RNAscope

RNAscope® Multiplex v.2 (ACDbio) *in situ* hybridization was employed for the co-detection of Grk2 and GnRH mRNA in GnRH neurons from POA region of hypothalamus of the G-GRKO mice. Whole brains from young female mice (n=4/group) were frozen and stored. By using a freezing microtome (Leica CM1850UV), brain coronal sections of 20 µm were cut and distributed into four sets of slides containing the main hypothalamic areas where GnRH neurons are located (medial septum and medial preoptic area). Sets of brain sections were fixed for 30 minutes in PFA 4% prior to dehydration. Four representative brain sections per group were selected for RNAscope assay, as well as two sections for positive and negative controls. RNAscope Multiplex v.2 protocol was followed as recommended. Briefly, cells from brain sections were permeabilize and pre-treated to unmask target RNA. Next, RNAscope probes were incubated for 2 hours to hybridize the target mRNA. For Gnrh mRNA hybridization, predesigned RNAscope® Probe- Mm-Gnrh1-O1 (ACDbio) was employed. Custom RNAscope® Probe- Mm-GRK2-C2 (ACDbio) was designed to target mRNA nucleotides corresponding to the LoxP flanked Grk2 sequence, ablated by the Cre recombinase activity in the G-GRKO double mutant mice. After washing, RNAscope reagents amplify the hybridization signals by consecutive amplifiers incubations. For detection of the mRNA probes, opal dye fluorophores (AKOYA biosciences, USA) were added. Opal dye 480 (1:350) and 570 (1:500) were employed for Gnrh and Grk2 visualization, respectively. Finally, sections were cover slipped with Fluoroshield™ with Dapi histology mounting medium (F6057, Sigma). *In situ* hybridization was visualized on a Zeiss LSM 710 confocal microscopy system using 63X lens, in the Unit of Micoscopy of IMIBIC. To search for co-localization, confocal images and

six Z-stacks were taken. For quantification of Gnrh-Grk2 co-localization, Mander's Coefficient was calculated with JaCop plug-in (ImageJ). Number of Grk2 co-localization events per GnRH neuron were counted in control neurons (n=13) and G-GRKO neurons (n=24) after region of interest (ROI) determination; 3D-images were obtained with 3D-viewer plug-in (ImageJ). Decrease in the number of events occurrence in G-GRKO neurons (co-localization events in control neurons minus co-localization events in G-GRKO neurons) was calculated prior to the estimation of the reduction in the percentage of co-localization events in G-GRKO neurons, as quotient of decrease in the number of events in G-GRKO neurons by total number of events in control neurons x 100.

6.10. Fluorescence-activated cell sorting

Fluorescence-activated cell sorting (FACS) was performed in enzymatically dissociated hypothalamic samples from mice. First, mice were intraperitoneally anesthetized with ketamine/xylazine (2:1 ratio) and intracardially perfused with cold artificial cerebrospinal fluid solution. Brains were extracted to dissect the hypothalamus from the *Kiss*$^{Cre:EYFP}$ mice, which were stereotaxically injected previously with viruses harboring vectors expressing miR-137-3p and mCherry under Cre activity. To perform digestion of the tissue, MBH isolation was done in cold aCSF, and was incubated for 50 minutes at 37°C in aCSF-enzymatic solution containing 20 units/mL of papain (PDS Kit, LK003176, Worthington) and 0.005% of DNase I (LK003172, Worthington). Next, tissues were mechanically dissociated by slow and soft pipetting, with progressive decreasing calibers. Then, homogenates were washed, filtered, centrifuged at 200g for 5 minutes at 4°C, and resuspended in 500 µL of recovery solution (HBSS 1X, 5% glucose, 0,2% BSA, 0,02% HCO_3^- in H_2O DEPC). Immediately, samples were placed on ice, and sorted with a FACS Aria III (Becton Dickinson) cell sorter at the Unit of Cytometry of IMIBIC. Purified cells were lysated (0.01% Triton-X, 35U RNasin®- Promega- in H_2O DEPC) to study RNA expression by TaqMan PCR analysis.

6.11. *In vitro* validation of miRNA repression

To confirm the regulatory action of miR-137-3p and miR-325-3p over the 3'UTR of *Kiss1*, the Secrete-Pair dual luciferase assay was performed in HEK293 cells (human embryonic kidney cells) in collaboration with the group of Prof. Marco A. Calzado, from the Department of Cell Biology, Physiology and Immunology of the University of Córdoba, Spain. Kiss1 3'UTR Gaussia luciferase (Gluc) reporter construct (217HmiR010098-MT05), precursor expression plasmid for hsa-miR-137-3p (217HmiR0011-MR04-B), precursor expression plasmid for hsa-miR-325- (217MmiR33334-MR04) and precursor miRNA scrambled control plasmid (217CmiR0001-MR04)

were obtained from Gene-Copeia (Rockville, MD, USA). Transient transfections were performed with Rotifect (Carl Roth, Karlsruhe, Germany) according to manufacturer's instructions (Promega, Madison, WI, USA).

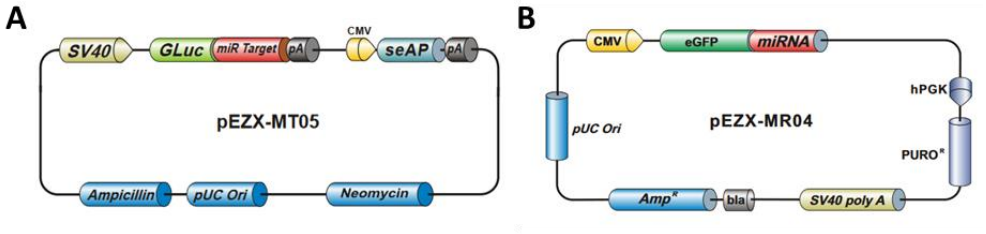

Figure 21. A) *KISS1 miTarget expressing vector (pEZX-MT05, picture taken from GeneCopeia).* ***B)*** *Precursor miRNA expression vector for hsa-mir-137-3p or has-miR-325-3p (pEZX-MR04 vector; picture taken from GeneCopeia).*

In detail, Secrete Pair Dual Luminescence Assay was performed following the manufacturer's instruction. HEK293 cells were maintained in DMEM (Dulbecco's modified Eagle's medium; Life Technologies, Grand Island, NY, USA) supplemented with 10% FBS (fetal bovine serum), 2 mM L-glutamine and 1% (v/v) penicillin/streptomycin at 37°C in a humidified atmosphere containing 5% CO2. Cells were co-transfected with (i) *Kiss1* 3'UTR Gluc reporter construct, (ii) *Kiss1* 3'UTR Gluc and scrambled miRNA vectors, (iii) 3'UTR control construct and hsa-miR-137-3p/hsa-miR-325-3p expression vector and (iv) *Kiss1* 3'UTR Gluc construct and hsa-miR-137-3p/hsa-miR-325-3p expression vector, at a concentration ratio 1:4 (250ng:1000ng), respectively. Transfections were performed using three replicates for each experimental condition. Cells were collected in PBS after 24h and lysate following the instructions of the luciferase assay kit. Luciferase activity was measured using an Autolumat LB 9510 (EG&G Berthold, USA).

6.12. *In vitro* calcium mobilization assay

Intracellular calcium mobilization responses were determined in collaboration with the group of Prof. Ursula B. Kaiser, from the Division of Endocrinology, Diabetes and Hypertension, Brigham and Women's Hospital, Harvard Medical School, USA, following their previously described protocol [257]. HEK293T-GPR54 were plated in black-walled, clear-bottom 96-well plates. They were washed with DMEM and Ham's F-12 Nutrient Mixture (DME/F12) and incubated in serum-free DME/F12 for 2 hours at 37°C before the beginning of the experiment. To measure intracellular calcium (Ca^{2+}) concentrations, the Fluo-4 Direct Kit (Invitrogen) was used. Next, cells were treated with Kp-10 (0 nM or 10 nM) and β-ARK1-I (0 µM or 150 µM) according to the design of the experiment 10. Then, changes in fluorescence activity were measured with POLARstar OPTIMA multifunction plate reader (BMG Labtech). Measurements were repeated every 15 seconds for 20 cycles. The intracellular calcium response was determined by calculating the ratio of the difference between the maximum and minimum fluorescence units over the minimum fluorescence units (relative fluorescence activity, RFI).

7. Bioinformatic analysis

MicroRNA prediction

With the aim to identify putative regulators of *KISS1/Kiss1* gene, we searched in several online available databases, in which the prediction algorithms and classification scores are based on different approaches listed in **Table 5**.

Method	Prediction and score based on	Web
TargetScan	Evolutionary conservation of binding site (sequence based)	https://www.targetscan.org/vert_80/
MiRDB	MiRTarget prediction algorithm (sequence based)	https://mirdb.org/
MicroT-CDS	MicroT algorithm (thermodynamic and evolutionary approach)	https://dianalab.e-ce.uth.gr/html/dianauniverse/index.php?r=microT_CDS
miRanda	Complementarity and thermodynamic stability	http://www.ebi.ac.uk/enrightsrv/microcosm/cgi-bin/targets/v5/search.pl
MirMap	Thermodynamic, evolutionary, probabilistic and sequence based	https://mirmap.ezlab.org/
MiRWalk	TarPMiR algorithm (sequenced based and experimentally verified interactions)	http://mirwalk.umm.uni-heidelberg.de/
RNAhybrid	Thermodynamic and sequence-based	https://bibiserv.cebitec.uni-bielefeld.de/rnahybrid/

Table 5: *Main miRNA databases employed.*

Genomic variant search

To corroborate miRNA functional role observed *in vivo* in animal models, with a functional role in humans, we inquired into several online available databases (**Table 6**). Our aim was to find genomic variants related with miRNA expression and associated phenotypes of altered puberty or reproductive function.

Database	Information provided	Web
Precocity DB	SNPs, pathways and ontology related with precocious puberty (manually curated)	https://precocity.bicnirrh.res.in/
Database of Genomic Variants (DGV)	Structural alterations in DNA (larger than 50 bp) in healthy controls	https://dgv.tcag.ca/dgv/app/home
gnomAD	Aggregation of exome and whole genome sequences form different disease-specific, population studies	https://gnomad.broadinstitute.org
Varsome	Tool for genomic variant calling. Add genomic context of the variant, related bibliography, regions of interest and ClinVar database information	http://varsome.com/
ClinVar	Genomic variation and its relationship with human health	https://www.ncbi.nim.nih.gov/clinvar
Decipher	Scientific resource with phenotypic and genotypic information from patients affected with any disorder.	http://www.deciphergenomics.org/
GTEX	Open access to gene expression, QTLs and histology images from human tissues	https://gtexportal.org/home

Table 6: *Genomic variants and gene expression online databases employed.*

8. Statistical analysis

8.1. General analyses

Statistical analyses were performed using Prism software (GraphPad Prism version 8.0 for Windows, GraphPad Software, La Jolla, California, USA, www.graphpad.com). Data represent mean ± SEM. The difference between two groups was analyzed by the unpaired Student t-test or paired Student T-test for repeated measures. Welch t-test correction was applied when SDs between groups were unequal. Differences between several groups were analyzed by one-way ANOVA (ANOVA) test followed by the Holm-Sidak test or Student-Newman-Keuls multiple comparison test. When comparing the influence of two different independent variables, experimental groups were subjected to two-way ANOVA (2-way ANOVA) followed by Student-Newman-Keuls multiple comparison test. P value of < 0.05 was considered statistically significant.

8.2. Area under the curve

Area under the curve (AUC) was calculated as integral measurement of glucose and insulin levels, in the case of GTT and ITT, or as integral measurement of hormonal secretion (for LH, FSH and T) over an intervention period. AUC represents mg/dL/min for glucose and insulin tolerance tests, in which time points of level determination were 20, 60 and 120 minutes since bolus injections of glucose or insulin. AUC represents ng/mL/day for LH, FSH and T from experiments 8, 9 and 21. In experiments 8 and 9, hormonal determination was done every 4 days during the 16 days of treatment. In experiment 21, hormonal determination was done in sequential intervals of 2, 3, 5 and 9 days through the 14 days of the experiment. AUC represents ng/mL/min for LH and FSH levels in experiments 15, 19, 20 and 22. In experiment 15, hormonal levels were determined after 15 and 60 minutes from the icv injection of Kp-10. In experiment 19, AUC was obtained from sampling every 5 minutes for 3 hours. In experiment 20, AUC was assessed during 4 hours with hormonal determination after 15 and 60 minutes from Kp-10 bolus injections. In experiment 22, AUC was assessed every 7 days for 28 days.

9. EXPERIMENTAL DESIGNS

The description of the experimental designs will be divided in four parts according to the objectives of the Thesis and their presentation in the section of Results. At the same time, each part will be subdivided in sets where groups of individual experiments will be displayed.

PART 1. MICRORNAS AND THE PHYSIOLOGICAL CONTROL OF PUBERTY

EXPERIMENTAL SET 1: Analyses of the hypothalamic expression of miR-137-3p, miR-325-3p and *Kiss1* during normal pubertal maturation and in models of perturbed puberty

After bioinformatic identification of potential miRNA regulators of *Kiss1* expression, our first set of experiments was focused on the analysis of the hypothalamic expression of the selected candidates, miR-137-3p and miR-325-3p, and the correlation with expression levels of *Kiss1*, in hypothalamic samples, both during normal postnatal development and in models of delayed puberty, due to postnatal underfeeding, chronic postweaning undernutrition and modification of the sex steroid milieu.

Experiment 1: Hypothalamic expression of miR-137-3p, miR-325-3p and *Kiss1* during postnatal development

The expression levels of miR-137-3p, miR-325-3p and *Kiss1* were assessed during early ontogeny in the following stages of female Wistar rats: neonatal stage (NEO; PND1 to PND7), infantile stage (INF; PND8 to PND20), juvenile stage (JUV; PND21 to PND32) and peripubertal stage (PUB; PND33 to PND37) in whole or divided hypothalamus (POA and MBH, n=3-10). Protein expression levels of kisspeptin were assessed at PND1 (NEO stage), PND10 (INF stage), PND20 (late INF stage), PND28 (JUV stage) and PND32 (late JUV/peripubertal stage) age (n=4). After decapitation of the animals, the whole hypothalamus, POA or MBH were isolated from the brain, frozen on liquid nitrogen and stored at -80°C until further processing, for qPCR or WB **(Figure 22).**

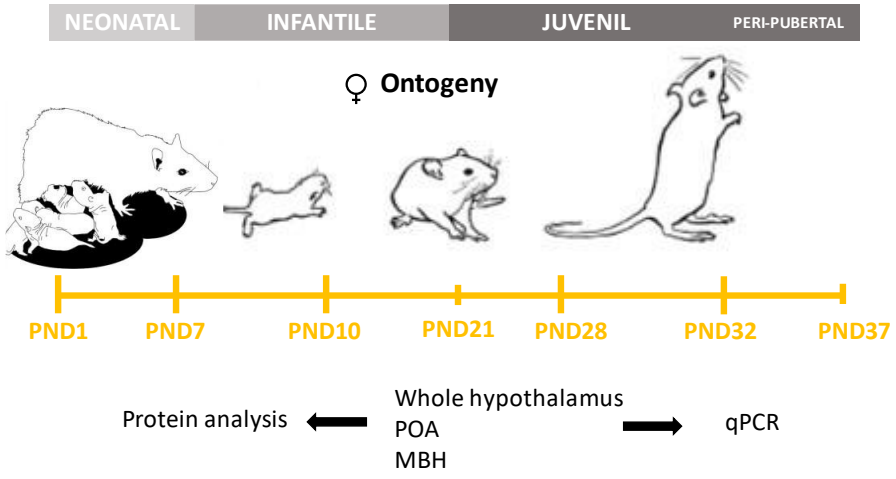

Figure 22. *Schematic representation of the Experiment 1, presenting PND of tissue collection.*

Experiment 2: Hypothalamic expression of miR-137-3p and miR-325-3p in models of delayed puberty

Since it is known that *Kiss1*/kisspeptin and LH levels, as well as timing of puberty, are affected in conditions of nutritional deprivation or modification of the sex steroid milieu [47], we explored expression profiles of our candidate miRNAs in different nutritional deprivation conditions, or after modification of the sex steroid milieu, previously validated as models of delayed puberty[5,258]. Hypothalamic samples were extracted, frozen on liquid nitrogen and stored at -80°C until processing for RNA extraction **(Figure 23)**. The following models were used.

Postnatal undernutrition. Female rats were subjected to postnatal underfeeding by rearing them in large litters (LL, 20 pups/mother), as this is proven to be a model of delayed puberty [5] when compared to control group reared in normal litters (NL, 12 pups/ mother). After weaning, female rats were fed *ad libitum* and euthanized at PND35 (n=4-6).

Peripubertal subnutrition. As model of caloric restriction post-weaning, peripubertal female rats (PND23-PND35) were submitted to a 30% caloric restriction of their daily food ration in comparison to pair aged rats fed *ad libitum* (n=5-9).

Neonatal sex steroid milieu manipulation. Neonatal female rats were submitted to supra-physiological doses of EB or TP to disrupt brain sexual differentiation in order to alter puberty onset and gonadotropic function [47]. Female rats (n=4-8) were injected subcutaneously (s.c.) on PND1 with olive oil (controls), EB dissolved in olive oil (10 µg /rat) or TP dissolved in olive oil (10 µg/rat).

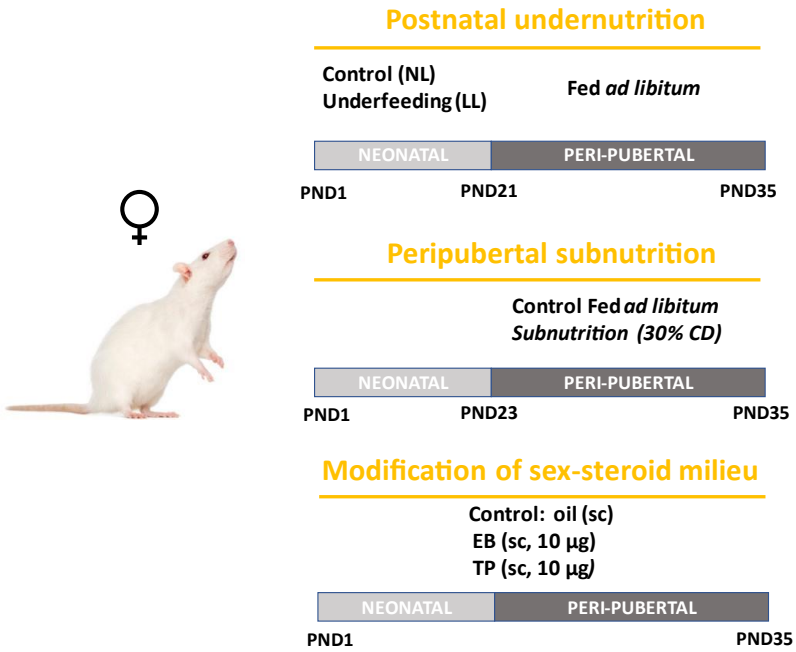

***Figure 23**. Schematic representation of the **Experiment 2**, showing the models of delayed puberty employed. EB: Estradiol benzoate; TP: Testosterone propionate.*

EXPERIMENTAL SET 2: Analyses of the functional role of miR-137-3p/miR-325-3p/Kiss1 pathway in the central control of puberty

The next set of experiments aimed to provide functional evidence for the potential role of the miR-137-3p/miR-325-3p/Kiss1 pathway in the central control of puberty, by using *in vivo* experimental approaches.

Experiment 3: Central administration of miRNA mimic nucleotides in prepubertal female rats

Evidence of the *in vivo* functional role of miR-137-3p and miR-325-3p in the regulation of *Kiss1* expression - and subsequently their implication in the control of puberty-, was further assessed by the employ of synthetic nucleotide sequences, miRCURY LNA miRNA Mimics. We injected them icv daily during the juvenile-peripubertal period (from PND25 to PND35), in order to evaluate the effects of mimicking the actions of endogenous miRNAs on *Kiss1* expression and pubertal development **(Figure 24)**. MiRNA mimics simulate naturally produced miRNAs by increasing the proportion of RISC complexes containing the guide strand miRNA. They are characterized by a design that includes three RNA strands: the miRNA guide strand with a sequence corresponding to the one annotated in miRbase and the passenger strand, that is divided in two LNA-enhanced strands. The segmented passenger strand assures that only the miRNA guide strand is loaded into the RISC complex. Mimic miR-137-3p and Mimic miR-325-3p (MiRCURY LNA miRNA mimics, Qiagen, Netherlands) were injected icv (0.2 mm posterior to bregma line; 1.2 mm lateral to bregma and 3 mm depth) after mixing the mimic with *in vivo*-jetPEI® (Polyplus®, France) in a jetPEI/nucleic acid ratio of 7, following manufacturer instructions. Doses of 40 pmol/5µL were administered daily during the period of treatment. Rats treated with vehicle (5% glucose -JetPEI) served as controls (n=7-12 per group). We recorded body weight, food intake, VO and first estrus. At the end of the experiment, we collected blood samples and hypothalamic tissue, and uterus and ovary weights were recorded and collected. Hypothalamic tissue was analyzed by WB to validate the effect of miRNA mimic on kisspeptin content.

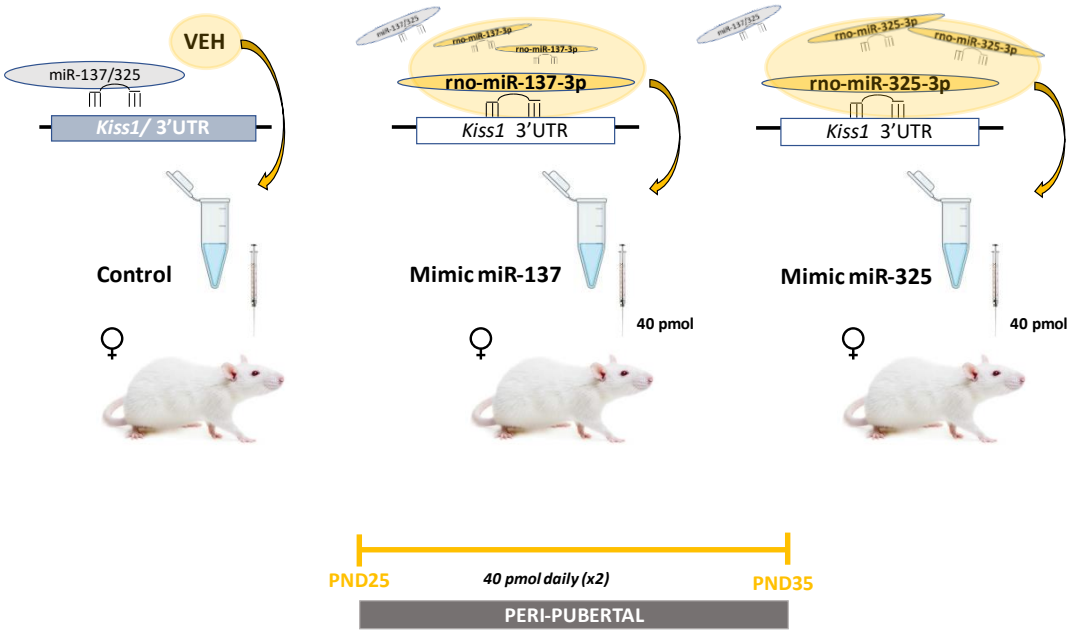

Figure 24. *Schematic representation of* ***Experiment 3****, showing the experimental groups that were analyzed.*

Experiment 4: Central administration of selective target site blockers (TSB) against 3'UTR of *Kiss1* gene in prepubertal female rats

With the aim of studying the role of endogenous miR-137-3p and miR-325-3p in the control of puberty, we implemented an experimental approach to avoid the natural binding of endogenous miR-137-3p and miR-325-3p miRNAs, specifically at the 3'UTR of *Kiss1,* by employing target site blockers (TSBs; miRCURY LNA™ microRNA Power Target Site Blocker *in vivo* use, Qiagen) for miR-137-3p and miR-325-3p binding site on 3'UTR of *Kiss1* (TSB 137/325/Kiss1; 5´TTATTGCACAAGTCTA3´ sequence). In detail, TSBs are LNA enhanced antisense oligonucleotide that bind to a specific miRNA target site of a mRNA, avoiding endogenous miRNAs to bind that site. LNA enhancement of TSB allows them to compete efficiently with the miRNA/RISC complex. Additionally, TSB/DNA mixmer avoids RNAse H-dependent degradation of mRNA and consequently increase the expression of that targeted mRNA. TSB 137/325/Kiss1 were diluted in TE buffer and were injected icv (100 pmol/5µL) once every four days, from PND24 to PND32 **(Figure 25).** TE buffer was employed as vehicle in the control group (n=11-12 per group). We recorded body weight, food intake, vaginal opening and first estrus. At the end of the experiment, we collected blood samples and hypothalamic tissue; uterus and ovary weights were recorded and collected. Hypothalamic tissue was analyzed by WB to validate the effect of TSB on kisspeptin expression.

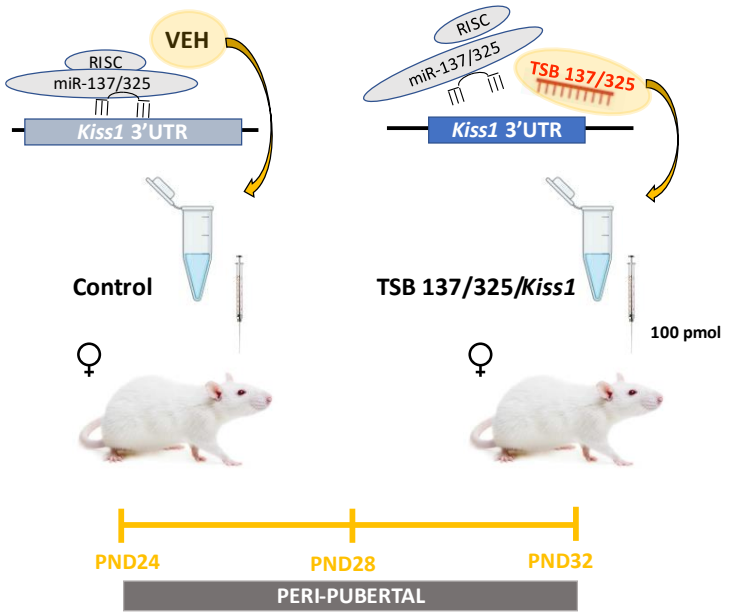

Figure 25. *Schematic representation of* ***Experiment 4****, showing the experimental groups and treatments.*

PART 2. PATHOPHYSIOLOGICAL ROLE OF MIR-137-3p AND MIR-325-3P IN MALE OIH

EXPERIMENTAL SET 3: Analyses of the functional role of miR-137-3p/miR-325-3p/Kiss1 pathway in OIH

The functional role of miR-137-3p on reproductive function during adulthood was evaluated with three different approaches: 1) by hypothalamic expression analysis of miR-137-3p in an OIH rat model; 2) by *in vivo* icv administration of miRNA mimics to adult male rats; and 3) by virogenetic overexpression, specifically in Kiss1-expressing neurons, of miR-137, using virogenetic tools in the *Kiss*$^{cre:GPF}$ and *Kiss*$^{cre:EYFP}$ mouse models.

Experiment 5: Hypothalamic expression of miR-137-3p and miR-325-3p in OIH

As a first approximation, we measured hypothalamic levels of miR-137-3p and miR-325-3p in samples collected from a previously model of OIH generated in our group. The RNA quality was checked previously to performance of RT and qPCR as previously described in the section 6.2.

Experiment 6: Central administration of miRNA mimic miR-137-3p in adult young male rats.

The central regulatory role of miR-137-3p on reproductive function was evaluated with a miRCURY LNA miRNA mimic, designed to simulate the natural miR-137-3p miRNA, administered centrally to adult young male rats, bred at NL and fed *ad libitum* (control conditions). Mimic miR-137-3p was injected icv (0.2 mm posterior to bregma line; 1.2 mm lateral to bregma and 3 mm depth) daily from PND60 to PND75, to analyze the effect on kisspeptin content and its surrogate marker, LH (**Figure 26**). Mimic miR-137-3p (MiRCURY LNA miRNA mimics, Qiagen) was mixed

with *in vivo*-jetPEI® (Polyplus®) in a jetPEI/nucleic acid ratio of 7, following manufacturer instructions. A dose of 40 pmol/5µL was administered daily during the period of treatment. Rats treated with vehicle (5% glucose -JetPEI) served as controls (n=10-12 per group). At the end of the experiment, we collected blood samples (to analyze circulating levels of LH and testosterone) and hypothalamic tissue. Hypothalamic samples were analyzed by WB to validate the effect of the miRNA mimic on kisspeptin content.

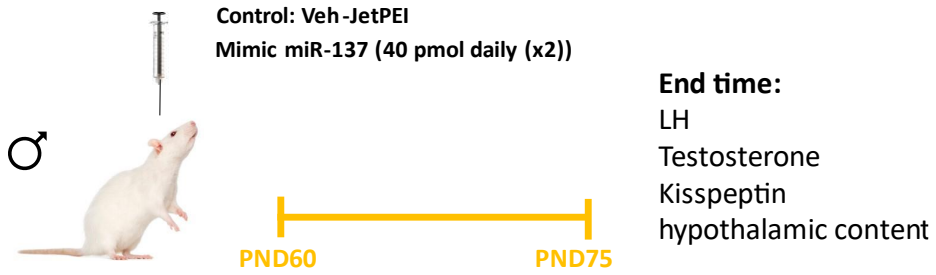

Figure 26. *Schematic representation of* ***Experiment 6****, showing the treatment employed in adult male rats.*

Experiment 7: Effects of virogenetic over-expression of miR-137 in Kiss1 neurons

To study the functional role of miR-137-3p specifically in Kiss1-expressing neurons, we performed stereotaxic injections in the ARC of the hypothalamus with a viral vector expressing miR-137-3p in the mouse lines, *Kiss*$^{Cre:GFP}$ *(v2)* and *Kiss*$^{Cre:EYFP}$.

The viral vector, VB210304-1205 XHC (Vector Builder, Chicago), was designed to contain mmu-miR-137 and mCherry reporter flanked by loxP sites, that are susceptible to be excised by the Cre recombinase that is active specifically in Kiss1-expressing cells in the above mouse models. In detail, adult *Kiss*$^{Cre:GFP}$ male mice (PND90) were bilaterally injected with 200 nL of the viral vector, titrated to 5 x 10^{12} genome copies (gc)/mL by dilution in TE buffer 1X (- 2.1 mm posterior to bregma, 0.25 mm to each lateral of the midsagittal suture and -5.9 mm, dorsoventrally). Control mice were infected with scramble viral vector containing mCherry solely, flanked by LoxP sites. Expression of the virus was allowed until PND150, when mice were sacrified. Body weight and food intake were followed weekly, body composition was analyzed before and at the end of the experiment (n=3/11 per group). At that time, blood was collected and mice were perfused to fix the brain that was intended to immunohistochemistry analysis (n=3 per group). In parallel, adult *Kiss*$^{Cre:EYFP}$ male mice (PND90) were unilaterally injected with 200 nL (2.38 x 10^{13} gc/mL) of the viral vector using the same coordinates as above and were maintained during one month (n=4 per group). After that time, mice were euthanized, hypothalami were extracted and FACS sorting was performed to isolate EYFP+ expressing neurons and EYPF+/mCherry+ neurons **(Figure 27).**

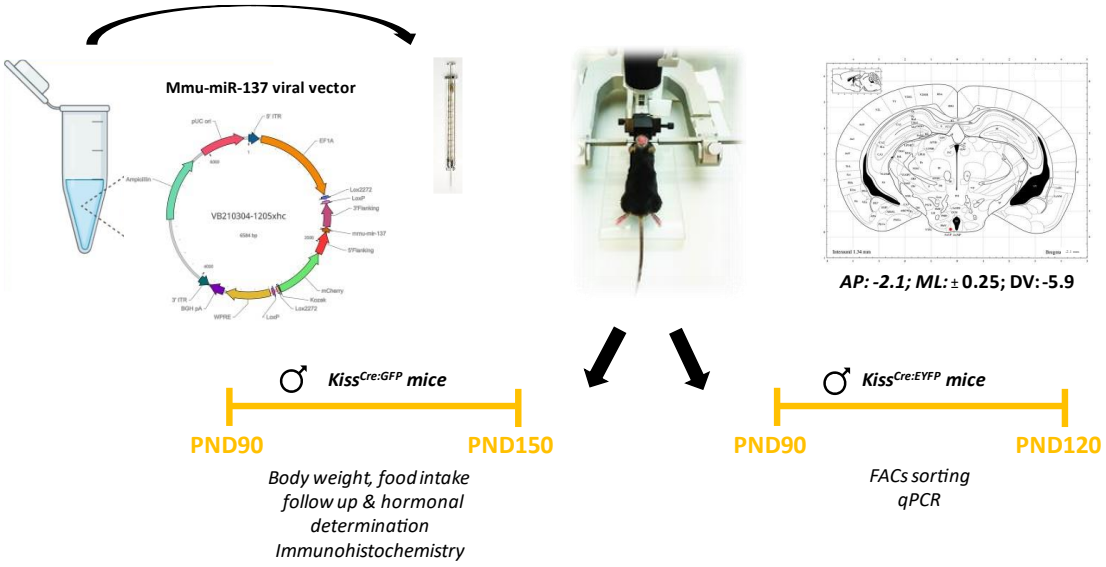

Figure 27. *Schematic representation of* ***Experiment 7****, showing stereotaxic injections of the viral vector in the mouse lines,* $Kiss^{Cre:GFP}$ and $Kiss^{Cre:EYFP}$.

EXPERIMENTAL SET 4: MiR-137-3p/miR-325-3p studies in the OIH model

This set of experiments were focus on the generation of the OIH model in male rats, where central hypogonadism was prompted via administration of an obesogenic diet post-weaning in male rats reared in small litters, as previously reported in the literature [229]. In this model, we studied the effect of central administration of TSB-miR-137-3p, Kp-10 and peripheral testosterone replacement over the hypogonadal phenotype.

Experiment 8: Generation of the male OIH model and evaluation of TSB-miR-137-3p treatment

As previously reported [229], for the generation of central OIH, male rats were randomly reared in normal litters (NL, 12 pups per mother) or in small litters (SL, 4 pups per mother) from PND1. After weaning at PND21, NL rats were fed *ad libitum* with control diet (CD; D12450B; 3.85 kcal/g: 10% of calories from fat, 20% from protein, and 70% from carbohydrate); these NL rats were employed as control group (n=12) and treated icv with vehicle (TE 1X buffer). SL rats were fed *ad libitum* with high-fat diet (HFD; D12451, 4.73 kcal/g: 45% of calories from fat, 20% from protein, and 35% from carbohydrate; Research Diets Inc) from weaning onwards. At PND150, SL/HFD rats (n=36) were allocated in 2 experimental groups and treated from PND150 to PND166, as follows: (1) SL/HFD control group (n=12) was treated with vehicle (VEH, TE 1X buffer); (2) SL/ HFD TSB 137/325/Kiss1 (n=12), was treated icv with TSB 137/325 (100 pmol/5µL) once every 4 days. Analyses in these experimental groups included pre-treatment body composition, follow-up of body weight and food intake, GTT and ITT, and SBP measurement.

During treatment, periodic blood extraction was performed an hour after treatment injection. At the end of the treatment, systolic blood pressure, body composition, GTT and ITT were assessed (**Figure 28**). Hypothalamic tissue was collected at the end of the experiment, while cardiovascular performance was analyzed in collaboration with the team of Professor Mercedes Salaices Sánchez and Ana Mª Briones, at the Department of Pharmacology of the Faculty of Medicine from Autonomous University of Madrid.

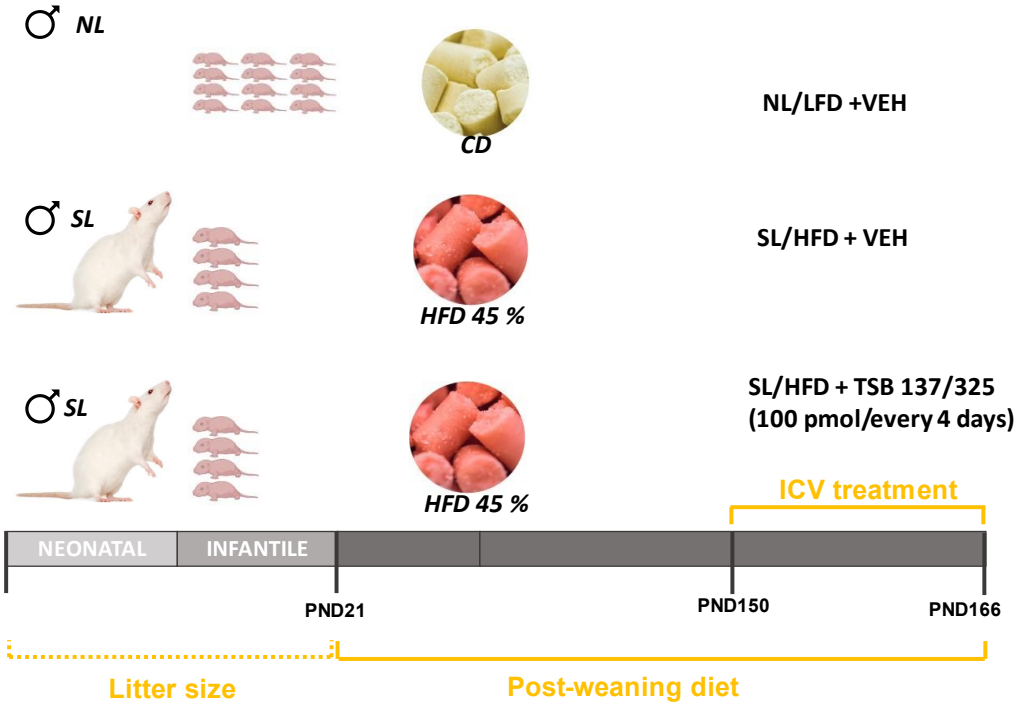

Figure 28. *Schematic representation of* ***Experiment 8****, showing the two obesogenic manipulations applied to induce OIH and the treatments applied to the experimental groups.*

Experiment 9: Kp-10 and testosterone treatments in the OIH male rat model

For the generation of central OIH, a similar protocol of sequential exposure to two obesogenic insults (SL/HFD) was applied. At PND150, SL/HFD rats (n=36) were allocated in 3 experimental groups and treated from PND166 to PND180, as follows: (1) SL/HFD control group (n=12), treated with vehicle (saline); (2) SL/ HFD Kp-10 (n=12), treated twice daily icv with 10 pmol/5µL of Kisspeptin (110–119)-NH2 (Kp-10; Phoenix Pharmaceuticals, Belmont, CA) (n=12); and (3) SL/HFD Testosterone (n=12) group, subcutaneously implanted with silastic capsules [length 2 cm; inner diameter (ID) 1.98 mm; outer diameter (OD) 3.18 mm; Dow Corning, Seneffe, Belgium] containing testosterone (T, 17β-Hydroxy-3-oxo-4-androstene; Sigma-Aldrich, St Louis, MO, USA). Phenotypic analysis included pre-treatment body composition, follow-up of body weight and food intake, GTT and ITT and systolic blood pressure measurement. During treatment blood extraction was performed one hour after treatment injection at days 1, 4, and 8 of treatment.

Systolic blood pressure, body composition, GTT and ITT were recorded and blood samples and hypothalamic tissue were collected at the end of the experiment **(Figure 29)**.

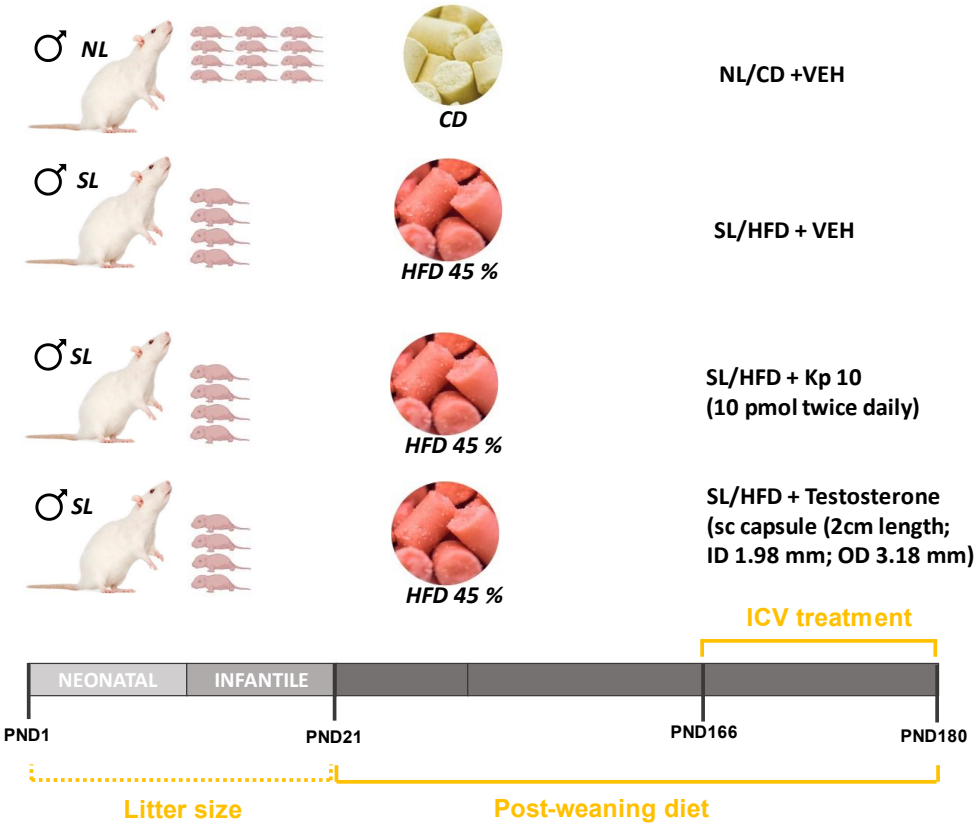

Figure 29. *Schematic representation of* ***Experiment 9****, according to the experimental groups and treatments applied.*

PART 3. GRK2 REGULATION OF Kiss1/GPR54 SIGNALING DURING NUTRITIONAL DEPRIVATION

EXPERIMENTAL SET 5: GRK2 regulation of GPR54 and the reproductive axis

In an initial set of experiments, we focused on the evaluation of GPR54 regulation by GRK2, that was assessed by *in vitro* and *in vivo* approaches.

Experiment 10: *In vitro* assessment of GRK2 control of GPR54 function

The role of GRK2 in the regulation of GPR54-mediated signaling was evaluated *in vitro* by measuring intracellular calcium responses to kisspeptin administration in the presence of the GRK2 inhibitor, β-ARK1-I, or vehicle in a HEK293T cell line, stably transfected with a vector including the coding sequence of the human kisspeptin receptor, termed HEK293T-GPR54. Cells were exposed to an effective concentration of β-ARK1-I (150 µM) or vehicle, and the Ca^{2+} mobilization responses to an effective dose of Kp-10 (10nM) were analyzed **(Figure 30)**. As reference value, cells were also exposed to vehicle or β-ARK1-I alone, to detect their basal calcium mobilization.

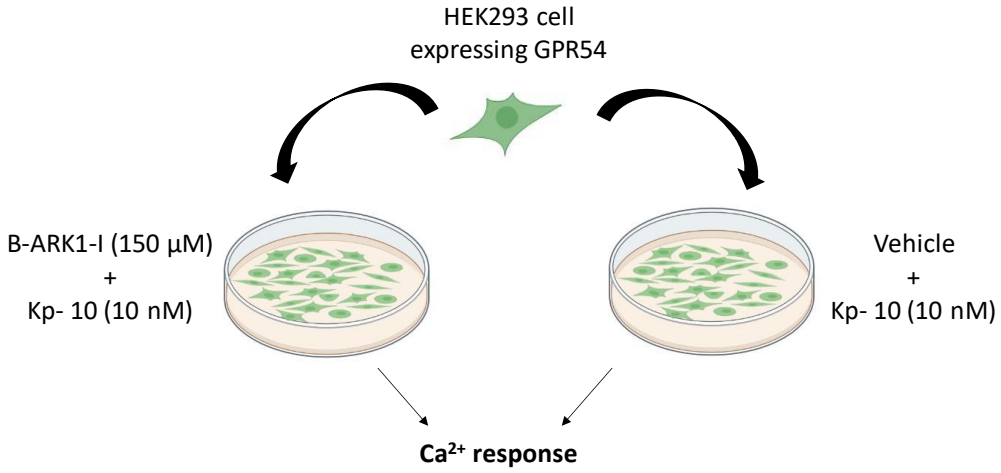

***Figure 30**. Schematic representation of **Experiment 10** showing study of Ca^{2+} response to Kp-10 in presence of β-ARK1-I or vehicle.*

Experiment 11: Assessment of regulatory actions of GRK2 on GPR54 *in vivo*

The physiological relevance of GRK2 in the modulation of *in vivo* responsiveness to major central regulators of the gonadotropic axis, acting via GPCRs, was evaluated in pubertal female rats. Thus, female rats were icv injected at PND28 with vehicle (VEH, DMSO) or GRK2-inhibitor, β-ARK1-I (6.53 nmol per injection), 13-h and 1-h before of central icv injection of a bolus of Kp-10 (1 nmol). Blood samples were obtained before (0 min) and at 15, and 60 min after icv injection of Kp-10. To test the gonadotropin-releasing effects of the agonist of NK3R, Senktide, a similar approach was used. A bolus of 600 pmol Senktide was icv injected after twice injection of β-ARK1-I (13-h and 1-h before of central icv injection of a bolus of Senktide) and blood samples were obtained at 0, 15 and 60 min for LH and FSH determinations **(Figure 31)**.

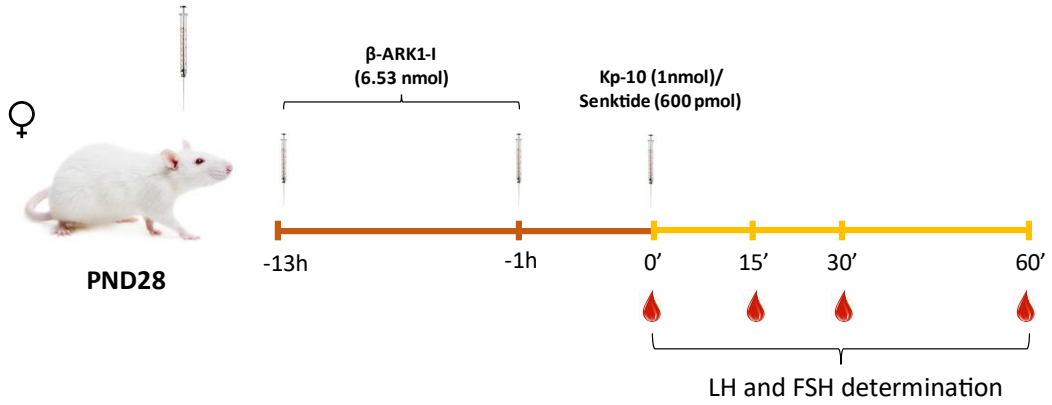

***Figure 31.** Schematic representation of **Experiment 11** showing β-ARK1-I injection before applying a single bolus of Kp-10 or Senktide to determine LH and FSH, as surrogate markers of GnRH activation.*

EXPERIMENTAL SET 6: Analysis of hypothalamic expression of GRK2 during postnatal maturation and in models of perturbed puberty

This experimental set was focused on assessment of hypothalamic expression of *Grk2*/GRK2 in rats during normal postnatal development and in models of delayed puberty. For this purpose, we used samples collected from the Experiments 1 and 2 of this Thesis.

Experiment 12. Hypothalamic GRK2 expression during normal postnatal maturation

The expression levels of *Grk2* were assessed during early postnatal maturation in the following stages of female Wistar rats: neonatal stage, infantile stage, juvenile stage and peripubertal stage), in whole or divided hypothalamus (POA and MBH, n=3-10). An additional group of adult female rats at diestrus was used for reference. Age-points for GRK2 protein levels measurement were neonatal (PND1), infantile (PND8), juvenile (PND21), late juvenile/early pubertal (PND28), and peripubertal (PND37). We refer to **Figure 22** for schematic representation of Experiment 1, as source of samples.

Experiment 13: Hypothalamic GRK2 expression in models of delayed puberty

Hypothalamic expression analyses of GRK2 were conducted in two of the models of delayed female puberty developed in Experiment 2, namely, postnatal underfeeding during lactation and chronic undernutrition during the juvenile period. In all the groups, blood and hypothalamic samples were obtained at the end of the experiment, for mRNA and protein analyses. We refer to **Figure 23** for schematic representation of Experiment 2, as source of samples.

EXPERIMENTAL SET 7: Effects of blockade of GRK2 on pubertal development

Protocols of pharmacological blockade of GRK2 or genetic elimination of its expression specifically at GnRH neurons were applied to study its effects on puberty and reproduction.

Experiment 14: Effects of pharmacological blockade of GRK2 on pubertal maturation

The impact of chronic blockade of central GRK2 signaling on the onset of puberty was evaluated in female rats. To this end, rats were icv injected with the GRK2 inhibitor (β-ARK1-I; dose: 6.53 nmol) or vehicle (DMSO), every 12 h, from PND25 to PND34. During treatment, food intake (FI), body weight, vaginal opening and first estrus were daily monitored. Animals were euthanized at PND34, when trunk blood, uterus and ovaries were collected **(Figure 32)**.

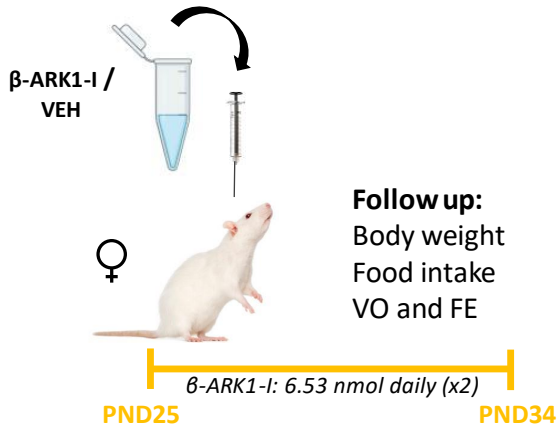

Figure 32. *Schematic representation of* ***Experiment 14*** *showing the study of the effects of GRK2 blockade on puberty by GRK2 inhibition with ß -ARK1-I.*

Experiment 15: LH responsiveness to a bolus of Kp-10 after GnRH-specific ablation of *Grk2*

Acute responses to a single bolus of Kp-10 (50 pmol; icv) were evaluated in G-GRKO and control mice. Adult males were used to allow drawing enough blood volume from repetitive sampling and to avoid the estrous cyclicity of females. Cannulation was performed as described earlier in this Methods section to deliver Kp-10 into the lateral cerebral ventricle. Blood samples were obtained before (0 min), 15- and 60-min after icv injection of Kp-10 (**Figure 33**).

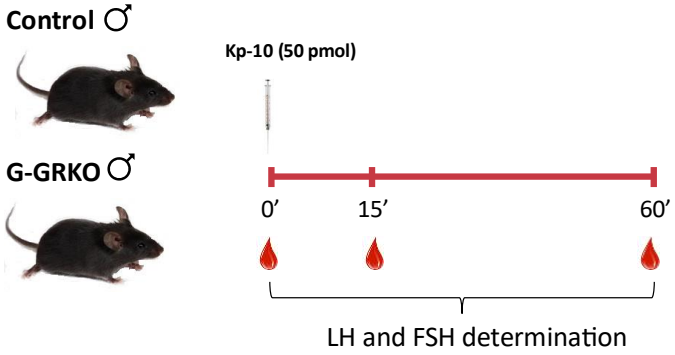

Figure 33. *Schematic representation of* ***Experiment 15*** *to analyze the acute LH response to Kp-10 in G-GRKO mice.*

Experiment 16: Conditional ablation of *Grk2* in GnRH neurons and impact on normal puberty

Similarly to experiment 14, pubertal progression was monitored in G-GRKO mice and their respective controls, by recording phenotypic markers of puberty. Body weight, food intake, VO and FE were analyzed in control and G-GRKO female mice between PND24 and PND43. Uterus and ovarian weights were also recorded, and ovarian sections were analyzed in both genotypes at the termination of the experiments (PND43). In parallel, somatic (body weight, food intake) and reproductive indices, such as BPS, as external sign of puberty, and testosterone levels, were assessed in pubertal G-GRKO male mice and their age-paired controls (**Figure 34**).

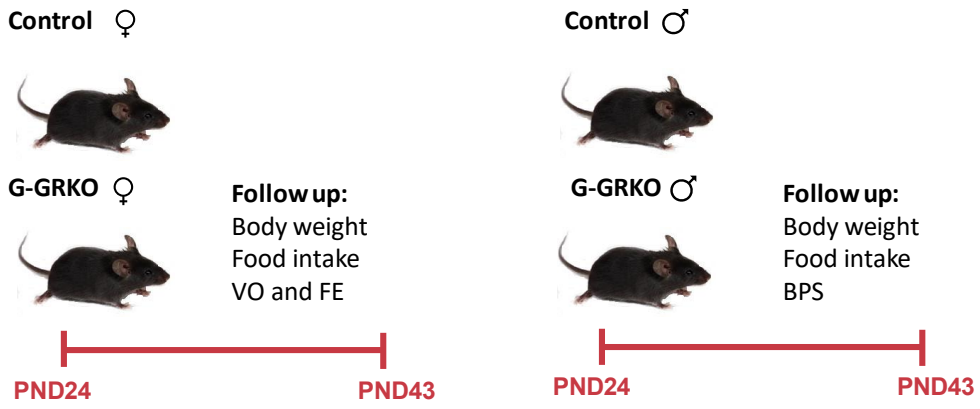

Figure 34. *Schematic representation of* ***Experiment 16*** *showing follow-up of puberty of G-GRKO mice.*

EXPERIMENTAL SET 8: GRK2 signaling and puberty under energy deprivation

The next set of experiments aimed to study puberty onset under conditions of nutritional deprivation, together with impaired GRK2 signaling by pharmacological or conditional blockade.

Experiment 17: Pharmacological blockade of GRK2 and puberty under energy deprivation

The contribution of central GRK2 signaling to the delay of puberty caused by conditions of negative energy balance was explored using a pharmacological approach in LL rats, as model of early undernutrition and delayed puberty. LL rats were icv injected with the GRK2 inhibitor (β-ARK1-I; dose: 6.53 nmol) or vehicle (DMSO), every 12 h, from PND25 to PND37. Body weight, food intake, VO and FE were daily monitored. Histological scoring of follicular maturation and ovulation were also conducted. Animals were euthanized at PND37, when trunk blood, uterus, and ovaries were collected (**Figure 35**).

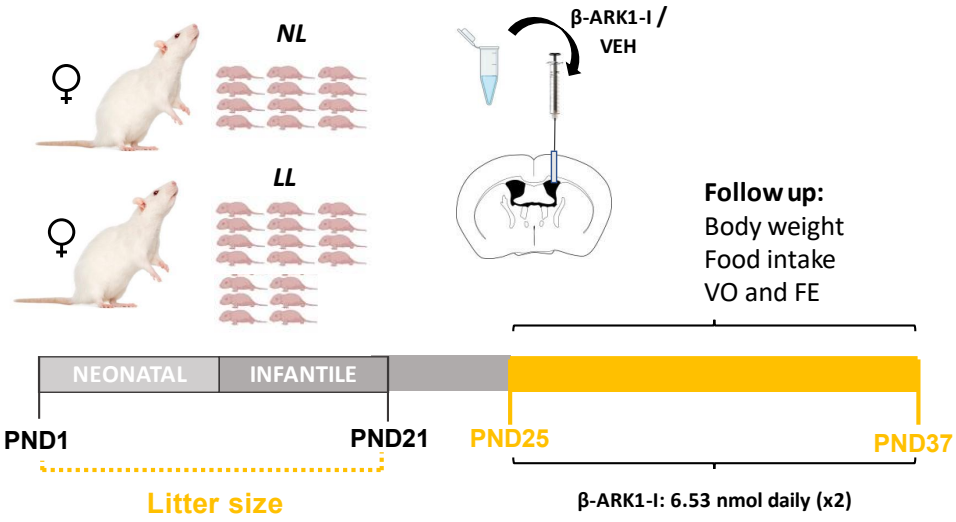

Figure 35. *Schematic representation of* ***Experiment 17*** *showing pharmacological blockade of GRK2 to study puberty in conditions of undernutrition.*

Experiment 18: Pubertal maturation in G-GRKO mice under nutritional deprivation

Similarly to Experiment 17, we evaluated the impact of chronic undernutrition (25% subnutrition) on pubertal progression in female G-GRKO mice. Body weight, food intake, VO and FE were daily monitored, from PND23 to PND50, in control female mice fed *ad libitum*, and in control and G-GRKO mice subjected to 20% caloric restriction from PND23 onwards (**Figure 36**). Euthanasia was applied at PND50, when trunk blood, uterus, and ovaries were collected.

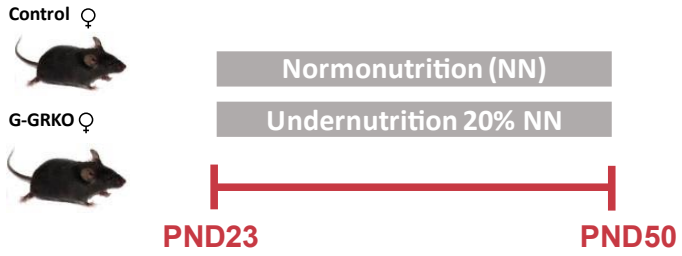

Figure 36. *Schematic representation of* ***Experiment 18*** *showing control and undernourished mice of the two genotypes submitted to pubertal follow-up.*

Experiment 19: LH pulsatile profile in G-GRKO mice

Pulsatile LH hormonal profiles were determined in G-GRKO and controls female mice in conditions of normo-nutrition and in conditions of 20% caloric restriction compared to control. Pulsatility tests were done in young adult females, as obliged by the habituation of mice required before performance of the test, and by the volume of blood collected. Habituation and blood sampling protocols, as described in Section 4.3. above, were applied (**Figure 37**).

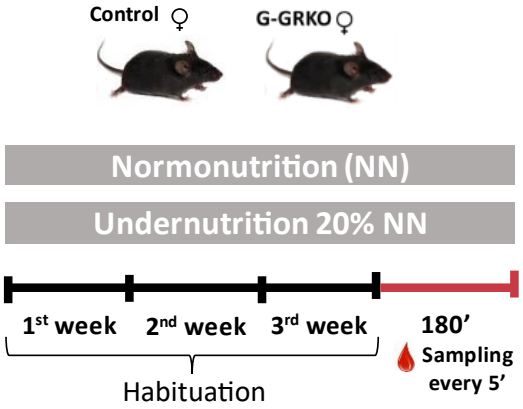

Figure 37. *Schematic representation of* ***Experiment 19*** *showing habituation (described previously in the 4.3 section of the methodology) and performance of the LH pulsatility test.*

PART 4. ANALYSIS OF THE ROLES OF GRK2 IN MALE OIH

The role of GRK2 in the control of the adult male gonadotropic axis and OIH was first assessed using models of pharmacological blockade of GRK2 with the inhibitor, β-ARK1-I.

Experiment 20: Acute inhibition of GRK2 with β-ARK-1 in male rats: Gonadotropin responses

The involvement of GRK2 in modulating GPR54 responses to repeated icv administration of Kp-10 was evaluated in adult male rats, subjected to pre-treatment with the GRK2 inhibitor. To this end, a β-ARK-1 group was treated icv with a dose of 6.53 nmol of the GRK2 inhibitor, β-ARK-1-I, 13h and 1h before the beginning of the experiment. Kp-10 was icv injected at a dose of 50 pmol or 1 nmol at time 0; then, Kp-10 was icv injected three additional times within a time lapse of one hour between injections. A control group was treated icv with VEH, 13h and 1 hour before the beginning of the experiment, and repeated Kp-10 injections were applied as above. Blood was taken by jugular venipuncture at basal time and 15' and 60' after the icv injections of Kp-10, with the aim of performing hormonal measurements of LH and FSH (**Figure 38**).

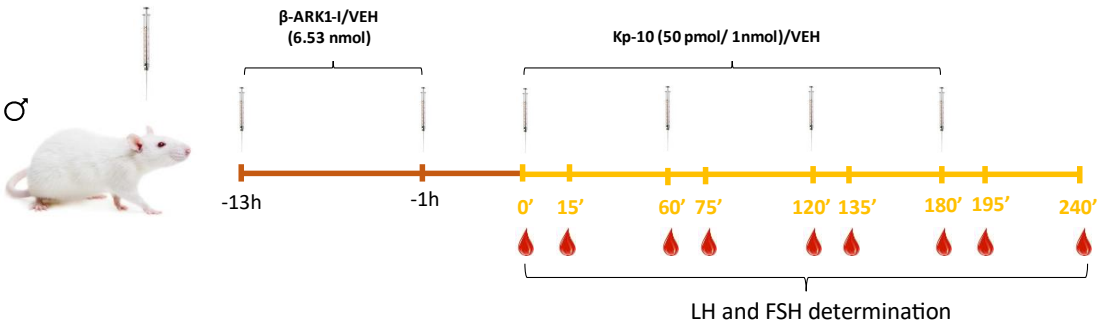

Figure 38. *Schematic representation of* ***Experiment 20*** *showing serial blood collection after central injection of Kp-10 in pre-treated β-ARK1-I male rats.*

Experiment 21: Pharmacological blockade of GRK2 in a rat model of OIH

First, we generated a rat model of OIH by breeding rats in SL and feeding them, after weaning, with an hypercaloric HFD (D12451: 4,73 kcal/g) until PND150, as described previously in this Methods Section (see Section 9, Part 2). From PND150, male SL/HFD were icv injected with the GRK2 inhibitor (β-ARK1-I; dose: 6.53 nmol) or vehicle (DMSO), every 12 h, until PND164. NL/CD (CD D12451: 3.85 kcal/g) male rats were employed as additional control group and were icv injected with vehicle. Body weight was daily monitored, and GTT and ITT were conducted. Blood was collected at PND150, PND152, PND155 and PND164, by venipuncture, for LH, FSH and T determination. Animals were euthanized at PND164, when hearts were collected, dried and weighted, and brain (for expression analysis of GRK2) and trunk blood were collected for additional determinations **(Figure 39).**

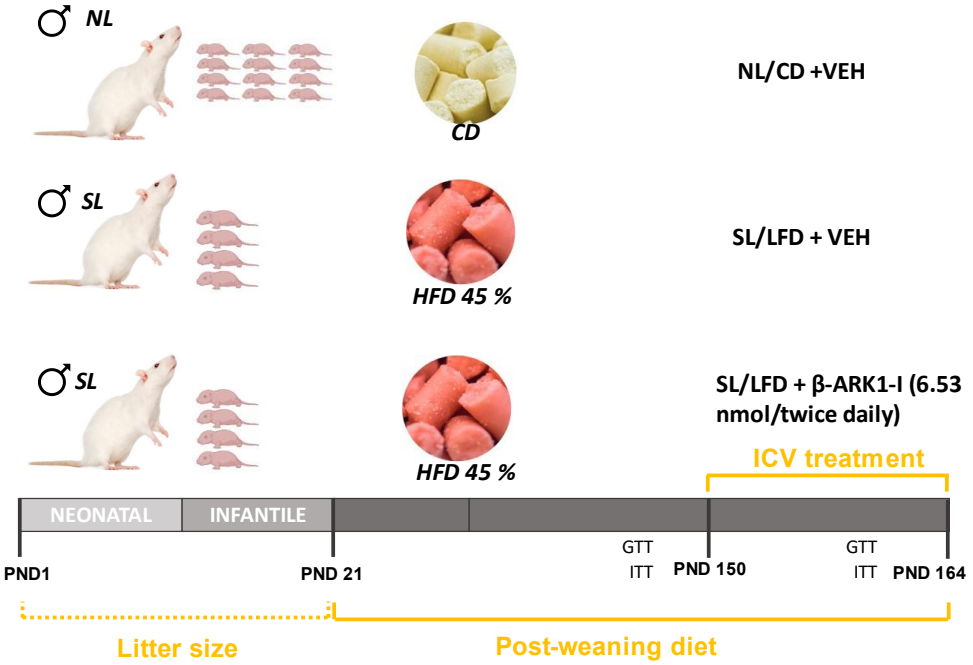

***Figure 39**. Schematic representation of **Experiment 21** showing experimental groups and treatment employed.*

Experiment 22: *Grk2* ablation from GnRH neurons in a mouse model of OIH

The role of GRK2 signaling in GnRH neurons in the pathophysiology of OIH was investigated via the induction of obesity in adult G-GRKO and control male mice. To this end, we fed adult male mice from both phenotypes with control diet (CD: A04 Panlab, 2,9 kcal/g) or HFD (HFD: D12451; 4.73 kcal/g) from PND60 to PND228. We evaluated central hypogonadism by the hormonal measurement of LH at different experimental time points. Additionally, we registered body weight, caloric intake, GTT and ITT. At PND228, mice were euthanized, and heart and trunk blood were collected for additional determinations **(Figure 40)**.

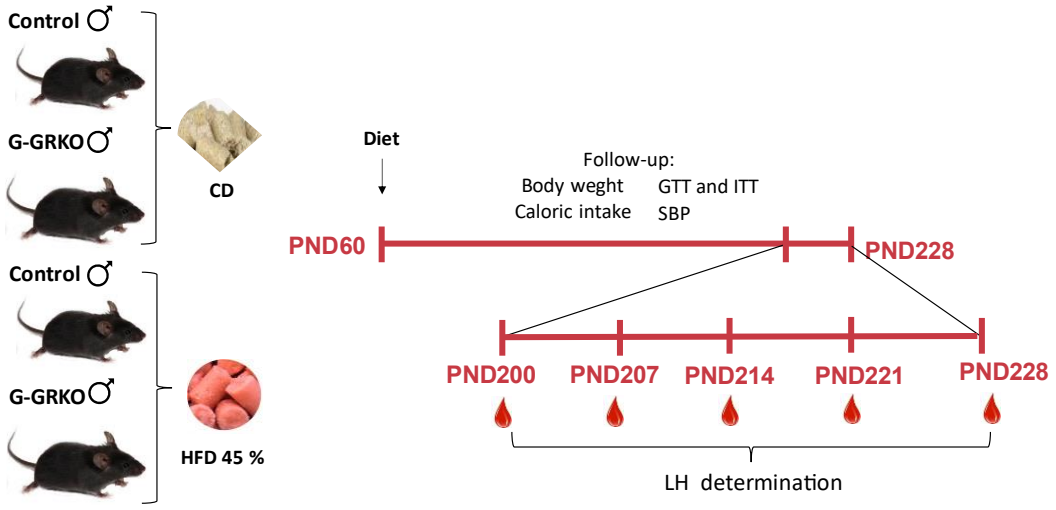

***Figure 40.** Schematic representation of **Experiment 22** showing the follow-up of the control and G-GRKO mice submitted to control or HFD.*

Results

Results

As mentioned in the Introduction, the Kiss1/GRP54 system has been proven as one of the main regulators of the HPG axis, in terms of modulation of both pubertal maturation and adult reproductive function. In this context, a relevant role for this system has been proposed both in the alterations associated with age of puberty (e.g., in adverse metabolic conditions), as well as in central hypogonadism associated to obesity in the male. However, the mechanisms responsible for the precise control of the Kiss1/GPR54 system in control and adverse conditions, remain ill defined. Therefore, this Thesis has been framed with the purpose of deepening in the knowledge of key regulators of the Kiss1/GPR54 system, mainly in relation with 1) the mechanisms of Kiss1 regulation by miRNAs; and 2) the mechanisms of regulation of GPR54 by GRK2.

PART 1. MiRNAs IN THE PHYSIOLOGICAL CONTROL OF PUBERTY

Given the lack of information in the literature on miRNAs that could putatively regulate *Kiss1*, as main component of the Kiss1 system, in the first part of the Thesis, we have focused on the study of miRNAs that could regulate *Kiss1*/kisspeptin expression, particularly in the context of puberty. Characterization of such potential regulatory miRNAs might shed light on the physiological mechanism controlling puberty and on the basis of pubertal alterations whose cause is still unknown.

1.1. *In silico* prediction of putative miRNA regulators of *KISS1/Kiss1*

To identify putative miRNA regulators of *KISS1/Kiss1*, bioinformatic analyses were performed using different online predictive algorithms, namely TargetScan, MirTarget, miRanda and microT-CDS. Selection of candidate microRNAs was based on three premises: 1) miRNAs had to be predicted as putative *Kiss1* regulators in at least one database; 2) miRNAs must be conserved in evolution at least between human, rat and mouse; and 3) miRNAs had to be found expressed at the hypothalamic level. As a result of these analyses, two miRNAs were selected for further analyses: miR-137-3p and miR-325-3p (**Figure 41**). Interestingly, miR-137-3p and miR-325-3p share the same seed region, understanding by seed region as the region that confers specificity and function to the miRNAs, whose location extends from nucleotide 2 to 7 of the 5'-end of the miRNA in question. This region must be complementary to the target mRNA [170]. In the case of the selected miRNAs, this seed region is similar in human, mouse and rat, as depicted in **Figure 41,** denoting a high degree of conservation in the evolution and its potential relevance. Additionally, previous literature and databases (tissue atlas) documented an abundant

expression of these miRNAs in the brain, especially in the hypothalamus, taken as pre-requisite for their potential regulation on *KISS1/Kiss1*.

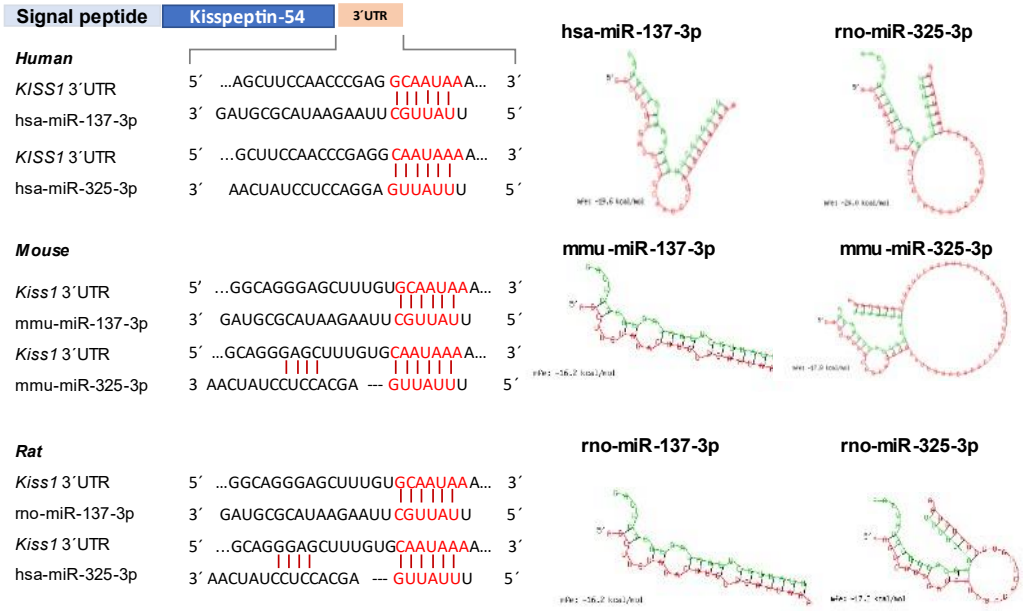

***Figure 41**. Schematic representation of predicted binding sites for miR-137-3p and miR-325-3p in human, mouse and rat 3'UTR of KISS1/Kiss1 gene. Seed regions of miR-137-3p and miR-325-3p are highlighted in red. Two-dimensional representations of repressive interaction miRNA/target in each species are presented in the right panels.*

Finally, it is also relevant to note that this is a relatively strong and stable interaction, since its binding spans 7 base pairs (bp) in each of the species in which it has been analyzed for both miRNAs.

1.2. Hypothalamic expression of miR-137/miR-325 in postnatal maturation and delayed puberty

In order to assess the potential role of these miRNAs during the pubertal transition, expression analyses of both miRNAs and *Kiss1* in the hypothalamus were performed during postnatal maturation in female rats.

First, we obtained hypothalamic samples from female rats at different postnatal stages: neonatal stage (NEO; PND0 to 7), infantile stage (INF; PND8 to 20), juvenile stage (JUV; PND21 to 32) and peripubertal stage (PUB; PND33 to 37). MiR-137-3p levels were found to increase in the POA and MBH from the infantile to juvenile period, and further into the pubertal stage (**Figure 42 A-B**). In the same vein, hypothalamic miR-325-3p levels increased along postnatal maturation, particularly during the juvenile period in the case of MBH, while the major increase of miR-325-3p levels occurred during the pubertal period in the POA (**Figure 42 C-D**). Of note, the rise in the expression levels of both miRNAs was accompanied by a progressive increase in kisspeptin content during postnatal maturation (**Figure 42 E**).

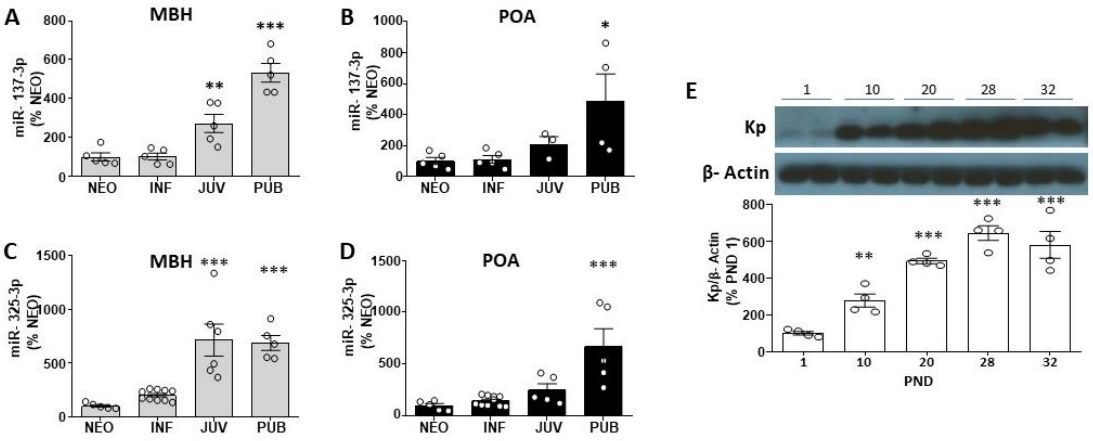

***Figure 42**. Expression profiles of miR-137-3p, mIR-325-3p and kisspeptin (Kp) in divided hypothalamus of female rats during the following stages of postnatal maturation: neonatal (NEO), infantile (INF), juvenile (JUV) and pubertal (PUB). **A)** miR-137-3p MBH expression, **B)** miR-137-3p POA expression, **C)** miR-325-3p MBH expression, and **D)** miR-325-3p POA expression in NEO, INF, JUV and PUB stages. **E)** Hypothalamic protein levels of Kp at PND1, 10, 20, 28 and 32. For data presentation, NEO stage or PND1 constitute 100% expression levels, and other data are normalized related to them. Data represent mean ±SEM. Group size: n=4-10. Statistical significance of the differences was assessed by ANOVA followed by Holm-Sidak test. *P<0.05, **P<0.01, ***P<0.001 vs NEO or PND1.*

In addition, the expression levels of these miRNAs were analyzed in hypothalamic samples from rat models of altered puberty. As mentioned earlier in this Thesis, proper functioning of the reproductive system is influenced by changes in nutritional status [220] and by exposure to sex steroids during critical periods of time [47]; perturbations in the nutritional and sex steroid milieu are known to alter hypothalamic kisspeptin levels and LH secretion, as well as timing of puberty. On this basis, we explored the role of these miRNAs in three stablished models of perturbed puberty [5,258], defined, among other phenotypic features, by pubertal delay [123,128,259]. Results from these models are presented below:

Postnatal underfeeding. Female rats were subjected to early undernutrition by breeding them in large litters (LL; 20 pups per mother), while the control group was reared in normal litters (NL; 12 pups per mother). This model was characterized by an overt decrease in body weight, accompanied by significant delay in the age of vaginal opening (VO), without changes in LH levels in female rats of PND35, in line with previous references [5]. In this model, hypothalamic levels of miR-137-3p increased by two-fold (**Figure 43 A**), while miR-325-3p levels did not increase when compared to NL group at pubertal (PND35) age (**Figure 43 D**).

Caloric restriction after weaning. Female rats submitted to 30% reduction in caloric intake during the peripubertal period displayed a very pronounced decrease in body weight, associated with low levels of LH and a delay in the age of VO, in line with previous reports [123,260]. This nutritional restriction was associated with a 50% significant increase in the hypothalamic levels of both, miR-137-3p and miR-325-3p, at PND36 (**Figure 43 B, E**).

Neonatal sex steroid manipulation. Neonatal exposure to EB or TP impairs puberty onset in female rats, as it has been documented by disturbed VO linked to low levels of LH [261]. In this condition, we observed a marked increase in miR-137-3p and miR-325-3p levels, close to a two-fold rise, as compared to control group at PND35 (**Figure 43 C, F**).

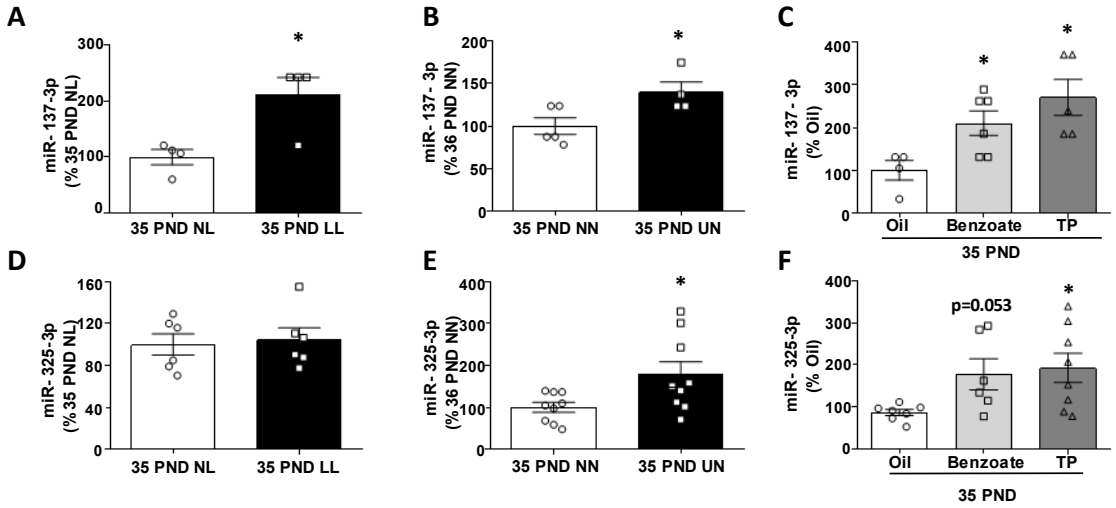

Figure 43. *Hypothalamic expression level of miR-137-3p and miR-325-3p at pubertal stage in female rats from models of delayed puberty.* ***A)*** *miR-137-3p expression in control (NL) and postnatally underfed (LL) rats at PND35.* ***B)*** *miR-137-3p expression in control (NN) and postweaning undernourished (UN) rats at PND35.* ***C)*** *miR-137-3p expression in female rats at PND35, after neonatal injection of estradiol benzoate (EB) or testosterone propionate (TP); oil-injected rats served as controls.* ***D)*** *miR-325-3p mRNA expression in NL and LL conditions at PND35.* ***E)*** *miR-325-3p expression in NN and UN at PND35.* ***F)*** *miR-325-3p expression in on oil, EB or TP groups at PND35. For data presentation, NL, NN and oil data represent 100% expression level, and the other data are normalized related to them. Data are presented as mean± SEM. Group size: n=4-9. Statistical significance was assessed by unpaired Student t-test or ANOVA followed by Holm-Sidak test (Panels C and F). *P<0.05 vs NL, NN or oil.*

1.3. *In vitro* validation of miR-137-3p and miR-325-3p repression over *Kiss1*

To confirm the *in silico* prediction obtained about the repressive role of miR-137-3p and miR-325-3p over *KISS1*, we performed Secrete-Pair dual luciferase assay in HEK293 cells. Here, the vector, pEZX-MT05, that carries a chimeric mRNA consisting of the 3' UTR sequence of the target (*KISS1*) plus the reporter Gluc, which is transcribed under the control of the SV40 promoter, was transfected into HEK293 cells. We transfected miExpress™ plasmids into the HEK293 expressing pEZX-MT05. MiExpress plasmids express the selected precursor miRNA (pre-miRNA) and eGFP reporter gene. As shown in **Figure 44**, co-transfection of the 3'UTR of *KISS1* and pre-miRNA-137-3p induced a significant, 20% decrease of the luciferase signal, while co-transfection with pre-miRNA-325-3p induced a 60% reduction of the luciferase signal, denoting effective repression for both miRNAs.

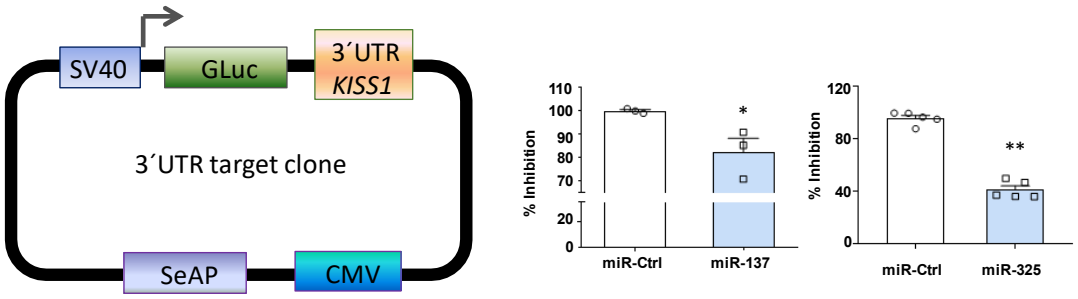

Figure 44. *In vitro analysis of miR-137-3p/miR-325-3p regulation of KISS1 expression. Luciferase assays were performed in cells transfected with 3' UTR KISS1 sequence expression plasmid and co-transfected with vectors expressing miRNA control (miR-Ctrl) or either pre-miRNA-137-3p or pre-miRNA-325-3p precursors. For presentation of data, expression levels of the control miRNA group were considered 100%, and the other values were normalized accordingly. Data represent mean ± SEM. Group size: n=3. Statistical significance was assessed by unpaired Student t-test *P<0.05 vs miRNA control.*

1.4. Assessment of miR-137-3p and miR-325-3p repression of *Kiss1 in vivo*

With the aim to validate the *in silico* predictions and the *in vitro* validation of the repressive actions of miR-137-3p and miR-325-3p on human *KISS1,* and to obtain *in vivo* evidence of such repressive interaction, we conducted experiments involving icv administration of synthetic mimic analogues with capacity to emulate the biological actions of given miRNAs at their corresponding targets. Initial experiments were conducted using a mimic-miR-137-3p, administered icv from PND25 to PND34 in female rats. During the treatment, we determined the evolution and day of VO, first estrus (FE) and ovarian maturation, as well as the ovarian and uterine relative weight, circulating levels of LH and hypothalamic levels of kisspeptin at the end the treatment (PND34).

In line with the predicted repressive action, the hypothalamic levels of kisspeptin protein were significantly decreased at PND34 in the whole hypothalamus of female rats treated with mimic-miR-137, with a drop of 20-40% compared to the control group (**Figure 45 A**).

Prepubertal administration of mimic-miR-137 did not significantly change body weight along pubertal transition, although some fluctuations in food intake were noticed between mimic- and vehicle-treated groups (**Figure 45 B-C**). Notably, treatment with mimic-miR-137 caused an overt delay in puberty onset, as denoted by the deferred age-course of accumulated vaginal opening vs. control group (**Figure 45 D**) and a significant delay in the mean age of VO, that was PND 32.67 in the mimic-miR-137 group vs. PND30.3 in the control group (**Figure 45 E**). In fact, while by PND32 100% of the animals in the control group displayed VO, by PND33 less than 50% of the animals in the mimic-miR-137 group exhibited VO (**Figure 45 D**).

In good agreement with VO data, the age of FE was substantially delayed in mimic-miR-137 treated female rats, as denoted by the age-course and mean age of FE (**Figure 45 F-G**). Thus, while the mean age of FE in the mimic-miR-137 group was PND33.12, it occurred at a mean of

PND31.9 in the control group (**Figure 45 G**). Likewise, the age-course of FE was also clearly delayed in mimic-miR-137 treated rats, and at PND32 the difference vs. the control group was greater than 60% (**Figure 45 F**).

In the same vein, ovarian weights were significantly decreased in female rats treated with the mimic of miR-137 (**Figure 45 H**), without changes in uterus weight (**Figure 45 I**) and a strong trend for decreased LH levels (**Figure 45 J**). In addition, histological analyses of the ovary also showed a delay in the age of follicular maturation in female rats treated with the mimic of miR-137, even if the percentage of ovulatory animals in mimic-treated animals was not grossly different vs. the vehicle group at the end of the treatment (**Figure 45 K**).

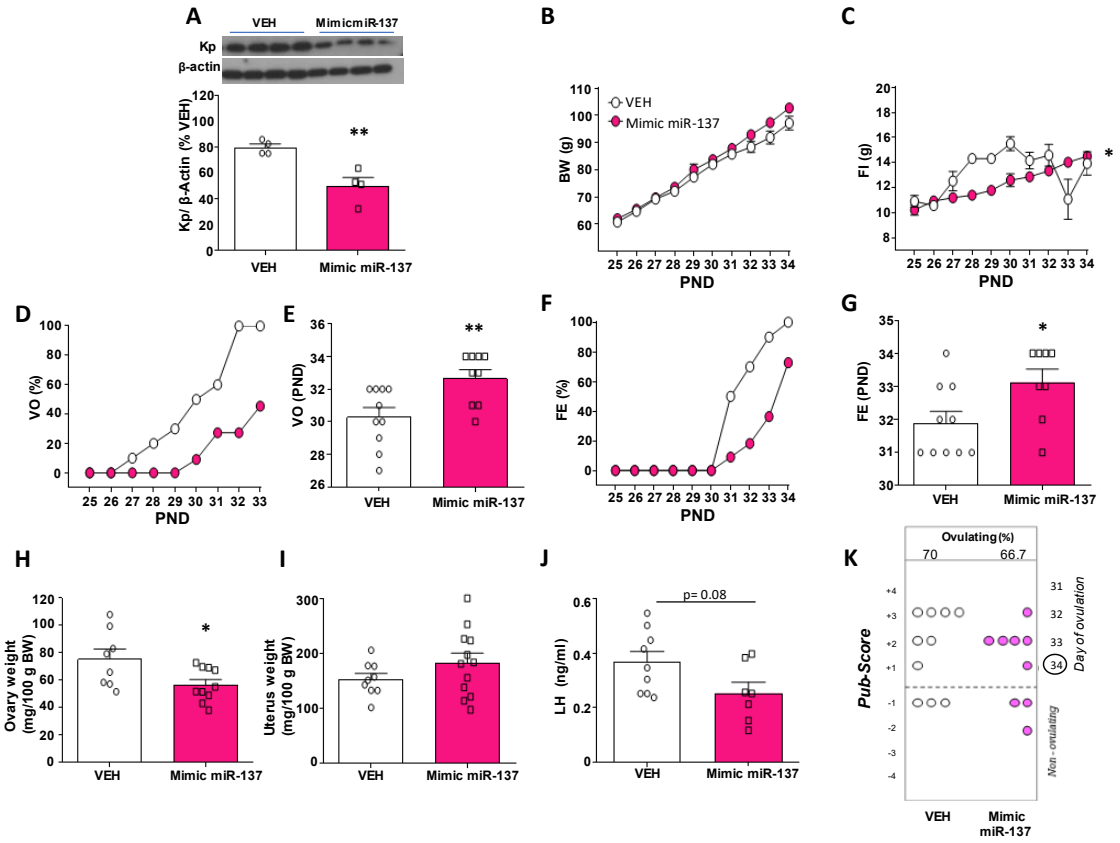

Figure 45. *Central (icv) administration of mimic-miR-137-3p delays puberty onset inducing a reduction in kisspeptin expression. Data from vehicle (VEH) group, as controls, and Mimic miR-137-3p (Mimic miR-137)-treated group, are presented.* ***A)*** *Hypothalamic kisspeptin (Kp) expression in female rats treated with VEH or Mimic miR-137.* ***B)*** *Follow up of body weight (BW) from PND25 to PND34.* ***C)*** *Food intake (FI) from PND25 to PND34.* ***D)*** *Cumulative percentage of vaginal opening (VO).* ***E)*** *Mean age of VO at PND34.* ***F)*** *Cumulative percentage of first estrus (FE).* ***G)*** *Mean age of FE at PND34.* ***H)*** *Relative ovary weight.* ***I)*** *Relative uterus weight.* ***J)*** *Serum LH levels at end of the treatment.* ***K)*** *Histological score for follicular maturation and ovulation (Pub-Score), representing day of first ovulation. Data represent mean ± SEM. Group size: n=10-11. Statistical significance was assessed by unpaired Student t-test or 2-way ANOVA followed by Student-Newman-Keuls test (Panels B and C). *P<0.05, **P<0.01 and ***P<0.001 vs VEH group.*

Using a similar experimental approach, peripubertal female rats were treated icv from PND25 to PND34 with the mimetic of miR-325-3p (mimic-miR-325) or vehicle, and pubertal parameters were assessed. First, hypothalamic kisspeptin content was measured by Western blot. These

analyses demonstrated a clear decrease in the hypothalamic levels of kisspeptin after treatment with mimic-miR-325, as compared with levels in the control VEH-treated group (**Figure 46 A**). Prepubertal icv administration of mimic-miR-325 from PND24 to PND34 did not change body weight or food intake (**Figure 46 B-C**); however, this treatment delayed pubertal maturation, as denoted by the deferral in the age-course of VO curve (**Figure 46 D**) and the delay in the mean age of VO, which occurred at PND32.72 in mimic-miR-325 treated female rats vs. PND30.3 in the control group (**Figure 46 E**). Regarding FE, a similar time lag was observed. Thus, while 100% control females reached FE at PND34, only 66.6 % of rats in the mimic-miR-325 group displayed FE at this age (**Figure 46 F**), denoting a clear delay in the age-course of FE in the mimic-treated group. Similarly, the mean age of FE was significantly delayed in mimic-miR-325 treated rats, that displayed FE at a mean age of PND33.54 vs. PND31.9 in the control group (**Figure 46 G**). In addition, relative ovarian weights were significantly decreased in the mimic miR-325 treated group (**Figure 46 H**), which also showed evidence for a moderate delay in follicular maturation and ovulatory rates; while 54.5% of female rats treated with mimic-miR-325 had ovulated at PND34, up to 70% of control rats had reached ovulation at this age (**Figure 46 K**). Yet, no significant differences were detected in terms of relative uterus weights (**Figure 46 I**) or LH levels (**Figure 46 J**) between vehicle- and mimic-treated groups.

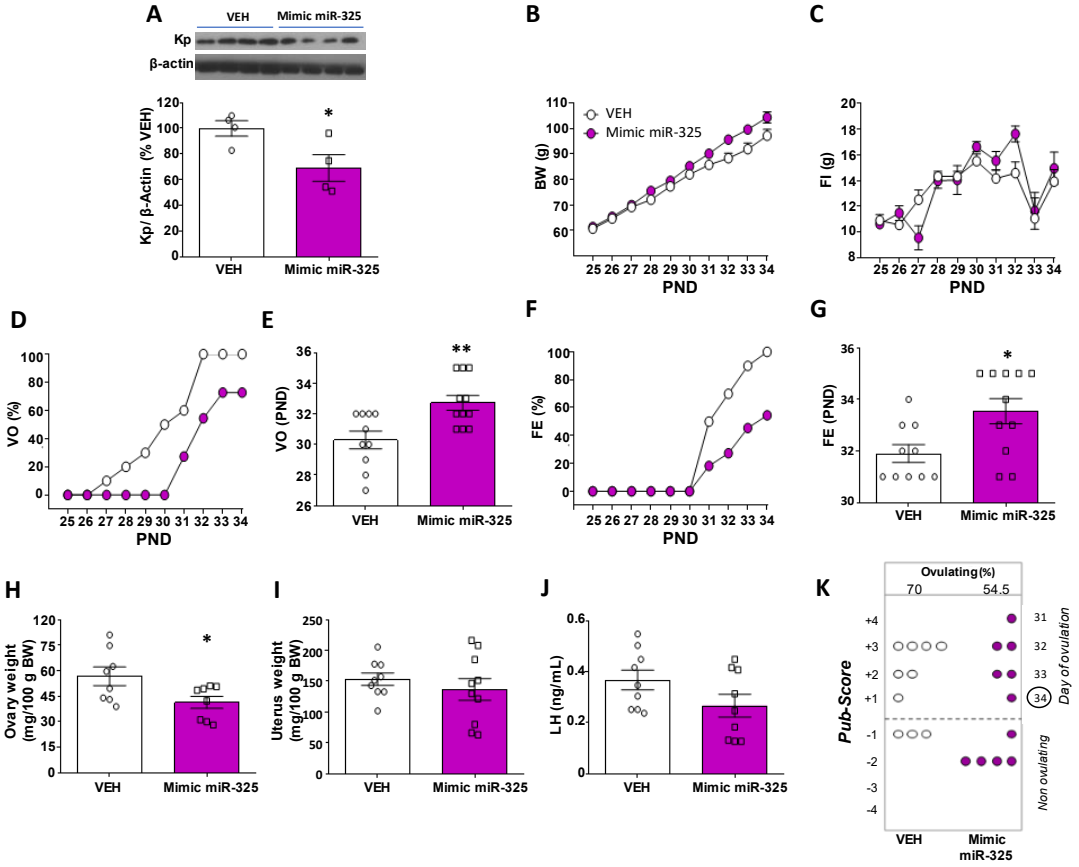

Figure 46. *Central (icv) administration of mimic-miR-325-3p delays puberty onset inducing a reduction in kisspeptin expression. Data from vehicle (VEH) group, as controls, and Mimic miR-325-3p (Mimic miR-325)-treated group, are presented.* ***A)*** *Hypothalamic kisspeptin (Kp) expression in female rats treated with VEH or mimic miR-325-3p.* ***B)*** *Follow up of body weight (BW) from PND25 to PND34.* ***C)*** *Food intake (FI) from PND25 to PND34.* ***D)*** *Cumulative percentage of vaginal opening (VO).* ***E)*** *Mean age of VO at PND34.* ***F)*** *Cumulative percentage of first estrus (FE).* ***G)*** *Mean age of FE at PND34.* ***H)*** *Relative ovary weight.* ***I)*** *Relative uterus weight.* ***J)*** *Serum LH levels at end of the treatment.* ***K)*** *Histological score for follicular maturation and ovulation (Pub-Score), representing day of first ovulation. Data represent mean ± SEM. n=10-12. Statistical significance was assessed by unpaired Student t-test or 2-way ANOVA followed by Student-Newman-Keuls test (Panel B). *P<0.05, **P<0.01, ***P<0.001 vs VEH group.*

1.5. Blockade of miR-137-3p/ miR-325-3p repression of *Kiss1 in vivo* advances puberty onset

Departing from the evidence that mimicking miR-137-3p and miR-325-3p actions at central levels causes a decrease in kisspeptin content and delay of puberty onset, we next evaluated the consequences of selective blockade of the repressive interaction between these miRNAs and *Kiss1* mRNA *in vivo*. To this end, the Target Site Blocker (TSB) technology was used, to design antisense oligonucleotides with locked nucleic acid (LNA) ends, which compete with greater affinity than the endogenous miRNA for the binding site and thus, prevent the repressive action of the selected miRNA on protein expression. Specificity in the blockade of the miRNA/mRNA interaction is given by including specific sequences of areas adjacent to the binding site at the 3'UTR of the target mRNA. In our experiment, central (icv) treatment with a TSB for the repressive action of miR-137/miR-325 (with common seed region) on the Kiss1 3'UTR was conducted from PND24 to PND32 in prepubertal female rats.

Central administration of TSB 137/325/Kiss1 was able to prevent the repressive interaction presumably established between miR-137-3p/miR-325-3p and *Kiss1*, as denoted by significant increases in hypothalamic levels of kisspeptin in the TSB-treated group (**Figure 47 A**), without changes in body weight or food intake (**Figure 47 B-C**). In line with the observed changes in Kp levels, there was an advancement of puberty onset caused by TSB treatment, as reflected by the age-course of cumulative percentage of VO, which was accelerated in the TSB group (**Figure 47 D**), as well as the mean age of VO, which displayed a strong trend for advancement, with a mean value of PND31.4 in the TSB 137/325/Kiss1 group, whereas it was PND32.8 in the vehicle group (P= 0.067) (**Figure 47 E**). In parallel with VO, FE occurred also earlier in the group treated with the TSB 137/325/Kiss1, as denoted by the age-course of cumulative percentage of female rats showing first estrus (**Figure 47 F**). These results are consistent with the observed rates of follicular maturation and ovulation, since 44% of female rats treated with TSB 137/325/Kiss1 reached an ovulatory stage by PND32, compared to 11% ovulation in the vehicle group (**Figure 47 L**). In contrast, no changes were observed in relative ovarian or uterine weights (**Figure 47 H-I**), neither there were changes in LH or FSH levels (**Figure 47 J-K**).

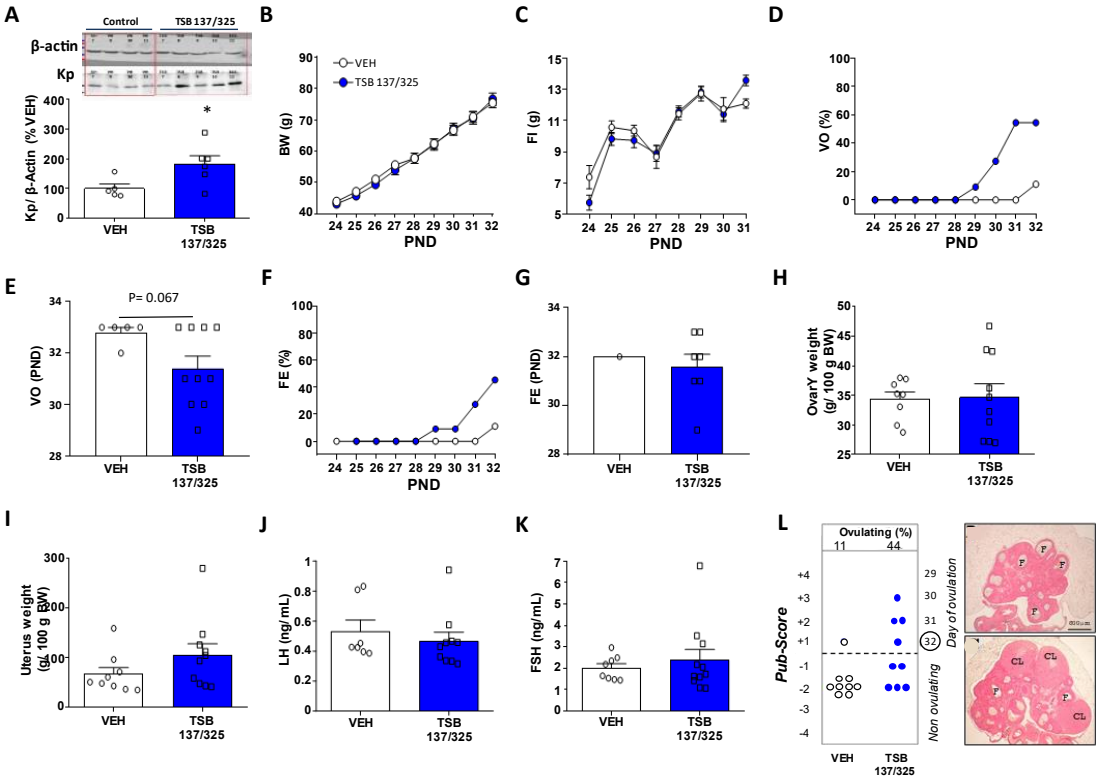

Figure 47. *Blockade of the repressive actions of miR-137-3p and miR-325-3p on Kiss1 in vivo advances puberty onset. The effects of central (icv) injection of a TSB 137/325/Kiss1 (TSB 137/325) or vehicle (VEH) in female rats between PND24 and PND32 are depicted.* ***A)*** *Hypothalamic kisspeptin (Kp) expression in female rats treated with VEH or TSB 137/325/Kiss1.* ***B)*** *Body weight from PND24 to PND32.* ***C)*** *Food intake (FI) from PND24 to PND31.* ***D)*** *Cumulative percentage of vaginal opening (VO).* ***E)*** *Mean age of VO at PND32.* ***F)*** *Cumulative percentage of first estrus (FE).* ***G)*** *Mean of FE at PND32.* ***H)*** *Relative ovary weight.* ***I)*** *Relative uterus weight.* ***J)*** *Serum LH levels at end of the treatment.* ***K)*** *Serum FSH levels at the end of the treatment.* ***L)*** *Pub-Score, representing day of first ovulation; a representative control histological ovarian section with unmature follicles (F), and a representative TSB-miR-137/325/Kiss1 (TSB) ovarian section with several corpora lutea (CL) are also presented. Data represent mean ± SEM. Group size: n=5-12. Statistical significance was assessed by unpaired Student t-test or 2-way ANOVA followed by Student-Newman-Keuls test (Panels B and C). *P<0.05, **P<0.01 vs VEH group.*

1.6. MiR137HG copy number variants in human precocious puberty

To further document the role of miR-137-3p and miR-325-3p in the regulation of puberty onset, we performed additional analyses seeking for evidence in favor of a conserved function of these miRNAs in the control of human puberty. For doing so, we inquired on different bibliography and public databases, such as Varsome, Precocity Database, GWAS catalog, Decipher and GTEX database, to check for putative alterations in the coding region of miRNAs in conditions of disordered puberty. This search identified the occurrence of copy number variants (CNV) – defined as microscopic or sub-microscopic structural variants of the genome, larger than 1kb [262] – associated with precocious puberty, in the region of the host gene of miR-137-3p (MIR137HG), which is located in the long arm of the chromosome 1. The identified clinical cases showed microdeletions in the 1p21.3 region, where the shortest overlapping region (SOR) spans 7,985,640 pb and includes MIR-137HG, LINC01776, SNX7, 7SX, PLPPR5 and PPLR4 genes (**Figure**

48). Additionally, our analyses revealed that the SNP encoded with the Reference SNP cluster ID (rs) rs11165924 is linked with the trait 'age at menarche' in the GWAS catalog. Moreover, this SNP qualifies as an expression quantitative trait locus (eQTLs), defined as a locus that explains a fraction of the genetic variance in the expression of a given gene [263], linked to MIR137HG expression in human brain tissue, as found in the GTEx database. Of note, the clinical cases linked to micro-deletions affecting MIR137HG are characterized in some cases by syndromic obesity or intellectual disability. Summary of this information can be found in **Figure 48**.

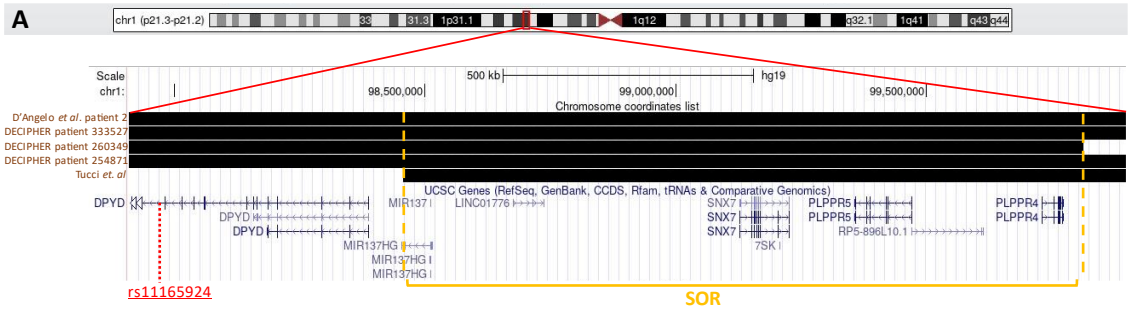

B

	D'Angelo et al. patient 2	DECIPHER patient 333527	DECIPHER patient 260349	DECIPHER patient 254871	Tucci et. al
Chromosome 1 postion (hg 19)	95,696,444 – 107,775,587	95,853,659 – 101,685,110	97,000,749 – 99,813,665	97,019,762 – 102,447,536	98,456,293 – 103,682,084
Gender	Female (syndromicobesity)	Male (overweight)	Male	Male	Male (syndromicobesity)
Age of precocious puberty detection	8 years 8 months	NA	NA	NA	9 years 5 months

Figure 48*. CNV and SNP affecting age of puberty in humans.* ***A)*** *Chromosome 1p21.3 microdeletions (black bars) related to precocious puberty. The shortest overlap region (SOR) is delimited by yellow lines. The assembly was performed with the UCSC Genome Browser on Human, Feb. 2009 (GRCh37/hg19). GWAS rs variant (highlighted in red) located in the gene DPYD, is related with 'age at menarche' trait and it is registered as an eQTL related with MIR137HG expression in the GTEX database, which resides within a highly conserved chromosomic region.* ***B)*** *Summary of 5 identified patients carrying microdeletions on MIR137HG region (1p21.3), with clinical evidence of precocious puberty.*

PART 2. PATHOPHYSIOLOGICAL ROLE OF MIR-137-3p AND MIR-325-3p IN MALE OIH

Departing from our *in silico*, *in vitro* and *in vivo* data (see Part 1), supporting a regulatory role of miR-137-3p and miR-325-3p on *Kiss1*, in the particular context of puberty, in this Thesis, we also evaluated the potential contribution of these miRNAs in the regulation of the reproductive system on adulthood, with a particular focus on their putative function in conditions of obesity-induced hypogonadism (OIH) in males, where it has been already reported that Kiss1 system is repressed [229].

2.1. Hypothalamic expression analysis of kisspeptin, miR-137-3p and miR-325-3p in OIH model

Expression analyses at central level were conducted in hypothalamic samples from a rat model of OIH. This model was generated by submitting rats reared in small litters (4 pump per mother) to a hypercaloric high fat diet (SL/HFD), from weaning until PND150. The control group (NL/CD) was reared in normal litters (12 pump per mother) and was fed with low fat diet the same period

of time. At PND150, hypothalamic samples (from MBH including ARC- and POA) of the two groups were collected to evaluate Kiss1 mRNA, kisspeptin protein contents, and miR-137-3p and miR-325-3p levels.

In line with previous studies from our group [229], hypothalamic Kiss1 mRNA was decreased, specifically in the MBH of the OIH male rats (**Figure 49 A**), with > 60% decline in relative *Kiss1* levels vs. controls. In addition, kisspeptin protein levels were diminished in the OIH group in both MBH and POA, with a drop in OIH animals of nearly 40% (**Figure 49 B**). Regarding the expression of miR-137-3p and miR-325-3p, a marked increase in their levels was found in the MBH of the OIH animals when compared to the control group (**Figure 49 C-D**). Thus, miR-137-3p displayed an increase on its levels of approx. 130% in the MBH of OIH males, with no changes between groups in the POA (**Figure 49 C**). Similar results were observed for miR-325-3p, with an increase of its levels that was greater than 60% in the OIH group and no significant changes in POA (**Figure 49 D**).

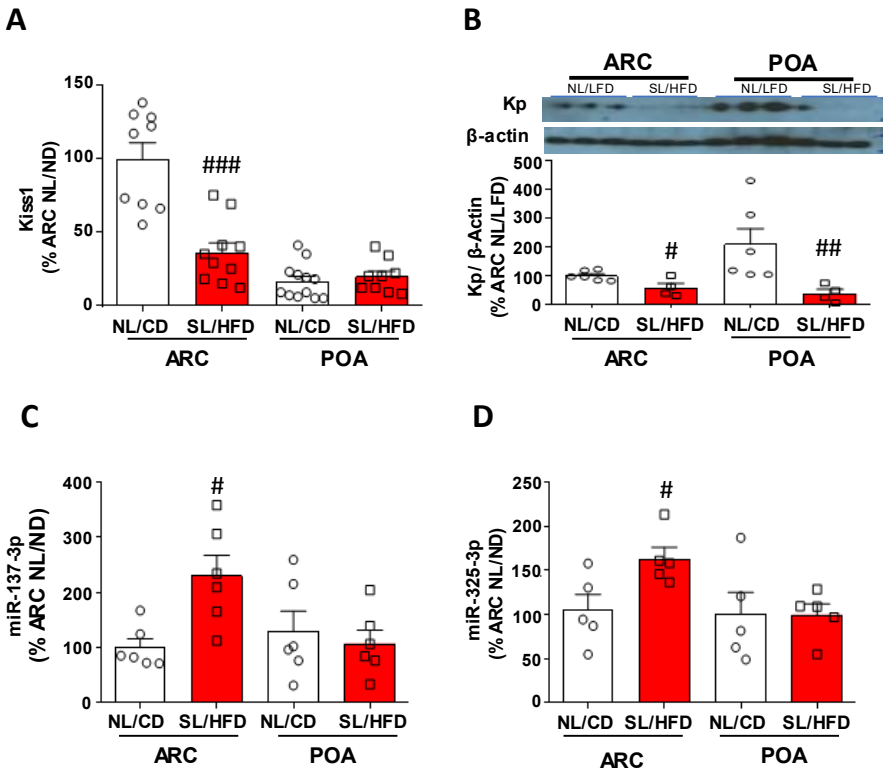

Figure 49. *Hypothalamic expression of Kiss1 mRNA, kisspeptin (Kp), miR-137-3p and miR-325-3p in control (NL/CD) and OIH (SL/HFD) conditions. Upper panels represent Kiss1 and Kp expression.* ***A)*** *Kiss1 mRNA expression in the MBH (including ARC) and POA of adult male rats.* ***B)*** *Kisspeptin (Kp) expression in ARC and POA of adult male rats. Lower panels present miRNA levels in divided hypothalamus.* ***C)*** *miR-137-3p expression in ARC and POA of adult male rats.* ***D)*** *miR-325-3p expression in ARC and POA. For presentation of data, the level of expression of RNA or protein from ARC in control condition (ARC, NL/CD) was taken as 100 %, and the other values were normalized accordingly. Data represent mean ±SEM. Group size: n=4-12. Statistical significance was assessed by unpaired Student t-test (comparison within hypothalamic area: MBH/ARC or POA). #P<0.05, ##P<0.01, ###P<0.001 vs NL/CD.*

2.2. *In vivo* validation of miR-137-3p repressive actions on *Kiss1* in adult male rats

Complementary to the *in silico*, *in vitro* and *in vivo* data (the latter in immature female rats) presented in Figures 41 and 43-47, adult male rats (PND60) were treated icv daily during 15 days with vehicle (VEH) or mimic-miR-137 (Mimic miR-137), in order to explore the effect of a central increase of miR-137-3p on the Kiss1 system and reproductive parameters in healthy young male rats. Treatment with the mimic of miR-137-3p at central level resulted in a marked and significant 50 % decrease of the hypothalamic levels of kisspeptin in young male rats. This was associated with trends for decreased LH and testosterone levels, which in the case of T was close to statistical significance (P= 0.059) when compared to the control (VEH) group (**Figure 50**).

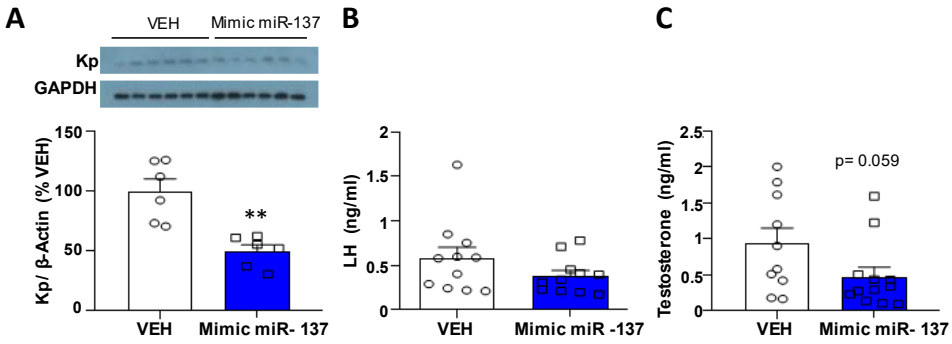

Figure 50. *Central administration of mimic-miR-137 induces downregulation of hypothalamic kisspeptin (Kp) levels.* ***A)*** *Hypothalamic expression levels of Kp in male rats treated with mimic-miR-137 compared to control group (VEH) (n=6 per group).* ***B)*** *LH levels in mimic vs. VEH group (n=11=).* ***C)*** *Testosterone levels in mimic vs. VEH group (n=10-12 per group). For presentation of protein data, expression levels of VEH were taken as 100%, and the other values were normalized accordingly. Data represent mean ± SEM. Statistical significance was assessed by unpaired Student t-test. **P<0.01 vs VEH group.*

2.3. Virogenetic over-expression of miR-137 in the ARC in *Kiss*$^{Cre:GFP}$ and *Kiss*$^{Cre:EYFP}$ mice

To further validate the capacity of miR-137 to repress Kiss1 in a physiological context, we conducted studies aimed at over-expressing this miRNA selectively in Kiss1 neurons in the ARC. To achieve this goal, we used a *Kiss*$^{Cre:GFP}$ mouse model characterized by presenting Cre recombinase activity under the control of the *Kiss1* promoter. Bilateral stereotaxic injections in the ARC of the hypothalamus (-2,1 mm caudally from bregma, ± 0,25 mm laterally and -5,9 mm ventrally) were carried out with a viral vector that allows over-expression of miR-137 and the reporter, mCherry, in a Cre-dependent manner. Control animals were injected with a viral vector expressing mCherry solely.

After stereotaxic injections, viral infection was monitored by immunohistochemical (IHC) detection of mCherry. In line with our predictions, mCherry immunoreactivity was limited to Kiss1-expressing neurons (denoted by green fluorescent protein, GFP, as this tag is expressed under the Kiss1 promoter), with a virtually complete colocalization of mCherry and GFP after the infection (**Figure 51 A**). IHC analyses demonstrated also that mice stereotaxically infected with

the miR-137 expressing virus displayed a clear tendency of decrease kisspeptin levels in the ARC, as compared to animals treated with the control adenovirus (**Figure 51 B-C**).

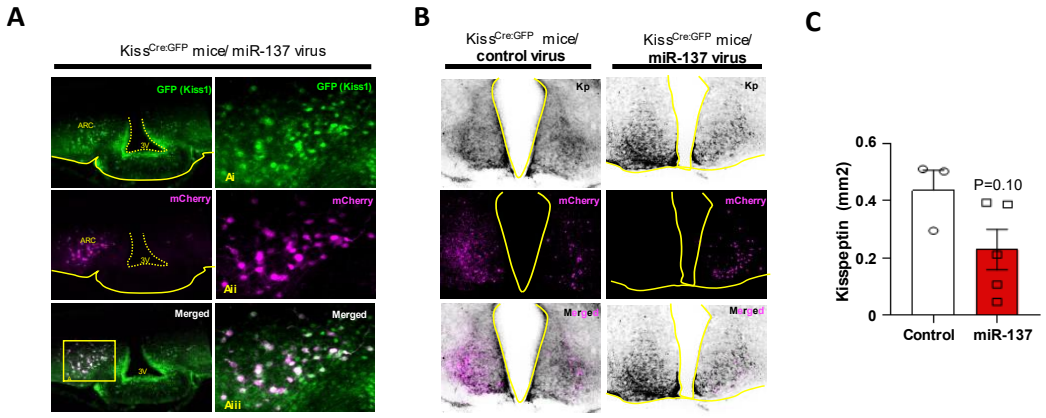

***Figure 51**. Strategy for Kiss1-neuron specific over-expression of miR-137 using viral vectors. **A**) Co-localization of GFP (labelling Kiss1-expressing cells) and infected cells with a viral construct for miR-137 over-expression (labelled by mCherry). **B**) Panels of the left, kisspeptin (Kp) expression reported by NiDAB, in neurons infected by the control virus (reported by mCherry); panel on the right, NiDAB IHC and mCherry fluorescent IHC of Kiss1 neurons infected by the virus miR-137. **C**) Kiss1 expression in ARC neurons infected with the virus overexpressing miR-137 vs. control virus group. Data represent mean ±SEM. Group size: n=3-5. Statistical significance was assessed by unpaired Student t-test.*

Next, we assessed the consequences of overexpression of miR-137 in ARC Kiss1 cells in terms of recapitulation of phenotypic features of OIH, by monitoring metabolic and reproductive parameters. In terms of metabolic parameters, our data showed that the *Kiss*$^{Cre:GFP}$ animals infected with the viral vector for miR-137 over-expression displayed greater weight gain throughout the treatment than those mice infected with the control virus (**Figure 52 A**). This increment in body weight gain was associated with a trend for higher adiposity, without changes in caloric intake during follow-up (**Figure 52 B-C**). Regarding reproductive parameters, targeted expression of miR-137 in ARC Kiss1 neurons was bound to a significant reduction in mean LH levels vs. circulating LH concentrations in the control group (**Figure 52 D**).

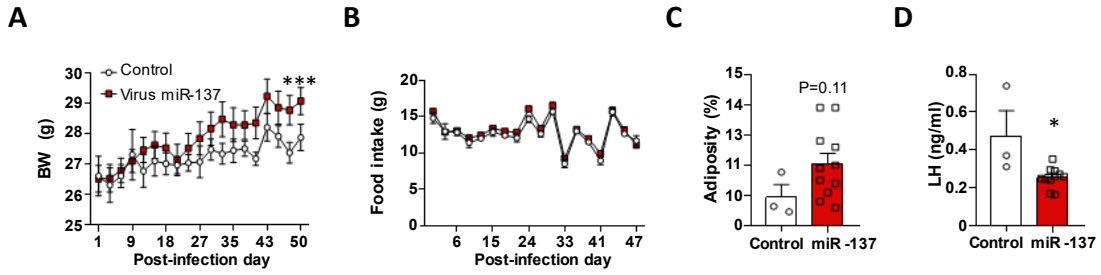

***Figure 52.** Metabolic and reproductive parameters in Kiss1$^{Cre:GFP}$ mice injected in the ARC with a viral vector for over-expression of miR-137. **A**) Evolution of body weight. **B**) Food intake. **C**) Percentage of adiposity, calculated as (fat %/fat +lean %)*100, at end of the treatment. **D**) Serum levels of LH. The above parameters were measured in mice stereotaxically injected with a control virus (control) or with the adenovirus miR-137/mCherry (miR-137). Data represent mean ±SEM. n=3-5. Statistical significance was assessed by 2-way ANOVA followed by Student-Newman-Keuls test (for BW and food intake) or by unpaired Student t-test. *p<0.05 vs control group.*

Additionally, stereotaxic injections of viruses in the ARC for Cre-mediated over-expression of mR-137 were conducted in young male *Kiss*$^{Cre:EYFP}$ mice, where EYFP expressing neurons display Cre recombinase and hence activate miR-137 over-expression after viral infection. Kiss1-EYFP^{+} neurons were isolated by FACS sorting, as a means to directly assess Kiss1 mRNA levels in infected cells, which co-express EYFP (used for FACS) and mCherry (viral infection). This group was compared with Kiss1 neurons not infected by the virus, that expressed only EYFP. Comparative analysis showed a >50% decrease in the Kiss1 mRNA levels in the Kiss1 neurons co-expressing EYFP (EYFP+) and mCherry (mCherry+), as compared to Kiss1 neurons expressing EYFP solely, and hence not over-expressing miR-137 (**Figure 53**).

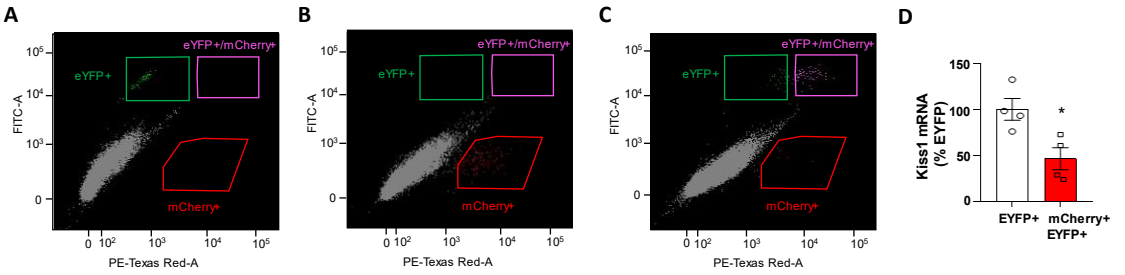

Figure 53. *FACS sorting of EYFP positive and mCherry positive cells.* ***A****) FACs plot representing EYFP positive cells (FITC-A channel, in green).* ***B****) FACS plot representing MiR-137-mCherry positive cells (PE-Texas Red-A channel, in red).* ***C****) double positive cells represented in pink.* ***D****) Kiss1 mRNA expression analysis from the populations sorted by FACS. Data represent mean ±SEM. n=4. Statistical significance was assessed by unpaired Student t-test- *P<0.05 vs control group (EYFP+).*

2.4. Hormonal and phenotypic characterization of the male rat OIH model

Based on data from previous literature, defining the SL/HFD male rat as valid model of OIH[229,264,265] , and our *in silico* predictions and current hypothalamic expression data (see **Figure 54**), pointing to a putative repressive interplay between miR-137/miR-325 and Kiss1, we next evaluated the impact of preventing such repressive interaction *in vivo* upon key reproductive, metabolic and cardiovascular parameters of our OIH model.

For sake of clarity, we consider relevant to summarize first in this section the detailed characterization of the male rat model of OIH per se, as a means to document the validity of our model to recapitulate the major features of OIH in humans. To this end, we present here the following parameters, that were compared between control (NL/CD) and OIH (SL/HFD) male rats: 1) reproductive parameters, such as serum gonadotropin (LH and FSH) and testosterone levels, as well as prostate hyperplasia ratio; 2) metabolic parameters; such as evolution of body weight, energy intake, body composition, leptin levels, basal glucose and insulin levels, ITT and GTT; 3) cardiovascular parameters; such as cardiac hypertrophy, systolic blood pressure and functional, structural and mechanical vascular alterations; and 4) markers of the inflammatory profile. Note that these parameters are graphed alongside the effects of treatment with the TSB

137/325/Kiss1, as described in detail in Section 2.5. The data described below correspond to the comparison between NL/CD and SL/HFD presented in Figures 54-56 and 59.

Regarding the reproductive profile, OIH male rats (SL/HFD) displayed a marked decrease (30%-50%) in the integral circulating levels (measured as AUC) of gonadotropins, LH (**Figure 54 B**) and FSH (**Figure 54 C**), as well as of testosterone levels (**Figure 54 D**), which was accompanied by a reduction on prostate hyperplasia ratio (171.1 ± 18.42 mg/cm in SL/HFD vs. 238.9 ± 26.53 mg/cm in NL/CD; P=0.012). In terms of metabolic parameters, evolution curves of body weights of control (NL/CD) and SL/HFD groups showed a progressive gain of weight, from the day of birth to the end of the experiment. This progressive increase was higher in the OIH group, with 30% higher gain of body weight than controls (**Figure 55 A**). Additionally, it was observed that OIH animals displayed higher energy consumption trends (P=0.06, **Figure 55 B**) and adiposity (**Figure 55 C**), which doubled the levels in controls. These results were paralleled by a strong trend for increased leptin levels (**Figure 55 D**; P= 0.059), associated with a marked increase in glucose levels and decreased insulin levels (**Figure 55 E-F**). In addition, OIH males showed evident insulin resistance (**Figure 55 G**) and glucose intolerance (**Figure 55 H**), as denoted by ITT and GTT, respectively. Further, OIH males displayed signs of cardiovascular impairment, as exemplified by cardiac hypertrophy (**Figure 56 A**) and increased systolic pressure (**Figure 56 B**), together with functional alterations in vessels, such as endothelial dysfunction and augmented (>30%) wall thickness, resulting in an increase in the media:lumen ratio, as well as elevation of cross-sectional area and an increased vascular stress from resistance vessels (**Figure 56 C-H**). Finally, OIH males manifested an evident inflammatory state, as denoted by elevated levels of relevant inflammatory cytokines, such as IL6, IL1, TNFα (**Figure 59**). Altogether, these hormonal and phenotypic data demonstrate that our model of SL/HFD male rats recapitulates the condition of OIH in humans, and its main comorbidities.

2.5. Central blockade of miR-137-3p/325-3p repression of *Kiss1 in vivo* in the OIH model

We applied a TSB strategy, similar to that used in pubertal studies, to address the functional consequences of preventing the repressive actions of miR-137/miR-325 on *Kiss1* in terms of phenotypic features of our model of male OIH.

Central administration of TSB 137/325/Kiss1 to OIH male rats was capable to significantly enhance the hypothalamic levels of kisspeptin, in line with the expected repression of elevated miR-137/325 levels in the MBH of OIH rats on kisspeptin expression (**Figure 54 A**). In the same vein, TSB-treated OIH males displayed an elevation in the accumulated levels of LH (50% increase; **Figure 54 B**) and FSH (12% increase; **Figure 54 C**). In addition, the significant drop in

testosterone levels that was observed in OIH rats was not detected when treated with the TSB (50% increase; **Figure 54 D**). In fact, the hormonal levels in TSB-treated rats were closer to control values, as observed in the NL/CD group.

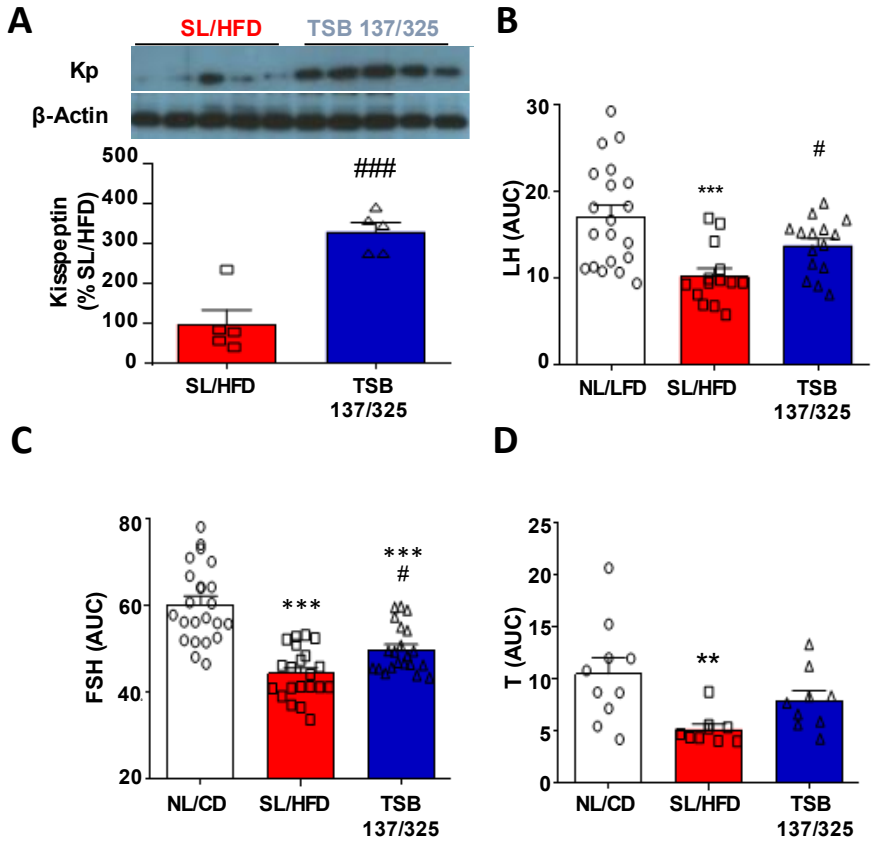

***Figure 54**. In vivo treatment with TSB 137/325/Kiss1 (TSB 137/325) enhances hypothalamic kisspeptin levels and improves reproductive alterations induced in OIH. **A)** Kisspeptin (Kp) expression in hypothalamus of OIH (SL/HFD) male rats treated with vehicle or TSB of miR-137/325/Kiss1. **B)** Area under curve (AUC) of LH secretory values, during the treatment. **C)** AUC of FSH secretory values, during the treatment. **D)** AUC of testosterone (T) secretory values, during the treatment. For presentation of protein level data, expression level of control (SL/HF) was taken as 100%, and the other values were normalized accordingly. Data represent mean ±SEM. Group size: n=9-12. Statistical significance was assessed by ANOVA followed by Holm-Sidak test. **P<0.01, ***P<0.001 vs NL/CD and #P<0.05, ###P<0.001 vs SL/HFD.*

In terms of metabolic parameters, treatment of OIH male rats with TSB 137/325/Kiss1 did not change body weight (**Figure 55 A**) but induced a 30% decrease in energy intake (**Figure 55 B**) and reduced adiposity (**Figure 55 C**), without significant changes in leptin levels (**Figure 55 D**). Treatment with TSB resulted also in improvement of glycemic and insulin homeostasis. Thus, TSB administration to OIH rats caused the normalization of basal glucose levels (**Figure 55 F**), as well as clear improvement of glucose intolerance and insulin sensitivity, as denoted by GTT and ITT (**Figure 55 G-H**). In addition, treatment with TSB 137/327/Kiss1 tended also to moderately increase basal insulin levels in OIH male rats (P=0.1; **Figure 55 E**).

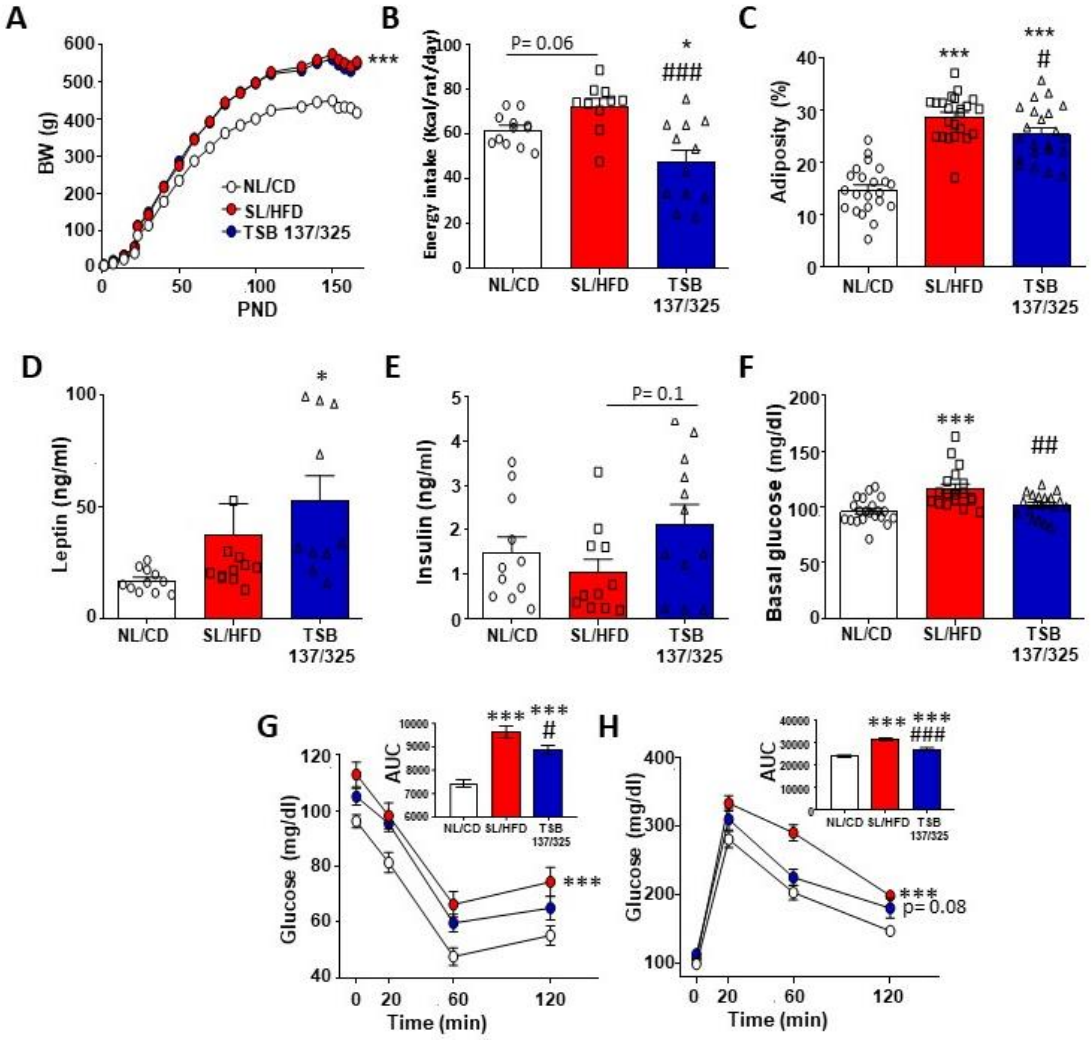

***Figure 55**. In vivo treatment with TSB 137/325/Kiss1 (TSB 137/325) improves the metabolic alterations observed in OIH male rats. **A)** Evolution of body weight from birth to the end of treatment. **B)** Energy intake. **C)** Percentage of adiposity, calculated as (fat %/fat +lean%)X100, at end of the treatment. **D)** Leptin levels at end of the treatment. **E)** Insulin levels at end of the treatment. **F)** Basal glucose levels. **G)** Insulin tolerance test (ITT), during treatment. **H)** Glucose tolerance test (GTT) during treatment. AUC (mg/dL/min) during 2 hours after glucose or inulin bolus are represented in the insets of panel G and H. Represented groups are control (NL/CD) and OIH (SL/HFD) treated with vehicle or TSB 137/325/Kiss1. Data represent mean ±SEM. Group size: n= 9-12. Statistical significance was assessed by ANOVA followed by Holm-Sidak test or 2-way ANOVA followed by Student-Newman-Keuls test (Panels A, G and H). *P<0.05, **P<0.01, ***P<0.001 vs control (NL/CD) and #P<0.05, ##P<0.01, ###P<0.001 vs OIH condition (SL/HFD).*

Regarding cardiovascular parameters, treatment of OIH male rats with TSB 137/325/Kiss1 was able to reverse cardiac hypertrophy (**Figure 56 A**), to decrease SBP (**Figure 56 B**), and to improve endothelial dysfunction linked to obesity (**Figure 56 C**), together with causing a slight rightward shift in the response to vasodilator, DEA-NO (**Figure 56 D**). Administration of TSB 137/325/Kiss1 also induced improvement in the cross-sectional area (**Figure 56 E**), the wall thickness (**Figure 56 F**) and the media:lumen ratio (**Figure 56 G**), which were all increased in the OIH model. Additionally, the treatment with TSB 137/325/Kiss1 prevented mechanical alterations in these resistance vessels generated by the double obesogenic manipulation (SL/HFD), as denoted in

parameters, such as vascular stress (**Figure 56 H**). In addition, TSB 137/325/Kiss1 also restored, beyond the control situation, the increased cytokine profile generated by OIH (see **Figure 59**).

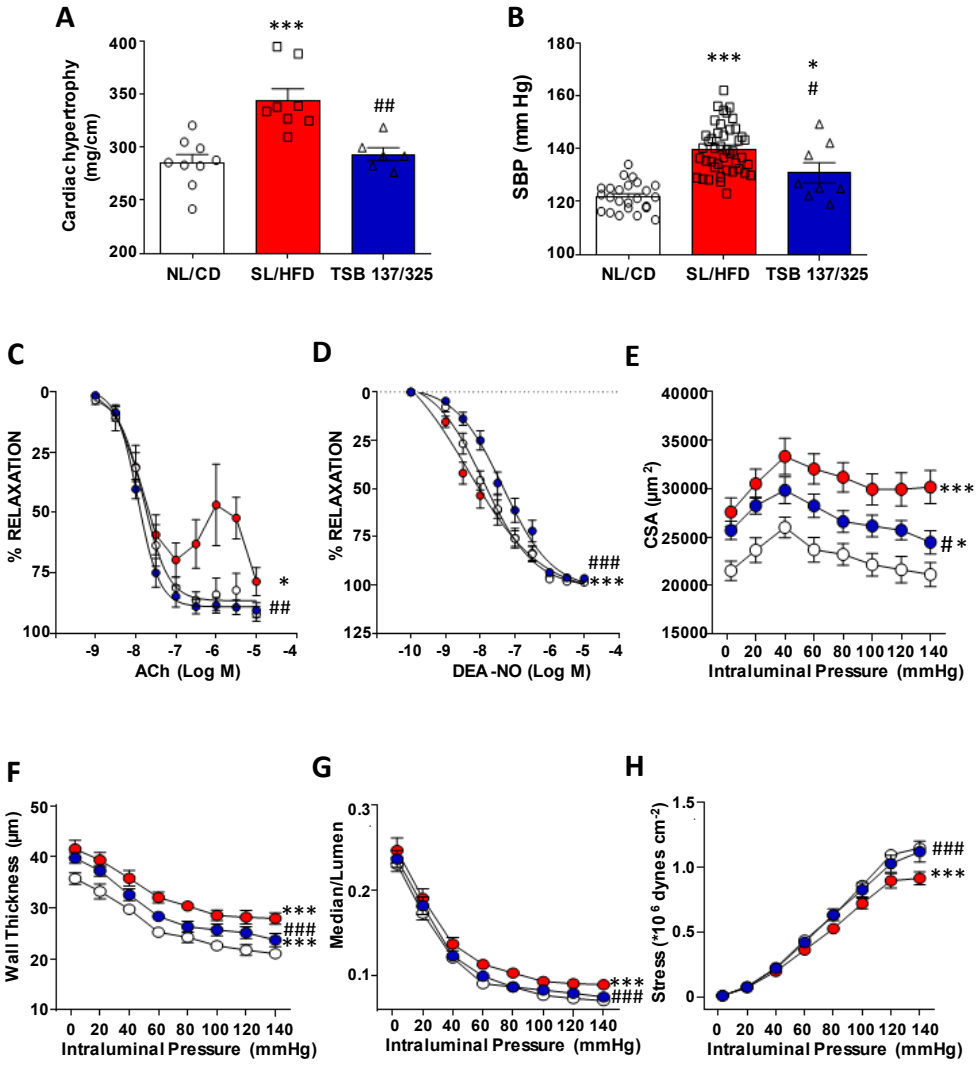

Figure 56. *In vivo treatment with TSB 137/325/Kiss1 (TSB 137/325) improves cardiovascular alterations in the OIH model.* ***A)*** *Cardiac Hypertrophy at the end of treatment.* ***B)*** *Systolic blood pressure (SBP) at the end of treatment.* ***C-D)*** *Dose-response curves to Acetylcholine (Ach) and diethylamine-NO complex (DEA-NO).* ***E-G)*** *Structural and* ***(H)*** *mechanical parameters in mesenteric resistance arteries, of the different experimental groups; control (NL/CD); OIH (SL/HFD) treated with vehicle; or OIH (SL/HFD) treated with TSB. Data represent mean ±SEM. Group size: n= 5-12. Statistical significance was assessed by 2-way ANOVA followed by Student-Newman-Keuls multiple range test. *p<0.05, ***P<0.001 vs control (NL/CD), and #P<0.05, ##P<0.01, ###P<0.001 vs OIH condition (SL/HFD).*

2.6. Effects of central Kp-10 or testosterone treatments on the OIH model

Based on results from section 2.5., we concluded that treatment with TSB 137/325/Kiss1 can substantially improve the main phenotypic manifestations of OIH in our male rat model, likely via elevation of *Kiss1* expression and restoration of reproductive parameters. On this basis, we aimed to evaluate next the effects of two additional treatments for comparative purposes: 1) central pharmacological treatment with Kp-10, or 2) testosterone replacement therapy, in form of chronic implant for sustained release of the androgen.

In relation to Kp-10 treatment, which was centrally applied twice daily for 15 days, we observed that Kp administration elevated LH and FSH levels, which reached values in or over the range of control lean males, together with a marked increase in testosterone levels (**Figure 57 A-C**). Yet, no change in prostate hyperplasia was found (**Figure 57 D**). Body weight, energy intake and adiposity remained unchanged after Kp-10 treatment in comparison with the SL/HFD group (**Figure 58 A-C**), although leptin levels decreased in Kp-treated SL/HFD males, reaching control values (**Figure 58 D**). No improvement of insulin resistance or glucose tolerance, cardiac hypertrophy or SBP was detected in SL/HFD males treated with Kp-10 (**Figure 58 E-J**). Regarding the inflammatory profile, modest changes in the cytokine concentration were noticed, with reduction being detected for IL17A and NT-3 levels (**Figure 59 A**).

Regarding testosterone replacement, this treatment was associated with a significant decrease in serum LH and FSH levels, but massive elevation of circulating testosterone levels (**Figure 57 A-C**), and elevation of prostate hyperplasia ratio (**Figure 57 D**), when compared to the SL/HFD group. Intriguingly, while there was a trend for increased basal insulin levels, ITT revealed no improvement in insulin resistance caused by testosterone treatment over vehicle-treated SL/HFD rats. At the same time, although basal glucose levels were partially reduced, GTT showed no amelioration of glucose intolerance (**Figure 58 E-H**). Increased energy intake was observed when compared with SL/HFD group (**Figure 58 B**), without changes regarding body weight, adiposity, leptin, cardiac hypertrophy or SBP (**Figure 58 A, C-D, I-J**). Regarding cytokine profiles, testosterone replacement was able to moderately improve some cytokine levels, such as IL1ra, IL17 or CCL3 (**Figure 59 A**).

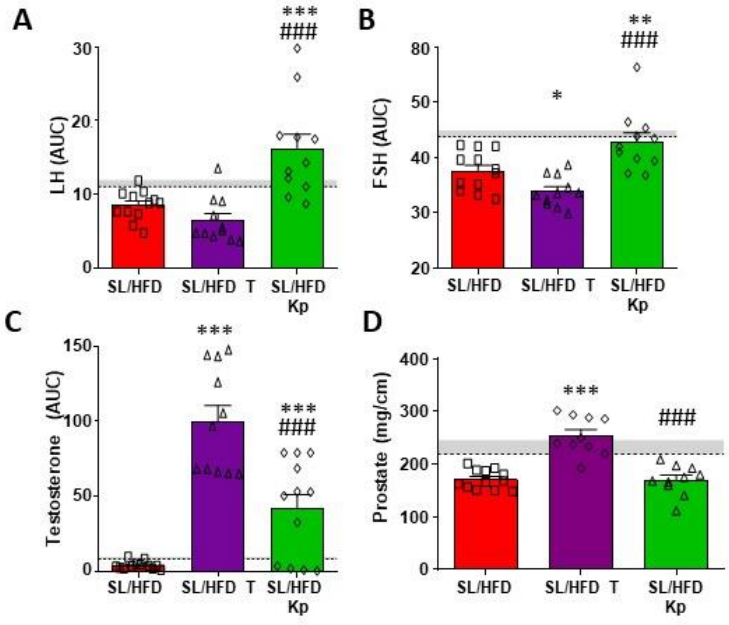

Figure 57*. Effects of Kp-10 and testosterone (T) replacement on reproductive parameters in the OIH model.* ***A****) Integral LH levels (AUC) during treatment.* ***B****) Integral FSH levels (AUC) during treatment.* ***C****) Integral T levels (AUC) during treatment.* ***D****) Prostate hyperplasia ratio (dry weight/ length of the tibia) at the end of the treatment. Control (NL/CD) values are depicted by a discontinuous line; OIH treated with vehicle (SL/HFD) and OIH groups treated with Kp-10 (SL/HFD Kp) or with testosterone (SL/HFD T) are compared. Data represent mean ±SEM. Group size: n= 9-12. Statistical analyses were assessed by ANOVA followed by Student-Newman-Keuls multiple range test. *P<0.05, ***P<0.001 vs control (SL/HFD).*

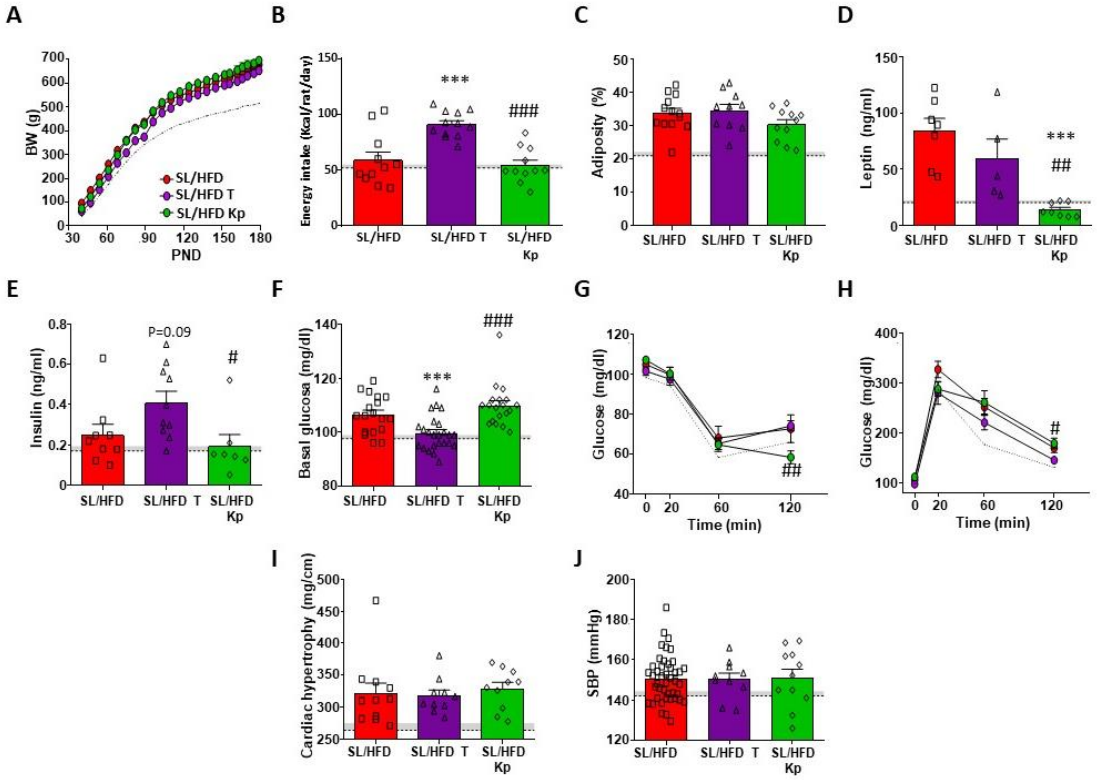

Figure 58*. Effects of Kp-10 and testosterone (T) replacement on metabolic and cardiovascular parameters in the OIH model.* ***A****) Evolution of body weight from PND40 to the end of treatments.* ***B)*** *Energy intake, at the end of treatment.* ***C)*** *Percentage of adiposity, calculated as (fat %/fat +lean %)*100, at the end of the treatment.* ***D****) Leptin levels, at the end of the treatments.* ***E****) insulin levels, at the end of the treatments.* ***F****) Basal glucose levels measured after an overnight fast.* ***G****) Insulin tolerance test (ITT). H) Glucose tolerance test (GTT).* ***I****) Cardiac hypertrophy, at the end of the treatments.* ***J****) Systolic blood pressure (SBP) , at the end of the treatments. Control (NL/CD) values are depicted by a discontinuous line; OIH treated with vehicle (SL/HFD) and OIH groups treated with Kp-10 (SL/HFD Kp) or with testosterone (SL/HFD T) are compared. Data represent mean ±SEM. N= 9-12. Statistical significance was assessed by ANOVA followed by Holm-Sidak test or 2-way ANOVA followed by Student-Newman-Keuls test (Panels A, F and G). ***P<0.001 vs control OIH (SL/HFD), #P<0.05, ##P<0.01 and ###P<0.001 vs SL/HFD T.*

Finally, since the aim of the studies assessing the effects of Kp-10 or testosterone treatments was to compare their effects with the data obtained after central TSB 137/325/Kiss1 treatment, in **Figure 59 B**, we present a graphical summary, in the form of heatmaps, comparatively depicting the overall effects evoked by the different treatments in the OIH male rat model.

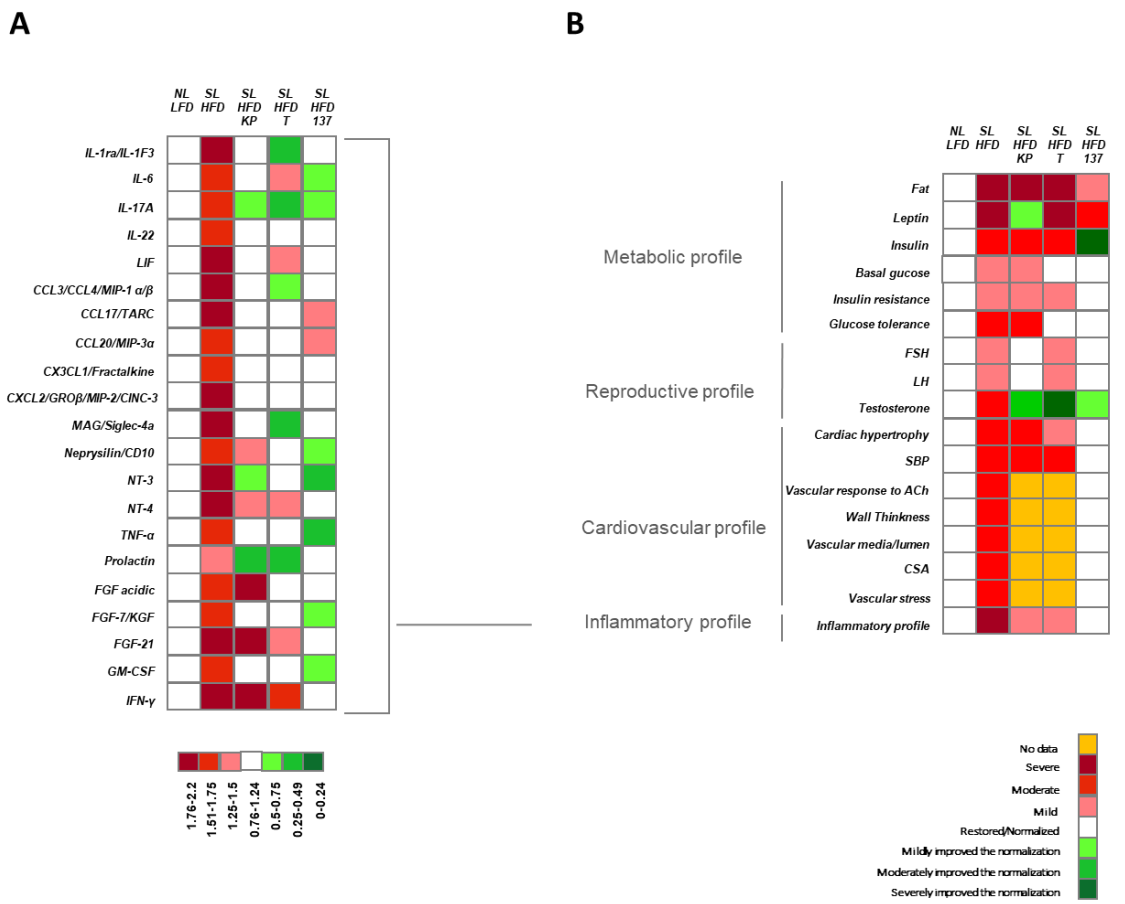

Figure 59. ***A****) Cytokine profiles in the different experimental groups: control (NL/CD) and OIH (SL/HFD) treated with vehicle, kisspeptin, testosterone, or TSB 137/325/Kiss1 (noted as 137). Data represent average density of duplicates. n= 9-12.* ***B****) Graphical summary in the form of heatmap of changes in the different parameters evaluated in OIH (vs. control NL/CD represented in white) and the effect of the different treatments: kisspeptin, testosterone or TSB 137/325/Kiss1 in OIH males. Taken from data presented in Figures 54-58 and 59A. Color codes are included.*

PART 3. GRK2 AS A NOVEL REGULATOR OF GPR54: ROLES IN PUBERTY AND NUTRITIONAL DEPRIVATION

While most of the studies on the regulatory mechanisms controlling the Kiss1 system have been focused on the regulation of the ligand (i.e., *Kiss1* expression and kisspeptin interplay with upstream modulatory systems), little attention has been paid so far to evaluate regulatory mechanisms controlling its receptor, GPR54, which may have also relevant roles. Therefore, as part of this Thesis, we set out experiments to evaluate the role of GRK2, a GPCR desensitizing kinase, in the control of puberty and its modulation by metabolic cues operating via GPR54.

3.1. Evaluation of GRK2-mediated modulation of responses to Kp-10 *in vitro* and *in vivo*

GRK2 is proven to modulate the action of GPCRs, and specifically of GPR54, in cells [136], but no information was available in its physiological relevance. On this basis, we evaluated: 1) *In vitro* responses to Kp-10 in the presence of the GRK2 inhibitor, β-ARK-1-I; and 2) The ability of GRK2 to control GnRH responses to Kp-10 *in vivo*, under conditions of acute and chronic stimulation with Kp-10.

In vitro responses to Kp-10 in control conditions and under the inhibitory action exerted on GRK2 by β-ARK-1 inhibitor were assessed using a cell line stably expressing the human receptor, GPR54, namely HEK293T-GPR54 cells. The cells were stimulated with Kp-10, which induced a maintained increase in intracellular calcium levels (**Figure 60 A**). When cells were stimulated with Kp-10 in the presence of β-ARK-1-I, the increment of calcium levels was further enhanced, while inhibition of GRK2 with β-ARK-1-I in the absence of Kp-10 administration did not significantly modify the amount of intracellular calcium mobilization (**Figure 60 A**).

In addition, the role of GRK2 in the modulation of GnRH responses to Kp-10 *in vivo* was evaluated by pharmacological experiments involving inhibition of GRK2 by pre-treatment with β-ARK-1-I icv. After central administration of effective doses of Kp-10, we evaluated LH and FSH levels, as surrogate markers of GnRH responses. In addition, hormonal responses to Kp-10 were compared with the effects of Senktide, as selective agonist of NK3R (the GPCR mediating the effects of NKB). In the absence of GRK2 inhibitor, central administration of Kp-10 induced a peak in LH levels after 15 minutes, which gradually decreased to reach values close to basal levels 60 minutes after injection. Inhibition of GRK2 provoked an exacerbated peak of LH after 15 minutes, with an AUC around 50 % greater than in control conditions. A grossly similar response was observed in the case of FSH levels (**Figure 60 B-C**). On the contrary, gonadotropin responses to central administration of Senktide were not altered after icv administration of β-ARK-1-I (**Figure 60 D-E**).

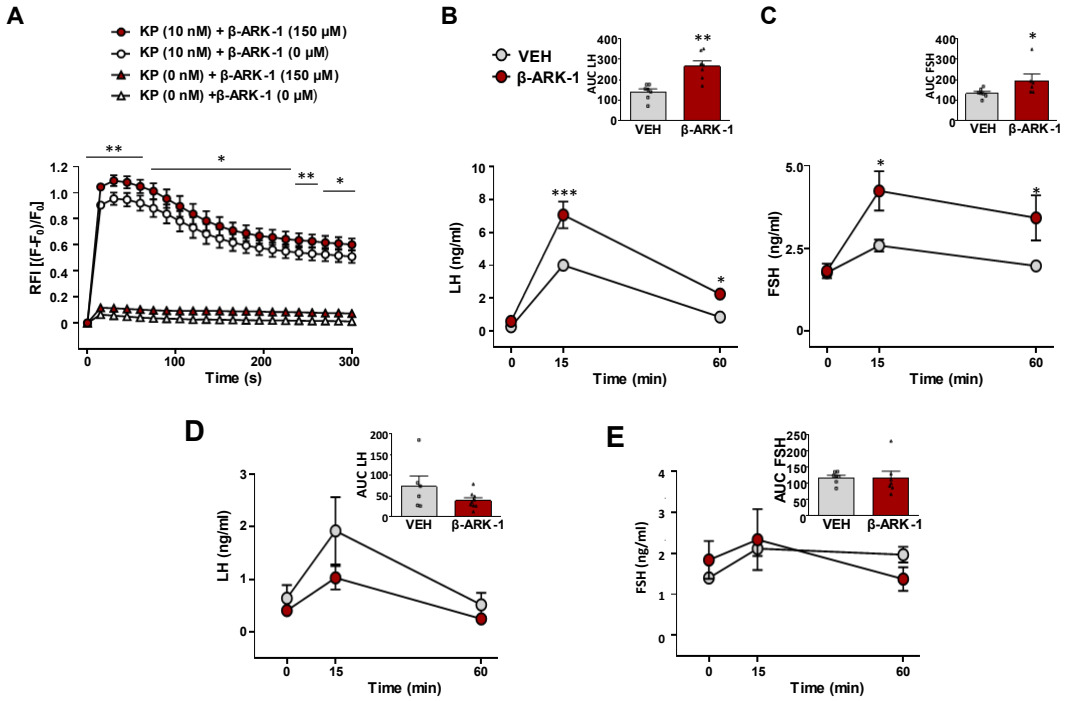

Figure 60. *GRK2 modulation of kisspeptin signaling.* ***A****) Data on calcium mobilization responses to Kp-10 stimulation in a cell line stably expressing the human kisspeptin receptor (HEK293T-GPR54), pre-treated with β-ARK-1 inhibitor or vehicle; RFI= relative fluorescence activity.* ***B****) LH and* ***C****) FSH responses to icv administration of Kp-10 in female rats, pre-treated with the GRK2-inhibitor, β-ARK-1-I, or vehicle; in addition to time-course profiles, integral (AUC) secretory responses are shown in the insets.* ***D****) LH and* ***E****) FSH responses to icv administration of a single bolus of 600 pmol of Senktide in female rats, pre-treated with VEH or β-ARK-1-I; integral secretory responses, calculated as AUC, are also shown. Data represent mean ± SEM. Group size: n=6-9. Statistical significance of the differences was assessed by ANOVA followed by Student-Newman–Keuls multiple range tests (time-course hormonal data) or paired Student t-test (AUC and in vitro data). *P < 0.05, **P < 0.01, ***P < 0.001 vs. corresponding vehicle-treated groups.*

3.2. Hypothalamic GRK2 expression through postnatal maturation and in delayed puberty

Grk2 mRNA levels were analyzed in the hypothalamus of female rats across different stages of postnatal maturation (neonatal, infantile, juvenile, early pubertal, pubertal and adult period). Grk2 mRNA levels increased consistently from neonatal period to early pubertal period, when *Grk2* expression achieved the highest levels in the whole hypothalamus or in the POA (**Figure 61 A, C**). In the MBH, the highest levels of Grk2 mRNA were found during the juvenile period (**Figure 61 D**). At the protein level, a similar pattern was observed, with the greatest hypothalamic content of GRK2 protein being detected during the early pubertal and pubertal period (**Figure 61 B**).

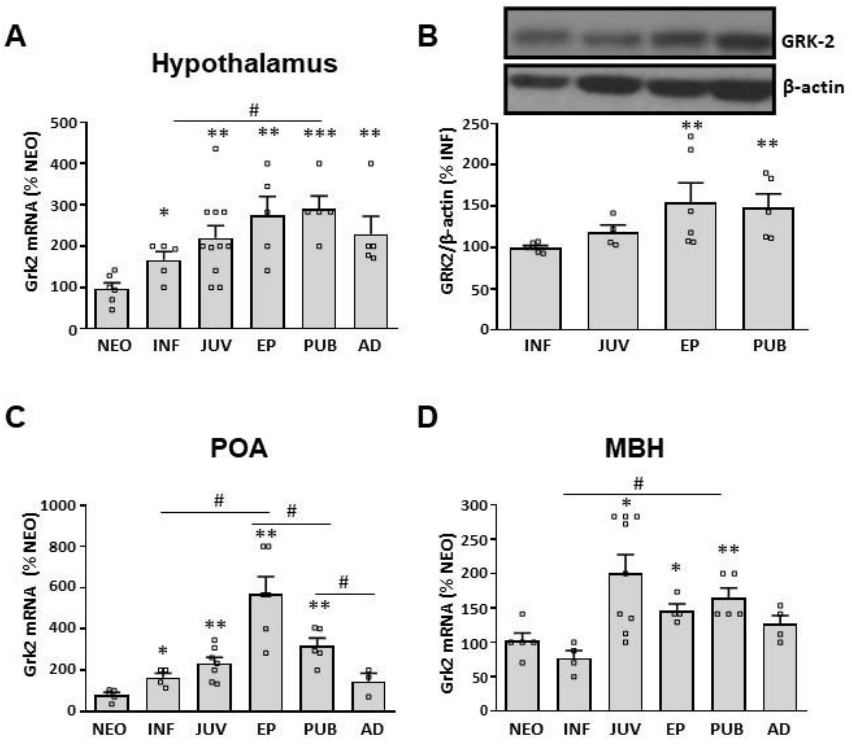

Figure 61. *Grk2/GRK2 expression in the rat hypothalamus during ontogeny.* ***A****) Grk2 mRNA expression and* ***B****) GRK2 protein content in whole hypothalamic samples from female rats at different stages of postnatal development.* ***C****) Data on Grk2 mRNA expression in the preoptic area (POA) and* ***D****) the medio-basal hypothalamus (MBH) of female rats at different stages of postnatal development are also shown. For presentation of data, the level of expression of Grk2 mRNA in neonatal samples (NEO), or protein content in infantile samples (INF), were taken as 100%, and the other values were normalized accordingly. Data represent mean ± SEM. Group sizes are: n= 6 for NEO, INF and EP stage, n =11 for JUV stage and n= 5 for AD stage in panels A-D. Statistically significant differences were assessed by ANOVA followed by Student-Newman-Keuls multiple range test. *P < 0.05, **P < 0.01, ***P < 0.001 vs reference (NEO or INF) values; # P < 0.05 vs the indicated paired groups (denoted by the continuous overline). NEO: neonatal; INF: infantile; JUV: juvenile; EP: early pubertal; PUB: pubertal; AD: adult.*

In addition, the expression levels of *Grk2* were assessed in hypothalamic samples from models of pubertal delay, similar to those analyzed in Part 1, namely, postnatal or lactational underfeeding (LL) and chronic caloric restriction post-weaning (UN), as previously validated in our laboratory[5].

In conditions of underfeeding during lactation (LL), hypothalamic *Grk2* mRNA levels at PND5, 15 and 35 were higher than those of control (NL) animals at the same ages (**Figure 62 A**). Similarly, hypothalamic protein levels of GRK2 were found to increase by 50 % in the LL group, as compared to NL at PND35 (**Figure 62 B**). Regarding female rats submitted to 30% chronic undernutrition post-weaning (UN; namely, allowed to eat only 70% of the normal daily ration of pair-aged rats fed *ad libitum* from PND23 to PND35), *Grk2* mRNA levels were found to increase in the POA of hypothalamus (**Figure 62 C**), while GRK2 protein levels increased in both, POA and MBH, when compared with the control group (**Figure 62 D**).

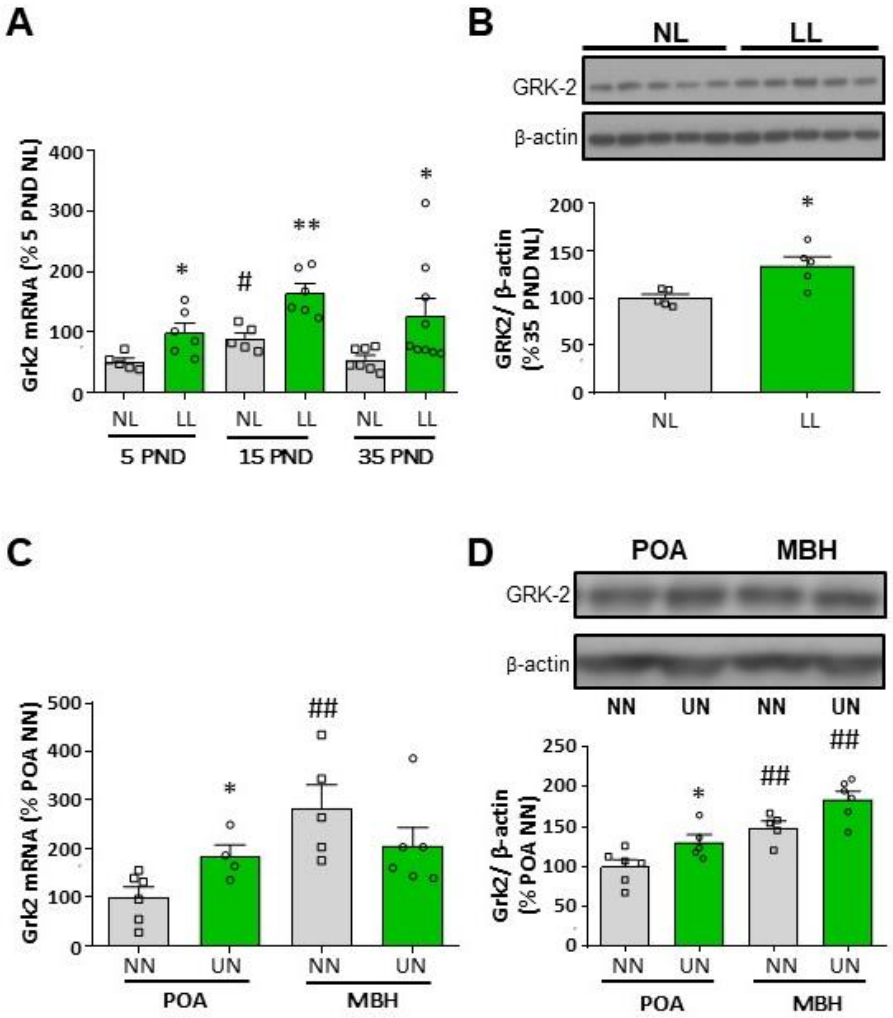

***Figure 62**. Hypothalamic expression of Grk2/GRK2 in rat models of delayed puberty. In the upper panels, a model of postnatal underfeeding is presented. Female rats from normal litters (NL, 12 pups/litter) served as controls. **A**) Hypothalamic expression of Grk2 mRNA was assayed in NL and LL rats at PND5, 15 and 35, while in **B**) GRK2 protein content was measured at PND35. In the lower panels, data from a model of chronic undernutrition (UN) are shown. Female rats fed ad libitum (NN) served as controls. **C**) Hypothalamic levels of Grk2 mRNA and **D**) GRK2 protein content in the POA and MBH of UN and NN rats at PND35, are shown. Data represent mean ± SEM. Group sizes: n = 10 for the NL and the LL group; yet, mRNA expression and protein content analyses in NN and UN rats were conducted in a subset of representative samples of each group. For panels C-D, n = 4-6. Statistical difference was assessed by Student t-test or ANOVA followed by Student–Newman–Keuls multiple range tests. *P < 0.05, **P < 0.01 vs corresponding control (NL or NN) groups. #P <0.05, ##P < 0.01 vs PND5 NL or POA NN.*

3.3. Blockade of GRK2 and pubertal development: Pharmacological and genomic approaches

Based on the results obtained above, which suggest that GRK2 could contribute to the regulation of puberty during reproductive maturation, we wanted to verify if chronic blockade of GRK2 at central levels would affect normal pubertal development. We pursue this goal in two ways: (i) through central administration of the pharmacological inhibitor, β-ARK-1-I, during the prepubertal period in female rats; and (ii) by the specific ablation of *Grk2* in GnRH neurons, in the so-called G-GRKO (GnRH-specific, Grk2 knock-out) mouse model, to specifically target the contribution of GRK2 at the level of the GnRH neuron, which is the primary site of action of kisspeptin, operating via GPR54.

3.3.1. Central pharmacological inhibition of GRK2 and puberty onset

Female rats injected icv twice daily, from PND25 to PND34, with an effective dose of the GRK2 inhibitor, β-ARK-1-I, or with VEH, were monitored to check pubertal progression. Treatment with β-ARK-1-I advanced the onset of puberty, as denoted by the moderate advance in the ages of VO and first estrus (**Figure 63 A-B**), which were associated with an increase in mean LH and FSH levels, as well as ovary and uterus relative weights (**Figure 63 C-F**). Histological analysis of the ovaries documented a marginal advancement of the follicular maturation stage and no changes in the percentage of ovulatory females at the end of the treatment (**Figure 63 G-H**).

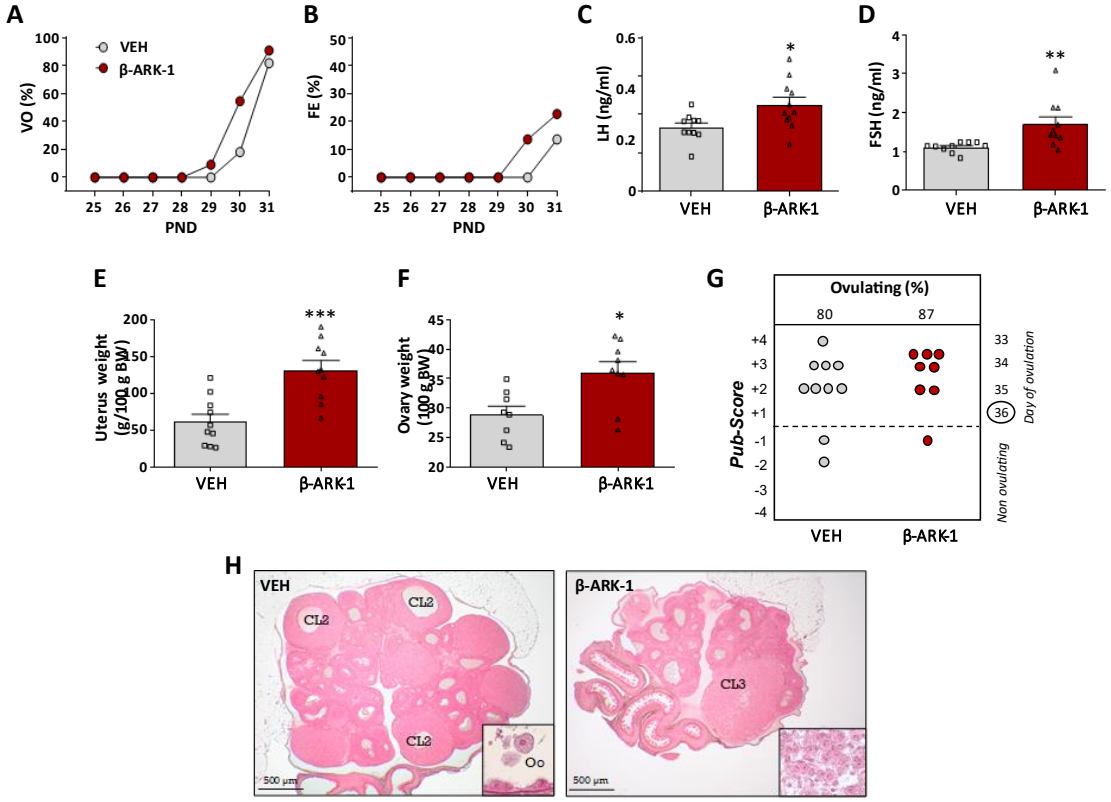

***Figure 63**. Impact of central blockade of GRK2 on the timing of puberty onset in female rats. Immature female rats were injected icv with the GRK2 inhibitor, β-ARK-1-I (red symbols), every 12 h, from PND25 to PND34; females injected icv with vehicle (VEH; grey symbols) served as controls The parameters presented are **A**) Cumulative percentage of vaginal opening (VO); and **B**) First estrus (FE). **C**) LH and **D**) FSH levels. **E**) Uterus and **F**) Ovary relative weights. In addition, **G**) histological score of follicular development/ovulation (Pub-score), and **H**) representative images of ovarian maturation are presented from both groups. CL: corpus luteum. Group size: n = 11 rats/group. Statistical significance was assessed by unpaired Student t-test. *P < 0.05, **P < 0.01, ***P < 0.001 vs. the vehicle-treated group.*

3.3.2. Conditional ablation of *Grk2* in GnRH neurons and puberty onset

Regarding specific ablation of *Grk2* in GnRH neurons *in vivo*, we generated a conditional GRK2 KO mouse line, called G-GRKO, by using the Cre-loxP technology. A well validated GnRH-Cre mouse line was crossed with homozygous mice harboring modified *Grk2* alleles, which contained the DNA region coding exons 3 to 6 flanked by loxP sites (**Figure 64 A**). Validation of the mouse model was conducted by PCR, where the excision of the floxed region documented

the presence of *Grk2* recombination events in the region where most GnRH neurons are localized, the POA, but not in other tissues (**Figure 64 B**). Additionally, we documented effective *Grk2* ablation by performing dual *in situ* hybridization using RNAscope probes. These analyses demonstrated abundant co-localization of *Grk2* mRNA in GnRH expressing cells in control mice, whereas in G-GRKO mice, co-expression of *Grk2* in GnRH neurons was significantly decreased (**Figure 64 C**), with an average number of co-localization events of 18.91 ± 2.19 per GnRH neuron in control mice vs. 6.26 ± 0.55 co-localization events in GnRH neurons from G-GRKO mice. This represents a 66.9% suppression of co-expression in our conditional null mouse line. These data confirm that GnRH neurons normally express *Grk2*, but this is markedly blunted in GnRH cells from G- GRKO animals.

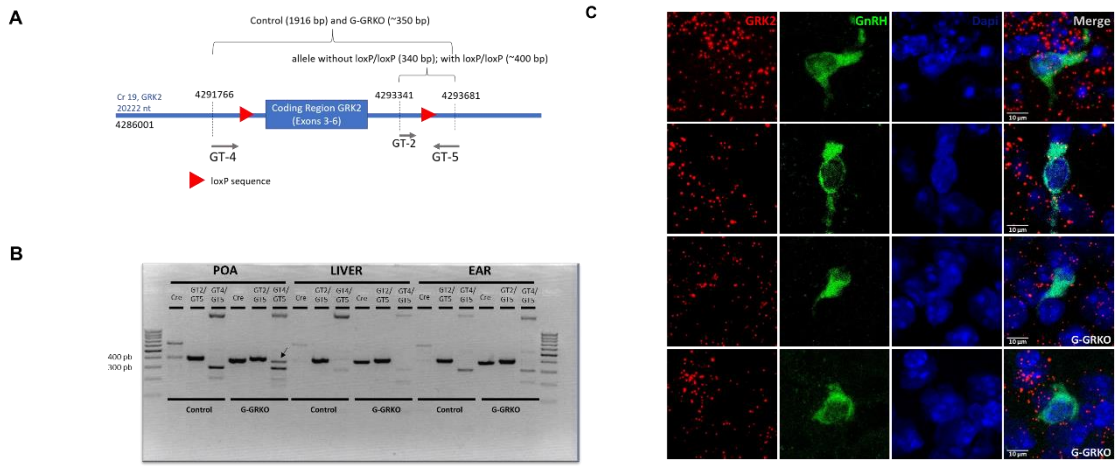

***Figure 64**. Validation of G-GRKO mouse model, where there is a GRK2 deletion in GnRH neurons. **A**) Genetic map of GRK2, in which is shown the location of the flox sequences, including the amplification regions of the primers and the size of the amplicons generated. **B**) PCR showing the presence or absence of Cre recombinase in POA, liver and ear (band of ~400 base pairs, bp), and the presence (band of 400 bp, GT2/GT5) or absence (band of 350 bp, GT4/GT5) of the Grk2 floxed allele, in POA, liver and ear, in control or G-GRKO mice, respectively. Arrow points to the 350 bp band detected in the POA of G-GRKO mice when PCR amplification is performed with the GT4/GT5 primer pair. **C**) In situ hybridization assay from control and G-GRKO mice for co-labelling Grk2 and GnRH; in the G-GRKO mouse, the probe for Grk2 targets the excised regions and hence impairs detection after recombination events.*

Regarding pubertal and reproductive indices, we performed functional tests involving icv injection of an effective bolus of Kp-10 in mice with specific deletion of GRK2 in GnRH neurons. GnRH responsiveness to kisspeptin stimulation was assessed using LH and FSH levels as surrogate markers of GnRH activation. LH and FSH responses to icv injection of Kp-10 were significantly augmented in G-GRKO mice, which displayed also elevated basal LH levels (**Figure 65 A-D**).

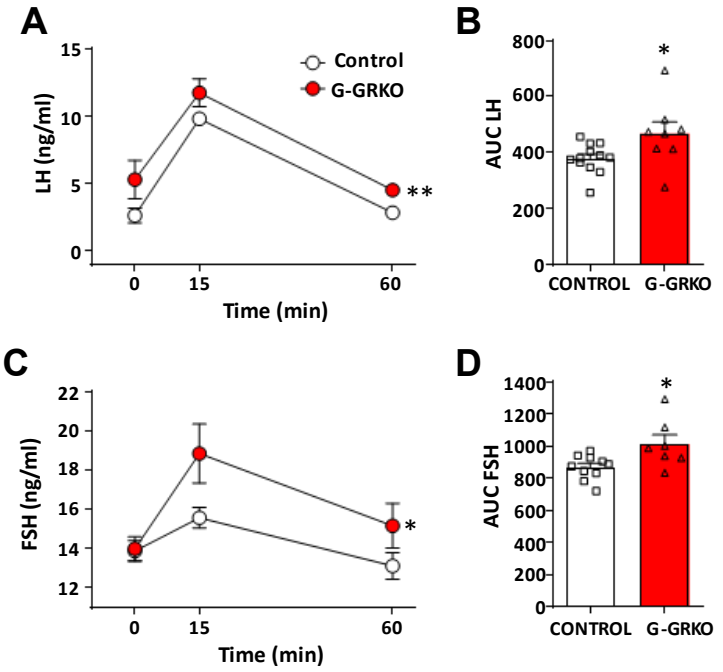

***Figure 65**. Characterization of mice with conditional ablation of GRK2 in GnRH cells (G-GRKO). **A**) Patterns of LH and **C**) FSH responses to Kp-10 stimulation in control and G-GRKO young male mice are presented. Hormonal determinations were conducted at 0- (basal), 15- and 60-min after Kp-10 injection. In addition to time-course profiles, **B**) integral (AUC) LH and **D**) FSH secretory responses are shown. Data represent mean ±SEM. Group sizes: n=12 for controls; n=8 for G-GRKO mice. Statistical significance was assessed by unpaired Student t-test. *P < 0.05, **P < 0.01, vs. the control group.*

Additionally, pubertal maturation was monitored in G-GRKO mice of both sexes. Regarding females, analysis of phenotypic markers of puberty revealed an advancement of pubertal onset, as denoted by earlier VO, with a mean age of PND35.6, which was associated with trends for earlier FE -as denoted by cumulative percentage of mice displaying first estrus- (**Figure 66 A-D**), along with a significant increase in the uterus and ovary weights (**Figure 66 E-F**). These results were confirmed by histological analyses of the ovaries of G-GRKO mice, which demonstrated a significant advancement of the state of follicular maturation and an increase in the percentage of ovulatory animals in G-GRKO mice *vs* controls, with an earlier expected mean age of first ovulation in the G-GRKO group (**Figure 66 G-H**). These phenotypic changes occurred in the absence of detectable changes in body weight or food intake during the pubertal maturation (**Figure 66 I-J**).

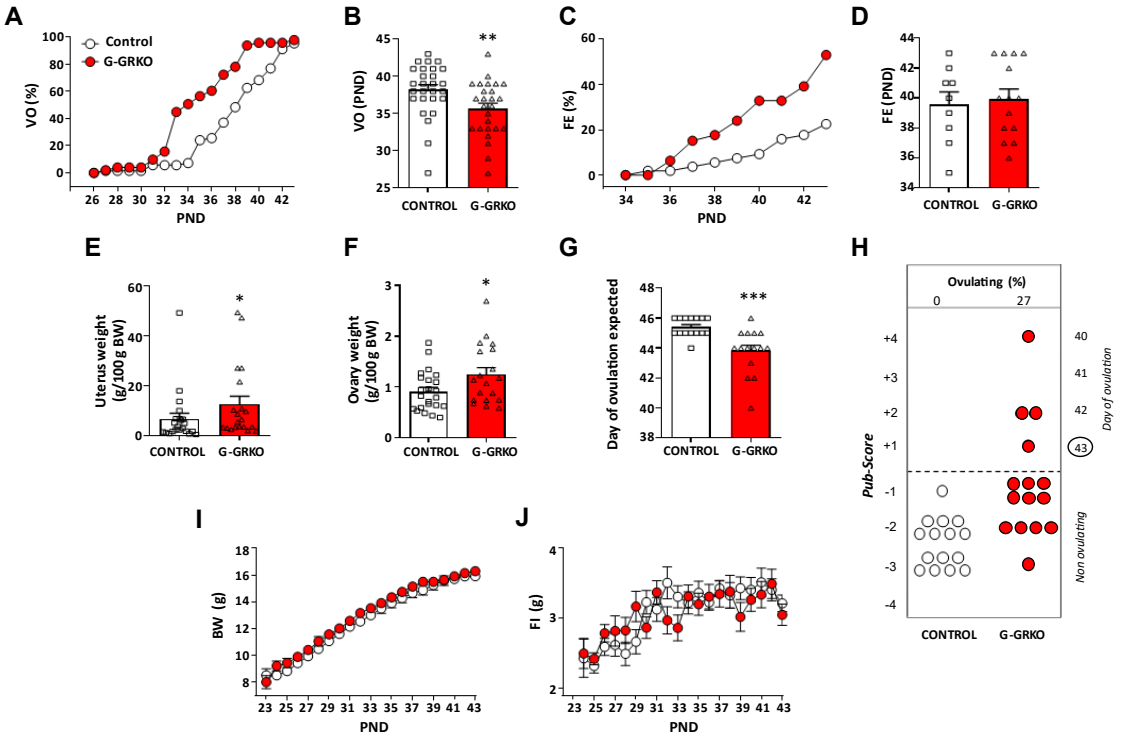

Figure. 66. *Phenotypic characterization of puberty onset in control and G-GRKO female mice.* ***A****) Cumulative percentage of vaginal opening (VO).* ***B****) Mean age of vaginal opening.* ***C****) Cumulative percentage of first estrus (FE).* ***D****) Mean age of FE.* ***E****) Uterus and* ***F****) ovary weights.* ***G****) Expected mean age of first ovulation, calculated based on the stage of follicular maturation, and* ***H****) Histological score of follicular development/ovulation (Pub-score) from both groups.* ***I****) Body weight (BW), and* ***L****) Food intake (FI) during experimental follow-up. Data represent mean ± SEM. n = 23 for controls; n = 19 for G-GRKO mice. Statistical significance was assessed by paired Student t-test. *P < 0.05, **P <0.01***P < 0.001 vs. corresponding control group.*

For comparative purposes, we also analyzed markers of puberty in male counterparts of both genotypes. In line with the female phenotype, and despite the lack of changes in body weight or food intake during the pubertal transition (**Figure 67 A-B**), the age of preputial separation, as an external sign of puberty, was advanced, and the circulating levels of testosterone were increased in G-GRKO male mice, when compared to control mice (**Figure 67 C-D**).

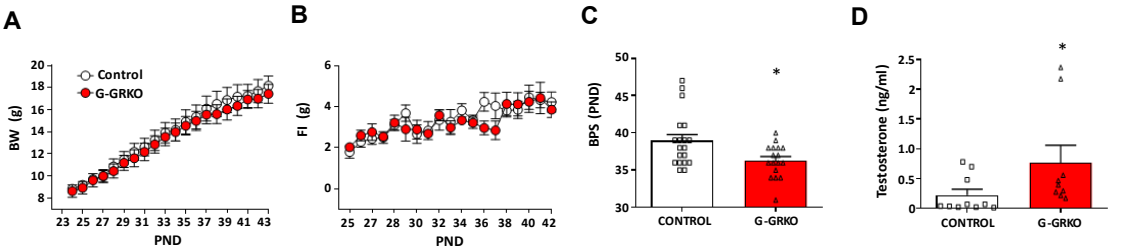

Figure 67*. Phenotypic characterization of puberty onset in control and G-GRKO male mice.* ***A****) Body weight (BW), and* ***B****) Food intake (FI) during experimental follow-up.* ***C****) Mean age of preputial separation (BPS).* ***D****) Mean testosterone levels at final time. Data represent mean ± SEM. n = 12-16 in panels A-C, n=9-10 for panel D. Statistical significance was assessed by 2-way ANOVA (Panels A-B) and paired Student t-test. *P < 0.05, vs. corresponding control group.*

To explore the basis for such accelerated puberty onset in G-GRKO mice, we assessed the profiles of pulsatile LH secretion in G-GRKO mice, in young adult females. Ablation of *Grk2* in GnRH neurons significantly decreased basal LH levels, with a concomitant reduction of mean,

total and integral LH secretion over the 3-h period of analysis (**Figure 68 A-D**). In contrast, G-GRKO mice displayed a significant increase in LH pulsatility, with double number of pulses (on average) per 3-h than the corresponding controls (**Figure 68 E**). Representative LH secretory profiles from control and G-GRKO mice are shown in **Figure 68 F-G**.

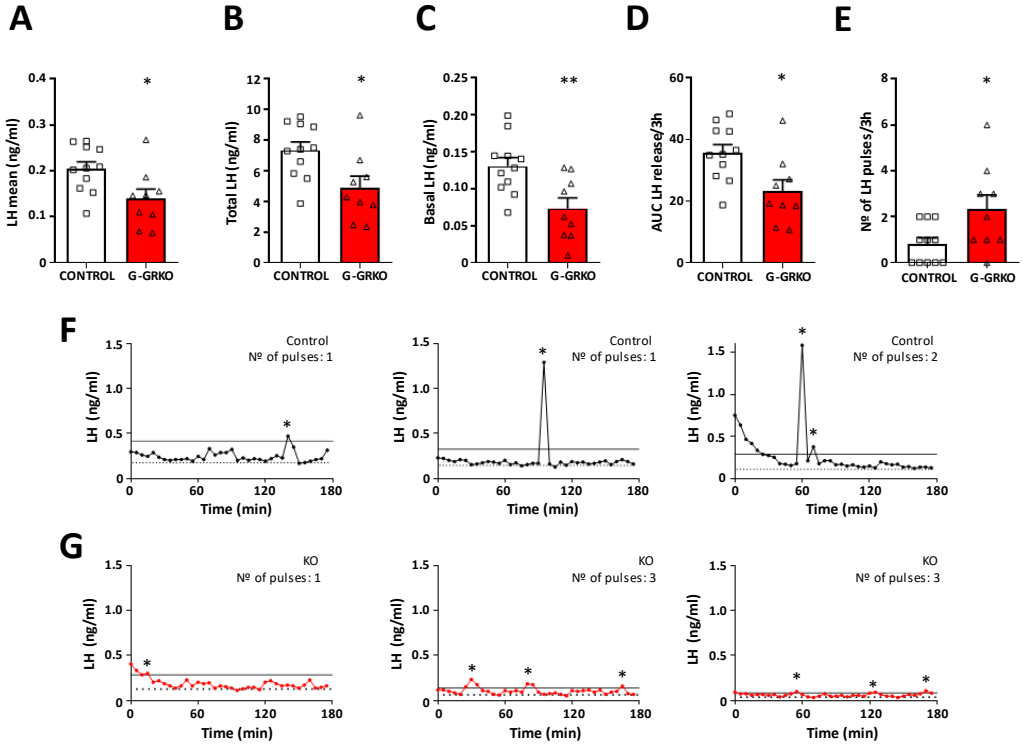

Figure 68. *LH pulsatility in female G-GRKO mice, with conditional ablation of GRK2 in GnRH cells. LH secretory profiles were characterized in young adult, control and G-GRKO mice. The following parameters of LH secretion are presented in the upper panels: **A**) mean LH, **B**) total LH and **C**) basal LH levels. **D**) The area under the curve (AUC) of LH release and **E**) the number of LH pulses during the 3-h study period are shown. In the lower panels, **F**) three representative individual LH secretory profiles of control and **G**) G-GRKO female mice are displayed. n = 11 for controls; n = 9 for G-GRKO mice. Statistical significance was assessed by Student t-test. *p < 0.05, **p < 0.01 vs. corresponding control group. In panels F-G, pulses are denoted by asterisks, dotted lines represent basal LH levels and continuous lines represent the 125% peak threshold level.*

3.4. Blockade of GRK2 and pubertal development: Studies in models of delayed puberty

As the results above confirm a role for *Grk2* in the regulation of kisspeptin responsiveness in GnRH neurons during normal pubertal development, next, we aimed to address if central pharmacological inhibition of GRK2 or its conditional ablation in GnRH neurons are able to prevent the delayed pubertal phenotypes linked to nutritional deprivation.

3.4.1. Central pharmacological inhibition of GRK2 in conditions of nutritional deprivation

As model of delayed puberty in female rats, we used LL rats. Pharmacological inhibition of GRK2 was achieved with β-ARK-1-I, that was daily injected during the prepuberal period. NL female rats were fed *ad libitum* and treated with vehicle (VEH NL), while LL were treated either with vehicle (VEH LL) or β-ARK-1 inhibitor (β-ARK-1 LL). As expected, VEH LL female rats treated with vehicle displayed decreased body weight as consequence of nutritional restriction (**Figure 69 A-**

B). Under this condition, VEH LL female rats exhibited delayed puberty, as demonstrated by the delay in the age of VO and FE, together with a trend for lower uterus (p=0.07) and ovary relative weights, without changes in LH or FSH levels, but a moderate reduction in the ovulatory rate (**Figure 69 C-I**). Treatment of LL female rats with the inhibitor, β-ARK-1-I, despite reduction in body weight linked to nutritional deprivation (**Figure 69 A**), partially normalized indices of pubertal maturation, as denoted by the ages of VO and FE, which exhibited an intermediate phenotype between VEH NL and VEH LL rats (**Figure 69 C-D**). Uterus and ovary relative weights were restored (**Figure 69 E-F**); as were follicular maturation and the estimated day of first ovulation (**Figure 69 I-J**). LH and FSH hormonal levels did not change between groups (**Figure 69 G-H**).

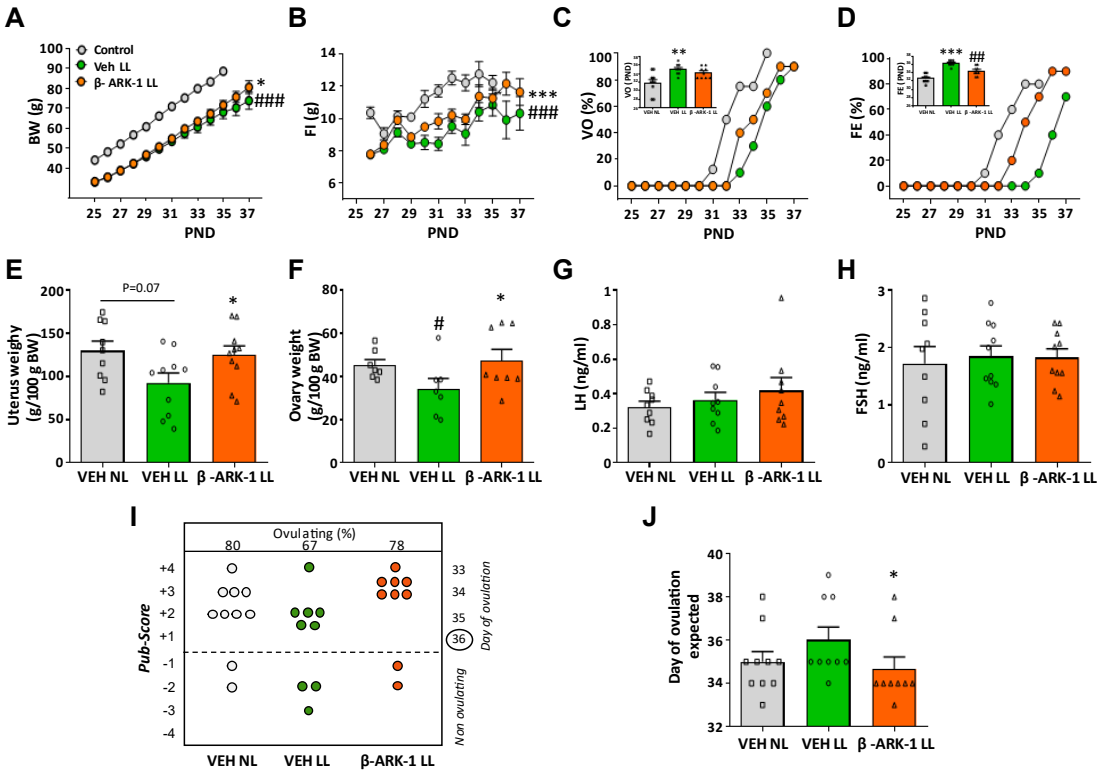

Figure 69. *Central blockade of GRK2 partially rescues pubertal delay caused by postnatal undernutrition in female rats. Female rats reared in large litters (LL) were icv injected with GRK2 inhibitor, β-ARK-1, or vehicle every 12 h, from PND25 to 37. Reference values from control (NL) females icv injected with vehicle (VEH) served as controls. The parameters presented are:* ***A****) body weight,* ***B****) daily food intake (FI),* ***C****) cumulative percentage of vaginal opening (VO), and* ***D****) first estrus (FE). In addition,* ***E****) uterus and* ***F****) ovary weights, as well as* ***G****) LH and* ***H****) FSH levels are shown, together with* ***I****) the histological score of follicular development/ovulation (Pub-score), and* ***J****) the mean age of expected first ovulation, calculated based on the stage follicular maturation. Data represent mean ± SEM. Group size: n= 10/group. Statistical significance was assessed by ANOVA followed by Student Newman–Keuls multiple range tests or 2way ANOVA. *P < 0.05, **p<0.01, ***P < 0.001 vs VEH LL. #P < 0.05, ##P < 0.01, ###P < 0.001 vs VEH NL.*

3.4.2. Conditional ablation of *Grk2* in GnRH neurons in conditions of delayed puberty

Complementary to the experiment described above, a protocol of chronic food restriction was applied from PND23 to PND49 to control and G-GRKO female mice. An average 20 % food restriction (UN) compared to the control daily ration, caused a substantial drop in body weight

gain, along with lower daily food intake (**Figure 70 A-B**), as expected due to restricted food availability. UN caused a delay in pubertal onset, evidenced by deferred progression and mean age of VO (**Figure 70 C-D**), together with delayed FE (**Figure 70 E**), and reduced LH levels, uterus (P = 0.07) and ovary relative weights (**Figure 70 F-H**). Ablation of *Grk2* in GnRH cells partially rescued this pubertal delay, as denoted by partial normalization of VO progression and complete rescue of the mean age of VO, as well as relative uterus and ovary weights. In addition, FE progression was moderately advanced, while LH levels remained suppressed in G-GRKO female mice subjected to UN (**Figure 70 C-H**). To get insight into the underlying hormonal basis for this partial rescue, pulsatile LH secretion was assessed in G-GRKO female mice subjected to UN. As shown in **Figure 70 I-L**, 25% UN caused a reduction in mean, basal and integral LH secretion, as well as a suppression of the number of LH pulses, over a 3-h period in control mice. In contrast, G-GRKO female mice subjected to a similar regimen of UN displayed higher number of LH pulses than the corresponding UN controls; their pulse frequency being similar to that of controls fed *ad libitum.* Notwithstanding, mean, basal and integral LH secretion over the 3-h period was equally suppressed by UN in G-GRKO and control mice (**Figure 70 I-K**).

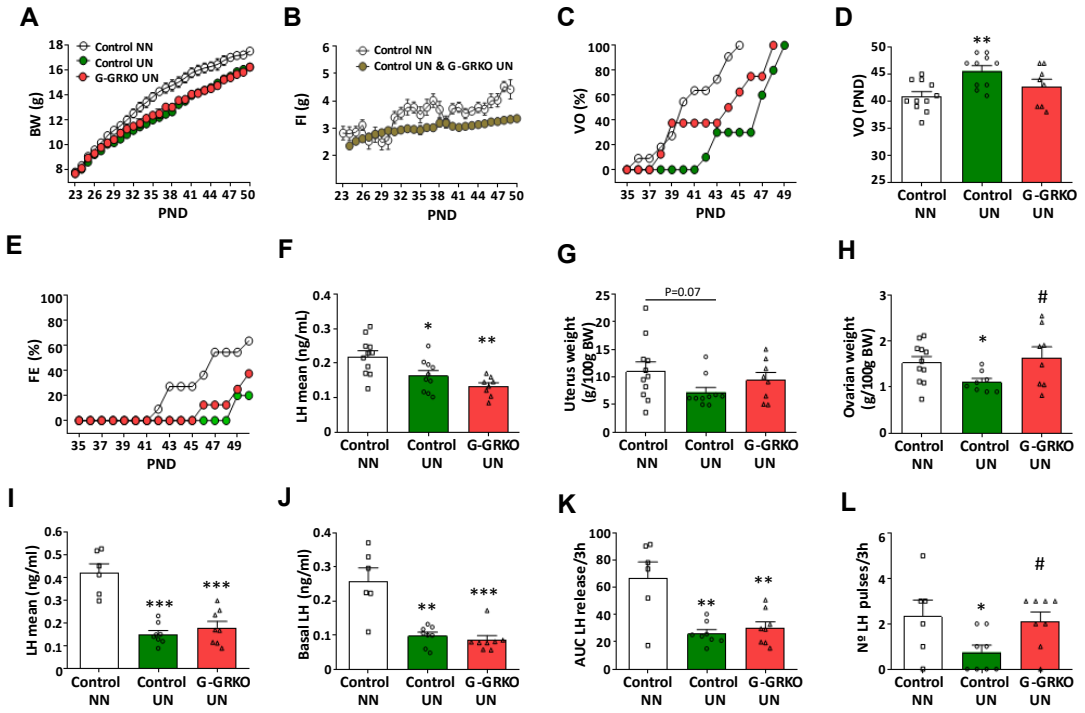

Figure 70. *Grk2 ablation in GnRH cells partially prevents the impact of undernutrition on puberty onset and LH pulsatility.* ***A****) Body weight,* ***B****) daily food intake,* ***C****) cumulative percentage of VO,* ***D****) mean age of VO, and* ***E****) cumulative percentage of first estrus (FE) in control and G-GRKO female mice subjected to chronic undernutrition (UN) are presented. Pair-aged, control female mice fed ad libitum (NN) served as controls.* ***F****) Mean LH levels,* ***G****) uterus and* ***H****) ovary relative weights in pubertal control and G-GRKO mice are also presented. Features of LH secretory profiles of young adult female control and G-GRKO mice subjected to UN are also shown:* ***I****) mean LH and* ***J****) basal LH levels, as well as* ***K****) the area under the curve (AUC) of LH release and* ***L****) the number of LH pulses during the 3-h study period. Data represent mean ± SEM. Group sizes: n = 11 for NN control group; n = 10 for UN control group; and n = 8 for UN G-GRKO group (panels A-H). In panels I-L, n= 6 for NN control group; n =9 for UN control group; and n = 8 for UN G-GRKO group. Statistical significance was assessed by 2way ANOVA, or ANOVA followed by Student Newman-Keuls multiple range test. *P < 0.05, **P < 0.01, ***p < 0.001 vs control NN group; #P < 0.05 vs control UN group.*

PART 4. ROLES OF CENTRAL GRK2 IN OBESITY-INDUCED HYPOGONADISM OF THE MALE

After demonstration of the role of GRK2 in the metabolic control of puberty, putatively acting via modulation of GPR54 signaling in GnRH neurons, we also aimed to assess the potential function of GRK2, at central and GnRH neuronal level, in the pathophysiology of OIH during adulthood in males.

4.1. Inhibition of GRK2 enhances gonadotropin responses to repeated kisspeptin stimuli

First, we explored if central inhibition of GRK2, using the inhibitor, β-ARK-1-I, was able to influence responses to repeated GPR54 activation, under normal nutritional conditions, in adult male rats submitted to sequential icv administration of Kp-10. Male rats were icv injected with β-ARK-1-I, 13 hours and 1 hour prior to the beginning of Kp-10 injections. We observed, by measuring LH and FSH levels -as surrogate markers of the activity of Kiss1/GPR54 signaling pathway- in a time course of 4 hours, that repeated injection of 50 pmol or 1 nmol of Kp-10 every 60 minutes induced an exacerbated response to Kp-10 in the group treated with β-ARK-1-I. Thus, 50 pmol Kp-10 administration doubled the circulating levels of LH and FSH (**Figure 71 A, C**), while 1 nmol Kp-10 injections triplicated the serum concentrations of LH and doubled FSH serum levels in the group pre-treated with the inhibitor β-ARK-1-I (**Figure 71 B, D**).

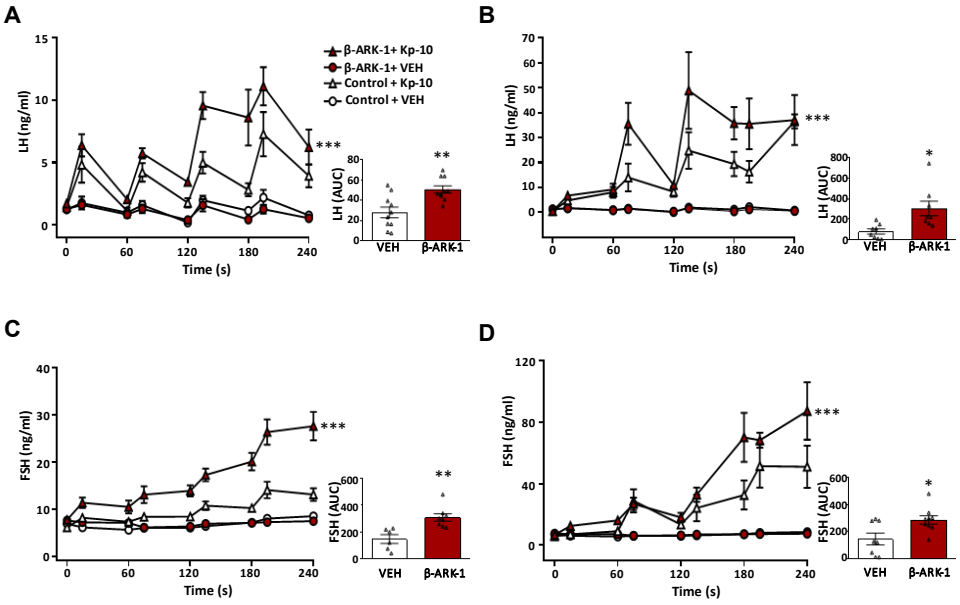

*__Figure 71__. Central administration of the GRK2 inhibitor, β-ARK-1, enhances gonadotropin responses after repeated central icv administration of Kp-10 in young male rats. Time-course analyses of LH responses to repeated injections of a bolus of 50 pmol (__A__) or 1 nmol (__B__) doses of Kp-10 every hour, over a period of 240 min, in the control group or β-ARK-1-I pre-treated animals, are presented. In addition, time-course analyses of FSH responses to repeated injections of a bolus of 50 pmol (__C__) or 1 nmol (__D__) of Kp-10 in the control group or β-ARK-1-I pre-treated animals are also shown. AUC (ng/mL/min for 4 hours) of the time-course profiles are represented In the insets of panels A-D. Groups are: control treated with vehicle (control + VEH), control treated with Kp-10 (control + Kp10), β-ARK-1-I treated with VEH (β-ARK-1+ VEH) and β-ARK-1-I treated with Kp-10. Data represent mean ± SEM. Group size: n=6-10. Statistical significance was assessed by 2- way ANOVA followed by Student-Newman-Keuls test or paired Student t-test for statistical significance of AUC. **P < 0.01, ***p < 0.001 vs control+ Kp-10 group.*

4.2. Hypothalamic expression of GRK2 in the rat model of OIH

Next, we evaluated hypothalamic levels of *Grk2*/GRK2 in our preclinical model of OIH. Grk2 mRNA and GRK2 protein levels were measured in the hypothalamus of control (NL/CD) and OIH male rats (SL/HFD), in separate tissue blocks encompassing either the MBH (that includes the ARC) or POA. Hypothalamic levels of Grk2 mRNA were higher in the MBH than in the POA; a similar phenomenon was detected for the protein content of GRK2 (**Figure 72**). OIH was associated to a 25% decrease in Grk2 mRNA and GRK2 protein levels in the MBH. While no significant differences of expression were found in mRNA levels in the POA between NL/CD and SL/HFD groups, GRK2 protein content decreased in the MBH and POA in OIH male rats (**Figure 72**).

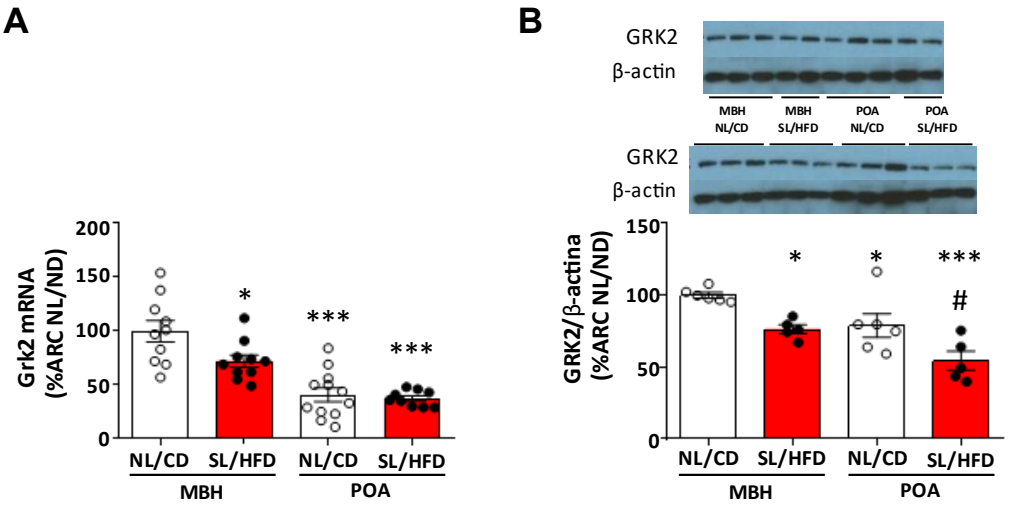

Figure 72. *Hypothalamic levels of Grk2 mRNA and GRK2 protein content in control (NL/CD) and OIH (SL/HFD) male rats.* ***A****) Grk2 mRNA levels, and* ***B****) GRK2 protein levels in both MBH (encompassing ARC) and POA of the hypothalamus of the experimental groups. Data represent mean ± SEM. Group sizes: n= 7-10 for mRNA analysis and n=5-6 for protein analysis. Statistical significance of the differences was assessed by ANOVA followed by Student Newman-Keuls multiple range test. *P < 0.05, ***p < 0.001 vs MBH NL/CD group; #P < 0.05 vs POA NL/CD.*

4.3. Effects of central pharmacological blockade of GRK2 in the rat model of OIH

Given the proposed role of GRK2 as repressor of kisspeptin signaling (see Section 4.1.), we assessed the effect of central pharmacological blockade of GRK2 in our rat model of OIH. To this end, SL/HFD male rats were treated icv with effective doses of vehicle or the GRK2 inhibitor, β-ARK-1-I, from PND150 to 164. As additional control group, male rats bred in normal litters and fed control low fat diet (NL/CD) were also included. Central (icv) treatments were done twice daily and body weight, reproductive parameters and metabolic indices were assessed. As expected, SL/HFD induced a 50% decrease in LH and a 10% decrease in FSH and testosterone levels (**Figure 73**) vs. control values in NL/CD rats, which documented the occurrence of central hypogonadism induced by obesity in our model.

Central administration of the GRK2 inhibitor to SL/HFD males partially improved LH levels, both as integral secretory mass (AUC) and final concentrations at the end of the treatment (**Figure 73 A-C**). A similar trend was detected for testosterone levels, which were not lower than control values in the β-ARK-1-I treated group (**Figure 73 G-I**). Likewise, the 10% drop in integral (AUC) FSH levels was not detected in SL/HFD rats treated with the GRK2 inhibitor, albeit no differences between the experimental groups were detected in final concentrations of FSH at the end of the treatment (**Figure 73 D-F**).

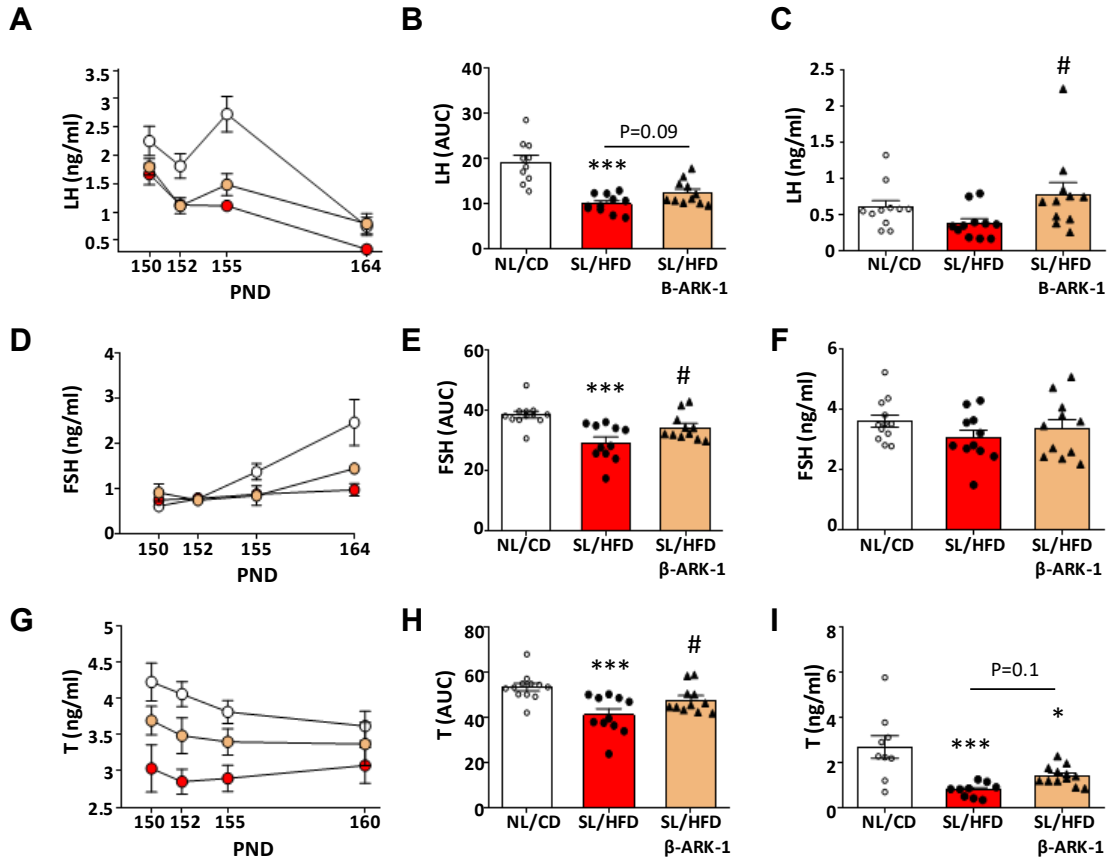

Figure 73*. Pharmacological blockade of GRK2 in SL/HFD male rats partially reverses reproductive indices of OIH.* ***A****) Serum LH levels along the treatments;* ***B****) Integral LH secretory mass, calculated as under the curve (AUC); and* ***C****) Final serum LH levels at the end of the treatments. Similar parameters are presented for FSH and Testosterone (T).* ***D****) Serum FSH levels along the treatments;* ***E****) Integral FSH secretory mass, calculated as under the curve (AUC); and* ***F****) Final serum FSH levels at the end of the treatments; and* ***G****) Serum T levels along the treatments;* ***H****) Integral T secretory mass, calculated as under the curve (AUC); and* ***I****) Final serum T levels at the end of the treatments. Data represent mean ± SEM. Group sizes: n = 10-12. Statistical significance of the differences was assessed by 2-way ANOVA or ANOVA followed by Student Newman-Keuls multiple range test. *P < 0.05, ***p < 0.001 vs NL/CD group; #P < 0.05 vs SL/HFD group.*

In addition, SL/HFD male rats displayed a significant increase in body weight gain (**Figure 74 A**), accompanied by increased basal levels of glucose (**Figure 74 B**), diminished circulating insulin (**Figure 74 C**), and impaired responses in insulin and glucose tolerance test (**Figure 74 D-E**). In addition, moderate cardiac hypertrophy was observed (**Figure 74 F**), together with a significant increase in systolic blood pressure vs. the levels in the control NL/CD group (**Figure 74 G**).

In contrast, SL/HFD male rats treated with the GRK2 inhibitor, β-ARK-1-I, displayed a strong improvement of the metabolic profile, with circulating glucose and insulin levels being in the range of control values in NL/CD males (**Figure 74 B-C**). In addition, glucose tolerance was improved and insulin resistance was ameliorated (**Figure 74 D-E**). In the same vein, cardiac hypertrophy was corrected and systolic blood pressure reduced (**Figure 74 F-G**). All these changes occurred despite no significant differences were observed in body weight in the SL/HFD group treated with the GRK2 inhibitor vs. values in vehicle-treated SL/HFD males (**Figure 74 A**).

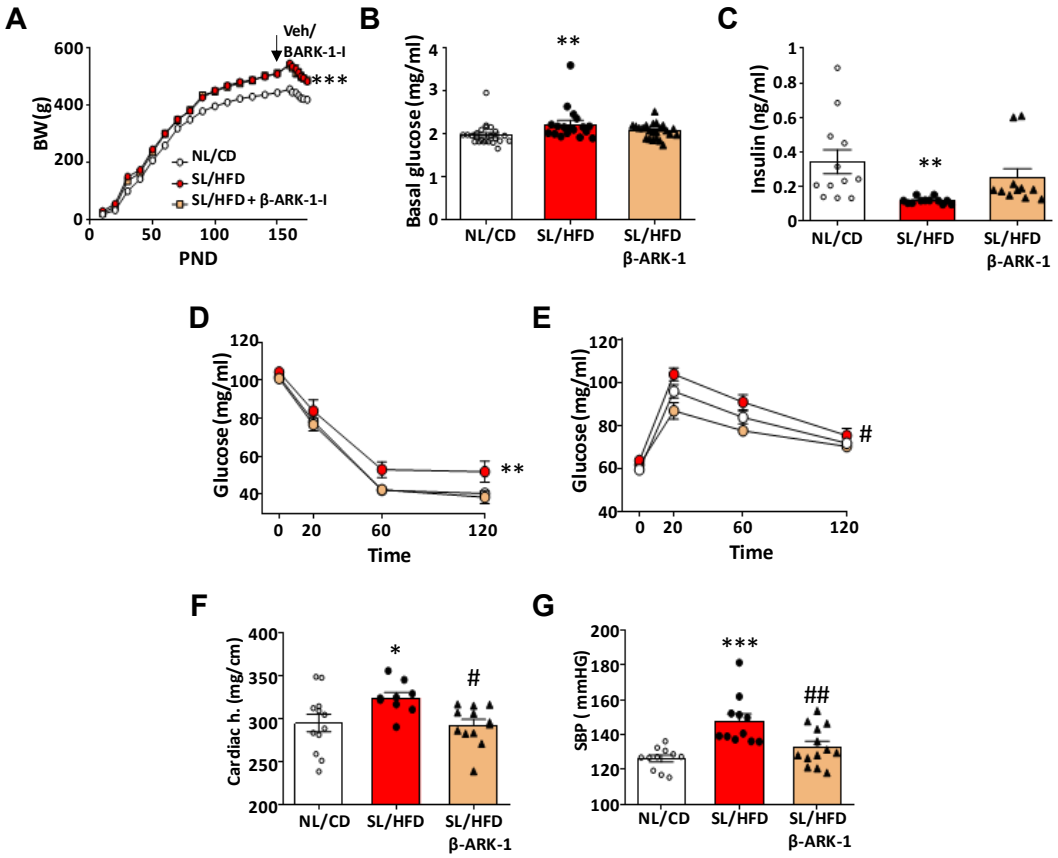

Figure 74. *Pharmacological blockade of GRK2 in OIH conditions.* ***A****) Body weight (BW) follow up from birth to PND150 in the NL/CD, SL/HFD and SL/HFD + β-ARK-1-I (β-ARK-1 groups);* ***B****) Basal glucose levels, and* ***C****) Serum insulin levels at PND150.* ***D****) Insulin tolerance tests, and* ***E****) Glucose tolerance tests.* ***F****) Cardiac hypertrophy (Cardiac h.), and* ***G****) Systolic blood pressure (SBP) in the different experimental groups. Data represent mean ± SEM. Group sizes: n = 12-13; except for basal glucose levels where n=24-26. Statistical significance of the differences was assessed by 2-way ANOVA or ANOVA followed by Student Newman Keuls multiple test. *P < 0.05, **P<0.01, ***p < 0.001 vs NL/CD group; #P < 0.05, ##P < 0.01 vs SL/HFD group.*

4.4. Effects of conditional ablation of *Grk2* in GnRH neurons in the mouse model of OIH

In order to evaluate the effect of specific ablation of *Grk2* from GnRH neurons in OIH conditions, we employed the G-GRKO mouse model. In line with the previous pharmacological approach, we fed adult G-GRKO and control male mice with HFD (G-GRKO HFD and control HFD groups), from PND60 onwards, with the aim of comparing the hypogonadal state linked to obesity in both

conditions. In parallel, we evaluated G-GRKO mice fed control diet (G-GRKO CD) and control mice fed control diet (control CD), to perform the comparative analysis between groups. First, to assess the presence of central hypogonadism in control and KO mice, we mainly evaluated serum LH levels, which showed a decrease in the control-HFD group compared to control-CD group, that was close to the 50% in the evolution curve of the last 28 days, as estimated by the AUC (p=0.05), as well as in the final LH measurement (**Figure 75 A-C**). This was accompanied by an evident reduction in the relative weights of testis (**Figure 75 D**). However, testosterone levels, which were in the low range already in control-CD, were not further decreased in control-HFD male mice (**Figure 75 E**).

Complementary, comparative analysis between control and G-GRKO groups were performed, in order to explore the consequences of the lack of GRK2 in GnRH neurons, in adult male mice under OIH conditions. Interestingly, while integral (AUC) and final LH levels were not significantly different between control and G-GRKO mice fed CD, ablation of *Grk2* in GnRH neurons greatly mitigated the adverse effects induced by obesity in terms of LH secretion in control mice, as these parameters were in the normal range in G-GRKO mice fed HFD (**Figure 75 A-C**). Yet, relative testis weights were reduced after HFD in G-GRKO mice, albeit this reduction was modestly lower that the one observed in control HFD mice (**Figure 75 D**). In addition, no differences in serum testosterone levels were detected between control and G-GRKO mice fed HFD (**Figure 75 E**).

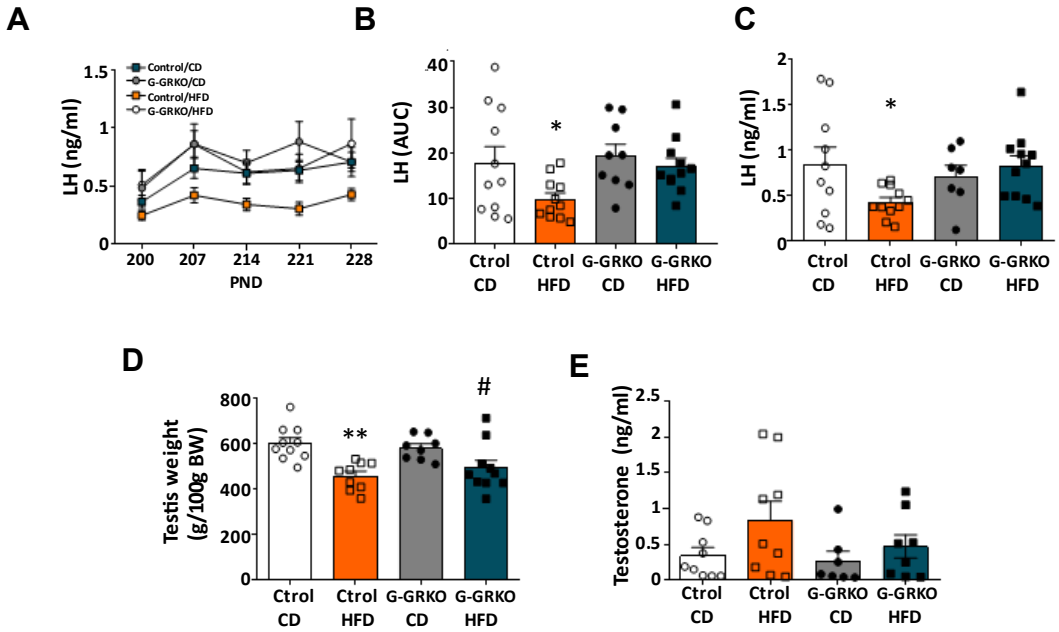

***Figure 75**. Conditional ablation of Grk2 in GnRH neurons, in the G-GRKO mice, and central OIH in HFD conditions. **A**) Dynamic LH levels. **B)** Integral LH (AUC) hormonal levels; and **C**) Final LH levels at the end of the experiment. **D**) Relative testis weight; and **E**) Testosterone levels at the end of the experiment. Data represent mean ± SEM. Group sizes: n = 7-11. Statistical significance of the differences was assessed by 2-way ANOVA (Panel A), one-way ANOVA followed by Student-Newman-Keuls test (for multiple comparisons in Panels B-E) or Student t-test for paired comparison in Control (Ctrl) or G-GRKO groups. *P<0.05, ***p < 0.001 vs Control CD group; #P < 0.01 vs Control G-GRKO group.*

Finally, cardiometabolic indicators were also comparatively explored in control and G-GRKO mice fed CD and their respective HFD groups. Regarding the metabolic and cardiovascular profiles, a prominent increase of body weight was detectable in G-GRKO HFD and control-HFD mice, in comparison to their respective controls (**Figure 76 A**). Both HFD fed groups showed also an increase in the calorie intake (**Figure 76 B**). In addition, both, the control-HFD and G-GRKO HFD groups displayed increased insulin levels, together with impaired glucose tolerance and insulin resistance, as well as cardiac hypertrophy, linked to a moderate 20 % increase in the SBP (**Figure 76 C-H**).

Comparative analyses between control and G-GRKO mice fed HFD revealed that, while body weight gain and energy intake tended to be greater in G-GRKO animals (**Figure 76 A-B**), ablation of *Grk2* in GnRH neurons had a moderate beneficial impact on basal glucose levels, both in CD and HFD conditions (**Figure. 76 D**), since G-GRKO mice displayed lower serum glucose levels than controls, regardless of the nutritional regimen. Conversely, no clear effects were observed during glucose and insulin tolerance tests (**Figure 76 E-F**), neither there were changes in the cardiovascular parameters analyzed, as cardiac hypertrophy and SBP were similar between control and G-GRKO groups, irrespective of the feeding conditions (**Figure 76 G-H**).

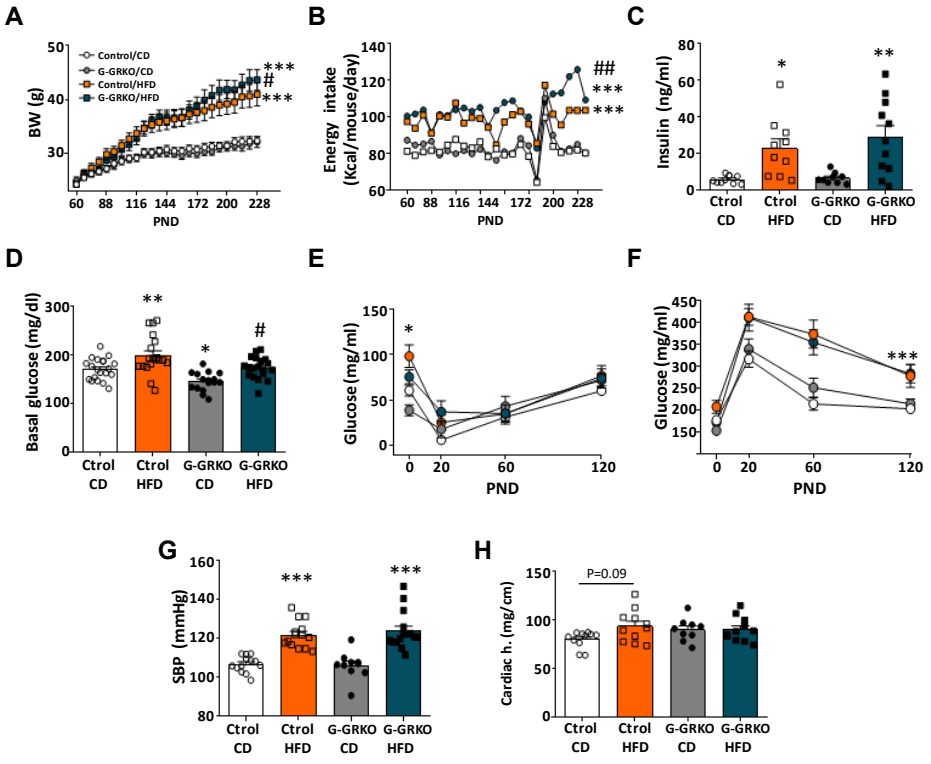

Figure 76. *Conditional ablation of Grk2 in GnRH neurons, in the G-GRKO mice, and metabolic indices in HFD conditions. **A**) Body weight (BW); **B**) Calorie intake; **C**) Insulin levels; **D**) Basal glucose; **E**) Insulin tolerance test; **F**) Glucose tolerance test; **G**) Systolic blood pressure (SBP); and **H**) Cardiac hypertrophy (Cardiac h.) for the experimental groups control CD, G-GRKO CD, Control HFD and G-GRKO HFD. Data represent mean ± SEM. Group sizes: n = 7-11, except for basal glucose levels where n=24-26. Statistical significance of the differences was assessed by 2-way ANOVA (Panels A-B, E-F) or ANOVA followed by Student-Newman-Keuls multiple range test. *p<0.05, ** p<0.01, ***p < 0.001 vs Control CD group; #P < 0.05, ##P < 0.01 vs Control HFD group.*

Discussion

Discussion

Compelling evidence gathered over the last two decades strongly supports that kisspeptins and their canonical receptor, GPR54, are essential components of the central mechanisms controlling puberty and reproductive capacity. A plethora of signals, both arising from different tissues or originating from the environment, have been shown to converge onto the Kiss1/ GPR54 system to precisely modulate pubertal maturation and the HPG axis [129,266–268]. Among them, nutritional and metabolic cues are known to play prominent roles in the control of reproduction, operating in part via modulation of components of the Kiss1/GPR54 system. This interplay is important for several reasons. In one hand, it might explain, at least partially, the trends for alterations in pubertal timing, particularly advanced puberty onset, which are seemingly occurring in girls, and possibly also in boys, in different countries. The rapid instauration of these trends for pubertal acceleration speaks in favor of a prominent role of environmental influences, which can include chemical disruptors and, prominently nutritional alterations, such as child obesity [269], whose prevalence is escalating worldwide. On the other hand, disordered puberty and perturbed gonadal function are also risk factors for metabolic conditions; in fact, perturbations in the age of puberty onset have been found to be linked to several pathologies, including greater risk of cardiometabolic diseases [270,271].

In this context, it becomes clear that deeper understanding of the mechanisms for the control of puberty and adult reproductive function, centered around the crucial roles of the elements of the Kiss1/GRP54 system, is mandatory, also to broaden our knowledge of the basis of prevalent reproductive and metabolic alterations, and to improve the current strategies to tackle them. In this context, and despite the astonishing progress in this area, little is still known regarding the epigenetic control mediated by miRNAs on *Kiss1*/kisspeptin expression, or on the mechanisms controlling GPR54 signaling, under physiological or stress conditions. Thus, with the aim to enlarge the current understanding of the mechanisms involved in the physiological control of puberty and adult reproductive function, and their alterations in conditions of nutritional stress, in this Doctoral Thesis, we explored (i) the putative role of specific miRNAs in the physiological control of puberty via regulation of *Kiss1*, by a combination of *in silico*, *in vitro* and *in vivo* studies; (ii) the pathophysiological role of selected miRNAs in obesity-induced hypogonadism of the male, focusing on their interplay with *Kiss1* and potential therapeutic implications; (iii) the role of GRK2 in the control of puberty and the HPG axis through regulation of GPR54 in normal conditions and under nutritional stress, by a combination of expression, pharmacological and functional genomic studies; and (iv) the implication of GRK2 in male,

obesity-induced hypogonadism, via GPR54 regulation, as assessed by pharmacological and functional genomic analyses.

For sake of clarity and concision of our Discussion, this section has been divided into four sub-sections, each one corresponding to one of the four objectives of this Thesis, followed by a final joint section of Conclusions.

MicroRNAs in the physiological control of puberty via regulation of *Kiss1*

A large body of evidence has pointed out the relevant role of microRNAs, from fetal life onwards, in the control of different aspects of reproductive maturation and function [128,159,162,167,259]. While in humans, studies are almost limited to their role as circulating biomarkers of reproductive perturbations [163,272,273], experimental studies in preclinical (animal) models have begun to reveal putative regulatory roles of miRNAs in the modulation of different components of the reproductive axis. However, most of the analyses so far have focused on early developmental or direct gonadal roles of miRNAs, even though the roles of miRNA biogenesis or specific miRNA species in the control of key cell types of the HPG axis, including pituitary gonadotrophs [274] and major hypothalamic circuits [128,159,167,259], have begun to be explored in recent years. Importantly, however, despite the central role of *Kiss1* in the control of the reproductive system along the lifespan, very little is known about putative miRNAs with capacity to directly regulate *Kiss1*/kisspeptin expression, except for a previous study of our group on the potential role of miR-324 as regulator of early embryonic/placental expression of *KISS1* in humans, whose deregulation may contribute to ectopic pregnancy [163].

This Thesis provides the first evidence for a major role of the miRNA tandem, miR-137-3p and miR-325-3p, as direct regulators of *Kiss1*/kisspeptin expression in the hypothalamus, thereby operating as a key component for the timed control of puberty. Our findings are congruent with the growing body of evidence supporting a major role of epigenetic pathways in the control of *Kiss1*, as major regulatory phenomenon in the precise modulation of puberty onset, but adds for the first time experimental evidence for the miRNA-mediated direct control of hypothalamic *Kiss1*/kisspeptin expression, as relevant element in this phenomenon. Further, our present data-set is in line with recent reports from our group showing that proper miRNA biogenesis in Kiss1 neurons is mandatory for complete pubertal maturation in female mice [167]. It must be noted, though, that in this previous study, congenital ablation of Dicer, as key enzyme for the synthesis of mature miRNAs, resulted in pubertal arrest and *Kiss1* suppression, likely via enhanced expression of major repressors of *Kiss1*, while our present data demonstrate that miR-137-3p and miR-325-3p seemingly operate as selective repressors of *Kiss1*, which can advance or delay

pubertal timing, depending of their suppression or activation, respectively. This illustrates a delicate role of this particular miRNA tandem in the precise control of the age of pubertal maturation, operating selectively via *Kiss1*.

The putative function of miR-137-3p and miR-325-3p to regulate *Kiss1*/kisspeptin expression was predicted by *in silico* analyses and later confirmed by a combination of *in vitro* and *in vivo* studies. Of note, not only the seed region of both miRNAs is totally conserved between humans and rodents, but also previous studies have documented that miR-137 expression is enriched in the CNS in rodents and humans [275,276], including robust hypothalamic expression in rats and mice[157,277]. Intriguingly, despite consistent *in vitro* evidence for a clear repressive role of both miRNAs on *Kiss1* expression, using reporter assays, our expression analyses in hypothalamic tissue from female rats at different stages of postnatal development revealed a concomitant increase in the relative levels of miR-137-3p and miR-325-3p together with the expected rise of kisspeptin content along postnatal maturation. A tenable explanation for this somewhat counterintuitive phenomenon is that, in physiological conditions, the elevation of hypothalamic expression of both miRNAs serves as safeguard mechanism to keep kisspeptin levels at check, to avoid inappropriately elevated kisspeptin levels that may lead to premature puberty. This interpretation is further supported by the fact that in three different models of delayed puberty, the hypothalamic expression of miR-137-3p and miR-325-3p was further augmented, as potential contributor for the pubertal delay observed in these conditions of nutritional deprivation or altered sex steroid milieu, in keeping with our *in vivo* experiments involving central infusion of mimics of miR-137-3p and miR-325-3p. Of note, the capacity of conditions of early subnutrition, either during lactation or post-weaning, to alter hypothalamic expression of miR-137-3p and miR-325-3p points out the eventual role of these miRNAs in the metabolic control of puberty, and is congruent with previous results from unbiased, large-scale expression analyses, showing altered expression of miR-137-3p and miR-325-3p in the hypothalamus of adult male rats subjected to nutritional manipulations [157].

Functional analyses of the interplay between miR-137-3p/miR-325-3p and *Kiss1* mainly involved gain- and loss-of-function approaches in immature female rats *in vivo*, using mimic and TSB tools, respectively. In the former, central icv administration of mimics of miR-137-3p and miR-325-3p, to simulate conditions of activation of their repressive actions, not only suppressed kisspeptin content in the hypothalamus, but also caused a consistent delay of pubertal maturation, as documented by a combination of phenotypic indices, including deferred ages of vaginal opening and first estrus, as well as partial delay of follicular maturation and (trends for) decreased LH levels. Admittedly, while icv injection of miRNA mimics allows central targeting of

regulatory elements, as *Kiss1* expression, it does not provide sufficient discrimination among the multiple central targets of the given miRNA, which are likely affected by the analogue. However, combination with TSB studies enables a more precise delineation of the *Kiss1*-dependent mechanisms of action, since in the case of blocker LNAs, these are specifically designed to interact, and hence prevent, the repressive interaction of miRNA targets at a specific biding site at the 3'UTR of the gene target of interest. Hence, our TSB miR137/325/*Kiss1* operates as specific antagonist, preventing the binding of both miR-137-3p and miR-325-3p (which share the seed region) at their specific binding site the 3'UTR of *Kiss1*. Accordingly, the effects caused by this TSB are seemingly mediated by blocking these specific repressive actions, as documented also by the marked increase in hypothalamic kisspeptin content following icv injection of TSB miR137/325/*Kiss1*. Moreover, opposite to mimic experiments, in which the repressive actions of the miRNAs are artificially modeled by the exogenous administration of synthetic compounds, in TSB studies, the observed effects should derive from preventing the action of endogenous miRNAs, in our case, miR-137-3p and miR-325-3p, on the target (in our case, Kiss1) mRNA, therefore reinforcing the physiological relevance of the findings.

Indeed, by preventing the repressive action of miR-137-3p and miR-325-3p selectively on *Kiss1*, not only hypothalamic kisspeptin levels were enhanced, but pubertal maturation was clearly accelerated, as denoted by different phenotypic indices. Taken together with the mirror effects of mimic administration, these data strongly support a major role of changes in hypothalamic levels of this miRNA tandem in the physiological control of puberty.

Of note, while TSB have been reported to easily enter into the cells after *in vivo* administration[159] due to their particular chemistry, mimics are less prone to cell incorporation after *in vivo* injection, and protocols for co-administration with *in vivo* transfecting agents are usually implemented to favor cellular access of the mimics [278,279]. This was the case in our experiments, in which miR-137-3p and miR-325-3p mimics were co-injected with the agent JetPEI. While this compound has been previously used for *in vivo* studies, our preliminary optimization studies (*not included in this Thesis*) demonstrated that (i) JetPEI co-administration is mandatory for full manifestation of the effects of the mimics *in vivo*, but (ii) JetPEI alone tended to cause a moderate but detectable acceleration of pubertal onset, whose basis is currently under investigation. This is the reason for the slight differences in pubertal timing between control (vehicle) groups between mimic and TSB experiments (see Figures 45-46 vs. 47). Anyhow, pubertal indices are fully reliable in both experimental sets, as all of them included their own corresponding controls (in the case of mimic experiments, JetPEI vs. JetPEI + mimic). Moreover, the fact that miR-137-3p and miR-325-3p mimics were able to suppress kisspeptin content and

delay pubertal onset even against the trend for acceleration of pubertal maturation caused by JetPEI alone further emphasizes the capacity of these miRNAs to repress puberty onset acting at central levels.

Different studies have documented pleiotropic roles of miR-137-3p and/or miR-325-3p, including neuronal development and differentiation, cell cycle regulation and proliferation, as well as sleep and circadian rhythms [280–283] to mention some prominent examples. This, together with their evolutionary conservation, argues in favor of a preserved role of these miRNAs in the control of essential bodily functions. According to our current data, these are likely to include also pubertal maturation. The translational dimension of these findings is reinforced by results from our search in clinical databases, which have identified the occurrence of precocious puberty in patients with microdeletions in chromosomic regions containing miR-137. Additionally, evidence for a SNP at this region linked to age at menarche in girls and that also acts as an eQTL related with the expression of the host gene of miR-137-3p, MIR137HG, was found in previously published databases. While these data do not unambiguously demonstrate the specific role of miR-137-3p in the control of human puberty, as microdeletions affected larger regions and were presented, in most patients, as syndromic cases, taken together with our experimental data, our findings strongly support a physiological role of miR-137-3p, and its related miR-325-3p, in the control of mammalian puberty, with a potential function in its modulation by early nutritional stress. While our experiments were selectively carried out in female rats, the fact that pubertal precocity linked to microdeletions affecting 1p21.3 chromosomic region, where the locus encoding miR-137 is found, were found predominantly in boys, suggests that this regulatory function may also apply to male puberty; a possibility that warrants specific investigation.

Pathophysiological role of miR-137-3p and miR-325-3p in male OIH via regulation of *Kiss1*

The *in silico* and experimental evidence gathered in the first part of this Thesis prompted us to explore the putative function of miR-137-3p and miR-325-3p in the control of hypothalamic *Kiss1*, in other conditions of nutritional stress, namely, obesity-induced hypogonadism (OIH) in the adult male. Additional reasons for these analyses were two-fold: (i) compelling experimental data had previously documented that, at least partially, OIH is linked to central suppression of *Kiss1*, as documented in male rodent and rabbit models [229,284,285]; and (ii) previous large-scale analyses of changes in miRNA levels in the hypothalamus of male rats under different conditions of nutritional stress, from caloric restriction to obesity, had suggested changes in the expression levels of both miRNAs [157].

OIH is a common, usually underrecognized condition that affects up to 50% of adult men suffering long-term obesity. Besides its potential reproductive implications, ranging from low sexual desire and erectile dysfunction to subfertility, persistently suppressed testicular function has been claimed to contribute to the deterioration of metabolic health, defining sort of vicious circle, in which progressive obesity leads to greater hypogonadism, which in turn aggravates the cardiometabolic complications of obesity. Using a male rat model of sequential exposure to obesogenic manipulations since early postnatal life, in this Thesis we aimed to define, using a combination of expression and functional studies, the potential pathogenic role of deregulated miR-137-3p and miR-325-3p in OIH of the male, via suppression of hypothalamic *Kiss1*.

Our expression data was fully compatible with this working hypothesis, since our OIH not only recapitulated the main phenotypic (reproductive, hormonal and metabolic) features of obese, hypogonadal males, and displayed decreased hypothalamic expression of Kiss1 mRNA and kisspeptin content, mainly in the MBH, where the prominent population of ARC Kiss1 neurons is located, but showed also increased levels of miR-137-3p and miR-325-3p, in line with their putative repressive role on *Kiss1*/kisspeptin expression in the context of OIH. Of note, previous data, from miRNA arrays in whole hypothalamic tissue from adult male rats, had suggested that, among other, both miRNAs display altered expression in conditions of nutritional stress, including short-term obesity [157]. Our present findings refine those previous observations, and conclusive document an inverse relationship between the hypothalamic levels of expression of *Kiss1*/kisspeptin (decreased) and miR-137-3p/miR-325-3p (increased) in the context of OIH. The fact that our mimic experiments in young adult males replicated our results in pubertal female rats, with as significant suppression of kisspeptin content after central injection of mimic miR-137-3p, which tended to cause also decrease T, and to a lesser extent, LH levels, further support a mechanistic role of elevated miR-137-3p and miR-325-3p levels as driving force for the central suppression of *Kiss1* and the HPG axis in obese male rats.

More incisive approaches, involving selective over-expression of miR-137-3p in Kiss1 neurons *in vivo*, further confirmed this putative miRNA/*Kiss1* repressive pathway in male rodents. Using engineered mouse lines to selectively express Cre recombinase and suitable fluorescent markers selectively in Kiss1 cells, couple to virogenetic approaches to target miR-137 expression in a Cre-dependent manner, our study is the first to document the repressive effects of *in vivo* upregulation of a given miRNA, in our case, miR-137, in Kiss1 neurons, upon *Kiss1* expression and different functional markers. Altogether, our data document our capacity to achieve effective over-expression of the miRNA of interest, which repressed *Kiss1* and suppressed markers of HPG axis function *in vivo*, such as LH levels. Interestingly, over-expression of miR-137

in Kiss1 cells also caused an elevation of body weight and tended to increase adiposity, suggesting a possible contribution of enhanced miR-137 expression in this neuronal population to the metabolic phenotype of diet-induced obese males.

Based on these expression and functional data, we also assessed whether preventing the repressive interplay between endogenous miR-137-3p/miR-325-3p and *Kiss1 in vivo* may ameliorate the reproductive and metabolic traits of OIH observed in our rat model, using a TSB strategy similar to that of our pubertal studies. Results of our *in vivo* experiments conclusively demonstrate that, indeed, by specifically interfering the repressive action of this miRNA tandem on the 3'UTR of *Kiss1*, the state of OIH can be largely reversed, with a detectable increase in integral LH, FSH and T levels, together with a substantial increase in hypothalamic content of kisspeptin. Equally interesting, the effects of TSB miR137/325/*Kiss1* on hormonal parameters and kisspeptin content were bound to a marked improvement of key metabolic indices in OIH males, including partial correction of excess of adiposity, glucose intolerance, insulin resistance, cardiac hypertrophy (as index of increased peripheral vascular resistance) and systolic blood pressure. In addition, different indices of vascular reactivity and the pro-inflammatory cytokine prolife of obese male rats suffering central hypogonadism were largely improved or even normalized by the TSB treatment. These findings not only support a major pathogenic role of deregulated miR-137-3p and miR-325-3p expression at the hypothalamus for the generation of the constellation of alterations of OIH, but also pave the way for the potential use of TSB-based therapies for the effective management of obesity and hypogonadism of the male.

Not only central hypogonadism associated to obesity is usually under-diagnosed, but the therapeutic options to properly manage this condition are mostly symptomatic and in many cases of limited efficacy. These include lifestyle changes, as modification of the alimentary habits or promotion of exercise may help to improve also gonadal function in obese men [230,233,237]. Yet, this first line intervention is often unsatisfactory and additional treatments, ranging from bariatric surgery to GLP1 analogues or testosterone replacement have been employed. Of note, testosterone supplementation might allow correction of hypogonadism, and therefore, may operate at the pathogenic basis of some of the manifestations of OIH. However, due to the difficulty to achieve physiological replacement, testosterone treatments are not commonly used, except when string sexual symptoms exist, especially since these are bound to some secondary effects that must be carefully considered [230,233,237].

In this context, we found relevant to compare the efficacy of our protocol of central TSB administration with that of treatment with T implants or repeated Kp-10 administration, as alternative means to rescue hypogonadism in our model. Our comparative data clearly

documented that repeated TSB administration outperforms pharmacological treatments with Kp-10 and T in terms of integral reversion of the metabolic and inflammatory traits of OIH in our rat model. Importantly, of the three protocols tested, only TSB allowed a partial reversion of the central hypogonadal state without causing supra-physiological levels of gonadotropins and/or testosterone. Hence, it can be argued that, while restoration of the physiological levels of *Kiss1* and gonadotropins/T, by preventing the repressive action of miR-137-3p and miR-325-3p is optimal to reverse the main manifestations of OIH, the pharmacological effects of either Kp-10 or T replacement, while improving some parameters, are clearly inappropriate to globally ameliorate the metabolic and inflammatory profile of obese male rats. This finding has important translational implications for future design of personalized strategies for the pharmacological management of OIH in men.

GRK2 as a novel regulator of GPR54: Roles in Pubertal control and nutritional deprivation

As stated in the Introduction of this Thesis, a large body of evidence has documented a sophisticated developmental program, affecting Kiss1 neurons and kisspeptin actions during pubertal maturation, which includes not only an increase in *Kiss1* expression and kisspeptin content in the hypothalamus during the pubertal transition but also plastic changes in Kiss1 neuronal populations and their projections to GnRH neurons, which substantially increase at puberty [112,268,286]. Characterization of these presynaptic components of kisspeptin signaling, and their changes during puberty onset, has drawn substantial attention in recent years and has dominated the search for the mechanisms controlling pubertal timing, and its modulation by metabolic and nutritional factors. This is epitomized by recent studies addressing the roles of cellular energy sensors in the transcriptional control of *Kiss1* in conditions of metabolic stress, such as subnutrition and obesity, bound to altered puberty [123,217]. However, initial evidence suggested that during the pubertal transition, postsynaptic changes affecting kisspeptin signaling are likely to occur also, leading to an increase in kisspeptin responsiveness [287,288], whose basis remained totally unexplored.

Our current dataset discloses a novel role of GRK2 in GnRH neurons, as a key component of the kisspeptin signaling-regulatory machinery, with a physiological function in the control of puberty. GRK2 would operate as repressor signal and counterbalance for excessive activation of GnRH neurons by kisspeptins, therefore aiding to keep puberty at check and preventing precocious pubertal maturation. Considering that powerful stimulatory actions of kisspeptins on the gonadotropin axis manifest already during the infantile/juvenile period [287,288], such inhibitory mechanism appears crucial to ensure the proper timing of puberty onset. Among the different

GPCR kinases, GRK2 is the most extensively studied, with proven pathophysiological actions in multiple bodily functions, including prominently the cardiovascular and metabolic systems[134,135]. However, the putative link of GRK2 with the central mechanisms governing puberty and reproduction remained virtually unexplored, except for very few biochemical studies addressing the role of GRK2 in the modulation of GnRH receptor *in vitro* [289,290], which is expressed at the pituitary to elicit gonadotropin secretion. In addition, a single report had documented, using heterologous (HEK293) cellular systems, that GRK2 can interact with GPR54 and may contribute to mediate kisspeptin-induced desensitization of the kisspeptin receptor *in vitro* [136]. While that biochemical study set the grounds of our current analyses, it did not provide evidence for the potential pathophysiological relevance of GRK2 in the control of kisspeptin signaling, or its putative role in the modulation of puberty. Interestingly, over-expression of GRK2 in HEK293T cells suppressed GPR54 signaling, as measured by inositol-phosphate (IP) formation, in basal and kisspeptin-stimulated conditions, but did not affect GPR54 surface expression or receptor internalization [136], which are hallmarks of desensitization. These data would suggest alternative modes of action of GRK2 in the tuning of GPR54 signaling, in line with recent mounting evidence demonstrating that multiple actions of GRK2 are actually conducted independently of its GPCR-desensitization effects [134,291]. In good agreement, our current results demonstrate that either pharmacological blockade of central GRK2 or selective ablation of *Grk2* from GnRH neurons result in a clear augmentation of acute responses to kisspeptin, suggesting that GRK2 conducts a repressive action on kisspeptin signaling in basal conditions, which contributes to shape the activation of GnRH secretion and, hence, the timing of puberty.

Whereas pharmacological tests involving central administration of the GRK2 inhibitor, β-ARK1-I, already suggested a role of GRK2 in controlling kisspeptin signaling and puberty onset, conclusive demonstration of the primary site and physiological relevance of such GRK2 regulatory system came from our studies in the G-GRKO mouse. A combination of conditional ablation of *Grk2* in GnRH-expressing cells *in vivo* and testing of the releasing effects of kisspeptin on LH secretion, as a surrogate marker of GnRH, demonstrated that GRK2 in GnRH neurons operates as a repressive signal that restrains the stimulatory actions of kisspeptins in this cell population. Reducing this restraint, either via genetic or pharmacological means, results in acceleration of puberty, which is especially evident when *Grk2* inactivation is selectively applied in GnRH neurons. Notably, pubertal G-GRKO mice displayed elevation of LH levels in single point measurements, together with advanced puberty onset and first ovulation in females. A similar acceleration of puberty seems to take place also in males, where external signs of puberty were advanced and testosterone levels were elevated in pubertal mice. Altogether, this evidence

attests a sustained inhibitory action of GRK2 in the control of GnRH neurons during the pubertal transition, at least partially via repression of kisspeptin signaling.

In addition, our current LH pulsatility analyses in G-GRKO mice, which were conducted in young adult mice for operational reasons, further support a sustained role of GRK2 in the regulation of adult gonadotropic axis, as denoted by changes in LH pulsatility after congenital ablation of *Grk2* in GnRH neurons. Intriguingly, such elimination resulted in diminished basal and total levels but significantly increased LH pulsatility, therefore pointing out that elimination of the restrain imposed by GRK2 in GnRH neurons contribute to the physiological shaping of LH pulse frequency, as major determinant for appropriate reproductive function [292].

Our data not only suggest that GRK2 plays a role in the physiological control of puberty, but also identify GRK2 as a novel regulatory node for the metabolic modulation of pubertal maturation. Indeed, conditions of early-onset negative energy balance, such as postnatal undernutrition during lactation and after weaning, which cause a substantial delay of puberty onset [217,293,294] were associated with a significant increase in *Grk2* expression, at mRNA and protein levels, in the hypothalamus, including the POA, where most GnRH neurons reside. Moreover, central pharmacological blockade of GRK2 partially rescued the pubertal delay imposed by early undernutrition, therefore attesting to the relevance of enhanced GRK2 signaling in the suppression of puberty caused by conditions of negative energy balance. In good agreement, mice congenitally devoid of *Grk2* in GnRH neurons were partially protected from the deleterious impact of chronic subnutrition on pubertal onset, as denoted by normalization of several phenotypic and hormonal markers of pubertal initiation. Interestingly, young adult females with congenital elimination of *Grk2* from GnRH neurons maintained higher LH pulsatility when subjected to subnutrition, when compared to underfed controls, although they did not display rescued LH secretory mass. These observations further attest to the key role of GRK2 in GnRH neurons in modulating LH pulsatility and strongly suggest that preserved LH pulsatility is seemingly a major contributor for preservation of pubertal progression in G-GRKO mice despite undernutrition. Recent data from our laboratory have documented that a key component of the pubertal suppression caused by early subnutrition is the transcriptional repression of *Kiss1* expression, mediated via activation of AMPK and SIRT1 in Kiss1 neurons, that results in the inhibition of the major stimulatory drive (kisspeptins) on GnRH neurons [123,217]. Our present findings disclose another, previously unnoticed regulatory layer, operating within GnRH neurons, whereby kisspeptin effects would be physiologically restrained and further inhibited in conditions of energy deficit that cause pubertal delay. These data are compatible with a distinct role of other nutrient-sensing mechanisms in GnRH neurons (e.g., AMPK), as putative

transducers for at least part of the control of puberty and the reproductive axis by metabolic cues [218] . While the ubiquitous nature of GRK2 and its capacity to modulate different GPCR makes feasible that part of its suppressive effects on puberty may be GPR54-independent, our current findings, including those in the mouse model of conditional ablation of *Grk2*, strongly argue in favor of a role of this kinase in the modulation of kisspeptin signaling in GnRH neurons. Considering that GRK2 has been proposed as a potential target for the treatment of various pathological conditions, our present data have translational potential, as they open up the possibility for the design of novel pharmacological strategies, targeting GRK2, for the management of pubertal disorders, and eventually other reproductive alterations, including those linked to metabolic perturbations.

Roles of central GRK2 in obesity-induced hypogonadism of the male

Departing from our studies on the inhibitory role of GRK2 on GPR54 signaling in GnRH neurons, as element for the modulation of puberty and its delay in conditions of negative energy balance, we aimed to explore also the putative contribution of central GRK2 signaling, and particularly in GnRH neurons, in mediating, at least partially, the impact of obesity on gonadotropic function in the male, using pharmacological tools and functional genomic approaches in rat and mouse models of obesity. Notably, GRK2 has been proposed as a major node for the control of cellular metabolism [133,134], and its levels have been shown to be altered (mainly, increased) under different adverse metabolic and cardiovascular conditions, both in animal models and human tissues, such as liver, heart, blood vessels, pancreas, adrenal gland or adipose tissue [134]. Thus, perturbations of GRK2 signaling have been identified in different pathologies, including heart disease, obesity, type 2 diabetes, pain and inflammation, or neurodegeneration [295]. Yet, although it was known that GRK2 participates in neurohormonal homeostasis, neurotransmitter signaling or circadian rhythms, studies connecting brain regulation of metabolism with GRK2 function remained scarce [139]. Likewise, the role of central GRK2 signaling in the control of the adult HPG axis had not been explored in detail to date.

Our data conclusively demonstrate that, as is the case in pubertal animals, central GRK2 signaling plays a role in the control of the adult gonadotropic axis, as documented initially by our pharmacological studies in male rats. In keeping with its role as repressor of GPR54 signaling, suggested by our pubertal studies, central infusion of a GRK2 inhibitor significantly enhanced LH and FSH responses to repeated Kp-10 injections, therefore supporting that endogenous GRK2 operates to restrain GPR54 responsiveness to kisspeptin stimulation in adult male rats. In fact, despite doubling or tripling LH and FSH secretory responses to kisspeptin, no evidence for

desensitization was obtained in male rats pre-treated with the GRK2 antagonist, pointing out a role of endogenous GRK2 in the central control of gonadotropin responses to repeated kisspeptin stimulation. Intriguingly, however, relative expression levels of *Grk2* and GRK2 protein content in the hypothalamus, and particularly in the MBH and/or POA, tended to be decreased in conditions of obesity causing central hypogonadism. While according to our pharmacological experiments, such a decrease of GRK2 expression might be linked to enhanced, rather than suppressed responsiveness to kisspeptin, we must take into consideration that OIH is bound to a decrease in the endogenous expression of kisspeptins, so that the observed decrease in GRK2 might be a compensatory response in face of the diminished tone of the ligand. In addition, given the lack of cellular resolution of our expression analyses, it is possible that the global decrease in *Grk2*/GRK2 levels detected in POA and/or MBH fragments might not translate into similar changes at the level of GnRH neurons.

In any event, implementation of pharmacological and functional genomic tools, to inactivate GRK2 in models of obesity in rodents, allowed us to identify tenable functions of central GRK2 in the generation/manifestation of phenotypic features of OIH. Thus, both pharmacological inhibition of GRK2, in a male rat model, and conditional ablation of *Grk2* in GnRH neurons, in our G-GRKO mouse line, partially or totally reversed some of the cardinal manifestations of OIH, with variable penetrance depending on the approach used. For instance, inhibition of GRK2 in male rats and ablation of *Grk2* in GnRH neurons in male mice partially prevented the inhibitory impact of obesity on gonadotropin secretion, and in the case of male rats, also on testosterone levels. Notably, in our mouse model of obesity, despite clear suppression of LH levels caused by obesity no overt changes in serum testosterone concentrations were detected, possibly due to the state of low basal androgen levels detected already in control animals. Notwithstanding, altogether, these results confirms the central inhibitory impact of obesity on the gonadotropic axis, and strongly suggest that GRK2 signaling likely contributes to this phenomenon, at least in part by acting in GnRH neurons, since ablation of *Grk2* effects ameliorates the gonadotropic profiles of obese male rodents.

In the same vein, both strategies of blockade of GRK2 activity in obese male rats and mice were able to reverse, to some extent, the metabolic manifestations of OIH. Of note, however, the effects of central pharmacological inhibition of GRK2 clearly outperformed those of genetic ablation of *Grk2* in GnRH neurons. Thus, while obese male rats treated with the inhibitor, β-ARK-1-I, displayed clear improvement of multiple cardiometabolic parameters, worsened by obesity, such as basal glucose and insulin levels, glucose tolerance, insulin resistance and systolic blood pressure, the metabolic profile of G-GRKO male mice subjected to obesity was only marginally

improved, with modest decreases in basal glucose levels and absence of cardiac hypertrophy, but without other major changes in key metabolic parameters, such as glucose tolerance or insulin resistance. Several explanations may justify these partially divergent responses. First, while pharmacological blockade of GRK2 was caused by central infusion of the antagonist, which reaches also non-GnRH neuronal targets, our genetic model enabled us to selectively ablate *Grk2* from GnRH neurons; hence, part of the metabolic improvement caused by central GRK2 suppression would stem from targets other than GnRH neurons. Alternatively, since clear changes in testosterone levels following GRK2 manipulations were detected only in rats treated with the inhibitor, but not in conditional KO mice, it might be argued that the greater effectiveness detected in the former might be linked to the positive effects on testosterone levels. Finally, it must be considered also that *Grk2* ablation in GnRH neurons does not exclusively affect GPR54, but is likely to impact also on the wide range of GPCR receptors expressed in these cells, with potential divergent effects that, when congenitally applied, might have masked the consequences of the blockade of GRK2 actions selectively on GPR54. In any event, when collectively considered, our data strongly supports a discernible role of GRK2 signaling, at least in part in GnRH neurons, in the manifestation of the central suppression of the gonadotropic axis in conditions of obesity, and in the metabolic alterations linked to this condition.

Conclusions

Conclusions

The **main conclusions** of this Doctoral Thesis are the following:

1. The microRNAs, miR-137-3p and miR-325-3p, which are evolutionary conserved and share their seed region, operate as putative regulators of puberty, acting via repression of *Kiss1*, as documented by expression and functional studies in female rats. This mechanism may contribute to pubertal regulation in conditions of early nutritional stress and, based on initial findings in clinical databases, might operate also in humans.
2. The microRNAs, miR-137-3p and miR-325-3p, are also involved in the pathogenesis of obesity-induced hypogonadism (OIH) in the male, as major driving force for suppression of hypothalamic *Kiss1* in conditions of obesity. Prevention of the repressive action of miR137/ 325 on *Kiss1* not only ameliorates reproductive indices, but also improves metabolic, cardiovascular and inflammatory markers, outperforming the effects of pharmacological treatments with either Kp-10 or testosterone in a rat model of rat obesity.
3. GRK2, acting in GnRH neurons, exerts a repressive effect on kisspeptin signaling, likely via modulation of GPR54; this phenomenon plays a relevant role in the control of pubertal maturation in rats, and contributes to inhibition of puberty onset in conditions of early undernutrition.

4. GRK2 signaling, acting at least in part in GnRH neurons, contributes to central suppression of the gonadotropic axis in conditions of obesity, with a discernible role of central GRK2 in the manifestation of the cardiometabolic alterations linked to this condition.

As a sum, the results of this Doctoral Thesis allow us to set as **global conclusion** that:

5. Novel repressive regulatory mechanisms, involving both the direct interplay between miR-137-3p/miR-325-3p and *Kiss1*, and the inhibitory actions of GRK2 on GPR54 in GnRH neurons, play a major role in the regulation of pubertal timing and its modulation by metabolic cues, particularly in situations of undernutrition, and likely contribute to the reproductive and metabolic manifestations of OIH. These pathways pose clear physiological interest and may pave the way for the definition of novel targets for the personalized management of prevalent reproductive and metabolic disorders, ranging from pubertal alterations to adult obesity and infertility.

Bibliography

Bibliography

1. Wise, J. Puberty timing has profound effect on later health, study finds. *BMJ* **350**, h3318 (2015).

2. Kaya, G., Abali, Z. Y., Bas, F., Poyrazoglu, S. & Darendeliler, F. Body mass index at the presentation of premature adrenarche is associated with components of metabolic syndrome at puberty. *Eur J Pediatr* **177**, 1593–1601 (2018).

3. Soliman, A. T., Sanctis, V. De, Elalaily, R. & Bedair, S. Advances in pubertal growth and factors influencing it: Can we increase pubertal growth? *Indian J Endocrinol Metab* **18**, S53–S62 (2014).

4. Unni, J. C. Onset of Puberty in Relation to Obesity. *Indian Pediatr* **53**, 379–380 (2016).

5. Sánchez-Garrido, M. A. *et al.* Metabolic programming of puberty: Sexually dimorphic responses to early nutritional challenges. *Endocrinology* **154**, 3387–3400 (2013).

6. Manfredi-Lozano, M. *et al.* Defining a novel leptin-melanocortine kisspeptin pathway involved in the metabolic control of puberty. *Mol Metab* **5**, 844–857 (2016).

7. Quennell, J. H. *et al.* Leptin deficiency and diet-induced obesity reduce hypothalamic kisspeptin expression in mice. *Endocrinology* **152**, 1541–1550 (2011).

8. Blüher, M. Obesity: global epidemiology and pathogenesis. *Nat Rev Endocrinol* **15**, 288–298 (2019).

9. Drucker, D. J. Diabetes, obesity, metabolism, and SARS-CoV-2 infection: the end of the beginning. *Cell Metab* **33**, 479–498 (2021).

10. Chooi, Y. C., Ding, C. & Magkos, F. The epidemiology of obesity. *Metabolism* **92**, 6–10 (2019).

11. Martin, J. *et al.* Neuroanatomy: Text And Atlas. *McGraw Hill* (1997).

12. Marchant, N. J., Zayra Millan, E. & McNally, G. P. The hypothalamus and the neurobiology of drug seeking. *Cell Mol Life Sci* **69**, 581–597 (2012).

13. Bear, M. H., Reddy, V. & Bollu, P. C. Neuroanatomy, Hypothalamus. *StatPearls* (2022).

14. Jones, R. E. & Lopez, K. H. Human reproductive biology.*Elsevier* (2006).

15. Goodman, R. L. & Lehman, M. N. Kisspeptin Neurons from Mice to Men: Similarities and Differences. *Endocrinology* **153**, 5105 (2012).

16. Burgus, R. *et al.* Primary structure of the ovine hypothalamic luteinizing hormone-releasing factor (LRF) (LH-hypothalamus-LRF-gas chromatography-mass spectrometry-decapeptide-Edman degradation). *Proc Natl Acad Sci U S A* **69**, 278–282 (1972).

17. Fernald, R. D. & White, R. B. Gonadotropin-releasing hormone genes: phylogeny, structure, and functions. *Front Neuroendocrinol* **20**, 224–240 (1999).

18. Millar, R. P., Pawson, A. J., Morgan, K., Rissman, E. F. & Lu, Z. L. Diversity of actions of GnRHs mediated by ligand-induced selective signaling. *Front Neuroendocrinol* **29**, 17–35 (2008).

19. Casoni, F. *et al.* Development of the neurons controlling fertility in humans: new insights from 3D imaging and transparent fetal brains. *Development* **143**, 3969–3981 (2016).

20. Forni, P. E. & Wray, S. GnRH, anosmia and hypogonadotropic hypogonadism–where are we? *Front Neuroendocrinol* **36**, 165–177 (2015).

21. Roa, J. & Tena-Sempere, M. Unique Features of a Unique Cell: The Wonder World of GnRH Neurons. *Endocrinology* **159**, 3895–3896 (2018).

22. Bear, M. F., Connors, B. W. & Paradiso, M. A. Neuroscience: Exploring the Brain. *Lippincott Williams & Wilkins* (2001).

23. Xie, Q. *et al.* The Role of Kisspeptin in the Control of the Hypothalamic-Pituitary-Gonadal Axis and Reproduction. *Front Endocrinol (Lausanne)* **13**, 1353 (2022).

24. Maggi, R. Physiology of gonadotropin-releasing hormone (Gnrh): beyond the control of reproductive functions. *MOJ Anat Physiol* **Volume 2**, (2016).

25. Clarkson, J. *et al.* Definition of the hypothalamic GnRH pulse generator in mice. *Proc Natl Acad Sci U S A* **114**, E10216–E10223 (2017).

26. Hall, J. E., Guyton, A. C. & Hall, M. E. Guyton & Hall. Tratado de fisiología médica. *Elsevier* (2021).

27. Moore, A. M., Coolen, L. M. & Lehman, M. N. *In vivo* imaging of the GnRH pulse generator reveals a temporal order of neuronal activation and synchronization during each pulse. *Proc Natl Acad Sci U S A* **119** (6), e2117767119 (2022).

28. Anderson, R. C., Newton, C. L., Anderson, R. A. & Millar, R. P. Gonadotropins and Their Analogs: Current and Potential Clinical Applications. *Endocr Rev* **39**, 911–937 (2018).

29. Keutmann, H. T., Mason, K. A., Kitzmann, K. & Ryan, R. J. Role of the beta 93-100 determinant loop sequence in receptor binding and biological activity of human luteinizing hormone and chorionic gonadotropin. *Mol Endocrinol* **3**(3),526-531 (1989).

30. Segaloff, D. L. & Ascoli, M. Thyroid-Stimulating Hormone/Luteinizing Hormone/Follicle-Stimulating Hormone Receptors. *Encyclopedia of Biological Chemistry: Second Edition* 387–391 (2013).

31. Picton, H. M. Activation of follicle development: the primordial follicle. *Theriogenology* **55**, 1193–1210 (2001).

32. Hansen, K. R. *et al.* A new model of reproductive aging: the decline in ovarian non-growing follicle number from birth to menopause. *Hum Reprod* **23**, 699–708 (2008).

33. McGee, E. A. & Hsueh, A. J. W. Initial and cyclic recruitment of ovarian follicles. *Endocr Rev* **21**, 200–214 (2000).

34. Park, S. U., Walsh, L. & Berkowitz, K. M. Mechanisms of ovarian aging. *Reproduction* **162**, R19 (2021).

35. Gutierrez-Castellanos, N., Husain, B. F. A., Dias, I. C. & Lima, S. Q. Neural and behavioural plasticity across the female reproductive cycle. *Trends in Endocrinology and Metabolism* **33**(11), 769-785 (2022).

36. Wang, C. Male Reproductive Function. *Springer* (1999).

37. Ruwanpura, S. M., McLachlan, R. I. & Meachem, S. J. Hormonal regulation of male germ cell development. *J Endocrinol* **205**, 117–131 (2010).

38. Krieger, D. T. & Hughes, J. C. Neuroendocrinology, the interrelationships of the body's two major integrative systems in normal physiology and in clinical disease. *Oxford University Press* (1980).

39. Turcu, A., Smith, J. M., Auchus, R. & Rainey, W. E. Adrenal androgens and androgen precursors: definition, synthesis, regulation and physiologic actions. *Compr Physiol*. **4**(4), 1369-1381 (2014).

40. Handelsman, D. J. Androgen Physiology, Pharmacology, and Abuse. Endotext *(2020)*.

41. Lee, J. H. *et al.* KiSS-1, a novel human malignant melanoma metastasis-suppressor gene. *J Natl Cancer Inst* **88**, 1731–1737 (1996).

42. Kotani, M. *et al.* The Metastasis Suppressor Gene KiSS-1 Encodes Kisspeptins, the Natural Ligands of the Orphan G Protein-coupled Receptor GPR54. *Journal of Biological Chemistry* **276**, 34631–34636 (2001).

43. Lee, D. K. *et al.* Discovery of a receptor related to the galanin receptors. *FEBS Lett* **446**, 103–107 (1999).

44. Kanda, S. & Oka, Y. Handbook of Hormones: Comparative Endocrinology for Basic and Clinical Research: Kisspeptin. *Academic Press Books* (2016).

45. De Roux, N. *et al.* Hypogonadotropic hypogonadism due to loss of function of the KiSS1-derived peptide receptor GPR54. *Proc Natl Acad Sci U S A* **100**, 10972 (2003).

46. Seminara, S. B., DiPietro, M. J., Ramaswamy, S., Crowley, W. F. & Plant, T. M. Continuous human metastin 45-54 infusion desensitizes G protein-coupled receptor 54-induced gonadotropin-releasing hormone release monitored indirectly in the juvenile male Rhesus monkey (Macaca mulatta): a finding with therapeutic implications. *Endocrinology* **147**, 2122–2126 (2006).

47. Pinilla, L., Aguilar, E., Dieguez, C., Millar, R. P. & Tena-Sempere, M. Kisspeptins and Reproduction: Physiological Roles and Regulatory Mechanisms. *Physiol Rev* **92**, 1235–1316 (2012).

48. Gottsch, M. L., Clifton, D. K. & Steiner, R. A. From KISS1 to Kisspeptins: An Historical Perspective and Suggested Nomenclature. *Peptides* **30**(1), 4-9 (2009).

49. Mead, E. J., Maguire, J. J., Kuc, R. E. & Davenport, A. P. Kisspeptins: a multifunctional peptide system with a role in reproduction, cancer and the cardiovascular system. *Br J Pharmacol* **151**, 1143–1153 (2007).

50. Lee, E. B. *et al.* Sexual Dimorphism in Kisspeptin Signaling. *Cells* **11**, 1146 (2022).

51. Fiorini, Z. & Jasoni, C. L. A Novel Developmental Role for Kisspeptin in the Growth of Gonadotrophin-Releasing Hormone Neurites to the Median Eminence in the Mouse. *J Neuroendocrinol* **22**, 1113–1125 (2010).

52. Bilban, M. *et al.* Kisspeptin-10, a KiSS-1/metastin-derived decapeptide, is a physiological invasion inhibitor of primary human trophoblasts. *J Cell Sci* **117**, 1319–1328 (2004).

53. Gottsch, M. L. *et al.* A Role for Kisspeptins in the Regulation of Gonadotropin Secretion in the Mouse. *Endocrinology* **145**, 4073–4077 (2004).

54. Smith, J. T., Clifton, D. K. & Steiner, R. A. Regulation of the neuroendocrine reproductive axis by kisspeptin-GPR54 signaling. *Reproduction* **131**, 623–630 (2006).

55. Clarke, S. A. & Dhillo, W. S. Kisspeptin across the human lifespan: evidence from animal studies and beyond. *Journal of Endocrinology* **229**, R83–R98 (2016).

56. Irwig, M. S. *et al.* Kisspeptin activation of gonadotropin releasing hormone neurons and regulation of KiSS-1 mRNA in the male rat. *Neuroendocrinology* **80**, 264–272 (2004).

57. Uenoyama, Y., Inoue, N., Nakamura, S. & Tsukamura, H. Central mechanism controlling pubertal onset in mammals: A triggering role of kisspeptin. *Front Endocrinol (Lausanne)* **10**, 312 (2019).

58. Foradori, C. D., Amstalden, M., Goodman, R. L. & Lehman, M. N. Colocalisation of Dynorphin A and Neurokinin B Immunoreactivity in the Arcuate Nucleus and Median Eminence of the Sheep. *J Neuroendocrinol* **18**, 534–541 (2006).

59. Burke, M. C., Letts, P. A., Krajewski, S. J. & Range, N. E. Coexpression of dynorphin and neurokinin B immunoreactivity in the rat hypothalamus: Morphologic evidence of interrelated function within the arcuate nucleus. *J Comp Neurol* **498**, 712–726 (2006).

60. Goodman, R. L. *et al.* Kisspeptin Neurons in the Arcuate Nucleus of the Ewe Express Both Dynorphin A and Neurokinin B. *Endocrinology* **148**, 5752–5760 (2007).

61. Skrapits, K. *et al.* Colocalization of cocaine- and amphetamine-regulated transcript with kisspeptin and neurokinin B in the human infundibular region. *PLoS One* **9**, (2014).

62. Molnár, C. S. *et al.* Morphological evidence for enhanced kisspeptin and neurokinin B signaling in the infundibular nucleus of the aging man. *Endocrinology* **153**, 5428–5439 (2012).

63. Hrabovszky, E. *et al.* The kisspeptin system of the human hypothalamus: sexual dimorphism and relationship with gonadotropin-releasing hormone and neurokinin B neurons. *Eur J Neurosci* **31**, 1984–1998 (2010).

64. Hrabovszky, E. *et al.* Low degree of overlap between kisspeptin, neurokinin B, and dynorphin immunoreactivities in the infundibular nucleus of young male human subjects challenges the KNDy neuron concept. *Endocrinology* **153**, 4978–4989 (2012).

65. Zhu, N., Zhao, M., Song, Y., Ding, L. & Ni, Y. The KiSS-1/GPR54 system: Essential roles in physiological homeostasis and cancer biology. *Genes Dis* **9**, 28 (2022).

66. Tresguerres, J. Fisiología humana. *McGraw Hill* (2009).

67. Naftolin F; *et al.* The formation of estrogens by central neuroendocrine tissues. *Recent Prog Horm Res* **31**, 295–319 (1975).

68. McCarthy, M. M. *et al.* Mini-Symposium: The Epigenetics of Sex Differences in the Brain. *J Neurosci* **29**, 12815 (2009).

69. Kuiri-Hänninen, T., Sankilampi, U. & Dunkel, L. Activation of the Hypothalamic-Pituitary-Gonadal Axis in Infancy: Minipuberty. *Horm Res Paediatr* **82**, 73–80 (2014).

70. Winter, J. S. D., Faiman, C., Hobson, W. C., Prasad, A. V. & Reyes, F. I. Pituitary-gonadal relations in infancy. Patterns of serum gonadotropin concentrations from birth to four years of age in man and chimpanzee. *J Clin Endocrinol Metab* **40**, 545–551 (1975).

71. Andersson, A.-M. *et al.* Longitudinal reproductive hormone profiles in infants: peak of inhibin B levels in infant boys exceeds levels in adult men. *J Clin Endocrinol Metab* **83**, 675–681 (1998).

72. Devillers, M. M., Mhaouty-Kodja, S. & Guigon, C. J. Deciphering the Roles & Regulation of Estradiol Signaling during Female Mini-Puberty: Insights from Mouse Models. *Int J Mol Sci*. **23** (22), *13695* (2022).

73. Delli, V. *et al.* Male minipuberty involves the gonad-independent activation of preoptic nNOS neurons. *Free Radic Biol Med* **194**, 199–208 (2023).

74. Clarkson, J. *et al.* Systems/Circuits Sexual Differentiation of the Brain Requires Perinatal Kisspeptin-GnRH Neuron Signaling. (2014).

75. Castellano, J. M. & Tena-Sempere, M. Kisspeptins and Puberty. *Conferencias. Rev Esp Endocrinol Pediatr* 8–14 (2017).

76. Ramirez, D. V. & McCann, S. M. Comparison of the regulation of luteinizing hormone (LH) secretion in immature and adult rats. *Endocrinology* **72**, 452–464 (1963).

77. Goodman, R. L., Herbison, A. E., Lehman, M. N. & Navarro, V. M. Neuroendocrine control of gonadotropin-releasing hormone: Pulsatile and surge modes of secretion. *J Neuroendocrinol* **34**, e13094 (2022).

78. Parkash, J. *et al.* Phosphorylation of N-methyl-D-aspartic acid receptor-associated neuronal nitric oxide synthase depends on estrogens and modulates hypothalamic nitric oxide production during the ovarian cycle. *Endocrinology* **151**, 2723–2735 (2010).

79. De Tassigny, X. D. A. *et al.* Coupling of neuronal nitric oxide synthase to NMDA receptors via postsynaptic density-95 depends on estrogen and contributes to the central control of adult female reproduction. *J Neurosci* **27**, 6103–6114 (2007).

80. Hanchate, N. K. *et al.* Kisspeptin-GPR54 Signaling in Mouse NO-Synthesizing Neurons Participates in the Hypothalamic Control of Ovulation. *J Neurosci* **32**, 932 (2012).

81. Herbison, A. E. The Gonadotropin-Releasing Hormone Pulse Generator. *Endocrinology* **159**, 3723–3736 (2018).

82. Torres, E. *et al.* Congenital ablation of Tacr2 reveals overlapping and redundant roles of NK2R signaling in the control of reproductive axis. *Am J Physiol Endocrinol Metab* **320**, E496–E511 (2021).

83. Yeo, S. H. & Colledge, W. H. The role of Kiss1 neurons as integrators of endocrine, metabolic, and environmental factors in the hypothalamic-pituitary-gonadal axis. *Front Endocrinol (Lausanne)* **9**, (2018).

84. Plant, T. M. & Zeleznik, A. J. *Physiology of Reproduction*. *Elsevier* (2015).

85. Rance, N. E. & Bruce, T. R. Neurokinin B gene expression is increased in the arcuate nucleus of ovariectomized rats. *Neuroendocrinology* **60**, 337–345 (1994).

86. Hrabovszky, E. *et al.* Substance P immunoreactivity exhibits frequent colocalization with kisspeptin and neurokinin B in the human infundibular region. *PLoS One* **8**, (2013).

87. Navarro, V. M. Metabolic regulation of kisspeptin - the link between energy balance and reproduction. *Nat Rev Endocrinol* **16**, 407–420 (2020).

88. De Croft, S., Boehm, U. & Herbison, A. E. Neurokinin B activates arcuate kisspeptin neurons through multiple tachykinin receptors in the male mouse. *Endocrinology* **154**, 2750–2760 (2013).

89. Navarro, V. M. *et al.* The integrated hypothalamic tachykinin-kisspeptin system as a central coordinator for reproduction. *Endocrinology* **156**, 627–637 (2015).

90. Maguire, C. A. *et al.* Tac1 Signaling Is Required for Sexual Maturation and Responsiveness of GnRH Neurons to Kisspeptin in the Male Mouse. *Endocrinology* **158**, 2319–2329 (2017).

91. Leon, S. & Navarro, V. M. Novel Biology of Tachykinins in Gonadotropin-Releasing Hormone Secretion. *Semin Reprod Med* **37**, 109–118 (2019).

92. Livadas, S. & Chrousos, G. P. Control of the onset of puberty. *Curr Opin Pediatr* **28**, 551–558 (2016).

93. Wang Luhong, Burger Laura L., Greenwald-Yarnell Megan L., Myers Martin- G. & Moenter Suzanne M. Glutamatergic Transmission to Hypothalamic Kisspeptin Neurons Is Differentially Regulated by Estradiol through Estrogen Receptor α in Adult Female Mice. *J Neurosci* **38**, 1061–1072 (2018).

94. di Giorgio, N. P., Bizzozzero-Hiriart, M., Libertun, C. & Lux-Lantos, V. Unraveling the connection between GABA and kisspeptin in the control of reproduction. *Reproduction* **157**, R225–R233 (2019).

95. Gallo, R. V. Kappa-opioid receptor involvement in the regulation of pulsatile luteinizing hormone release during early pregnancy in the rat. *J Neuroendocrinol* **2**, 685–691 (1990).

96. Weems, P. W. *et al.* κ-Opioid Receptor Is Colocalized in GnRH and KNDy Cells in the Female Ovine and Rat Brain. *Endocrinology* **157**, 2367–2379 (2016).

97. Barabás, K. *et al.* Stereology of gonadotropin-releasing hormone and kisspeptin neurons in PACAP gene-deficient female mice. *Front Endocrinol (Lausanne)* **13**, (2022).

98. Cheng, L. *et al.* Direct effect of RFRP-3 microinjection into the lateral ventricle on the hypothalamic kisspeptin neurons in ovariectomized estrogen-primed rats. *Exp Ther Med* **23**, (2022).

99. Leon, S. *et al.* Sex-Biased Physiological Roles of NPFF1R, the Canonical Receptor of RFRP-3, in Food Intake and Metabolic Homeostasis Revealed by its Congenital Ablation in mice. *Metabolism* **87**, 87–97 (2018).

100. Dufourny, L., Delmas, O., Teixeira-Gomes, A. P., Decourt, C. & Sliwowska, J. H. Neuroanatomical connections between kisspeptin neurones and somatostatin neurones in the female and male rat hypothalamus: A possible involvement of SSTR1 in kisspeptin release. *J Neuroendocrinol* **30**, e12593 (2018).

101. Sugimoto, A. *et al.* Central somatostatin-somatostatin receptor 2 signaling mediates lactational suppression of luteinizing hormone release via the inhibition of glutamatergic interneurons during late lactation in rats. *J Reprod Dev* **68**, 190–197 (2022).

102. Mitra, S. W. *et al.* Immunolocalization of estrogen receptor beta in the mouse brain: comparison with estrogen receptor alpha. *Endocrinology* **144**, 2055–2067 (2003).

103. Herbison, A. E. & Pape, J.-R. New evidence for estrogen receptors in gonadotropin-releasing hormone neurons. *Front Neuroendocrinol* **22**, 292–308 (2001).

104. Nadal, A., Díaz, M. & Valverde, M. A. The estrogen trinity: membrane, cytosolic, and nuclear effects. *News Physiol Sci* **16**, 251–255 (2001).

105. Smith, S. S., Aoki, C. & Shen, H. Puberty, steroids and GABA(A) receptor plasticity. *Psychoneuroendocrinology* **34**, Suppl 1:S91-S103 (2009).

106. Adachi, S. *et al.* Involvement of anteroventral periventricular metastin/kisspeptin neurons in estrogen positive feedback action on luteinizing hormone release in female rats. *J Reprod Dev* **53**, 367–378 (2007).

107. Christian, C. A., Glidewell-Kenney, C., Jameson, J. L. & Moenter, S. M. Classical estrogen receptor alpha signaling mediates negative and positive feedback on gonadotropin-releasing hormone neuron firing. *Endocrinology* **149**, 5328–5334 (2008).

108. Wintermantel, T. M. *et al.* Definition of estrogen receptor pathway critical for estrogen positive feedback to gonadotropin-releasing hormone neurons and fertility. *Neuron* **52**, 271–280 (2006).

109. Clarkson, J. Effects of estradiol on kisspeptin neurons during puberty. *Front Neuroendocrinol* **34**, 120–131 (2013).

110. Mayer, C. *et al.* Timing and completion of puberty in female mice depend on estrogen receptor α-signaling in kisspeptin neurons. *Proc Natl Acad Sci U S A* **107**, 22693–22698 (2010).

111. Göcz, B. *et al.* Estrogen differentially regulates transcriptional landscapes of preoptic and arcuate kisspeptin neuron populations. *Front Endocrinol (Lausanne)* **13**, 1940 (2022).

112. Clarkson, J., Boon, W. C., Simpson, E. R. & Herbison, A. E. Postnatal Development of an Estradiol-Kisspeptin Positive Feedback Mechanism Implicated in Puberty Onset. *Endocrinology* **150**, 3214 (2009).

113. Bronson, F. H. The regulation of luteinizing hormone secretion by estrogen: relationships among negative feedback, surge potential, and male stimulation in juvenile, peripubertal, and adult female mice. *Endocrinology* **108**, 506–516 (1981).

114. Goto, T. *et al.* Identification of hypothalamic arcuate nucleus-specific enhancer region of Kiss1 gene in mice. *Mol Endocrinol* **29**, 121–129 (2015).

115. Altarejos, J. Y. *et al.* The Creb1 coactivator Crtc1 is required for energy balance and fertility. *Nat Med* **14**, 1112–1117 (2008).

116. Mitchell, D. C. *et al.* Regulation of KiSS-1 metastasis suppressor gene expression in breast cancer cells by direct interaction of transcription factors activator protein-2alpha and specificity protein-1. *J Biol Chem* **281**, 51–58 (2006).

117. Mueller, J. K. *et al.* Transcriptional regulation of the human kiss1 gene. *Mol Cell Endocrinol* **342**, 8 (2011).

118. Sanz, E. *et al.* Fertility-Regulating Kiss1 Neurons Arise from Hypothalamic Pomc-Expressing Progenitors. *J Neurosci* **35**, 5549 (2015).

119. Leon, S. *et al.* Sex-specific pubertal and metabolic regulation of Kiss1 neurons via Nhlh2. *Elife* **10**, e69765 (2021).

120. Jaenisch, R. & Bird, A. Epigenetic regulation of gene expression: how the genome integrates intrinsic and environmental signals. *Nat Genet* **33**, 245–254 (2003).

121. McCarthy, M. M. A piece in the puzzle of puberty. *Nat Neurosci* **16** (3), 251–253 (2013).

122. Lomniczi, A., Wright, H. & Ojeda, S. R. Epigenetic regulation of female puberty. *Front Neuroendocrinol* **36**, 90 (2015).

123. Vazquez, M. J. *et al.* SIRT1 mediates obesity- and nutrient-dependent perturbation of pubertal timing by epigenetically controlling Kiss1 expression. *Nat Commun* **9**, 1–15 (2018).

124. Ojeda, S. R. & Lomniczi, A. Unravelling the mystery of puberty. *Nat Rev Endocrinol* **10**, 67–69 (2013).

125. Abreu, A. P. *et al.* MKRN3 inhibits the reproductive axis through actions in kisspeptin-expressing neurons. *J Clin Invest* **130**, 4486–4500 (2020).

126. Abbara, A. & Dhillo, W. S. Makorin rings the kisspeptin bell to signal pubertal initiation. *J Clin Invest* **130**, 3957–3960 (2020).

127. Mariani, M. *et al.* MKRN3 circulating levels in Prader–Willi syndrome: a pilot study. *J Endocrinol Invest* **45**, 2165–2170 (2022).

128. Heras, V. *et al.* Hypothalamic miR-30 regulates puberty onset via repression of the puberty-suppressing factor, Mkrn3. *PLoS Biol* **17**, (2019).

129. Sobrino, V., Avendaño, M. S., Perdices-López, C., Jimenez-Puyer, M. & Tena-Sempere, M. Kisspeptins and the neuroendocrine control of reproduction: Recent progress and new frontiers in kisspeptin research. *Front Neuroendocrinol* **65**, (2022).

130. Lomniczi, A. & Ojeda, S. R. The Emerging Role of Epigenetics in the Regulation of Female Puberty. *Endocr Dev* **29**, 1–16 (2016).

131. Elks, C. E. *et al.* Thirty new loci for age at menarche identified by a meta-analysis of genome-wide association studies. *Nat Genet* **42**, 1077–1085 (2010).

132. Perry, J. R. B. *et al.* Parent-of-origin-specific allelic associations among 106 genomic loci for age at menarche. *Nature* **514**, 92–97 (2014).

133. Ciccarelli, M., Cipolletta, E. & Iaccarino, G. GRK2 at the Control Shaft of Cellular Metabolism. *Curr Pharm Des* **18**, 121–127 (2012).

134. Murga, C. *et al.* G protein-coupled receptor kinase 2 (GRK2) as a potential therapeutic target in cardiovascular and metabolic diseases. *Front Pharmacol* **10**,112 (2019).

135. Cipolletta, E. *et al.* Antidiabetic and Cardioprotective Effects of Pharmacological Inhibition of GRK2 in db/db Mice. *Int J Mol Sci* **20** (6), 1492 (2019).

136. Pampillo, M. *et al.* Regulation of GPR54 signaling by GRK2 and β-arrestin. *Molecular Endocrinology* **23**, 2060–2074 (2009).

137. Menéndez, F. M. GRKs y arrestinas en la regulación de receptores cerebrales. *Monografías de la Real Academia Nacional de Farmacia* 113–138 (2010).

138. Penela, P., Ribas, C., Sánchez-Madrid, F. & Mayor, F. G protein-coupled receptor kinase 2 (GRK2) as a multifunctional signaling hub. *Cell Mol Life Sci* **76**, 4423–4446 (2019).

139. Mayor, F. *et al.* G protein-coupled receptor kinase 2 (GRK2) as an integrative signalling node in the regulation of cardiovascular function and metabolic homeostasis. *Cell Signal* **41**, 25–32 (2018).

140. Sorriento, D. *et al.* The Metabolic Role of GRK2 in Insulin Resistance and Associated Conditions. *Cells* **10**, 1–15 (2021).

141. Arcones, A. C., Cruces-Sande, M., Ramos, P., Mayor, F. & Murga, C. Sex Differences in High Fat Diet-Induced Metabolic Alterations Correlate with Changes in the Modulation of GRK2 Levels. *Cells* **8**, (2019).

142. Arcones, A. C. *et al.* Cardiac GRK2 Protein Levels Show Sexual Dimorphism during Aging and Are Regulated by Ovarian Hormones. *Cells **10**,* 673 (2021).

143. Pitcher, J. A. *et al.* The G protein-coupled receptor kinase 2 is a microtubule-associated protein kinase that phosphorylates tubulin. *J Biol Chem* **273**, 12316–12324 (1998).

144. Lafarga, V., Aymerich, I., Tapia, O., Mayor, F. & Penela, P. A novel GRK2/HDAC6 interaction modulates cell spreading and motility. *EMBO J* **31**, 856–869 (2012).

145. Chen, M. *et al.* Prodeath signaling of G protein-coupled receptor kinase 2 in cardiac myocytes after ischemic stress occurs via extracellular signal-regulated kinase-dependent heat shock protein 90-mediated mitochondrial targeting. *Circ Res* **112**, 1121–1134 (2013).

146. Whalen, E. J. *et al.* Regulation of beta-adrenergic receptor signaling by S-nitrosylation of G-protein-coupled receptor kinase 2. *Cell* **129**, 511–522 (2007).

147. Iwakawa, H.-O. & Tomari, Y. Life of RISC: Formation, action, and degradation of RNA-induced silencing complex. *Mol Cell* **82**, 30–43 (2022).

148. David P. Bartel. MicroRNAs: Genomics, Biogenesis, Mechanism, and Function. *Cell* **116**, 281–297 (2004).

149. Bartel, D. P. Metazoan MicroRNAs. *Cell* **173**, 20–51 (2018).

150. de Sousa, M. C., Gjorgjieva, M., Dolicka, D., Sobolewski, C. & Foti, M. Deciphering miRNAs' Action through miRNA Editing. *Int J Mol Sci* **20**, 6249 (2019).

151. Sayed, D. & Abdellatif, M. MicroRNAs in development and disease. *Physiol Rev* **91**, 827–887 (2011).

152. Michlewski, G. & Cáceres, J. F. Post-transcriptional control of miRNA biogenesis. *RNA* **25**, 1 (2019).

153. Adams, L. Pri-miRNA processing: structure is key. *Nat Rev Genet* **18**, 145–145 (2017).

154. Tafrihi, M. & Hasheminasab, E. MiRNAs: Biology, Biogenesis, their Web-based Tools, and Databases. *Microrna* **8**, 4–27 (2019).

155. Cao, C. *et al.* Reproductive role of miRNA in the hypothalamic-pituitary axis. *Mol Cell Neurosci* **88**,130-137 (2018).

156. Zhu, H. *et al.* Lin28a transgenic mice manifest size and puberty phenotypes identified in human genetic association studies. *Nat Genet* **42**, 626–630 (2010).

157. Sangiao-Alvarellos, S., Pena-Bello, L., Manfredi-Lozano, M., Tena-Sempere, M. & Cordido, F. Perturbation of hypothalamic microRNA expression patterns in male rats after metabolic distress: impact of obesity and conditions of negative energy balance. *Endocrinology* **155**, 1838–1850 (2014).

158. Wang, H. *et al.* Gonadotrope-specific deletion of Dicer results in severely suppressed gonadotropins and fertility defects. *J Biol Chem* **290**, 2699–2714 (2015).

159. Messina, A. *et al.* A microRNA switch regulates the rise in hypothalamic GnRH production before puberty. *Nat Neurosci* **19**, 835–844 (2016).

160. Iivonen, A. P., Känsäkoski, J., Vaaralahti, K. & Raivio, T. Screening for mutations in selected miRNA genes in hypogonadotropic hypogonadism patients. *Endocr Connect* **8**, 506 (2019).

161. LaPierre, M. P., Lawler, K., Godbersen, S., Farooqi, I. S. & Stoffel, M. MicroRNA-7 regulates melanocortin circuits involved in mammalian energy homeostasis. *Nat Commun* **13**, 1–17 (2022).

162. Ahmed, K. *et al.* Loss of microRNA-7a2 induces hypogonadotropic hypogonadism and infertility. *J Clin Invest* **127**, 1061–1074 (2017).

163. Romero-Ruiz, A. *et al.* Deregulation of miR-324/KISS1/kisspeptin in early ectopic pregnancy: mechanistic findings with clinical and diagnostic implications. *Am J Obstet Gynecol* **220**, 480.e1-480.e17 (2019).

164. Alkafaji, H. A. *et al.* Up-regulation of KISS1 as a novel target of Let-7i in melanoma serves as a potential suppressor of migration and proliferation in vitro. *J Cell Mol Med* **25**, 6864–6873 (2021).

165. Ulasov, I. *et al.* MicroRNA 345 (miR345) regulates KISS1-E-cadherin functional interaction in breast cancer brain metastases. *Cancer Lett* **481**, 24–31 (2020).

166. Gaytan, F. *et al.* Distinct expression patterns predict differential roles of the miRNA-binding proteins, Lin28 and Lin28b, in the mouse testis: studies during postnatal development and in a model of hypogonadotropic hypogonadism. *Endocrinology* **154**, 1321–1336 (2013).

167. Roa, J. *et al.* Dicer ablation in Kiss1 neurons impairs puberty and fertility preferentially in female mice. *Nat Commun* **13** (1), 4663 (2022).

168. Mendes, N. D., Freitas, A. T. & Sagot, M. F. Current tools for the identification of miRNA genes and their targets. *Nucleic Acids Res* **37**, 2419–2433 (2009).

169. Kozomara, A., Birgaoanu, M. & Griffiths-Jones, S. MiRBase: From microRNA sequences to function. *Nucleic Acids Res* **47**, D155–D162 (2019).

170. Lewis, B. P., Burge, C. B. & Bartel, D. P. Conserved seed pairing, often flanked by adenosines, indicates that thousands of human genes are microRNA targets. *Cell* **120**, 15–20 (2005).

171. McGeary, S. E. *et al.* The biochemical basis of microRNA targeting efficacy. *Science* **366**, (2019).

172. Liu, W. & Wang, X. Prediction of functional microRNA targets by integrative modeling of microRNA binding and target expression data. *Genome Biol* **20**, (2019).

173. Vejnar, C. E. & Zdobnov, E. M. MiRmap: comprehensive prediction of microRNA target repression strength. *Nucleic Acids Res* **40**, 11673–11683 (2012).

174. Ding, J., Li, X. & Hu, H. TarPmiR: a new approach for microRNA target site prediction. *Bioinformatics* **32**, 2768–2775 (2016).

175. Enright, A. J. *et al.* MicroRNA targets in Drosophila. *Genome Biol* **5**, 1–14 (2003).

176. Rehmsmeier, M., Steffen, P., Höchsmann, M. & Giegerich, R. Fast and effective prediction of microRNA/target duplexes. *RNA* **10**, 1507–1517 (2004).

177. Kowarsch, A., Preusse, M., Marr, C. & Theis, F. J. MiTALOS: Analyzing the tissue-specific regulation of signaling pathways by human and mouse microRNAs. *RNA* **17**, 809–819 (2011).

178. Ludwig, N. *et al.* Distribution of miRNA expression across human tissues. *Nucleic Acids Res* **44**, 3865–3877 (2016).

179. Liu, C. J. *et al.* MiRNASNP-v3: A comprehensive database for SNPs and disease-related variations in miRNAs and miRNA targets. *Nucleic Acids Res* **49**, D1276–D1281 (2021).

180. Baker, E. R. Body weight and the initiation of puberty. *Clin Obstet Gynecol* **28**, 573–579 (1985).

181. Talbi, R. & Navarro, V. M. Novel insights into the metabolic action of Kiss1 neurons. *Endocr Connect* **9**, R124–R133 (2020).

182. Grossmann, M. Hypogonadism and male obesity: Focus on unresolved questions. *Clin Endocrinol (Oxf)* **89**, 11–21 (2018).

183. Wahab, F., Atika, B., Ullah, F., Shahab, M. & Behr, R. Metabolic impact on the hypothalamic kisspeptin-kiss1r signaling pathway. *Front Endocrinol (Lausanne)* **9**, 123 (2018).

184. Bowe, J. E. *et al.* Kisspeptin stimulation of insulin secretion: mechanisms of action in mouse islets and rats. *Diabetologia* **52**, 855–862 (2009).

185. Hussain, M. A., Song, W. J. & Wolfe, A. There is Kisspeptin - and then there is Kisspeptin. *Trends Endocrinol Metab* **26**, 564 (2015).

186. Kim, G. L., Dhillon, S. S. & Belsham, D. D. Kisspeptin Directly Regulates Neuropeptide Y Synthesis and Secretion via the ERK1/2 and p38 Mitogen-Activated Protein Kinase

Signaling Pathways in NPY-Secreting Hypothalamic Neurons. *Endocrinology* **151**, 5038–5047 (2010).

187. Higo, S., Iijima, N. & Ozawa, H. Characterisation of Kiss1r (Gpr54)-Expressing Neurones in the Arcuate Nucleus of the Female Rat Hypothalamus. *J Neuroendocrinol* **29**(2), 10.1111/jne.12452 (2017).

188. Millington, G. W. M. The role of proopiomelanocortin (POMC) neurones in feeding behaviour. *Nutrition & Metabolism* **4**, 1–16 (2007).

189. Manfredi-Lozano, M. *et al.* Defining a novel leptin-melanocortine kisspeptin pathway involved in the metabolic control of puberty. *Mol Metab* **5**, 844–857 (2016).

190. Kristensen, P. *et al.* Hypothalamic CART is a new anorectic peptide regulated by leptin. *Nature* **393**, 72–76 (1998).

191. Li, H. Y., Hwang, H. W. & Hu, Y. H. Functional characterizations of cocaine- and amphetamine-regulated transcript mRNA expression in rat hypothalamus. *Neurosci Lett* **323**, 203–206 (2002).

192. Zheng, H., Patterson, L. M. & Berthoud, H. R. CART in the dorsal vagal complex: Sources of immunoreactivity and effects on Fos expression and food intake. *Brain Res* **957**, 298–310 (2002).

193. True, C., Verma, S., Grove, K. L. & Smith, M. S. Cocaine- and amphetamine-regulated transcript is a potent stimulator of Gnrh and kisspeptin cells and may contribute to negative energy balance-induced reproductive inhibition in females. *Endocrinology* **154**, 2821–2832 (2013).

194. Elias, C. F. *et al.* Leptin differentially regulates NPY and POMC neurons projecting to the lateral hypothalamic area. *Neuron* **23**, 775–786 (1999).

195. Wu, Q., Whiddon, B. B. & Palmiter, R. D. Ablation of neurons expressing agouti-related protein, but not melanin concentrating hormone, in leptin-deficient mice restores metabolic functions and fertility. *Proc Natl Acad Sci U S A* **109**, 3155–3160 (2012).

196. Moore, A. M., Coolen &, L. M. & Lehman, M. N. Kisspeptin/neurokinin B/Dynorphin (KnDy) cells as integrators of diverse internal and external cues: evidence from viral-based monosynaptic tract-tracing in mice. *Sci Rep* **9**(1):14768 (2019).

197. Childs, G. v., Odle, A. K., MacNicol, M. C. & MacNicol, A. M. The Importance of Leptin to Reproduction. *Endocrinology* **62**(2),bqaa204 (2021).

198. Ramos-Lobo, A. M. *et al.* Long-term consequences of the absence of leptin signaling in early life. *Elife* **8**, e40970 (2019).

199. Patel, R. & Smith, J. T. Novel actions of kisspeptin signaling outside of GnRH-mediated fertility: a potential role in energy balance. *Domest Anim Endocrinol* **73**, (2020).

200. Talbi, R. & Navarro, V. M. Novel insights into the metabolic action of Kiss1 neurons. *Endocr Connect* **9**, R124–R133 (2020).

201. Dudek, M., Ziarniak, K. & Sliwowska, J. H. Kisspeptin and Metabolism: The Brain and Beyond. **9**, 16 (2018).

202. Obici, S., Feng, Z., Karkanias, G., Baskin, D. G. & Rossetti, L. Decreasing hypothalamic insulin receptors causes hyperphagia and insulin resistance in rats. *Nat Neurosci* **5**, 566–572 (2002).

203. Woods, S. C., Lotter, E. C., McKay, L. D. & Porte, D. Chronic intracerebroventricular infusion of insulin reduces food intake and body weight of baboons. *Nature* **282**, 503–505 (1979).

204. Qiu, X. *et al.* Delayed Puberty but Normal Fertility in Mice With Selective Deletion of Insulin Receptors From Kiss1 Cells. *Endocrinology* **154**, 1337–1348 (2013).

205. Qiu, X. *et al.* Insulin and Leptin Signaling Interact in the Mouse Kiss1 Neuron during the Peripubertal Period. *PLoS One* **10**, e0121974 (2015).

206. Roa, J. *et al.* Metabolic Control of Puberty Onset: New Players, New Mechanisms. *Mol Cell Endocrinol* **324**(1-2),87-94 (2010)

207. Tschöp, M. *et al.* Post-prandial decrease of circulating human ghrelin levels. *J Endocrinol Invest* **24**, RC19–RC21 (2001).

208. Nakazato, M. *et al.* A role for ghrelin in the central regulation of feeding. *Nature* **409**, 194–198 (2001).

209. Chen, H. Y. *et al.* Orexigenic action of peripheral ghrelin is mediated by neuropeptide Y and agouti-related protein. *Endocrinology* **145**, 2607–2612 (2004).

210. Szlis, M., Wójcik-Gładysz, A. & Przybył, B. J. Central obestatin administration affect the LH and FSH secretory activity in peripubertal sheep. *Theriogenology* **145**, 10–17 (2020).

211. Xu, Y. *et al.* Distinct Hypothalamic Neurons Mediate Estrogenic Effects on Energy Homeostasis and Reproduction. *Cell Metab* **29**, 1232 (2019).

212. Morentin, P. B. M. De *et al.* Estradiol regulates brown adipose tissue thermogenesis via hypothalamic AMPK. *Cell Metab* **20**, 41–53 (2014).

213. López, M., Nogueiras, R., Tena-Sempere, M. & Diéguez, C. Hypothalamic AMPK: a canonical regulator of whole-body energy balance. *Nat Rev Endocrinol* **12**, 421–432 (2016).

214. Mittelman-Smith, M. A. *et al.* Arcuate kisspeptin/neurokinin B/dynorphin (KNDy) neurons mediate the estrogen suppression of gonadotropin secretion and body weight. *Endocrinology* **153**, 2800–2812 (2012).

215. Conde, K. *et al.* Testosterone Rapidly Augments Retrograde Endocannabinoid Signaling in Proopiomelanocortin Neurons to Suppress Glutamatergic Input from Steroidogenic Factor 1 Neurons via Upregulation of Diacylglycerol Lipase-α. *Neuroendocrinology* **105**, 341–356 (2017).

216. Hardie, D. G., Ross, F. A. & Hawley, S. A. AMPK: a nutrient and energy sensor that maintains energy homeostasis. *Nature Reviews Molecular Cell Biology* **13**, 251–262 (2012).

217. Roa, J. *et al.* Metabolic regulation of female puberty via hypothalamic AMPK–kisspeptin signaling. *Proc Natl Acad Sci* **115**(45):E10758-E10767 (2018).

218. Franssen, D. *et al.* AMP-activated protein kinase (AMPK) signaling in GnRH neurons links energy status and reproduction. *Metabolism* **115**, 154460 (2021).

219. Sadria, M. & Layton, A. T. Interactions among mTORC, AMPK and SIRT: a computational model for cell energy balance and metabolism. *Cell Commun Signal* **19**, 1–17 (2021).

220. Vazquez, M. J., Velasco, I. & Tena-Sempere, M. Novel mechanisms for the metabolic control of puberty: implications for pubertal alterations in early-onset obesity and malnutrition. *J Endocrinol* **242**, R51–R65 (2019).

221. Pita, J. *et al.* Circulating kisspeptin levels exhibit sexual dimorphism in adults, are increased in obese prepubertal girls and do not suffer modifications in girls with idiopathic central precocious puberty. *Peptides* **32**, 1781–1786 (2011).

222. Mancini, A. *et al.* Evaluation of Kisspeptin levels in prepubertal obese and overweight children: sexual dimorphism and modulation of antioxidant levels. *Eur Rev Med Pharmacol Sci* **25**, 941–949 (2021).

223. Navarro, V. M. & Tena-Sempere, M. Neuroendocrine control by kisspeptins: role in metabolic regulation of fertility. *Nat Rev Endocrinol* **8**, 40–53 (2011).

224. Castellano, J. M. *et al.* Expression of hypothalamic KiSS-1 system and rescue of defective gonadotropic responses by kisspeptin in streptozotocin-induced diabetic male rats. *Diabetes* **55**, 2602–2610 (2006).

225. Morelli, A. *et al.* Sex steroids and leptin regulate the 'first Kiss' (KiSS 1/G-protein-coupled receptor 54 system) in human gonadotropin-releasing-hormone-secreting neuroblasts. *J Sex Med* **5**, 1097–1113 (2008).

226. Castellano, J. M. *et al.* Changes in Hypothalamic KiSS-1 System and Restoration of Pubertal Activation of the Reproductive Axis by Kisspeptin in Undernutrition. *Endocrinology* **146**, 3917–3925 (2005).

227. Luque, R. M., Kineman, R. D. & Tena-Sempere, M. Regulation of hypothalamic expression of KiSS-1 and GPR54 genes by metabolic factors: analyses using mouse models and a cell line. *Endocrinology* **148**, 4601–4611 (2007).

228. de Lorenzo, A. *et al.* MOSH syndrome (Male obesity secondary hypogonadism): Clinical assessment and possible therapeutic approaches. *Nutrients* **10**, 474 (2018).

229. Sánchez-Garrido, M. A. *et al.* Obesity-induced hypogonadism in the male: Premature reproductive neuroendocrine senescence and contribution of Kiss1-mediated mechanisms. *Endocrinology* **155**, 1067–1079 (2014).

230. Molina-Vega, M., Muñoz-Garach, A., Damas-Fuentes, M., Fernández-García, J. C. & Tinahones, F. J. Secondary male hypogonadism: A prevalent but overlooked comorbidity of obesity. *Asian J Androl* **20**, 531–538 (2018).

231. Dimakopoulou, A. *et al.* Animal Models of Diabetes-Related Male Hypogonadism. *Front Endocrinol (Lausanne)* **10**, 628 (2019).

232. Rey, R. A. *et al.* Male hypogonadism: an extended classification based on a developmental, endocrine physiology-based approach. *Andrology* **1**, 3–16 (2013).

233. Kumar, P., Kumar, N., Thakur, D. S. & Patidar, A. Male hypogonadism: Symptoms and treatment. *J Adv Pharm Technol Res* **1**(3), 297–301 (2010).

234. Cohen, P. G. The hypogonadal-obesity cycle: Role of aromatase in modulating the testosterone-estradiol shunt - A major factor in the genesis of morbid obesity. *Med Hypotheses* **52**, 49–51 (1999).

235. George, J. T., Millar, R. P. & Anderson, R. A. Hypothesis: Kisspeptin mediates male hypogonadism in obesity and type 2 diabetes. *Neuroendocrinology* **91**, 302–307 (2010).

236. Sarchielli, E. *et al.* Tumor necrosis factor-α impairs kisspeptin signaling in human gonadotropin-releasing hormone primary neurons. *J Clin Endocrinol Metab* **102**, 46–56 (2017).

237. Fernandez, C. J., Chacko, E. C. & Pappachan, J. M. Male obesity-related secondary hypogonadism – pathophysiology, clinical implications and Management. *Eur Endocrinol* **15**, 83–90 (2019).

238. Martin, L. J. & Touaibia, M. Improvement of testicular steroidogenesis using flavonoids and isoflavonoids for prevention of late-onset male hypogonadism. *Antioxidants* **9**, 237 (2020).

239. Dandona, P. *et al.* Hypogonadotrophic hypogonadism in type 2 diabetes, obesity and the metabolic syndrome. *Curr Mol Med* **8**, 816–828 (2008).

240. Pivonello, R. *et al.* Metabolic Disorders and Male Hypogonadotropic Hypogonadism. *Front Endocrinol (Lausanne)* **10**, 1–13 (2019).

241. Dandona, P., Dhindsa, S., Ghanim, H. & Saad, F. Mechanisms underlying the metabolic actions of testosterone in humans: A narrative review. *Diabetes Obes Metab* **23**, 18–28 (2021).

242. Padilla, S. L., Johnson, C. W., Barker, F. D., Patterson, M. A. & Palmiter, R. D. A Neural Circuit Underlying the Generation of Hot Flushes. *Cell Rep* **24**, 271–277 (2018).

243. Srinivas, S. *et al.* Cre reporter strains produced by targeted insertion of EYFP and ECFP into the ROSA26 locus. *BMC Dev Biol* **1**, 1–8 (2001).

244. Yoon, H., Enquist, L. W. & Dulac, C. Olfactory inputs to hypothalamic neurons controlling reproduction and fertility. *Cell* **123**, 669–682 (2005).

245. Matkovich, S. J. *et al.* Cardiac-specific ablation of G-protein receptor kinase 2 redefines its roles in heart development and beta-adrenergic signaling. *Circ Res* **99**, 996–1003 (2006).

246. Won, K. A. *et al.* The Glial–Neuronal GRK2 Pathway Participates in the Development of Trigeminal Neuropathic Pain in Rats. *J Pain* **15**, 250–261 (2014).

247. Taguchi, K., Matsumoto, T., Kamata, K. & Kobayashi, T. Inhibitor of G Protein-Coupled Receptor Kinase 2 Normalizes Vascular Endothelial Function in Type 2 Diabetic Mice by Improving β-Arrestin 2 Translocation and Ameliorating Akt/eNOS Signal Dysfunction. *Endocrinology* **153**, 2985–2996 (2012).

248. Navarro, V. M. *et al.* Characterization of the Potent Luteinizing Hormone-Releasing Activity of KiSS-1 Peptide, the Natural Ligand of GPR54. *Endocrinology* **146**, 156–163 (2005).

249. García-Galiano, D. *et al.* Kisspeptin signaling is indispensable for Neurokinin B, but not glutamate, stimulation of gonadotropin secretion in mice. *Endocrinology* **153**, 316–328 (2012).

250. Gaytan, F. *et al.* Development and validation of a method for precise dating of female puberty in laboratory rodents: The puberty ovarian maturation score (Pub-Score). *Sci Rep* **7**, 46381 (2017).

251. McQuillan, J., Han, S. Y., Cheong, I. & Herbison, A. E. GnRH Pulse Generator Activity Across the Estrous Cycle of Female Mice. *Endocrinology* **160**, 1480–1491 (2019).

252. Avendaño, M. S. *et al.* mPGES-1 (Microsomal Prostaglandin E Synthase-1) Mediates Vascular Dysfunction in Hypertension Through Oxidative Stress. *Hypertension* **72**, 492–502 (2018).

253. Griffiths, K. & Madhani, M. The Use of Wire Myography to Investigate Vascular Tone and Function. *Methods Mol Biol* **2419**, 361–376 (2022).

254. Avendaño, M. S. *et al.* Role of COX-2-derived PGE2 on vascular stiffness and function in hypertension. *Br J Pharmacol* **173**, 1541–1555 (2016).

255. Pfaffl, M. W. A-Z of Quantitative PCR: Quantification strategies in real-time PCR. *Bustin, A., Ed.; International University Line* (2004).

256. Steyn, F. J. *et al.* Development of a methodology for and assessment of pulsatile luteinizing hormone secretion in juvenile and adult male mice. *Endocrinology* **154**, 4939–4945 (2013).

257. Min, L. *et al.* RF9 acts as a KISS1R agonist in vivo and in vitro. *Endocrinology* **156**, 4639–4648 (2015).

258. Navarro, V. M. *et al.* Persistent impairment of hypothalamic KiSS-1 system after exposures to estrogenic compounds at critical periods of brain sex differentiation. *Endocrinology* **150**, 2359–2367 (2009).

259. Sangiao-Alvarellos, S. *et al.* Changes in hypothalamic expression of the Lin28/let-7 system and related microRNAs during postnatal maturation and after experimental manipulations of puberty. *Endocrinology* **154**, 942–955 (2013).

260. Perdices-Lopez, C. *et al.* Connecting nutritional deprivation and pubertal inhibition via GRK2-mediated repression of kisspeptin actions in GnRH neurons. *Metabolism* **129**, (2022).

261. Heras, V. *et al.* Central Ceramide Signaling Mediates Obesity-Induced Precocious Puberty. *Cell Metab* **32**, 951-966.e8 (2020).

262. Scherer, S. W. *et al.* Challenges and standards in integrating surveys of structural variation. *Nat Genet* **39**, S7 (2007).

263. Nica, A. C. & Dermitzakis, E. T. Expression quantitative trait loci: present and future. *Philos Trans R Soc Lond B Biol Sci* **368** (1620), 20120362 (2013).

264. Barroso, A. *et al.* Neonatal exposure to androgens dynamically alters gut microbiota architecture. *J Endocrinol* **247**, 69–85 (2020).

265. Santos-Marcos, J. A. *et al.* Interplay between gonadal hormones and postnatal overfeeding in defining sex-dependent differences in gut microbiota architecture. *Aging* **12**, 19979–19999 (2020).

266. Terasawa, E., Guerriero, K. A. & Plant, T. M. Kisspeptin and Puberty in Mammals. *Adv Exp Med Biol* **784**, 253 (2013).

267. Ruiz-Pino, F. *et al.* Environmentally Relevant Perinatal Exposures to Bisphenol A Disrupt Postnatal Kiss1/NKB Neuronal Maturation and Puberty Onset in Female Mice. *Environ Health Perspect* **127**, (2019).

268. Avendaño, M. S., Vazquez, M. J. & Tena-Sempere, M. Disentangling puberty: novel neuroendocrine pathways and mechanisms for the control of mammalian puberty. *Hum Reprod Update* **23**, 737–763 (2017).

269. Nieuwenhuis, D., Pujol-Gualdo, N., Arnoldussen, I. A. C. & Kiliaan, A. J. Adipokines: A gear shift in puberty. *Obesity Reviews* **21** (6), e13005 (2020).

270. Golub, M. S. *et al.* Public health implications of altered puberty timing. *Pediatrics* **121 Suppl 3**, S218-S230 (2008).

271. Day, F. R., Elks, C. E., Murray, A., Ong, K. K. & Perry, J. R. B. Puberty timing associated with diabetes, cardiovascular disease and also diverse health outcomes in men and women: the UK Biobank study. *Sci Rep* **5**, 11208 (2015).

272. Romero-Ruiz, A. *et al.* Molecular diagnosis of polycystic ovary syndrome in obese and non-obese women by targeted plasma miRNA profiling. *Eur J Endocrinol* **185**, 637–652 (2021).

273. Vashisht, A. & Gahlay, G. K. Using miRNAs as diagnostic biomarkers for male infertility: opportunities and challenges. *Mol Hum Reprod* **26**, 199–214 (2020).

274. Wang, H. *et al.* Gonadotrope-specific deletion of Dicer results in severely suppressed gonadotropins and fertility defects. *J Biol Chem* **290**, 2699–2714 (2015).

275. Landgraf, P. *et al.* A mammalian microRNA expression atlas based on small RNA library sequencing. *Cell* **129**, 1401–1414 (2007).

276. Lagos-Quintana, M. *et al.* Identification of tissue-specific microRNAs from mouse. *Curr Biol* **12**, 735–739 (2002).

277. Herzer, S., Silahtaroglu, A. & Meister, B. Locked nucleic acid-based *in situ* hybridisation reveals miR-7a as a hypothalamus-enriched microRNA with a distinct expression pattern. *J Neuroendocrinol* **24**, 1492–1504 (2012).

278. Wang, Y., Miao, L., Satterlee, A. & Huang, L. Delivery of oligonucleotides with lipid nanoparticles. *Adv Drug Deliv Rev* **87**, 68–80 (2015).

279. Höbel, S. & Aigner, A. Polyethylenimines for siRNA and miRNA delivery *in vivo*. *Wiley Interdiscip Rev Nanomed Nanobiotechnol* **5**, 484–501 (2013).

280. Mahmoudi, E. & Cairns, M. J. MiR-137: an important player in neural development and neoplastic transformation. *Mol Psychiatry* **22**, 44-55 (2017).

281. Sha, N. *et al.* The role of pineal microRNA-325 in regulating circadian rhythms after neonatal hypoxic-ischemic brain damage. *Neural Regen Res* **16**, 2071–2077 (2021).

282. Wang, F., Wang, F., Zhang, S. & Xu, X. MicroRNA-325 inhibits the proliferation and induces the apoptosis of T cell acute lymphoblastic leukemia cells in a BAG2-dependent manner. *Exp Ther Med* **21** (6), 631 (2021).

283. Carvelli, A. *et al.* A multifunctional locus controls motor neuron differentiation through short and long noncoding RNAs. *EMBO J* **41** (13), e108918 (2022).

284. Morelli, A. *et al.* Physical activity counteracts metabolic syndrome-induced hypogonadotropic hypogonadism and erectile dysfunction in the rabbit. *Am J Physiol Endocrinol Metab* **316**, E519–E535 (2019).

285. Minabe, S., Iwata, K., Tsuchida, H., Tsukamura, H. & Ozawa, H. Effect of diet-induced obesity on kisspeptin-neurokinin B-dynorphin A neurons in the arcuate nucleus and luteinizing hormone secretion in sex hormone-primed male and female rats. *Peptides* **142**, 170546 (2021).

286. Herbison, A. E. Control of puberty onset and fertility by gonadotropin-releasing hormone neurons. *Nat Rev Endocrinol* **12**, 452–466 (2016).

287. Castellano, J. M. *et al.* Ontogeny and mechanisms of action for the stimulatory effect of kisspeptin on gonadotropin-releasing hormone system of the rat. *Mol Cell Endocrinol* **257–258**, 75–83 (2006).

288. Han, S. K. *et al.* Activation of gonadotropin-releasing hormone neurons by kisspeptin as a neuroendocrine switch for the onset of puberty. *J Neurosci* **25**, 11349–11356 (2005).

289. Neill, J. D., Musgrove, L. C., Duck, L. W. & Sellers, J. C. High efficiency method for gene transfer in normal pituitary gonadotropes: adenoviral-mediated expression of G protein-coupled receptor kinase 2 suppresses luteinizing hormone secretion. *Endocrinology* **140**, 2562–2569 (1999).

290. Neill, J. D., Duck, L. W., Musgrove, L. C. & Sellers, J. C. Potential regulatory roles for G protein-coupled receptor kinases and beta-arrestins in gonadotropin-releasing hormone receptor signaling. *Endocrinology* **139**, 1781–1788 (1998).

291. Evron, T., Daigle, T. L. & Caron, M. G. GRK2: multiple roles beyond G protein-coupled receptor desensitization. *Trends Pharmacol Sci* **33**, 154–164 (2012).

292. Stamatiades, G. A. & Kaiser, U. B. Gonadotropin regulation by pulsatile GnRH: Signaling and gene expression. *Mol Cell Endocrinol* **463**, 131–141 (2018).

293. Caron, E., Ciofi, P., Prevot, V. & Bouret, S. G. Alteration in neonatal nutrition causes perturbations in hypothalamic neural circuits controlling reproductive function. *J Neurosci* **32**, 11486–11494 (2012).

294. Castellano, J. M. *et al.* Early Metabolic Programming of Puberty Onset: Impact of Changes in Postnatal Feeding and Rearing Conditions on the Timing of Puberty and Development of the Hypothalamic Kisspeptin System. *Endocrinology* **152**, 3396–3408 (2011).

295. Zhai, R., Snyder, J., Montgomery, S. & Sato, P. Y. Double life: How GRK2 and β-arrestin signaling participate in diseases. *Cell Signal* **94**, (2022).

296. Gupta, P., Mahapatra, A., Suman, A., & Kumar Singh, R. Effect of Endocrine Disrupting Chemicals on HPG Axis: A Reproductive Endocrine Homeostasis. *IntechOpen* (2021).

297. Koebele, S. V., & Bimonte-Nelson, H. A. Modeling menopause: The utility of rodents in translational behavioral endocrinology research. *Maturitas* **87**, 5–17 (2016).